ISSN 0973-8916

# Current Trends in Biotechnology and Pharmacy

Volume- 18 issue 2 APRIL 2024


www.abap.co.in

**Current Trends in Biotechnology and Pharmacy**
ISSN 0973-8916 (Print), 2230-7303 (Online)



www.abap.co.in

ISSN 0973-8916

# Current Trends in Biotechnology and Pharmacy

(An International Scientific Journal)

Volume- 18 issue 2 April 2024


www.abap.co.in

Indexed in Chemical Abstracts, EMBASE, ProQuest, Academic SearchTM, DOAJ, CAB Abstracts, Index Copernicus, Ulrich's Periodicals Directory, Open J-Gate Pharmoinfonet.in Indianjournals.com and Indian Science Abstracts.

## Association of Biotechnology and Pharmacy
## (Regn. No. 28 OF 2007)

The Association of Biotechnology and Pharmacy (ABAP) was established for promoting the science of Biotechnology and Pharmacy. The objective of the Association is to advance and disseminate the knowledge and information in the areas of Biotechnology and Pharmacy by organising annual scientific meetings, seminars and symposia.

**Members**

The persons involved in research, teaching and work can become members of Association by paying membership fees to Association.

The members of the Association are allowed to write the title MABAP (Member of the Association of Biotechnology and Pharmacy) with their names.

**Fellows**

Every year, the Association will award Fellowships to the limited number of members of the Association with a distinguished academic and scientific career to be as Fellows of the Association during annual convention. The fellows can write the title FABAP (Fellow of the Association of Biotechnology and Pharmacy) with their names.

**Membership details**

| (Membership and Journal) | India | SAARC | Others |
|---|---|---|---|
| Individuals – 1 year ` | Rs. 600 | Rs. 1000 | $100 |
| LifeMember | Rs. 4000 | Rs. 6000 | $500 |
| Institutions – 1 year | Rs. 1500 | Rs. 2000 | $200 |
| (Journal only) Life member | Rs.10000 | Rs.12000 | $1200 |

Individuals can pay in two instalments, however the membership certificate will be issued on payment of full amount. All the members and Fellows will receive a copy of the journal free.


## Association of Biotechnology and Pharmacy
(Regn. No. 28 OF 2007)
#5-69-64; 6/19, Brodipet
Guntur – 522 002, Andhra Pradesh, India

# Current Trends in Biotechnology and Pharmacy
**ISSN 0973-8916**

**Volume 18 (2)** **CONTENTS** **April 2024**

# Information to Authors

The Current Trends in Biotechnology and Pharmacy is an official international journal of Association of Biotechnology and Pharmacy. It is a peer reviewed quarterly journal dedicated to publish high quality original research articles in biotechnology and pharmacy. The journal will accept contributions from all areas of biotechnology and pharmacy including plant, animal, industrial, microbial, medical, pharmaceutical and analytical biotechnologies, immunology, proteomics, genomics, metabolomics, bioinformatics and different areas in pharmacy such as, pharmaceutics, pharmacology, pharmaceutical chemistry, pharma analysis and pharmacognosy. In addition to the original research papers, review articles in the above mentioned fields will also be considered.

**Call for papers**

The Association is inviting original research or review papers and short comunications in any of the above mentioned research areas for publication in Current Trends in Biotechnology and Pharmacy. The manuscripts should be concise, typed in double space in a general format containing a title page with a short running title and the names and addresses of the authors for correspondence followed by Abstract (350 words), 3 – 5 key words, Introduction, Materials and Methods, Results and Discussion, Conclusion, References, followed by the tables, figures and graphs on separate sheets. For quoting references in the text one has to follow the numbering of references in parentheses and full references with appropriate numbers at the end of the text in the same order. References have to be cited in the format below.

Mahavadi, S., Rao, R.S.S.K. and Murthy, K.S. (2007). Cross-regulation of VAPC2 receptor internalization by m2 receptors via c-Src-mediated phosphorylation of GRK2. Regulatory Peptides, 139: 109-114.

Lehninger, A.L., Nelson, D.L. and Cox, M.M. (2004). Lehninger Principles of Biochemistry, (4th edition), W.H. Freeman & Co., New York, USA, pp. 73-111.

Authors have to submit the figures, graphs and tables of the related research paper/article in Adobe Photoshop of the latest version for good illumination and allignment.

Authors can submit their papers and articles either to the editor or any of the editorial board members for onward transmission to the editorial office. Members of the editorial board are authorized to accept papers and can recommend for publication after the peer reviewing process. The email address of editorial board members are available in website www.abap.in. For submission of the articles directly, the authors are advised to submit by email to krssrao@abap.co.in or krssrao@yahoo.com.

Authors are solely responsible for the data, presentation and conclusions made in their articles/research papers. It is the responsibility of the advertisers for the statements made in the advertisements. 

Current Trends in Biotechnology and Pharmacy
Vol. 18(2) 1669-1679, April 2024, ISSN 0973-8916 (Print), 2230-7303 (Online)
DOI: 10.5530/ctbp.2024.2.15



# Improved, Efficient and Reliable Plant Regeneration Protocol for a Recalcitrant Black Rice (*Oryza sativa* cv. Chakhao amubi)

**Priyanka, Manchikatla Venkat Rajam***

Department of Genetics, University of Delhi - South Campus, Benito Juarez Marg, New Delhi 110021
*Corresponding author: rajam.mv@gmail.com; venkat.rajam@south.du.ac.in

**Abstract**

Rice tissue culture is very well established for the Indica and Japonica varieties in white rice. Black rice is recalcitrant for the regeneration due to their pigment. Since, there is a limited genetic transformation protocol available for the black rice so crop improvement efforts have not made so much progress. Here, we have developed an improved, efficient and reliable regeneration protocol for Chakhao amubi cultivar of black rice using mature seeds as an explant and through somatic embryogenesis pathway. The effects of growth regulators, gelling agent, and photoperiod, and various stages of complete protocol is well established. The regeneration protocol developed in this study will be well suited for introducing the agronomical important genes and functional genomic studies in black rice.

**Keywords:** Black rice, Chakhao amubi, Embryogenic callus induction, Somatic embryogenesis, Plant regeneration

## Introduction

Rice is the major staple food for the people in India and for more than 50% of the world's population. It is the primary source of nutrition for more than half of the world's population, primarily in Asia. It is grown on 43.86 million hectares in India, with a yield of 117.47 million tonnes (DAC & FW, 2019-20). It plays an important role in the nation's economy. Depending on the colour pericarp, there are many types of rice black, brown, purple and red and coloured rice provides several health benefits (1). Rice is a pre-eminent crop in North-East India and is widely grown in lowland, upland, and deep-water situations, accounting for around 72% of the total land area. This region is thought to be home to at least 10000 indigenous cultivars (2). The states of Arunachal Pradesh, Assam, Manipur, Meghalaya, Mizoram, Nagaland, Sikkim, and Tripura in Northern India have a rich array of regionally adapted non-Basmati aromatic germplasm. It is defined as a huge geographical area with high rainfall, humidity, variable topography, high natural selection pressures, and environmental stresses. Joha, chakhao, and tai cultivars grown in the states of Assam, Manipur, and Mizoram are the most prominent fragrant rice cultivars in this region (3). Chakhao landraces are a Manipur unique rice with a pleasant aroma and high quality. Manipur is one of India's eight North Eastern states and is noted for its numerous traditional rice types, cultivars, and landraces that are valued for their cultural and nutraceutical properties (4). Black rice is also known as Chak hao (meaning delicious rice) in Manipur, Chak means rice and hao means delicious. Recently, Black rice (Chak hao) has bagged GI tag in April 2020, with a certificate number 364. The application was registered by North Eastern Regional Agricultural Marketing Corporation Limited (NERAMAC).

In India, Manipur is the highest producer of Black rice cultivated by Meitei farmers. In Manipur, there are four landraces of black rice: Chakhao amubi, Chakhao angouba, Chakhao poireiton, and Chakhao angangba. This rice is gluten-free, cholesterol-free, and low in sugar, salt and fat. It is a whole grain, exceptionally nutritious rice that is high in fibre, anthocyanin, antioxidants, vitamin B complex, vitamin E, iron, thiamine, magnesium, niacin, and phosphorus. According to Cornell University researchers, antioxidants are nearly six times more abundant in black rice. Black rice is known as a treasure of macro and micro-nutrients as it contains many minerals and vitamins. It is estimated that 50 g of black rice per day offers 35% of the RDA for selenium, copper, zinc, and magnesium. Protein quality and quantity are better than in any other rice variety as it contains 18 amino acids. Being a natural iron-rich food, it is ideal for those who are concerned about receiving enough iron on plant-based diet (5). Calcium (Ca) and iron (Fe) are abundant in black rice (21.38/100 g), but sodium (Na) is low (10.19 mg/100g). It has a high magnesium and potassium content (Potassium 186.54 mg/100 g and Magnesium 107.21 mg/100 g). Among all rice varieties studied, black rice (5.89%) had the highest total saturated fatty acid and unsaturated fatty acid content (6). All rice samples included oleic and linoleic acid, with black rice having the highest concentration. The soluble dietary fibre (SDF) (%) in black rice is 8.17±0.07, while the insoluble dietary fibre (IDF) (%) is 14.49 ±0.07 (78). One half-cup cooked or one-fourth cup uncooked black rice contains (in daily recommended values) 160 kcal energy, 1.5 g fat, 34 g carbohydrate, 2 g fibre, 7.5 g protein, no saturated fat, and no cholesterol (5) and www.blackrice.com.

According to earlier research, black rice has higher antioxidant activity and phenolic content than white rice (7). Several studies have revealed that black rice is an excellent source of phytochemicals**.** The dehulled seeds of Japanese black-purple rice were qualitatively and quantitatively characterised for anthocyanin, flavones, flavonoids glycosides (Quercetin-3-O-glucoside, isorhamnetin-3-O-glucoside, and myricetin-7-O-Glucoside), carotenoids, vitamin E (tocopherols and tocotrienols), and y-oryzanols that gives health benefits, which also ensures the usage of black rice as a nutritious food (8). Chakhao rice takes 108 to 165 days to bloom flower and reaches a height of 130 to 165 cm. Chakhao cultivars have a narrow spikelet fertility range and yield few tillers and panicles per plant (9). Chakhao rice produces a yield of 1.3-5.01 tonnes ha-1, depending on the farming regime (9, 10). In spite of high nutritional and medicinal values, the yields of these cultivars are very poor as they are highly susceptible abiotic and biotic stresses. Efforts should be made to develop high yielding varieties without losing their aroma, cooking quality and grain quality.

Although during green revolution, conventional breeding had played a major significant role in crop production but those methods are not sufficient to feed today's growing population. Standardisation of protocols for effective regeneration and transformation systems for various crops has proven to be a challenging task, and biotechnology interventions for crop breeding have established an advantage over conventional approaches. Although, there are manyplant regeneration protocols for white rice are well established (11-14), but studies on *in vitro* culture and regeneration in black rice are very scarce. Attempts to develop a tissue culture-based methodology for regenerating black rice plants from calluses have so far either failed or produced extremely low regeneration frequencies. Development of extremely efficient and reliable plant regeneration systems have significant potential to assist in the genetic transformation of indica rice cultivars. In the present study, an improved, efficient and reliable regeneration protocol with high regeneration frequency was developed, which will be useful for generating black rice transgenics for its genetic improvement.

## Materials and Methods

### *Plant material and sterilization of seeds*

A Manipuri Black rice cultivar Chakhao amubi was selected for the present study. Seeds were collected from Assam Agriculture University, Assam, India. Dehusked healthy mature seeds were initially washed two times with sterile distilled water for removing dust particles. Seeds were sterilized with 70% ethanol (v/v) for 30 sec and then immediately rinsed with autoclaved distilled water. Seeds were surface sterilized using 4% sodium hypochlorite along with few drops of teepol for 20 min with intermittent shaking. The seeds were then washed thoroughly with autoclaved distilled water for removing the detergent. Sterilized seeds were soaked for overnight before they were inoculated on embryogenic callus induction medium.

### *Induction of embryogenic callus*

The over-night-soaked sterilized seeds were dried on sterile Whatman paper before inoculation. For embryogenic callus induction, 12-15 seeds per petri plate were inoculated on Callus Induction Medium (CIM) and kept under dark at 28±2˚C. CIM was supplemented with MS salts Himedia PT021 with different concentration of 2,4-D, 3% Maltose, 2.8 g/L proline, 0.6 g/L casein hydrolysate. Gelling agents used for solidifying the medium were 0.8 % agar and 0.4% phytagel. pH was adjusted to 5.8 before autoclaving. A total of three different combination of 2,4-D and gelling agents used were listed in Table 1. After 15 days, embryogenic calli were selected and cut it into two pieces and sub-cultured on CIM for multiplication. The frequency of callus induction was calculated by the following formula:

$$\text{Callus induction frequency (\%)} = \frac{\text{No. of seeds produced calli}}{\text{No. of seeds inoculated}} \text{ X } 100$$

Data obtained were subjected to two-way anova test analysis, based on 110 seeds per experiment, which was repeated thrice by using 110 seeds in each case for the induction of callus.

Table 1: Composition of various media used in the study

| Medium type | Medium | Medium composition | Plant hormones | Gelling agent |
|---|---|---|---|---|
| Callus Induction Medium | CIMI1 | MS Salts Himedia PT021, 3% Maltose, 2.8 g/L Proline, 600 mg/L CEH pH 5.8 | 2 mg/L 2,4-D | 0.8% Agar |
| | CIMI2 | MS Salts Himedia PT021, 3% Maltose, 2.8 g/L Proline, 600 mg/L CEH pH 5.8 | 2.5 mg/L 2,4-D | |
| | CIMI3 | MS Salts Himedia PT021, 3% Maltose, 2.8 g/L Proline, 600 mg/L CEH pH 5.8 | 3.0 mg/L 2,4-D | |
| | CIMII1 | MS Salts Himedia PT021, 3% Maltose, 2.8 g/L Proline, 600 mg/L CEH pH 5.8 | 2 mg/L 2,4-D | 0.4% Phytagel |
| | CIMII2 | MS Salts Himedia PT021, 3% Maltose, 2.8 g/L Proline, 600 mg/L CEH pH 5.8 | 2.5 mg/L 2,4-D | |
| | CIMII3 | MS Salts Himedia PT021, 3% Maltose, 2.8 g/L Proline, 600 mg/L CEH pH 5.8 | 3.0 mg/L 2,4-D | |

| | | | | |
|---|---|---|---|---|
| Shoot Regeneration Medium | MSRMIa | MS Salts Himedia PT021, 3% Maltose, 600 mg/L Proline, 2 g/L CEH, pH 5.8 | 2 mg/L BAP + 5 mg/L NAA | 0.4% Phytagel |
| | MSRMIb | MS Salts Himedia PT021, 3% Maltose, 600 mg/L Proline, 2 g/L CEH, pH 5.8 | 2 mg/L BAP 1 mg/l Kinetin + 0.5 mg/l NAA | |
| | MSRMIc | MS Salts Himedia PT021, 3% Maltose, 600 mg/L Proline, 2 g/L CEH, pH 5.8 | 4.5 mg/l Kinetin | |
| | MSRMId | MS Salts Himedia PT021, 3% Maltose, 600 mg/L Proline, 2 g/L CEH, pH 5.8 | 2.5 mg/l BAP + 0.5 mg/l NAA | |
| | MSRMIe | MS Salts Himedia PT021, 3% Maltose, 600 mg/L Proline, 2 g/L CEH, pH 5.8 | 2 mg/l Kinetin + 1 mg/l BAP + 0.2 mg/L NAA | |
| | MSRMI-Ia | MS Salts Himedia PT021, 3% Maltose, 600 mg/L Proline, 2 g/L CEH, pH 5.8 | 2 mg/L BAP + 0.5mg/L NAA | 0.8% Agarose |
| | MS-RMIIb | MS Salts Himedia PT021, 3% Maltose, 600 mg/L Proline, 2 g/L CEH, pH 5.8 | 2 mg/L BAP + 1 mg/l Kinetin + 0.5 mg/l NAA | |
| | MS-RMIIc | MS Salts Himedia PT021, 3% Maltose, 600 mg/L Proline, 2 g/L CEH, pH 5.8 | 4.5 mg/l Kinetin | |
| | MSRMI-Id | MS Salts Himedia PT021, 3% Maltose, 600 mg/L Proline, 2 g/L CEH, pH 5.8 | 2.5 mg/l BAP + 0.5 mg/l NAA | |
| | MS-RMIIe | MS Salts Himedia PT021, 3% Maltose, 600 mg/L Proline, 2 g/L CEH, pH 5.8 | 2 mg/l Kinetin + 1 mg/l BAP + 0.2 mg/L NAA | |
| Rooting Medium | RM | Half MS Salts Himedia PT021, 3% Sucrose | - | 0.4% Phytagel |

***Plant regeneration***

Calli obtained were cut into two pieces and sub-cultured on the same CIM for multiplication of calli. To get highly efficient regeneration, sub-cultured embryogenic calli were considered. A total of five different combination of media for regeneration tested were listed in Table 1. Different combination of BAP, NAA and along with Kn were used for regeneration in this study. Calli were inoculated on regeneration medium in the petri plates and kept under 16/8 photoperiod with a light intensity of 40 µE mol $m^{-2}s^{-1}$ at 28 ± 2°C. After shoot buds were initiated from calli, they were transferred to shoot elongation medium in jam bottles. Shoot regeneration frequency was calculated on the basis of number of calli cultured on shoot regeneration medium and number of calli with shoot regeneration.

$$\text{Shoot regeneration frequency} = \frac{\text{No. of calli showing shoot regeneration}}{\text{No. of calli inoculated}} \times 100$$

### *Rooting and hardening*

Healthy multiple shoots obtained were transferred to rooting medium (Table1) for induction and proliferation of roots for 15-20 days. The *in vitro* regenerated plants were gently rinsed with the autoclaved distilled water to remove the excess of agar to avoid any fungal contamination. Then the plants were transferred to pots containing soil and vermiculite in the ratio of 1:1 and covered with poly bags to maintain humidity and grown them in the tissue culture room with 26±1˚C and under 16/8 photoperiod with 40 µE mol $m^{-2}s^{-1}$ light intensity. After few days, polybags were removed upon the emergence of new leaves and then transferred to the field for further growth and development

## Results and Discussion

### *Effects of 2,4 D and gelling agent on callus induction*

We selected an important Black rice cultivar, i.e., Chakhao amubi for standardization of plant regeneration. Formation of embryogenic calli from seeds is the first step of any rice plant tissue culture system for subsequent regeneration of shoots and roots. We compared the callus induction frequency using the different sterilizing agents, different concentration of 2,4 -D and gelling agents. Initially, when the seeds were sterilized with 0.1% mercuric chloride and inoculated on callus induction media (CIMII1-3) with three different concentrations of 2,4-D no callus induction was observed in any medium (Fig. 1). But when we changed it to sodium hypochlorite and inoculated on CIMI1-3 and CIMII1-3 media, callus induction was initiated after 3 days from scutellar region of the embryo in all the combinations. After 5 days, vigorous callus proliferation was observed and healthy calli were obtained after 15 days of culture. In CIMI, gelling agent used was 0.8 % agar, CIMII medium gelled by 0.4% phytagel and 1,2 and 3 represent with different concentration of 2,4-D, *viz*., 2.0, 2.5 and 3.0 mg/L respectively. The callus induction frequency obtained was 31% in CIMI1, 40% in CIMI2 and 49% (highest) in CIMI3 (Fig. 2). In all the combination of CIMI1-3, cream, friable and unhealthy calli were developed when 0.8% agar gelling agent was used in all the concentration of 2,4-D (Fig 1). In case of CIMII, callus obtained were white compact, globular and healthy in all the combination of 2,4-D. Callus induction frequency obtained was 53% in CIMII1, 75% in CIMII2, and 96% in CIMII3. In all the combinations of CIMI and CIMII, highest callus induction frequency was obtained with CIMII3 when medium was supplemented with 3 mg/L 2,4-D and gelled with 0.4% phytagel (Fig. 1 and 2)). When the concentration of 2,4-D was increased to 3.5 and 4 mg/L, callus induction frequency was decreased to 60%. 2,4-D at 3 mg/L in combination with 0.4% phytagel gelling agent was found to be optimum for callus induction with high frequency. Hence, this concentration of 2,4-D and 0.4% phytagel gelling agent were selected for the subsequent experiments.

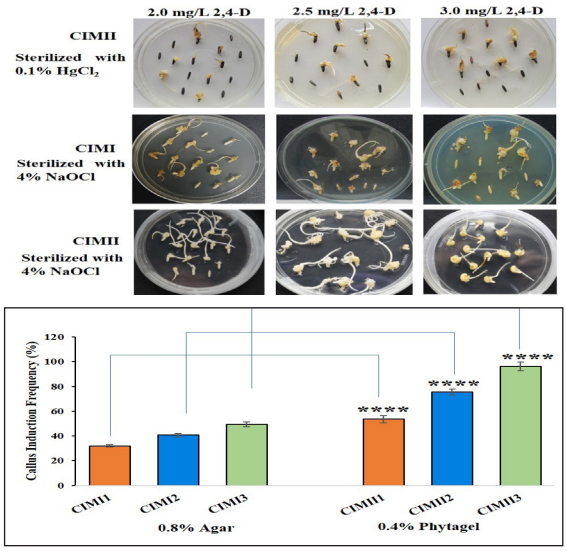


Figs. 1 and 2. Standardization of conditions for embryogenic callus induction in Black rice, cv. Chakhao amubi. Effect of 2,4-D, and sterilizing agent on embryogenic callus induction (Fig. 1) and gelling agent on callus frequency (Fig. 2) with their respective media CIMI (1-3) and CIMII (1-3) after 2 weeks of incubation. Data analysed by two-way analysis of variance (ANOVA) was statistically significant at $P < 0.05$.

### *Effects of phytohormones and gelling agent on regeneration frequency*

To obtain high regeneration frequency, MS medium supplemented with different combinations of BAP, Kn and NAA along with two different gelling agents, phytagel and agarose were used (Table1). Two types of regeneration media, MSRMI with 0.4% phytagel and MSRMII with 0.8% agarose were used. Both these media were fortified with different concentrations of BAP, NAA, and Kn. Calli showed maximum regeneration frequency in all the combinations of MSRMII. The regeneration frequency in MSRMI was in the range of 12 to 18%. In case of MSRMI, slightly higher shoot regeneration frequency, 15% and 18% were obtained in MSRMIa and MSRMIc respectively (Fig. 3 and 4).). While in case of MSRMII, high regeneration frequency, 35% to 47% was recorded and out of which maximum regeneration frequency was obtained in MSRMIId with the combination of 2.5 mg/L BAP and 0.5 mg/L NAA and MSRMIIe supplemented with 2 mg/L Kn, 1 mg/L BAP and 0.2 mg/L NAA. It was noticed that the increased concentration of Kn resulted in decrease in shoot regeneration frequency, and medium without BAP led to poor regeneration frequency. In all the combinations, maximum regeneration frequency was obtained in MSRMIId and MSRMIIe, and these concentrations were selected for the further experiments (Fig. 3 and 4).). Initially, green shoot buds appeared after 4-5 days embryogenic callus culture, then these shoot buds were transferred to jam bottles containing the respective medium for their development into shoots. The healthy multiple shoots obtained were transferred to rooting medium (Table1) for induction and proliferation of roots for 15-20 days (Fig. 5a). The regenerated plants were gently rinsed with the sterile distilled water to remove the traces of agar, and then the plants were transferred to pots (Fig. 5b), which were covered with poly bags to maintain humidity and following tissue hardening, they were transferred to the field for further growth and development.

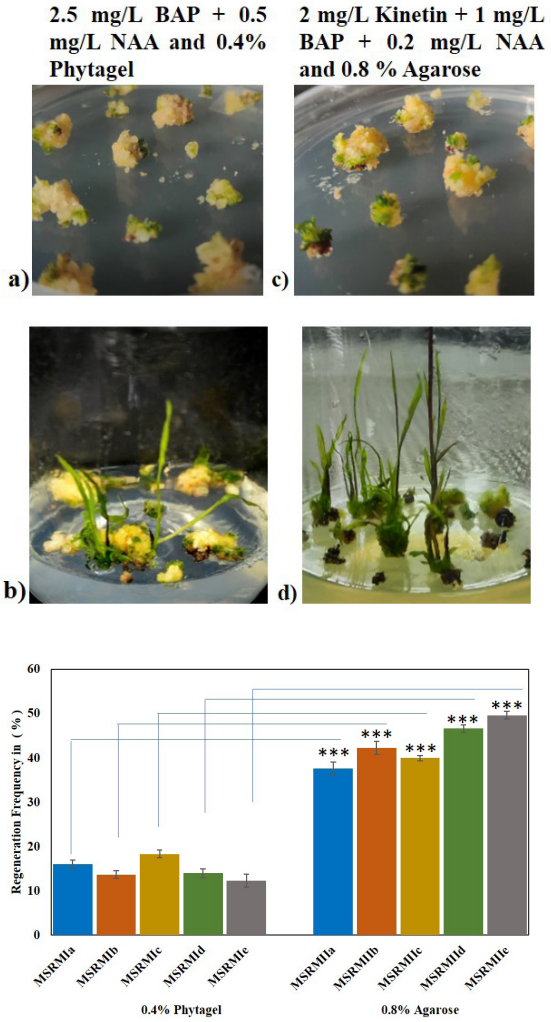


Figs. 3 and 4. Standardization of conditions for plant regeneration in Black rice, cv. Chakhao amubi. Effects of different phytohormones and gelling agent for regeneration in Oryza sativa cv. Chakhao amubi; Embryogenic sub-cultured callus on regeneration media MSRMI and MSRMII, and initiation of shoot buds (Fig. 3a and c) and elongated shoots (Fig. 3b and d); Effects of gelling agents and phytohormones on regeneration frequency (Fig. 4). Data analysed by two-way analysis of variance (ANOVA) was statistically significant at $P < 0.05$.

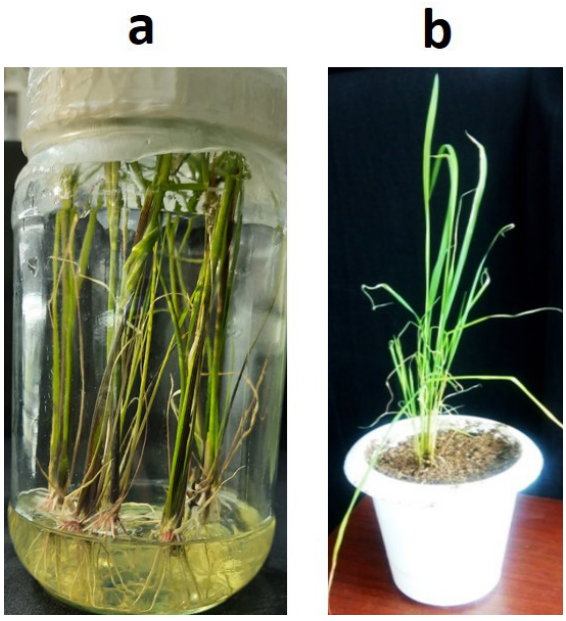


Fig. 5. Rooting of in vitro shoots, and hardening and acclimatation of regenerated plants. Healthy multiple shoots transferred to the rooting medium in the jam bottle containing only half-MS without phytohormones (Fig. 5a) Representative picture of fully regenerated chakhao amubi plant in the pot after 7 days of hardening (Fig. 5b).

## Discussion

The most crucial phase in rice tissue culture has long been regarded as embryogenic callus induction. The capacity for callus induction and the frequency of cell regeneration depends on the culture parameters such as the medium composition, genotype, and explant source. Even though there are numerous *in vitro* culture procedures for white rice available, the efforts to develop an efficient tissue culture regeneration protocol for Black rice with high regeneration frequency is absolutely required as the reported frequencies are very low. In this study, Chakhao amubi, an elite, popular and widely cultivated variety of Black rice was considered. Embryogenic callus induction was observed on both CIMI and CIMII. We observed that calli obtained in CIMI were yellowish, friable and unhealthy. On the other hand, calli obtained in CIMII were white, globular, compact and healthy after 15 days of inoculation. Callus induction frequency also varied in all three combinations of CIMI and CIMII of 1,2 and 3. Significant increase in callus induction frequency achieved with using 3 mg/L of 2,4-D in both the case of CIMI and CIMII. 2,4-D is an excellent source of auxin for induction of embryogenic callus, and this is supported by several previous studies (12,15-19). Seed sterilizing agent plays an important role in tissue culture protocol, it not only used for seed surface sterilization but also effects the callus induction and their frequency. Our results did not show any callus induction when the seeds were sterilized with 0.1% mercuric chloride and inoculated on CIM, On the contrary, seeds sterilized with 4% NaOCl showed very efficient callus induction in dark at 28˚C in MS fortified with 3% Maltose, 2.8 g/L proline, 600 mg/L CEH and 3 mg/L 2,4-D. Callus induction frequency also depends on gelling agent (12,20). We observed that when the seeds were inoculated on MS medium gelled with agar, callus obtained were friable, yellow and unhealthy. On the other hand, callus obtained using phytagel containing medium were healthy, compact, white and globular. As per the earlier reports, callus induction frequency also depends on the age of the explants and genotype and different basal medium composition (21-27). Further, we did not observe callus induction with seeds sterilized with mercuric chloride in our initial experiments, but callus induction was observed in CIMI and CIMII when seeds were sterilized with 4% sodium hypochlorite. Therefore, we continued our further standardization with sodium hypochlorite. The maximum callus induction frequency obtained with 3 mg/L 2,4-D as compared to 2.5 and 2 mg/L. According to (28), the optimal dose of 2,4-D for inducing embryogenic callus in indica rice is 0.5 mg/L. Optimal callus formation has also been reported by (29,30), at 2 mg/L of 2,4-D. It was also shown that the concentration of 2,4-D above 2 mg/L also causes reduction in callus induction frequency in Swarna cultivars

(20). Verma et al. (31) and Pawar et al. (32) also noted a decrease in callus induction frequency and callus bulk with an increase in 2,4-D concentration above 2 mg/L. It is evident, and also based on previous studies that the different concentrations of 2,4-D have an impact for callus induction in different rice cultivars. This variance in optimal 2,4-D concentrations for callus induction in rice cultivars imply genotype-dependent responses of the explants to the concentration of 2,4-D in the culture media.

While MS medium supplemented with MS salts, 3 % Maltose, 0.6 g/L CEH, 2.8 g/L proline, 2.5 mg/L BAP and 0.5 mg/L NAA, and gelled by 0.8 % agarose and other combination of 2 mg/L Kn, 1 mg/L BAP and 0.2 mg/L NAA and 0.8 % agarose (pH 5.8) resulted in significant higher regeneration frequency compared with other combinations mentioned in Table 1. There are many previous reports, which suggest that the combination of BAP, Kn and NAA leads to higher regeneration frequency. However, Mostafiz et al. (33) reported that while a combination of MS salts + 2 mg/L BAP + 2 mg/L Kn + 0.5 mg/L NAA resulted in 82 % regeneration in the Malaysian wetland variety MR220- CL2 and 68 % regeneration in the Malaysian wetland varieties MR220 and MR232, it only induced 40 % regeneration in the variety Bario. They attribute the differential reaction to the explant's genotype. Juturu et al. (20) reported that the range of 2-3 mg/L 2,4-D along with 0.5-1.0 mg/L NAA resulted in optimum regeneration frequency. As mentioned above that the gelling agents effect the callus induction frequency, but they also affect the regeneration frequency and similar results were also obtained by Sahoo et al. (12). The use of agarose as a gelling agent in shoot regeneration medium resulted in significant higher regeneration frequency as compared to phytagel and agar gelling agent. Several studies have been published on the effects of gelling agents on shoot regeneration in various rice types (12, 34-37) found no statistically significant differences in the frequency of regeneration of certain Indica rice types when several gelling agents were used in regeneration. Studies have been reported that there is significantly higher value in regeneration frequency in four rice cultivars (IR64, CSR10, Pusa Basmati 1 and Swarna) when 1% agarose used as a gelling agent (12). Mohamed et al. (37) also reported that gelling agents effect regeneration frequency. They found that using gelrite or phytagel as gelling agents increased the frequency of regeneration in the Egyptian rice cultivars Sakha104 and Giza178 as opposed to bacteriological agar. Consequently, just like with plant growth regulators, genotype determines how tissues react to various gelling agents.

## Conclusion

We optimised a protocol of plant regeneration of aromatic black rice Chakhao amubi with more than 40% regeneration efficiency. The developed protocol can be used for black rice transformation for its improvement by expressing novel genes that confer useful traits.

## Conflicts of Interest

The authors declare that there are no conflicts of interest.

## Acknowledgements

We are grateful to the Department of Biotechnology, New Delhi for generously funding black rice work (Grant No. DBT-NER/AGRI/29/2015) for a research grant on Black rice. MVR is grateful to the University Grants Commission (UGC) for BSR Faculty Fellowship. Priyanka is thankful to the UGC for fellowship. We also thank the UGC for SAP (DRS-III) programme, DST for FIST (Level 2) programme, and DU-DST PURSE (Phase II) grants. We acknowledge Dr. Tapan Kumar Mondal, ICAR-National Institute of Plant Biotechnology and Prof. Lingaraj Sahoo, Indian Institute of Technology Guwahati for their help.

## References

1. Kumari S (2020) "Black rice: An emerging "super food". Pantnagar Journal of Research, 18: 15-18.

2. Hore DK (2005) “Rice diversity collection, conservation and management in north-eastern India” Genetic Resources and Crop Evolution, 52:1129-1140.

3. Roy S, Banerjee A, Pattanayak A, Roy S., Rathi RS, Misra AK, Ngachan SV, Bansal KC (2014). Chakhao (delicious) rice landraces (*Oryza sativa* L.) of North-east India: collection, conservation and characterization of genetic diversity. Plant Genetic Resources, 12(3):264-272.

4. Asem ID, Imotomba RK, Mazumder PB, Laishram JM (2015) Anthocyanin content in the black scented rice (Chakhao): its impact on human health and plant defense. Symbiosis, 66:47-54.

5. Kushwaha UKS (2016) Health benefits of black rice. Black Rice*:* Research, History and Development, Springer. pp:151-183.

6. Tharmabalan RT, Bhat R, Yeoh TK (2016) Composition of amino acids, fatty acids, minerals and dietary fiber in some of the local and import rice varieties of Malaysia. International Food Research Journal, 22(3): 1148-1155.

7. Pal I (2018) Black rice-an extensive review. Paragon International Publishers, p 126.

8. Irakli MN, Samanidou VF, Katsantonis DN, Biliaderis CG, Papadoyannis IN (2016) Phytochemical profiles and antioxidant capacity of pigmented and non-pigmented genotypes of rice (*Oryza sativa* L.). Cereal Research Communications, 44(1):98-110.

9. Gangmei TP, George PJ (2017) Black rice CV. ‘Chakhao Amubi’ (*Oryza sativa* L.) response to organic and inorganic sources of nutrients on growth, yield and grain protein content. Journal of Pharmacognosy and Phytochemistry, 6(4):550-555.

10. Borah N, Athokpam FD, Semwal RL, Garkoti SC (2018) Chakhao (Black Rice; *Oryza sativa* L.): A culturally important and stress tolerant traditional rice variety of Manipur. Indian Journal of Traditional Knowledge 17(4):789-794.

11. Toki S, Hara N, Ono K, Onodera H, Tagiri A, Oka S, Tanaka H (2006) Early infection of scutellum tissue with *Agrobacterium* allows high-speed transformation of rice. The Plant Journal, 47(6):969-976.

12. Sahoo KK, Tripathi AK, Pareek A, Sopory SK, Singla-Pareek SL (2011) An improved protocol for efficient transformation and regeneration of diverse indica rice cultivars. Plant Methods, 7(1):1-11

13. Islam M, Roly ZY, Naim Z, Khalekuzzaman M (2015) *Agrobacterium* mediated genetic transformation and regeneration in elite rice (*Oryza sativa* L.) cultivar BRRI dhan56. African Journal of Biotechnology, 14(31):2415-2423.

14. Safitri FA, Ubaidillah M, Kim KM (2016) Efficiency of transformation mediated by *Agrobacterium tumefaciens* using vacuum infiltration in rice (*Oryza sativa* L.). Journal of Plant Biotechnology, 43(1):66-75.

15. Pandey SK, Ramesh B, Gupta PK (1994). Study on effect of genotype and culture medium on callus formation and plant regeneration in rice (*Oryza sativa* L.). Indian Journal of Genetics and Plant Breeding, 54(03):293-299.

16. Shankhdhar D, Shankhdhar SC,Pant RC (2002) Development of somatic embryos in rice. Indian Journal of Plant Physiology, 7(3):211-214.

17. Tam DM, Lang NT (2003) In vitro selection for salt tolerance in rice. Omonrice, 11:68-73.

18. Naqvi SMS, Sultana R, Rasheed H (2005) Tissue culture studies in *Oryza satva* L. cvs. Basmat 385 and super Basmat. Pakistan Journal of Botany, 37(4):823.

19. Jaseela F, Sumitha VR, Nair GM (2009) Somatic embryogenesis and plantlet regeneration in an agronomically important wild rice species *Oryza nivara*. Asian Journal of Biotechnology, 1(2):74-78.

20. Juturu VN, Mekala GK, Garladinne M, Reddy PCO Sekhar AC (2016) Optimization of in vitro regeneration protocol for a popular Indica rice (*Oryza sativa* L. cv Swarna). Annual Plant Science, 5:1395-1401.

21. Lin YJ, Zhang Q (2005) Optimising the tissue culture conditions for high efficiency transformation of indica rice. Plant Cell Reports, 23:540-547.

22. Ge X, Chu Z, Lin Y, Wang S (2006) A tissue culture system for different germplasms of indica rice. Plant Cell Reports 25,392-402.

23. Carsono N, Yoshida T (2006) Identification of callus induction potential of 15 Indonesian rice genotypes. Plant Production Science, 9(1):65-70.

24. Bhattacharya P, Sen SK (1980) Potentiality of leaf sheath cells for regeneration of rice (*Oryza sativa* L.) plants. Theoretical and Applied Genetics, 57:87-90.

25. Wernicke W, Brettell R, Wakizuka T, Potrykus I (1981) Adventitious embryoid and root formation from rice leaves. Zeitschrift für Pflanzenphysiologie, 103(4):361-365.

26. Abe T, Futsuhara Y (1986) Genotypic variability for callus formation and plant regeneration in rice (*Oryza sativa* L.). Theoretical and Applied Genetics, 72:3-10.

27. Oard JH, Rutger JN (1988) Callus induction and plant regeneration in elite US rice lines. Crop Science, 28(3):565-567.

28. Chen LJ, Luthe DS (1987) Analysis of proteins from embryogenic and non-embryogenic rice (*Oryza sativa* L.) calli. Plant Science, 48(3):181-188.

29. Kishor PK (1987) Energy and osmotic requirement for high frequency regeneration of rice plants from long-term cultures. Plant Science, 48(3):189-194.

30. Abe, T., & Futsuhara, Y. (1989) Selection of higher regenerative callus and change in isozyme pattern in rice (*Oryza sativa* L.). Theoretical and Applied Genetics, 78: 648-652.

31. Verma D, Joshi R, Shukla A, Kumar P (2011) Protocol for in vitro somatic embryogenesis and regeneration of rice (*Oryza sativa* L.). Indian Journal of Experimental Biology, 49(12):958-963.

32. Pawar BD, Bhaurupe JV, Kole PB, Markad NR (2015) Development of in vitro plant regeneration protocol in rice (*Oryza sativa* L.) using shoot tip explant. The Ecoscan, 9(1&2):231-233.

33. Mostafiz SB, Wagiran A (2018) Efficient callus induction and regeneration in selected indica rice. Agronomy, 8(5):77.

34. Jain RK, Jain S, Wu R (1996) Stimulatory effect of water stress on plant regeneration in aromatic indica rice varieties. Plant Cell Reports, 15:449-454.

35. Khaleda L, Al-Forkan M (2006) Stimulatory effects of casein hydrolysate and proline in in vitro callus induction and plant regeneration from five deep water rice (*Oryza sativa* L.). Biotechnology, 5(3):379-384.

36. Repalli SK, Geda CK, Pradhan NSN, Gjn R (2019) Influence of media type and carbon source on callus induction and regeneration response of different indica rice genotypes. Advances in Crop Science and Technology, 7(448):2.

37. Mohamed GM, Amer AM, Osman NH, Sedikc MZ, Hussein MH (2021) Effects of different gelling agents on the different stages of rice regeneration in two rice cultivars. Saudi Journal of Biological Sciences, 28(10):5738-5744.

Current Trends in Biotechnology and Pharmacy
Vol. 18(2) 1680-1687, April 2024, ISSN 0973-8916 (Print), 2230-7303 (Online)
DOI: 10.5530/ctbp.2024.2.16



# Green Synthesis Of silver Nanoparticles Using *Elettaria cardamomum*: Characterization and Antimicrobial Potential

**Nimisha D. Patel, [1]* Dharmesh A. Patel, [2] Gaurav D. Shrimali, [3] and Ritu Kamdar[1]**

[1]Department of Microbiology , Parul institute of applied science & research, Parul University, Limda, Waghodia, Vadodara, Gujarat, India 391769
[2]Quality Assurance, Kashiv Biosciences, Llc, 3440 S Dearborn St Ste 300 Chicago, IL, 60616-5149 United States
[3]School of Applied Sciences and Technology, Gujarat Technological University, Chandkheda, Ahmedabad, Gujarat, India 382424
*Corresponding author email: nimisha.patel@paruluniversity.ac.in

Graphical abstract

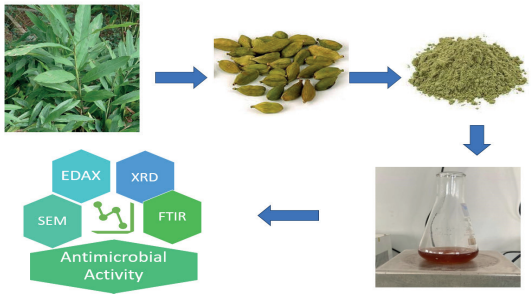


## Abstract

Recently, the eco-friendly production of silver nanoparticles (AgNPs) has become a focal point for researchers. In India, the quest for cost-effective, non-hazardous compounds suitable for reducing and stabilizing AgNPs has been limited. This study explores the synthesis of AgNPs using *Elettaria cardamomom* seed extract. We evaluated the efficiency of silver ion (Ag+) reduction and AgNP formation from an aqueous AgNO3 solution combined with the cardamom seed extract. Characterization of the AgNPs was carried out through UV-vis spectroscopy, XRD, SEM, EDAX, and FTIR. This research presents a practical and efficient strategy for AgNP production. A formulation using readily available 1 mm aqueous AgNO3, known for its accessibility and therapeutic properties, was created with cardamom seed extract serving as both a capping and reducing agent. Within 30 minutes, the silver ions were reduced to AgNPs, resulting in a change from golden to dark brown-reddish tint. Various analytical techniques, including UV-vis spectroscopy and Fourier-transform infrared spectroscopy, were employed for characterization. This study introduces an affordable, robust, and renewable method using *E. cardamomum* seeds for AgNP synthesis, which is entirely eco-friendly and devoid of toxic chemicals. AgNPs hold promise for applications in cancer treatment and diagnosis, setting them apart from other noble metals.

Keywords: Green synthesis, Silver Nanoparticles, Elettaria cardamomum, Nanotechnology, Surface Plasmon Resonance

## Introduction

The process of altering matter within a length range of 1 to 100 nm to create useful materials, tools, and systems is referred to as “nanotechnology.” At this scale, novel characteristics, and functions emerge(1). Nanotechnology is currently an expanding field of manufacturing processes. Notably, living cells represent some

Current Trends in Biotechnology and Pharmacy
Vol. 18(2) 1680-1687, April 2024, ISSN 0973-8916 (Print), 2230-7303 (Online)
DOI: 10.5530/ctbp.2024.2.16


of the best examples of nanoscale machines capable of a wide range of activities, including energy generation and material extraction(2). Nanoparticles can be created using a chemical synthesis process in a short period of time; however, this approach requires capping agents to stabilize the size of the nanoparticles. The chemicals used in the creation and stabilization of nanoparticles are dangerous and generate environmentally harmful byproducts. Recently, research in nanoparticle synthesis using microbes and plant extracts has gained more importance due to its eco-friendliness, versatility, and, most importantly, the avoidance of hazardous chemicals (3).

When compared to microbes, plant-mediated synthesis is frequently used *by* researchers for its advantages, such as avoiding the need to maintain microbial cultures, saving time, and cost-effectiveness(4). The need for ecologically safe synthetic processes for producing nanoparticles has led to increased interest in biological techniques that do not produce dangerous chemicals as by-products. Consequently, "green nanotechnology" is becoming increasingly popular(5). Green chemistry has recently become essential for producing environmentally friendly products(6).

Cardamom (*E. cardamomum*), widely recognized as the 'Queen of Spices' and belonging to the Zingiberaceae family, is one of the most important and readily available spices. The seeds of cardamom are the source of its aroma and flavor. Plants synthesize a wide variety of secondary metabolites, with a significant portion consisting of phenolic compounds and flavonoid compounds(7). Nowadays, medicinal plants(8), fruits(9-11), weeds(12), and spices(13) have been used for the synthesis of nanoparticles. Spices are a new frontier in green synthesis, and Singh et al. have already reported the synthesis of silver nanoparticles using clove buds. The presence of aromatic flavor compounds in the clove buds is likely responsible for the reduction of silver ions to silver nanoparticles(13).

## Materials and Methods

### *Collection and extraction of cardamom seeds*

A variety of plants in the families Elettaria and Amomum in the family Zingiberaceae produce seeds that are used to make the spice known as cardamom. We bought fresh Elettaria cardamom seeds from a local market of Ahmedabad district, cleaned them with distilled water, and let them air dry. The seeds were pulverized to a fine powder. 20 g of newly made dry seed powder was suspended in 200 ml of distilled water and heated at 75 °C for 30 minutes. Whatman Filter Paper No. 1 was used to filter the final solution before using it as an extract in the following experiment.

### *Synthesis of silver nanoparticles*

As a precursor, silver nitrate (AgNO3) was used to start the production of silver nanoparticles. 40 ml of various AgNO3 concentrations (0.16, 0.18, and 0.20 gm) and about 7 ml of *E. cardamomum* seed extract was mixed in a conical beaker. The solution's colour shifted from light brown to dark brown during the 30 minutes that it was brought to a boil at 75°C. The reduction of Ag+ ions to AgO was noticed by observing the UV-Vis spectra of various concentrations of the reaction mixture (silver nitrate solution and seed extract).

### *Optimization of synthesized silver nanoparticles*

With an increase in leaf extract concentration (10, 20, and 30 mL) in 10 mL of 1 mM silver nitrate, the concentration ratio of the leaf extract and silver nitrate was optimized (ratio1:1,2:1,3:1). The solution's absorbance was measured spectrophotometrically after two days of incubation. It was also done by changing quantities of the aqueous silver nitrate by 16,18 and 20ml. Also, the stability of the produced silver nanoparticles was checked after 10 days through UV spectrophotometry.

***Antibacterial activity study***

Antibacterial activity of synthesized AgNP was assessed by agar well diffusion method(14). In this method 0.2 ml of young test culture of *Bacillus subtilis* and *E. coli* was inoculated in sterile melted top agar previously cooled at 50°C. After solidification, two wells of 8mm size were created by sterile cup-borer. One well is loaded with antibiotic neomycin which is designated as A and other well is loaded with AgNPs synthesized by aqueous cardamom extract which is designated as S.

***Characterization studies***

The ability of colored materials to selectively absorb energy within the visible portion of the electromagnetic spectrum is what gives color its appearance. Energy absorption causes an electron to move from its ground state to its excited state. As a result, the principal characterization instrument to investigate the creation of metal nanoparticles is the UV visible absorption spectroscopy. UV-visible spectroscopy, which has proven to be a very helpful method for the investigation of nanoparticles, was used to characterize the nanoparticles in the main. With a resolution of 1 nm, UV-visible spectroscopy (nanodrop) analysis was performed(15). Using a UV-visible Spectrophotometer, the reduction of silver metal ions to silver nanoparticles was first examined (Perkin-Elmer) at regular intervals with wavelengths ranging from 360 to 700 nm. Using a (Bruker VERTEX-70) FT-IR spectrophotometer with a resolution of 4 cm-, it was feasible to identify potential biomolecules that oversaw the reduction and stability of silver nanoparticles(16). FTIR Spectra of neem leaf broth and synthesized AgNPs were recorded on ALPHA-T –Bruker model in the range of 4000 – 400 cm-1.

**Results and Discussion**

The current investigation thoroughly examines biological synthesis, characterization, process optimization, size-based separation and purification, mechanism of synthesis of silver nanoparticles, antimicrobial activity of plant material synthesized silver nanoparticles, and their potential antimicrobial mechanism. A straightforward method for the creation of silver nanoparticles was used for the screening of various plant components. So, the identification of new and potential biological nanoparticle manufacturing systems was based on the results of this screening.

There is evidence in the literature that plant extracts have the ability to convert metal ions into metal nanoparticles. Due to the presence of bioactive phytochemicals in the aqueous date seed extract such as phenolics, flavonoids, polyphenols, aldehydes, carboxylic acids, anthraquinone, saponin, terpenoids tannin, and proteins, they were able to stabilize the produced silver nitrate salt into AgNPs. The change of color in the reaction mixture from orange red to dark brown provided early proof that silver nanoparticles had been produced because of the surface Plasmon resonance phenomenon. (Fig. 1).

An important method to investigate how metal NPs develop in aqueous solutions is UVVis spectroscopy. UV-vis spectroscopy was employed to examine the characteristics of nanoparticles. UV-Vis spectroscopy is a vital technique to confirm the nanoparticles' size, shape, and stability. through the development of a brown tint from a light orangish golden(17). Visualization of AgNPs generation was possible. From 350 to 800 nm, the measured spectrum values were obtained. A single, strong, and broad surface Plasmon Resonance (SPR) peak was seen at 429 nm throughout the reaction period, indicating that the NPs were disseminated 27 in the aqueous solution. This peak was measured by analyzing the absorption spectra at a wavelength range of 200 to 800 nm (Fig. 2). Due to the plasmon resonance exhibited by AgNPs, it is known that AgNPs exhibit a UV-Vis absorption spectrum maximum in the range of 400–500 nm. The AgNPs' Surface Plasmon Resonance (SPR) absorption band's nearly identical, symmetrical shape (Fig. 3) indicates

Current Trends in Biotechnology and Pharmacy
Vol. 18(2) 1680-1687, April 2024, ISSN 0973-8916 (Print), 2230-7303 (Online)
DOI: 10.5530/ctbp.2024.2.16


that they formed into spherical nanoparticles without significant aggregation(18). Numerous reports have shown that Silver nanoparticles' resonance peak appears to be located between 300 and 480 nm(19,20).

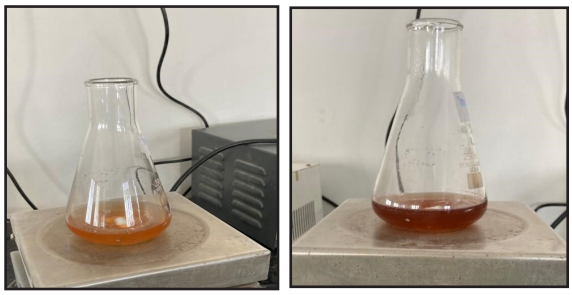

Fig. 1. Color change of leaf extracts containing silver before (left side) and after (right side) the synthesis of silver nanoparticles.

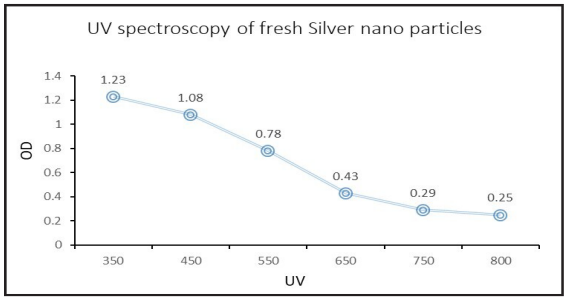


Fig. 2 UV-Visible absorption spectra of biosynthesized silver Nanoparticle from *E. cardamomum* depicting peak at 450nm.

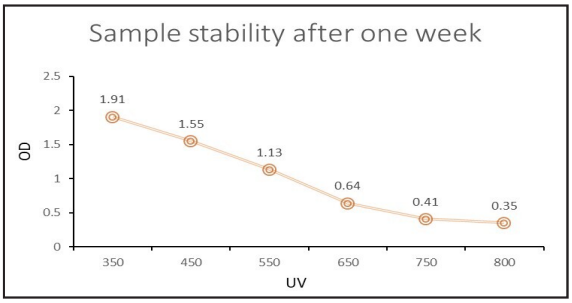


Fig. 3 UV-Visible absorption spectra of same biosynthesized silver nanoparticle after a week.

The FTIR spectra of the reduced AgNO3 solution with the plant extracts were found between the wave number ranges of 4000-600 cm1(Fig. 4). FTIR research was done at a resolution of 4 cm1 to determine the likely functional groups in plant extracts that are in charge of lowering the silver ion and capping the produced AgNPs. The occurrence of the FTIR peak at 3350 cm1 shows the presence of N-H bonds in amines, as opposed to the tiny peak at 2913 cm1, which reflects the H-C-H symmetric stretching of alkanes. Fig. 5 showing the FTIR spectra of silver nanoparticle synthesized using *E. cardamomom* seed broth. The alkaloid capsaicin with N-H stretch is responsible for both the coating of the nanoparticles and the bio-reduction of silver ions. The band at 1017 cm1 is caused by the ethers' C-O elongation in plant extract. Previous research has found that the harmonics of alcoholic O-H, alkanes C-H, phenolic O-H, and C-O stretches, respectively, are 3325-3198 cm1, 2917-2833 cm1, 1380-1360 cm1, and 1050-1025 cm(21,22).

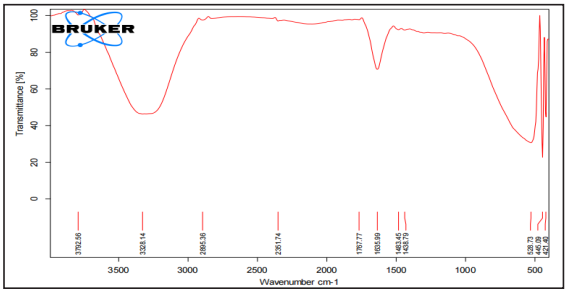


Fig. 4. FTIR spectra of *E. cardamomom* seed broth extract

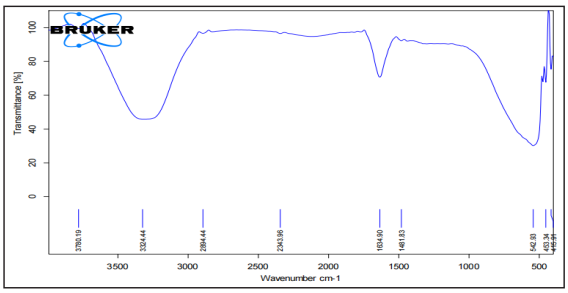


Fig. 5. FTIR spectra of silver nanoparticle synthesized using *E. cardamomom* seed broth

AgNps demonstrated antimicrobial efficacy against *E. coli* and *B. subtilis*, as demon-

strated by the findings and visible zones of inhibition on (Figure 6(a, b)). AgNps exhibited behavior that was dose dependent. At a concentration of 30 g/disc, generic Neomycin and nanoparticles were compared side by side. Biosynthesized AgNps displayed larger zones of inhibition at 30 g dosages. The ability of the AgNps to inhibit both Gram-positive and Gram-negative bacteria at the cellular level was amply demonstrated by this action in other words, compared to traditional antibiotics, AgNps were more efficient at preventing the growth of pathogenic germs. Numerous studies have discussed how effective silver's antibacterial action is against various infections(23,24). However, a few studies have produced some data and hypotheses: I (i) To interact with bacteria, they should have a spherical shape; (ii) Nanoparticles can enter bacteria and cause damage by likely working in conjunction with substances containing sulphur and phosphorus(25). All silver nanoparticles with a diameter of 1 to 10 nm attach to the cell membrane surface of bacteria and interfere with their ability to function(26). The antibacterial effect is likely generated from the electrostatic interaction between the positive charged Nanoparticles and the negative charged cell membrane of the bacterium(27,28). On the other hand(29), observed that the antibacterial activity of silver nanoparticles on Gram-negative bacteria was dependent on the concentration of Ag nanoparticles and was directly related to the creation of pits in the bacterial cell wall.

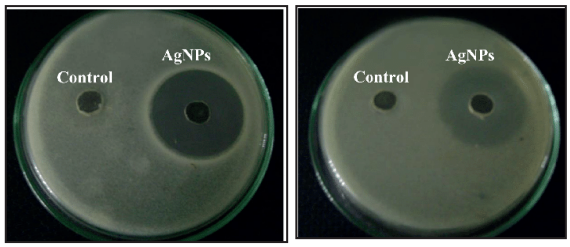


Fig. 6. The different zones formed by taking neomycin as control and (a) *Bacillus subtilis* (b) *E. coli.*

This research developed a simple, quicker, and more environmentally friendly method for creating AgNPs from cardamom seed aqueous extracts. monitoring of shifting FTIR peak locations of Spectra suggest that various functional categories of plant secondary metabolites may serve as capping and stabilizing agents. The Ag ion reduction will be complete in 4 hours due to how fast metal ions are reduced. Successfully produced silver nanoparticles underwent UV-vis and FTIR analysis. Two samples were tested in UV-VIS and compared to one another to show that as samples age, the particles tend to become denser. The functional group contained in the cardamom seeds is found using FTIR. The graph demonstrated the presence of the two major functional groups, 1,8 cineole and a-terpinyl acetate.

## Conclusion

The objective of our study was to explore the antimicrobial, antioxidant, and synthesis capabilities of AgNPs while also investigating the effects of sulfidation on these nanoparticles.

Our experimental results demonstrate the successful achievement of green synthesis of AgNPs utilizing *E. cardamomum* extract as both a capping and reducing agent. In terms of accessibility, environmental sustainability, affordability, and the simplicity of the reduction process, green synthesis outperformed traditional chemical reduction methods. Notably, the green synthesis approach has been optimized to yield AgNPs rapidly and in substantial quantities. Characterization of the synthesized AgNPs revealed nearly spherical shapes with sizes averaging around 50 nm, as confirmed through a series of comprehensive characterization techniques. AgNPs synthesized via green methods hold significant promise for various applications, including drug delivery, DNA analysis, gene therapy, cancer treatment, antimicrobial agents, biosensors, catalysis, surface-enhanced Raman spectroscopy (SERS), and magnetic resonance imaging (MRI). This study introduces a straightforward, simplified, and environmentally friendly method to produce AgNPs using aque-

ous extracts of cardamom seeds. The successful derivation of silver nanoparticles was confirmed through UV-vis spectroscopy, and further insights into the functional groups present in cardamom seeds were obtained through FTIR analysis. Notably, our FTIR analysis revealed the presence of two key functional groups, namely, 1,8 cineole and a-terpinyl acetate, as evident from the generated spectra.

**Acknowledgments**

The research was conducted at the Parul Institute of Applied Science and Research, Parul University. We extend our sincere appreciation to the esteemed management of Parul University for their invaluable support and provision of essential resources, which played a pivotal role in facilitating the successful completion of this study.

**References**

1. Poole Jr., C.P. and Owens, F.J. Introduction to Nanotechnology, John Wiley & Sons, Inc., Hoboken (2003).

2. D. Goodsell, Lessons from Nature, New Jersey: Wiley-Liss (2004).

3. S.Mann: Molecular tectonics in biomimetic materials chemistry, Nature, , pp 499 – 505 (1993).

4. M.D.A. Farooqui, P.S. chauhan, P. krishnamoorthy, and J.shaik: Extraction of silver Nanoparticle from the leaf extracts of Clerodendrum inerme, Digest journal of nanomaterials and biostructures, , 5, pp. 43 – 49 (2010).

5. Pradeep T. Coalescence of nanoclusters and the formation of sub micron crystallites assisted by Lactobacillus strains, Crystal growth and design, , 2(4), pp. 293-298 (2002).

6. Haohong Duan, Dingsheng Wang and Yadong Li: Green chemistry for nanoparticles synthesis," Chem. soc. Rev., , 44(16), pp. 5778- 5792 (2015).

7. Crozier, H. Ashihara, M.N. Clifford, Plant: Secondary Metabolites and the Human Diet, Oxford: Blackwell Publishing, (2006).

8. Thirumurugan, G.J. Jiflin, G. Rajagomathi, N.A. Tomy, S. Ramachandran, and R. Jaiganesh: Biotechnological synthesis of gold Nanoparticle of Azadirachta indica leaf extract, International Journal of Biological Technology,1, pp. 75-77 (2010).

9. Ankamwar, C. Damle, A. Ahmad, and M. Sastry: Biosynthesis of Gold and Silver Nanoparticle Using Emblica Officinalis Fruit Extract, Their Phase Transfer and Transmetallation in an Organic Solution, Journal of Nanoscience and Nanotechnology, , 5, pp. 1665-1671 (2005).

10. Jain, H. K. Daima, S. Kachhwaha, S. L. Kothari: Synthesis of plant-mediated silver Nanoparticle using papaya fruit extract and evaluation of their anti microbial activities, Digest journal of nanomaterials and biostructures, , 4, pp. 557 – 563 (2009).

11. G.S. Ghodake, N.G. Deshpande, Y.P. Lee, E.S. Jin, Pear fruit extract-assisted room-temperature biosynthesis of gold nanoplates, Colloids and Surfaces B: Biointerfaces , , 75 pp. 584-589 (2010).

12. V. Parashar, R. Parashara, B. sharma, A.C. Pandey, Parthenium leaf extract mediated synthesis of silver Nanoparticle: a novel approach towards weed utilization. Digest Journal of Nanomaterials and Biostructures, , 4, pp. 45-50 (2009).

13. A.K. Singh, M. Talat , D.P. Singh , O. N. Srivastava, Biosynthesis of gold and silver Nanoparticle by natural precursor clove and their functionalization with amine group, J. Nanopart Res, 12, pp. 1667-

1675 (2010).

14. Perez, C., Pauli, M. and Bazerque, P. An Antibiotic Assay by Agar Well Diffusion Method. Acta Biologiae et Medicinae Experimentalis, , 15, pp. 113-115 (1990).

15. Harekrishna Bar, D. k. Green synthesis of silver nanoparticles using latex of Jatropha curcas. Colloids and surfaces A Physiochemical and Engineering Aspects, , pp.134-139 (2009).

16. Nagarajan Kanipandian, S. K. Characterization, antioxidant and cytotoxicity evaluation of green synthesized silver nanoparticles using Cleistanthus collinus extract as surface modifier. Materials research Bulletin, , pp. 494-502 (2014).

17. P Prakash 1, P Gnanaprakasam, R Emmanuel, S Arokiyaraj, M Saravanan "Green synthesis of silver nanoparticles from leaf extract of Mimusops elengi, Linn. for enhanced antibacterial activity against multi drug resistant clinical isolates," Colloids Surf. B, , pp. 255-259 (2013).

18. Liqin Lin A B C D, Wenta Wang B C D, Jiale Huang B C D, Qingbiao Li A B C D, Daohua Sun B, Xin Yang B C D, Huixuan Wang B C D, Ning He B, Yuanpeng Wang B: Nature factory of silver nanowires: plant mediated synthesis using broth of Cassia fistula leaf," Chem. J., 16, pp. 852-858 (2010)

19. Ramana, M. V., Anuradha, G., Janaki Rama Rao, V. V., Anitha, P., & Lakshmi, P. S. Synthesis of Zinc Oxide Nanostructures Using Ocimum Gratissiumum Leaf Extract. In Proceedings of the UGC Sponsored Conference on ATOM-2014 (Advanced Technology Oriented Materials-, Rajahmundry, India pp. 8-9 (2104).

20. Zahir, A. A., & Rahuman, A. A. Evaluation of different extracts and synthesised silver nanoparticles from leaves of Euphorbia prostrata against Haemaphysalis bispinosa and Hippobosca maculata. Veterinary Parasitology, 187(3-4), , pp. 511-520 (2012).

21. R. S. V. Mishra, "Green synthesis of zinc oxide nanoparticles using fresh peels extract of Pumica granatum and its Antimicrobial activities," Int. J. Pharma. Res. Health Sci, 3,. pp 694-699 (2015).

22. M. Gomathi A, P.V. Rajkumar B, Prakasam A , K. Ravichandran B "Green synthesis of silver nanoparticles using Datura stramonium leaf extract and assessment of their antibacterial activity," Resour. Eff. Technol, no. 3, pp., pp. 280-284 (2017).

23. M. M. S. Jain, "Medicinal plant leaf extract and pure flavanoid mediated green synthesis of silver nanoparticles and their enhanced antibacterial property," Sci. Rep., no. 7, , pp. 1-13 (2017).

24. K. Y.-J. S. H. e. a. Singh P, "Biosynthesis of anistropic silver nanoparticles by Bhargavea indica and their synergistic effect with antibiotics against pathogenic microorganisms," J. Nanomater, pp. 4 (2015).

25. Hina Singh, Juan Du, Priyanka Singh, Tae Hoo Yi "Ecofriendly synthesis of silver and gold nanoparticles by Euphrasia officinalis leaf extract and its biomedical applications," Artif. Cells Nanomed. Biotechnol, no. 46 pp. 1163-1170 (2018).

26. Chao Wang , Yeon Ju Kim , Priyanka Singh , Ramya Mathiyalagan , Yan Jin , Deok Chun Yang "Green synthesis of silver nanoparticles by Bacillus methylotrophicus and their antimicrobial activity," Artif Cells Nanomed Biotechnol, pp. 1127-1132 (2015).

27. Yacaman, M. A.-T. Structure shape and

stability of nanometric sized particles. J. Vacuum Sci. Technol. B. Microelectron. Nanometer. Struct., , 1091-1103 (2001).

28. Burda, C. C.-S. Chemistry and properties of nanocrystals of different shapes. Chem. Rev., 1025-1102 (2005).

29. Sondi and B.S. Sondi, Silver nanoparticles as antimicrobial agent: a case study on *E. coli* as model for gram negative bacteria, J.colloid &interface science, 275,;177 -182 : (2004).

Current Trends in Biotechnology and Pharmacy
Vol. 18(2) 1688-1696, April 2024, ISSN 0973-8916 (Print), 2230-7303 (Online)
DOI: 10.5530/ctbp.2024.2.17


# Targeting Glucose Metabolism in Diabetes-A Homology Modeling and Active Site Identification for Inositol Monophosphatase

**Lavanya Gnanam[1] and Navaneetha Nambigari[1, 2*]**

[1]Department of Chemistry, University College of Science, Saifabad, Osmania University, Hyderabad - 500004, Telangana State, India.
[2]Department of Chemistry, University College of Science, Osmania University, Hyderabad - 500007, Telangana State, India.
[*]Corresponding author: navaneeta@osmania.ac.in

**Abstract**

Diabetes is a degenerative disease caused by either the body's inability to use insulin adequately or the pancreas's failure to release enough insulin. Diabetes is a glucose metabolic imbalance produced by the phosphodiesterase family of protein inositol monophosphatase (IMPase). Inositol monophosphatase, an enzyme involved in the phosphatidylinositol signalling pathway, is encoded by the IMPA1 gene.

Homology Modelling is used to create a 3D model of the IMPA1 protein (target). The FASTA sequence for the IMPase protein (265 amino acids) (Uniprot ID H0YBL1) is obtained from the Uniprot server. Jpred, and NCBI Blast servers are used to search for templates. Based on the query coverage (92%) and E-score, the protein with the PDB ID-1IMA is identified as a potential template. The structural alignment (by ClustalW) submitted to the SWISS-MODEL service yields a 3D model. The Swiss PDB viewer is used to minimise energy (E = - 10099.60 kcal/mole). Procheck, ERRAT, and the VERIFY 3D server validate the model.

The Ramachandran plot of the 3D model indicates that 93.5% of the amino acids are in the allowed region and none are in the forbidden region. The ERRAT result shows an overall quality factor of up to 96.17% for non-bonded atomic interactions. According to NCBI blast, the conserved domain is between 60 - 245 amino acids. The servers (ACTIVE SITE FINDER,) indicate binding pockets in the hydrophobic area, and Swiss dock is used to determine the active residues by protein - small ligand (Natural substrate, Fructose Biphosphatase- FBPase receptor ) docking to identify the active site residues (Asp 90 and Thr- 95) based on visualisations and a Swiss energy value. The glucose metabolism can be stopped by blocking these residues. Key Words: Diabetes, Phosphodiesterase family, Homology Modelling

## Introduction

Diabetes is the world's most serious health concern and the second biggest cause of mortality. Diabetes affects 537 million persons aged 20 to 79. Diabetes is expected to affect 643 million people by 2030 and 783 million by 2045. Three out of every four diabetic adults reside in low- and middle-income nations. Prevalence has been growing faster in low- and middle-income nations than in high-income countries. Diabetes and renal disease caused an estimated 2 million deaths in 2019 (1). In contrast, the likelihood of dying from any of the four major non-communicable illnesses (cardiovascular diseases, cancer, chronic respi-

ratory diseases, or diabetes) between the ages of 30 and 70 reduced by 22% globally.

Inositol monophosphatase 1 (IMPase) was shown to be significantly expressed in Triple Negative Breast Cancer (TNBC) tissues and to play carcinogenic functions via the mTOR pathway and the EMT process, making it an appealing method for boosting the treatment response of IMPA1-high TNBC tumours (3).

IMPase is necessary for dephosphorylating inositol monophosphates to produce inositol (4), which is a key metabolite as a precursor for producing phosphoinositide and hence has dramatic effects on gene expression and is essential for cell signalling and biological activities (5). Recent research has linked disruption of the inositol cycle to a number of human illnesses, including cancer, neurological disorders, and diabetes (6).

The Akt-mediated pathway is known to be involved in cell survival, growth, proliferation, angiogenesis, and glucose metabolism activation. It has been proven to be closely related to pulmonary hypertension(PAH) aetiology (7, 8). The proper synthesis or recycling of myo-inositol, the key precursor of all phosphatidylinositols, including phosphatidylinositol 3,4,5-trisphosphate (PIP3), which binds to Akt and recruits it to the plasma membrane, is required for this pathway to be activated. since a result, the molecular processes involved in myoinositol production or recycling are critical, since they may influence the shift into a highly proliferative phenotype.

Inositol monophosphatase 1 (IMPase) is a cytosolic enzyme that converts the highly osmotic glucose metabolite glucose 6-phosphate (G6P) to nonosmotic myo-inositol, therefore protecting cells from osmotic stress (9). Based on this feature, IMPA1 has been identified as a major contributor to the inositol cycle, including both de novo inositol synthesis and inositol polyphosphate recycling (10, 11). One of the most prominent features of PAH is metabolic reprogramming of the pulmonary vascular cells, which results in an increase in glucose absorption and metabolism.

**Materials and Methods**

The Homology modelling approach predicts the 3D structure of a protein as precisely as a low-resolution experimentally validated structure (12). The structural model of the target is created using sequence alignment and template structure (13). The protein's 3D structure is essential to understand its biology; comparative modelling approach. The amino acid sequence of the target protein (Uniprot ID: H0YBL1 _ HUMAN) is downloaded in FASTA format from the ExPASy Swiss-Prot (Expert protein analysis system) site (http://www.expasy.org).(14). Position -specific Iterative Basic Local Alignment Search Tool (PSI -BLAST) (15) Jpred (16) are used for template search. It is one of the most often used methodologies for protein structure prediction.

The pairwise alignment of the target protein, with the sequence of selected template is carried out with Clustal W tool which is a series of widely used computer programs used in Bioinformatics for multiple sequence alignment (17). The alignment file is used for model generation using the Swiss model (18). The protein structures are visualized and analyzed with SPDBV, which is an interactive molecular graphics program which analyzes several proteins at the same time (19). Clustal W is used to perform pairwise alignment of the target protein with the sequence of the selected template (17). The alignment file is used to generate models using the Swiss model (18). SPDBV, an interactive molecular graphics programme that analyses many proteins at the same time, is used to visualize and analyze the protein structures (19).

The refinement of the target protein's initial model is followed by energy minimization. SPDBV is used to minimize energy using a preset cutoff Root Mean Square Deviation (RMSD) of 0.3 A°. PROCHECK from the Structural Analysis and Verification Server (SAVES) validates

the model (20) predict the stereochemical quality of the resulting protein 3D model (21, 22). By measuring the dihedral angles phi and psi of the amino acid residues, the angle at the peptide bond is typically 180° because the partial double-bond feature preserves the peptide planar (23). ProSA server evaluates the quality of the local model (24).

### *Active Site Prediction*

Prediction of ligand-binding sites, a critical step in understanding a protein's molecular recognition mechanism and function. The putative active site was determined using the portion of the IMPase protein that binds to its receptor. The binding domain facilitates the interaction of IMPase with FBPase receptor proteins, resulting in the activation of a conserved pathway that governs critical elements of cell fate determination, migration, and polarity. The Active Site Finder server identifies the protein's active site area. The Protein Active Site Prediction service computes the cavities in a particular protein. The prediction of ligand-binding sites is a critical step in understanding a protein's molecular recognition mechanism and function (25). The identification of putative binding residues, active site prediction servers such as CASTp (26). The specific binding residues within the binding domain of the target protein.

## Results and Discussion

Using homology modelling, a 3D model of the IMPase protein was created. The IMPase protein amino acid sequence (UniprotKB ID: H0YBL1) was sent to template search server programmes such as NCBI BLAST and JPred to locate a suitable template sequence, and the results are shown in Table 1. Based on factors like as identity, sequence similarity, and E - value, the protein with the PDB ID - 1IMA is chosen as a template. 1IMA template protein shows a query coverage of is 92% and a sequence identity of 87.7% with the IMPase protein. As a consequence, the 1IMA protein is used as a template for creating the 3D model of the IMPase protein. ClustalW was used to perform pair-wise sequence alignment between the IMPase protein and the template protein 1IMA, as shown in Figure 1. The SWISS MODEL was used to construct the homology model once the alignment file and template coordinates were given.

Table 1: Tools for template Search.

| S.No. | Server | E- Score | Template (PDB) |
|---|---|---|---|
| 1. | NCBI | 4e-178 | 1IMA |
| 2. | JPred | 1e-135 | 1IMA |

Figure 1. Alignment of Target (HoYBL1) and template sequence using Clustal W.

Current Trends in Biotechnology and Pharmacy
Vol. 18(2) 1688-1696, April 2024, ISSN 0973-8916 (Print), 2230-7303 (Online)
DOI: 10.5530/ctbp.2024.2.17


The 3D model (*Figure 2*) was considered for further refinement and validation studies. Similar techniques were reported earlier for the identification of template and model building (27 - 29).

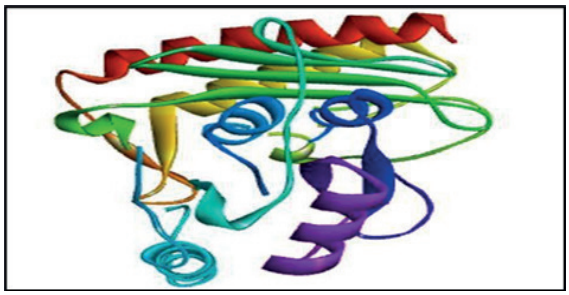

Figure 2: 3D model of IMPase protein.

The 3D model is further energy minimized using Swiss- PDB viewer (19) to assess the reliability of the generated 3D structure. The energies before and after energy minimization were –9476.8 kJ/mol and –10099.6 kJ/ mol respectively. The stereochemical quality of the protein structure was assessed by using Ramachandran plot (21) (*Figure 3*), which shows 202 (93.5%) of residues in the energetically most favored region, 13 (6%) of residues in the additionally allowed region, 1(0.5%) of the residues in the generously allowed region and none (0%) in the disallowed region. It can be seen that most of the amino acid residues are in the energetically favored region (Table 2). This shows that the protein was stereo chemically good which was generated after energy minimization.

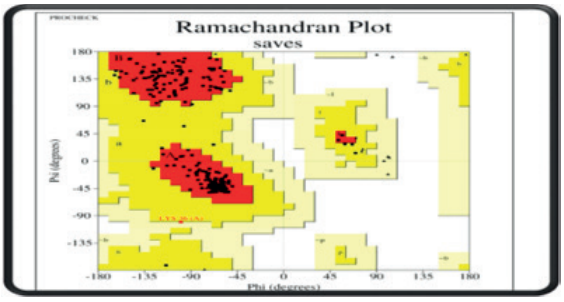


Figure 3. Ramachandran plot of the 3D protein.

Ramachandran plot obtained by Structural Analysis and Verification Server (SAVES). The red color in the plot indicates the most favorable region, yellow represents additionally allowed, light yellow indicates generously allowed and white field indicates disallowed region.

Table 2. Ramachandran plot statistics

| RESIDUES IN THE FOLLOWING REGION | NO.OF RESIDUES | PERCENTAGE |
|---|---|---|
| MOST FAVORED REGION[A,B,L] | 202 | 93.5% |
| ADDITIONAL ALLOWED REGION [a, b, l, p] | 13 | 6.0% |
| GENEROUSLY ALLOWED REGION[-a, -b, -l, -p] | 1 | 0.5% |
| DISALLOWED REGION | 0 | 0.0% |
| NO. OF NON- GLYCINE AND PROLINE RESIDUES | 216 | |
| NO. OF END RESIDUES (GLYCINE, PROLINE) | 14 | |
| NO. OF GLYCINE RESIDUES (SHOWN AS TRIANGLES) | 20 | |
| NO. OF PROLINE RESIDUES | 8 | |
| TOTAL NUMBER OF RESIDUES : 258 | | |

The Figure 4 depicts the Verify3D compatibility of the IMPase protein model (3D) with its own amino acid sequence (1D) (30, 31). The Verify3D server ascertained whether an atomic 1IMA model (3D) was compatible with its amino acid sequence (1D). For each of the 265 residues, the scores of a sliding 21-residue window (from –10 to +10) are added and plotted. The average 3D-1D score of 84.50 % of the residues is greater than 0.2.

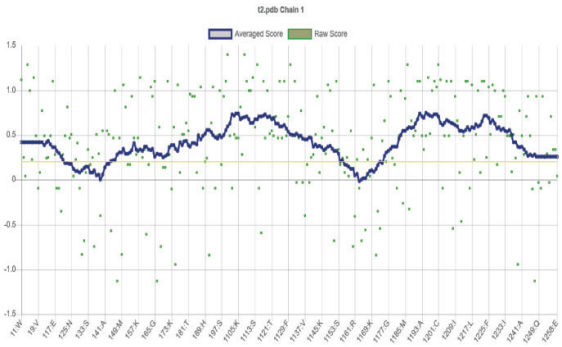


Figure 4. VERIFY 3D plot.

The validation of the selected protein after energy minimization is by PROCHECK and ProSA .The ProSA plot gives the local model quality (Figure 5) of the IMPase protein. The low

Z-score indicates a high overall model quality and compares the deviation of the ProSA server to calculate the energy required for protein folding architecture as a function of the amino acid sequence.

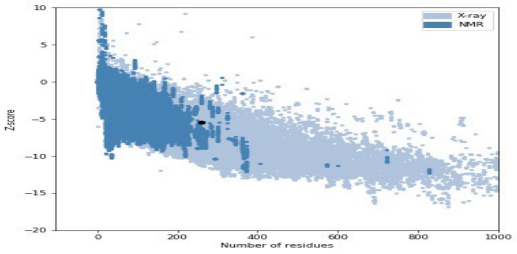


Figure 5. ProSA plot of IMPase. Black spot represents the 3D model falls in the NMR region with the Z- score= -5.42.

ProSA-Web Z-score determined by X-ray crystallography (light blue) and NMR spectroscopy for all proteins in the PDB (dark blue). The black spot in Figure 5 corresponds to the IMPase protein and has the Z-score value of –5.42.The low Z-score indicates good overall model quality and compares the structure's total energy deviation from an energy distribution derived from native conformations.

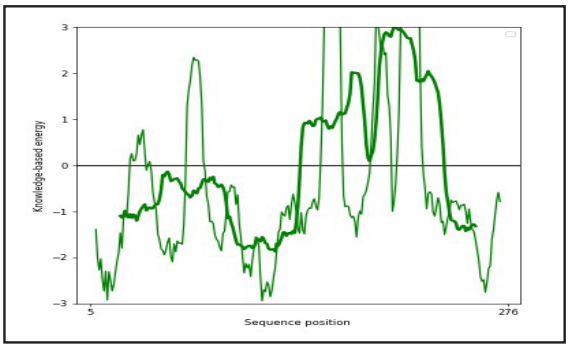


Figure 6. ProSA plot Energy Profile.

Overall, the folding energies of the protein residues are quite negative, with the model protein's folding energy in the range of native conformations having a Z-score of -5. 42. Figure 6 depicts the charting of energy as a function of amino acid sequence position. Positive values, in general, refer to problematic or incorrect sections of the input structure. The validation server tool findings indicate that the produced 3D structure of IMPase protein is stereo chemically and energetically stable. As a result, this protein is trustworthy for future research.

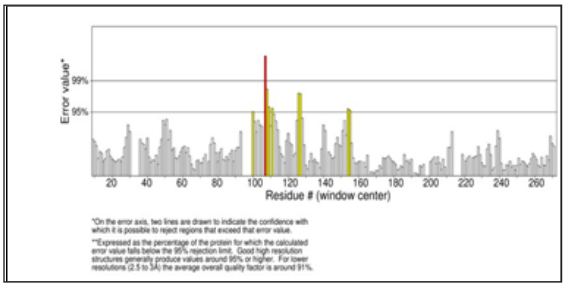


Figure 7. ERRAT Profile.

ERRAT is a program for verifying protein structures determined by crystallography. Error values are plotted as a function of the position of a sliding 9-residue window. The ERRAT Profile of the IMPase 3D model shows an overall quality factor of 96.17, against an average qulity factor 91% for a resolution of 2.5 – 3.0Å (32). The result of the ERRAT server shows a graph between residues and error values (Figure.7). The overall quality score of this input structure is 96.17% and this is considered good. If the input structure has good resolution, then it should have a quality score of greater than 95%.

IMPase has three hydrophilic hollow active sites, each of which bind water and magnesium molecules. The 3D Structure of the IMPase protein generated by homology modeling is presented in Figure 3. The detailed secondary structure of the protein is shown in Figure 8. The structure constitutes 9 Helices, 17 loops, 14 β sheets.

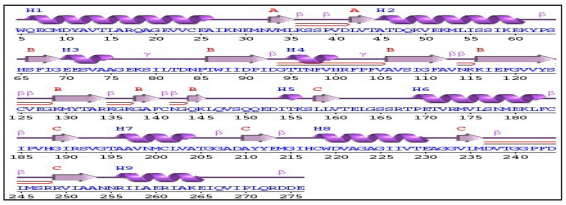

Figure 8. Secondary Structure of IMPase protein.

Current Trends in Biotechnology and Pharmacy
Vol. 18(2) 1688-1696, April 2024, ISSN 0973-8916 (Print), 2230-7303 (Online)
DOI: 10.5530/ctbp.2024.2.17


The secondary structure details along with the amino acid chain lengths are shown in Table 3. The topology of the target protein is shown in Figure 9. The topological analysis reveals that the N terminal region (Trp 5) and C terminal terminal region (Ile 266).

Table 3. Secondary structure Of IMPase protein

| HELICES | LOOPS | BETA SHEETS |
|---|---|---|
| Q 6 - A 26 | 5W | V 33 – L 35 |
| A 45 – K 61 | Y 62 – H 64 | L42 – T 44 |
| E 70 – A 75 | G 76 – P 85 | S 66 – G 69 |
| T 95 – H 100 | V 113 – K 115 | T 86 – I 92 |
| I 154 – K 156 | C 125 – G 128 | A 106 – A 112 |
| P 169- F 183 | K 135 – K 137 | K 116 – S 124 |
| A 196 – A 204 | C 141 – G 143 | K 129 – R 134 |
| C 218 – E 230 | L 146 – D 153 | G 138 – F 140 |
| R 256 – E 265 | S 153 | Q 144 – K 145 |
| | T 161 – T 168 | L 158- V 160 |
| | C 184 – H 188 | G 188- R 191 |
| | S 192 – T 195 | A 210 – E 213 |
| | T 205 – D 209 | V 234 – M 236 |
| | M 214- H 217 | R 249 A 253 |
| | A 231 – G 233 | |
| | D 237 – R 248 | |
| | N 254 – N255 | |

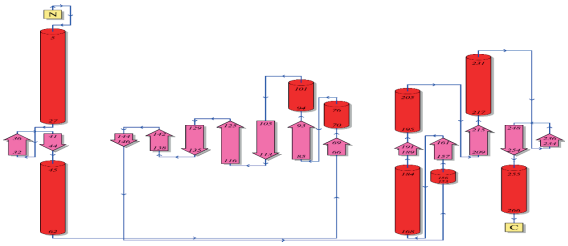

Figure 9. Topology of the amino acid residues

The conserved domains of the IMPase protein are characterized using the NCBI BLAST tool, as illustrated in Figure 10; NCBI blast also identified the binding site domains of the IMPase protein. The results demonstrate that the target protein includes a FIG domain (Amino Acid 28 – 264) from Insilico predictions of protein interactions utilising protein-ligand docking studies enable the discovery of major residue-residue contacts involving target interactions. IMPase protein binding site residues and cavity volumes were predicted using Active Site Finder based on hydrophobicity. SWISS dock server was used to perform protein-natural ligand docking between IMPase and FBPase proteins.

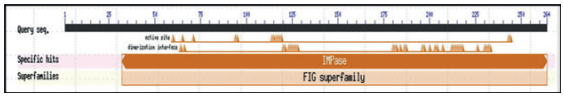


Figure 10. Conserved domain of IMPase protein. The domain shows FIG Superfamily.

The Active site Finder analysis shows a binding cavity which possess the following residues: 70, 90, 92- 95, 194- 196, 213, 220. The least energy value was selected to identify the specific binding site residues of the IMPase protein that interact with its natural receptor FBPase. The binding modes in the protein – receptor complex were analyzed using Discovery Studio Visualizer 3.5. The protein- small ligand binding interactions in the docked complex are presented in Figure 11.

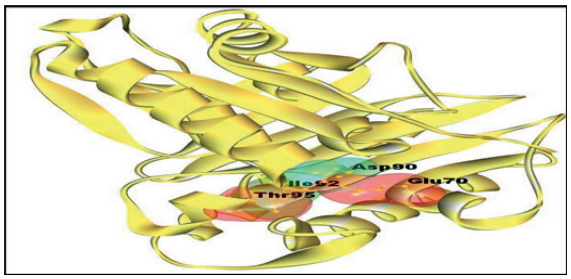


Figure 11. Interaction showing Protein- Small ligand Docking.

Table 4. Active site residues.

| RESIDUES | INTERNUCLEAR DISTANCE |
|---|---|
| GLU 70 | 2.50 A° |
| ASP 90 | 2.38 A° & 2.95 A° |
| ILE 92 | 2.49 A° |
| THR 95 | 2.85 A° |

The table 4 show the binding interactions of the target protein with its natural substrate (FBPse) are GLU 70, ASP 90, ILE 92, THR 95. The above residues participate in binding to FBPase protein.

## Conclusion

The homology modeling method provided a reliable structure of IMPase for further investigation. The 3D structure of the IMPase protein generated using 1IMA as a template is comparable to the X-ray resolved protein structure with 93.5% in favorable region in Ramachandran plot, an average 3D-1D score of 84.50

% of the residues is greater than 0.2 (Verify 3D), Z- Score of –5.42 comparable to X – Ray resolved structure (ProSA Server) and 96.17% score in ERRAT infers a reliable model for further research. The secondary structure analysis reveals the 9 Helices, 17 loops, 14 β sheets. Protein-ligand docking of IMPase with its natural receptor confirmed the binding residues in the active site region. The docking studies conclude that GLU 70, ASP 90, ILE 92, THR 95 of IMPase are involved in the binding of protein to receptor signals. Thus, by blocking these residue binding sites, protein regulates glucose metabolism thereby diabetes can be controlled.

**Acknowledgements**

The author GL and NNT is thankful to The Head, Department of Chemistry and the Principal, University College of Science, Saifabad, Osmania University, Hyderabad and DST FIST, New Delhi for the facilities to carry out this work.

**Author Declarations**

**Funding**

No financial support from any agency.

**Conflict of Interest**

The corresponding author states that there is no conflict of interest.

**Ethics approval/declarations (include appropriate approvals or waivers)**

Not Applicable.

**Availability of Data and material / Data availability**

All data generated or analyzed during this study are included in this published article (and its supplementary information files).

**Consent to participate**

Not applicable

**Code availability (software application or custom code)** -

Not applicable.

**References**

1. Diabetes mellitus, fasting blood glucose concentration, and risk of vascular disease: a collaborative meta-analysis of 102 prospective studies. Emerging Risk Factors Collaboration. Sarwar N, Gao P, Seshasai SR, Gobin R, Kaptoge S, Di Angelantonio et al. Lancet. 2010; 26; 375:2215-2222.

2. Causes of blindness and vision impairment in 2020 and trends over 30 years, and prevalence of avoidable blindness in relation to VISION 2020: the Right to Sight: an analysis for the Global Burden of Disease Study GBD 2019 Blindness and Vision Impairment Collaborators* on behalf of the Vision Loss Expert Group of the Global Burden of Disease Study† Lancet Global Health 2021;9: e141-e160.

3. Ying Yang, Yi- Fan Xie, Tai- Mei Zhang, Ling Deng, Li Liao, Shu-Yuan Hu, Yin-Ling Zhang, Fang- Lin Zhang, Da- Qiang. Inositol monophosphatase 1 (IMPA1) promotes triple- negative breast cancer progression through regulating mTOR pathway and EMT process. Cancer Med. 2023; 12:1602-1615. doi: 10.1002/cam4.4970

4. Andreassi C, Luisier R, Crerar H, et al. Cytoplasmic cleavage of IMPA1 3' UTR is necessary for maintaining axon integrity. Cell Rep. 2021;34(8):108778.

5. 9. Pillai RA, Islam MO, Selvam P, et al. Placental Inositol Reduced in Gestational Diabetes as Glucose Alters Inositol Transporters and IMPA1 Enzyme Expression. J Clin Endocrinol Metab. 2021;106(2):e875- e890.

6. 10. Hakim S, Bertucci MC, Conduit SE, Vuong DL, Mitch-

ell CA. Inositol polyphosphate phosphatases in human disease. Curr Top Microbiol Immunol. 2012; 362:247- 314.

7. Garat CV, Crossno JT Jr, Sullivan TM, Reusch JE, Klemm DJ. Inhibition of phosphatidylinositol 3-kinase/Akt signaling attenuates hypoxia-induced pulmonary artery remodeling and suppresses CREB depletion in arterial smooth muscle cells. J Cardiovasc Pharmacol 62: 539 – 548, 2013. doi:10.1097/FJC.0000000000000014.

8. Tang H, Chen J, Fraidenburg DR, Song S, Sysol JR, Drennan AR, Offermanns S, Ye RD, Bonini MG, Minshall RD, Garcia JG, Machado RF, Makino A, Yuan JX. Deficiency of Akt1, but not Akt2, attenuates the development of pulmonary hypertension. Am J Physiol Lung Cell Mol Physiol 308: L208–L220, 2015. doi:10.1152/ajplung.00242.2014.

9. Gardell AM, Yang J, Sacchi R, Fangue NA, Hammock BD, Kültz D. Tilapia (Oreochromis mossambicus) brain cells respond to hyperosmotic challenge by inducing myo-inositol biosynthesis. J Exp Biol 216: 4615– 4625, 2013. doi:10.1242/jeb.088906.

10. Figueiredo T, Melo US, Pessoa AL, Nobrega PR, Kitajima JP, Rusch H, Vaz F, Lucato LT, Zatz M, Kok F, Santos S. A homozygous loss-of-function mutation in inositol monophosphatase 1 (IMPA1) causes severe intellectual disability. Mol Psychiatry 21: 1125–1129, 2016. doi: 10.1038/mp.2015.150.

11. Bone R, Frank L, Springer JP, Pollack SJ, Osborne SA, Atack JR, Knowles MR, McAllister G, Ragan CI, Broughton HB, et al. Structural analysis of inositol monophosphatase complexes with substrates. Biochemistry. 1994 Aug 16;33(32):9460-7. doi: 10.1021/bi00198a011. PMID: 8068620.

12. Chothia, C.; Lesk, A. M. The Relation between the Divergence of Sequence and Structure in Proteins. EMBO J. 1986, 5 (4). https://doi.org/10.1002/j.1460-2075.1986.tb04288.x.

13. Martí-Renom, M. A.; Stuart, A. C.; Fiser, A.; Sánchez, R.; Melo, F.; Šali, A. Comparative Protein Structure Modeling of Genes and Genomes. Annu. Rev. Biophys. Biomol. Struct. 2000, 29 (1). https://doi.org/10.1146/annurev.biophys.29.1.291.

14. Altschul S. Gapped BLAST and PSI-BLAST: A New Generation of Protein Database Search Programs. Nucleic Acids Res. 1997. V. 25. No. 17. P. 3389–3402. doi: 10.1093/nar/25.17.3389

15. Altschul S. Gapped BLAST and PSI-BLAST: A New Generation of Protein Database Search Programs. Nucleic Acids Res. 1997. V. 25. No. 17. P. 3389–3402. doi: 10.1093/nar/25.17.3389

16. A protein secondary structure prediction server. Alexey Drozdetskiy Christian Cole James Procter Geoffrey J. Barton. Nucleic acids research (2015) 43: W1, w389-w394.

17. Improving the sensitivity of progressive multiple sequence alignment through sequence weighting, position specific gap penalties and weight matrix choice. Nucleic Acids res, Thompson JD, Gibson TJ, CLUSTAL W, (1994), 22:4673- 4680.

18. Guex, N.; Peitsch, M. C. SWISS-MODEL and the Swiss-Pdb Viewer: An Environment for Comparative Protein Modeling. Electrophoresis 1997, 18 (15). https://doi.org/10.1002/elps.1150181505.

19. Guex N., Peitsch M.C. SWISS-MODEL and the Swiss-Pdb Viewer: An Environment for Comparative Protein Modeling. Electrophoresis. 1997. V. 18. No. 15. P. 2714–2723. doi: 10.1002/elps.1150181505

20. PROCHECK: a program to check the stereo chemical quality of protein structure. Laskowsky RA, MacArthur MW, Moss DS, Thornton JM (1993), J Appl Crystallography 26: 283- 291.

21. Stereochemical quality of protein structure coordinates. Morris AL, MacArthur Mw, Hutchinson EG, Thornton JM, Proteins (1992), 12:345-364.

22. Stereochemistry of polypeptide chain configurations. Ramachandran GN, Ramakrishnan C, Sasisekharan V, J Mol Biol, (1963), 7:95-99.

23. Half a century of Ramachandran plots, Oliviero Carugo , Kristina Djinovic-Carugo, Acta Crystallographic Section D,2013, 69(8) : 1333-1341.

24. ProSA- web: interactive web service for the recognition of errors in the three – dimensional structure of proteins. Wiederstein M, Sippl MJ, Nucleic Acids res (2007), 35: w407- w410.

25. Laurie AT, J. R. Methods for the Prediction of Protein-Ligand Binding Sites for Structure-Based Drug Design and Virtual Ligand Screening. Curr Protein Pept Sci 2006, 7, 395–406. https://doi.org/10.2174/138920306778559386.

26. Dundas, J.; Ouyang, Z.; Tseng, J.; Binkowski, A.; Turpaz, Y.; Liang, J. CASTp: Computed Atlas of Surface Topography of Proteins with Structural and Topographical Mapping of Functionally Annotated Residues. Nucleic Acids Res. 2006, 34 (Web Server). https://doi.org/10.1093/nar/gkl282.

27. Navaneetha Nambigari*. 2023 Cancer therapeutics: A Structure-based drug design of inhibitors for a novel angiogenic growth factor. Math. Biol. Bioinform. 18(1): 72-88. http://doi.org/10.17537/2023.18.72 (IF = 0.687)

28. Jyothi Bandi, Vasavi Malkhed*and Navaneetha Nambigari*. 2022. An Insilico study of KLK - 14 protein and its inhibition with Curcumin and its derivatives. Chemical Papers. 76, 4955–496. http://doi.org/10.1007/s11696-022-02209-w (IF- 2.097).

29. Navaneetha Nambigari, Kiran Kumar Mustyala, Vasavi Malkhed, Bhargavi Kondagari, Sarita Rajender Potlapally, Ramasree Dulapalli, & Uma Vurupturi*. Angiogenesis: an insilico approach to angiogenic phenotype. Journal of Pharmacy Research. 5 (1): 583 - 588 (2012).

30. Recognition of errors in three-dimensional structures of proteins. Dr. Manfred J. Sippl. December 1993.Proteins 17, 355-362.

31. Lüthy, R., Bowie, J. & Eisenberg, D. Assessment of protein models with three-dimensional profiles. Nature 356, 83–85 (1992). https://doi.org/10.1038/356083a0

32. Colovos C, Yeates TO. Verification of protein structures: patterns of nonbonded atomic interactions. Protein Sci. 1993 Sep;2(9):1511-9. doi: 10.1002/pro.5560020916. PMID: 8401235; PMCID: PMC2142462.

Current Trends in Biotechnology and Pharmacy
Vol. 18(2) 1697-1704, April 2024, ISSN 0973-8916 (Print), 2230-7303 (Online)
DOI: 10.5530/ctbp.2024.2.18



# Phytochemical, Toxicological, and Anti-Hyperglycemic Evaluation of *Pennisetum purpureum* in Sprague-Dawley Rats

**Rahul Deo Yadav*[1,2], Himanshu Pandey[3], Man Singh[1,2], Shanti Bhushan Mishra[4], Shradhanjali Singh[4], Danish Ahmed[2]**

[1]Department of Pharmacy, MLN Medical College, Prayagraj 211001, India
[2]Department of Pharmaceutical Sciences, Sam Higginbottom University of Agriculture, Technology and Sciences, Prayagraj 211008, India
[3]Centre for Teacher Education, Central Institute of Higher Tibetan Studies, Sarnath, Varanasi, 221007, India
[4]United Institute of Pharmacy, Prayagraj 211010, India
*Corresponding Author: rahulyadav246@gmail.com

## Abstract

Many herbal extracts have been used for preventing and managing diabetes. In recent times it was documented that the herbal extracts in traditional Indian medicine are clinically effective in treating sugar imbalances associated with diabetes mellitus. Although it was considered that several bioactivities and phytochemicals have been attributed and it confirmed in terms of their toxicological profile and anti-diabetic activity. Herbal formulation and extract of the plant part of elephant grass plays an important role for the treatment of various diseases and disorders such as inflammation, pain, ulcer, cancer, bacterial infections, and fungal infections. Ethanolic extract of *Pennisetum purpureum* which was prepared by using 50%v/v and their fractions were prepared by using liquid-liquid extraction technique. There was quantitative estimation of gallic acid analyzed by HPTLC technique. The extract has been found safe at high dose through oral acute toxicity study. Antihyperglycemic activity was performed on Sprague-Dawley rats by inducing the diabetes through Streptozotocin. Gallic acid was quantitatively estimated in methanolic fraction of extract and was found to be 0.13%w/w. Extract showed positive response in the treatment of diabetes which was confirmed after performing histopathology of liver and pancreas. Finally in this study, it was found that *P. purpureum* showed no toxicity and ameliorative changes in the blood glucose level, antioxidant level and biochemical parameters viz. triglycerides, total cholesterol, high density lipoprotein, low density lipoprotein and very low-density lipoprotein.

**Keyword:** *Pennisetum purpureum*, Diabetes mellitus, Antihyperglycemic, Biochemical, Acute toxicity, Histopathology

## Introduction

The long-term complications of ineffectively or untreated diabetes include nephropathy, retinopathy, and peripheral neuropathy. This metabolic disorder is exemplified by symptomatic intolerance of glucose as well as fluctuations in protein and lipid metabolism. Moreover, diabetic patients have an increased risk of stroke and cardiovascular disease (1)**.** Hence, there is a strong need for effective and safe oral antihyperglycemic agents that offer the physician a broader range of options to prevent treat and manage diabetes. Many herbal extracts or derivatives have been documented in traditional

Indian medicine (TIM) to be clinically effective in treating sugar imbalances associated with diabetes mellitus.

*Pennisetum purpureum* (Elephant grass, family Poaceae) is important silage in the tropical and subtropical region. The young shoots and leaves are eaten by humans and can be cooked to prepare stews and soups (2). Leaf and stem infusions are used for its diuretic properties. The plant possesses several pharmacological activities including antifungal activity, antimicrobial activity (3), antioxidant activity, cytotoxic activity, anti-inflammatory activity (4), antiulcer activity (5), analgesic activity, and antimalarial activity (6).

Phytochemical analysis of *P. purpureum* revealed the presence of alkaloids, cyanogenic glycosides, flavonoids, oxalates, phytates, saponins, and tannins. Some bioactive phytochemicals have been isolated from *P. purpureum* methanolic extract includes dihydrocapsaicin, ethyl iso-allocholate, 2-hydroxy-4-methoxybenzaldehyde , 1,2-benzenediol , ergost-5-en-3-ol, stigmast-5-en-3β-ol, 1,2-Dihydroxybenzene, Ethyl iso-allocholate, 4-Hydroxy-3,5,5-trimethyl-4-(3-oxo-1–1-butenyl)−2cyclohexen-1-one, 5-Butylpyridine-2-carboxylic acid, 2,3-Di-O-phenylboranediyl-alpha-D-mannofuranose, 2-Hydroxy-4-methoxybenzaldehyde, 2,4a,5,8a-Tetramethyl-1,2,3,4,4a,7,8,8aoctahydronaphthalen-1-ol, Chlolest-4-en-3-one, Ergosta-4,22–dien-3-one, Stigmast-4-en-3-one, Cholest-4-ene-3,6–dione, N-methyl-adamantane acetamide, 3,5-Bis(1,1-dimethylethyl)−4-hydroxy-2–4cyclohexadien-1-one, and 4-Hydroxy-3,5,5-trimethyl-4-(3-oxo-1–1-butenyl)−2cyclohexen-1-one (7). Although several bioactivities and phytochemicals have been attributed to this plant in the literature, none of them have been confirmed in terms of their toxicological profile and anti-diabetic activity. Therefore, the study aims to justify the use of this plant as an anti-diabetic agent through preclinical study.

## Materials and Method

### Material

The plant was collected and authenticated in the Botanical Survey of India, Prayagraj and the voucher specimen number BSI/CRC/2021-22/448 was submitted in the department. The ethanolic extract of *P. Purpureum* was prepared by using 50%v/v ethanol at $55^0$ C by hot percolation method.

### *Preparation of sample*

Four fractions were prepared by using liquid-liquid extraction technique considering 100gm of extract in each solvent viz. chloroform, ethyl acetate, methanol and water.

### *Phytochemical screening and TLC*

The plant extract was qualitatively analyzed by TLC using Toluene: ethyl acetate: formic acid: methanol (6:1.5:1.5:1v/v/v/v). PPEE showed (03) spots at 365nm whereas PPMF showed (04) spots at 254nm. Further, PPEE and PPMF were subjected to preliminary phytochemical screening for the identification of various constituents by using standard procedures (8).

### *Quantitative estimation of gallic acid in methanolic fraction*

The standard solution of gallic acid was prepared by mixing 5mg gallic acid in 20 ml methanol.10 µl of the solution was spotted on HPTLC plate and developed at 365nm. 100mg of methanolic fraction was mixed with 5ml methanol. 10 µl of the solution was spotted on HPTLC plate and developed at 365nm using mobile phase Toluene: ethyl acetate: formic acid: methanol (6:1.5:1.5:1v/v/v/v).

### *Animals*

Sprague-Dawley rats, both sexes weighing 190-220 g, were used in the study. All animals were fed with standard pellet diet and water *ad libitum* throughout the study. The research protocol was approved by IAEC of Unit-

ed Institute of Pharmacy, Prayagraj with approval number UIP/IAEC/March-2023/19.

### *Acute oral toxicity*

The procedure for study was followed as per OECD 423 guidelines (9). A single dose of the extract (300 mg/kg, 2000 mg/kg and 5000 mg/kg body weight) was given orally to all animals (three each) and monitored continuously for any adverse effects till 14 days.

### *Induction of diabetes in experimental animals*

The rats were fasted for overnight but were allowed water *ad libitum*. Diabetes was induced in rats by intraperitoneal injection of STZ (60 mg/kg body weight) except group - Ist (10).. After two days of STZ administration, rats with blood glucose level more than 220mg/dl were considered diabetic and used in the study.

### *Design of experiment*

The experimental rats were divided into seven groups (n=6). Group 1 represents normal group receives saline orally. Group 2 represents diabetic control group received saline only. Group 3 represents standard drug metformin (100mg/kg) treated diabetic rats. Group 4 and group 5 received plant extract (PPEE) (100mg/kg b.w and 200g/kg b.w) respectively while group 6 and group 7 received methanolic fraction (PPMF) (100mg/kg b.w and 200g/kg b.w) respectively. The oral administration of saline, extract, and fractions was carried out for a duration of three weeks using an oral gavage tube on a daily basis. Blood samples were collected from the retro orbital puncture on Day 0, Day 7, Day 14, and Day 21 to measure the blood glucose level. The glucometer (SugarScan Thyrocare Technologies Limited, Mumbai, India) was used to determine the blood glucose level. The values of the treated groups were compared to those of the standard group, which was treated with Metformin. The animals were euthanized by intraperitoneal administration of high dose of thiopentone sodium and the liver, kidney, and pancreas were exposed and perfused with cold saline phosphate buffer (pH 7.4) for histopathological examination.

### *Biochemical parameters*

Parameters including total cholesterol, Triglyceride, HDL, LDL, VLDL were assessed in all groups by using diagnostic kits (Erba Mannheim, Mumbai, India).

### *In vivo antioxidant activity in diabetic rats*

Superoxide dismutase (SOD), Catalase (CAT), reduced glutathione (GSH), glutathione peroxidase (GPx) were estimated as per previously reported method (11).

### *Histopathology*

Histopathology analysis was performed as per previously reported standard method (12). The histopathological slides were examined and photographs were captured with a digital stereomicroscope (Olympus, B061, USA).

### *Statistical Analysis*

The statistical analysis of all pharmacological analysis was performed using software Graph Pad prism version 9.1.2 using Two-way ANOVA through Newman-keuls test. The values are represented as mean ± S.D. (n=6)

## Results

### *Preliminary phytochemical screening*

Phytochemical screening of PPEE ensure the presence of bioactives viz. alkaloids, phenolic compounds, steroids, flavonoids, tannins whereas PPMF shows presence of Tannic acid, Phenolic compounds, steroids, flavonoids, alkaloids, amino acids and proteins.

### *HPTLC fingerprinting analysis*

The qualitative HPTLC fingerprint analysis of PPEE was carried considering mobile phase as Toluene: ethyl acetate: formic acid: methanol (6:1.5:1.5:1v/v/v/v). The four spots at different rf value viz. 0.23 (39.95%), 0.43

(17.11%), 0.56 (36.59%), and 0.61 (6.35%) were obtained as shown in figure 1. The amount of gallic acid in PPMF by quantitative HPTLC method was found to be 0.13 %w/w.

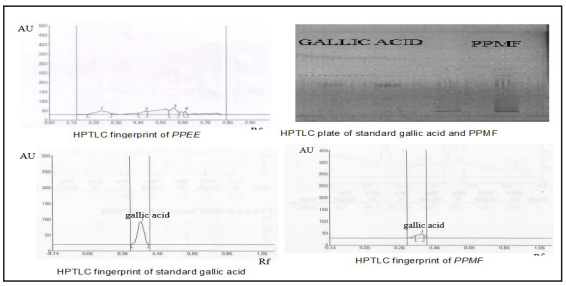


Figure 1: HPTLC finger printing analysis of PPEE, PPMF and standard Gallic acid

### *Acute oral toxicity*

The extract (PPEE) didn't show any mortality even at higher dose 5000 mg/kg b.w and found completely safe. Therefore, for further pharmacological study, two doses 100 and 200 mg/kg body weight have been selected.

### *Antihyperglycemic activity*

By the end of treatment, A decline in blood glucose value was seen in PPMF treated rats (100mg/kg and 200mg/kg) as (224.21± 2.75-122.78±1.25) and (224.21±2.75 – 108.33±4.03) ($p<0.001$) respectively; in PPEE treated rats (100mg/kg) & (200mg/kg) as (224.21±2.75 – 141.66±3.01) & (224.21±2.75 – 137.85±7.02) ($p<0.001$) respectively; whereas metformin reduces blood glucose value (224.21±2.75 to 102.33±3.07) ($p<0.001$). The results were moderately significant shown in figure 2.

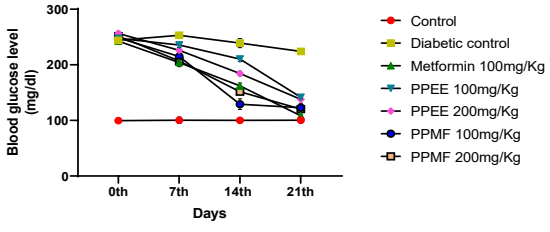


Figure 2: Antihyperglycemic effect of PPEE and PPMF

### *Effect of PPEE and PPMF on lipid profile*

Figure 3 revealed that on oral administration of PPEE (100 mg/kg) showed the significant amelioration in biochemical parameters as compared to diabetic group viz. TG (102.16 ± 4.16; $p<0.01$), TCh (120.66 ±2.58) HDL (20.66 ± 2.56), LDL (50.45±4.87) and VLDL (25.33 ±2.16) levels in diabetic rats. While in case of PPEE 200mg/kg treated animals, shows remarkable improvement in lipid profile as TG (96.45±6.23), TCh (106.85±8.54) HDL (20.25±6.80), LDL (48.5 ±3.67) and VLDL (23.87±3.21) levels in diabetic rats. Oral administration of methanolic fraction PPMF 100 mg/kg reveals diminution in TG level (81.99±8.25; $p<0.001$), Tch (89.25±9.22; $p<0.001$), LDL (46.98 ±2.85), and VLDL (21.96±3.41) in diabetic animals whereas enhancement in the level of HDL (21.45±6.23; $p<0.001$).

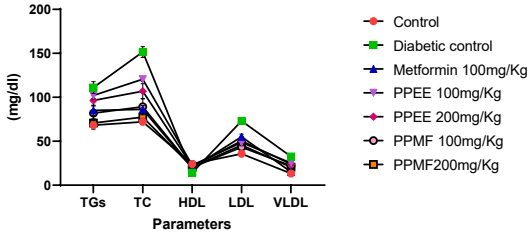


Figure 3: Effect of PPEE and PPMF on biochemical parameters

### *Effect of PPEE and PPMF on antioxidant parameters*

Table 1 shows significant reductions in GSH, GPx, SOD, and catalase enzymes in the diabetic control rats as compared to normal control rats. After 21 days treatment with 200 mg/kg of PPEE and PPMF, there is significant increase in GSH, GPx and CAT level in liver viz. 74.23 to 98.12 and 74.23 to 109.42; 5.42 to 6.48 and 5.42 to 8.62; and 31.45 to 47.32 and 31.45 to 78.2 respectively ($p<0.001$). From the results, it confirms that oral administration of PPEE and PPMF ameliorates oxidative stress in diabetic experimental animals.

Table 1: Effect of extract and fraction on antioxidant enzyme activities in STZ diabetic rats

| Parameters | Normal control | Diabetic control | Metformin 100mg/kg | PPEE 100mg/ kg | PPEE 200mg/ kg | PPMF 100 mg/kg | PPMF 200 mg/kg |
|---|---|---|---|---|---|---|---|
| | GSH (mM of DTNB conjugated/ mg protein) | | | | | | |
| Liver | 129.67 ± 2.6 | 74.23 ± 1.5 $^{z}$ | 124.78± 2.4$^{c}$ | 82.46± 2.2$^{a}$ | 98.12± 3.3$^{c}$ | 102.42± 3.6$^{c}$ | 109.42± 2.36$^{c}$ |
| Kidney | 118.77 ± 2.3 | 46.17 ± 2.4$^{z}$ | 88.18 ± 3.45 | 62.15± 3.5 | 69.38± 2.7 | 78.84± 5.34$^{c}$ | 92.84 ± 2.54 |
| | GPx (mg glutathione consumed/ min/ mg protein) | | | | | | |
| Liver | 9.46 ± 0.91 | 5.42 ± 0.88 $^{z}$ | 7.10 ± 0.21$^{b}$ | 5.87± 0.76$^{b}$ | 6.48± 0.44$^{c}$ | 7.85± 0.62$^{c}$ | 8.62± 0.95$^{c}$ |
| Kidney | 7.36 ± 0.14 | 4.98 ± 1.01$^{y}$ | 6.58 ± 0.25$^{a}$ | 5.18± 0.14$^{a}$ | 5.90± 0.26$^{c}$ | 6.89± 0.48$^{c}$ | 7.38± 0.6$^{4}$c |
| | CAT (mmol of $H_2O_2$ consumed/ min/ mg protein) | | | | | | |
| Liver | 71.25 ± 2.17 | 31.45± 1.71$^{z}$ | 83.5 ± 0.97$^{c}$ | 44.32± 2.5$^{b}$ | 47.32± 3.1$^{b}$ | 63.7± 0.97$^{c}$ | 78.2 ± 0.97$^{c}$ |
| Kidney | 38.33 ± 1.22 | 52.01± 1.58$^{z}$ | 28.8± 1.29$^{c}$ | 21.26± 1.0$^{a}$ | 21.56± 1.2$^{a}$ | 22.46± 1.5$^{c}$ | 25.7± 1.49$^{c}$ |
| | SOD (U/ min/ mg/ Hb) | | | | | | |
| Erythrocytes | 6.35 ± 0.17 | 3.45 ± 0.28 $^{z}$ | 4.29± 0.24$^{b}$ | 5.98± 0.66$^{b}$ | 5.42± 0.40$^{c}$ | 6.1 ±0.70$^{b}$ | 6.78 ±0.83$^{c}$ |

The values represent the means ± S. D. for six rats per group. $^{a}$p<0.05, $^{b}$p<0.01, $^{c}$p<0.001 compared to diabetic group. $^{z}$p<0.001 compared to normal group. SOD: superoxide dismutase; GSH: Glutathione; GPx: glutathione peroxidase; CAT: Catalase

### *Histopathological investigation*

#### Liver

Normal hepatic cells were observed in group (4a). In group II (4b) diabetic rats, shows degeneration and inflammatory infiltrate. In group III (4c), the hepatocytes portal tracts and central veins come out to be normal. In group IV (4d) lessened degeneration and necrosis is visible. In group V (4e) inflammatory infiltrate and degeneration of cells is seen. In group VI (4f) and VII (4g) normal architecture of liver cells are regained.

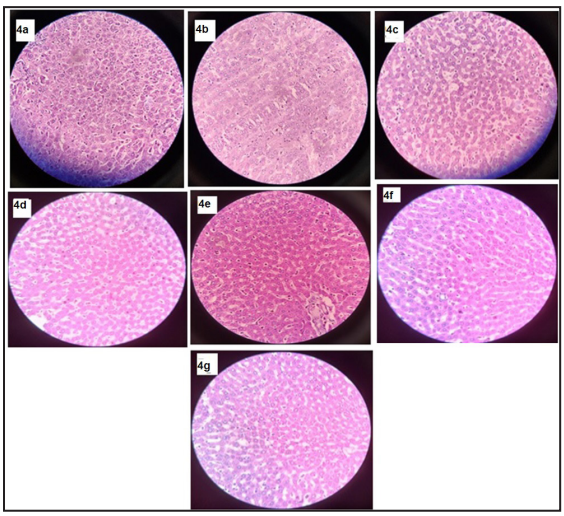


Figure 4: Histopathology of liver

#### Pancreas

Normal acini, cells and normal cellular islets of Langerhans were observed in group (5a). In group 2 (5b) vacuoles and wider intralobular duct is observed. In metformin group (5c) restoration of normal structure were observed. In group IV (5d) and group V (5e) reduction of vacuoles and thinning of intralobular duct were

observed. Group VI (5f) and group VII (5g) were observed with normal cells and architecture.

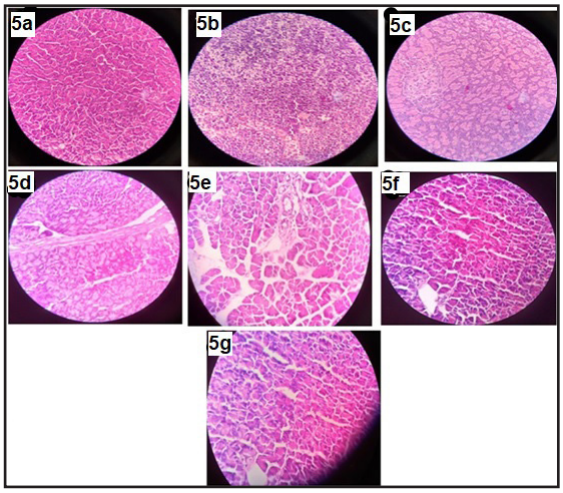


Figure 5: Histopathology of pancreas

## Discussion

The traditional use of *Pennisetum purpureum* for its antidiabetic properties prompted the current study. Streptozotocin-induced diabetes was used as a model in Sprague-Dawley rats, which partially damages beta cells and produces type 2 diabetes. The anti-hyperglycemic potential of PPEE and PPMF was investigated in which we observed reduction in elevated blood glucose concentration that might be due to the presence of Gallic acid in extract and fraction. Gallic acid was found to upregulate pAkt, PPAR-γ, and Glut4 that facilitate insulin sensitivity and glucose homeostasis; (13) moreover, the antidiabetic effects of Gallic acid could be mediated via regulation of TNF-α and adipocytokines expression. Gallic acid also improved the function of the β cells by inhibiting caspase-9-related cellular apoptosis (14). Acute toxicity studies showed that PPEE was safe even at higher dose 5000 mg/kg b.w. The test group exhibited a significant decline ($p \leq 0.001$) in serum glucose, serum total cholesterol, and serum triglycerides levels compared to the control group. Free radical generation and antioxidant resistance damage can lead to the oxidation of glucose, glycation of protein, and oxidative degradation of protein glycation. After intake of streptozotocin, oxidative stress increased due to a compromise in the antioxidant system in the diabetic condition (15). Herbal and edible plant that having this polyphenolic compound (Gallic acid) modulated different antidiabetic signaling pathways through its antioxidative potential in diabetic complications, and plays a major role in amelioration of cardiac complications, diabetic nephropathy, and neuropathy (16), moreover preventing oxidative stress induced hepatic and pancreatic injury. Therefore, the study suggests that *Pennisetum purpureum* extract having antioxidant, hypolipidemic and antidiabetic potential.

## Conclusion

In this study *Pennisetum purpureum* showed no toxicity and ameliorative changes in the elevated blood glucose level, antioxidant level and biochemical parameters Therefore could be considered as an ingredient in the development of antidiabetic herbal formulations. Further studies might be led to investigate the mode of action of the fraction in interacting with the oxidative and antidiabetic pathways.

## Acknowledgement

The authors acknowledge the contribution of United Diagnostic Centre, Prayagraj for providing histopathological data for the study. Authors are also grateful to Arbro laboratories, New Delhi for providing HPTLC data.

## *Statement and Declarations*

### *Competing Interests*

Author declares that there is no financial interest that are directly or indirectly related to the work submitted for publication.

## References

1. Jia, W., Gao, W., and Tang, L. (2003). Antidiabetic herbal drugs officially approved in China. Phytotherapy research, 17(10):

1127–1134. https://doi.org/10.1002/ptr.1398

2. Matore, Z. (2019). Bana Grass Growing in Sub Saharan. Africa Intech Open. doi: 10.5772/intechopen.82367

3. Jack, I. R., Clark, P. D., and Ndukwe, G. I. (2020). Evaluation of Phytochemical, Antimicrobial and Antioxidant Capacities of Pennisetum purpureum (Schumach) Extracts. Chemical Science International Journal, 29(4): 1–14.

4. Chen, Y., Wang, Y., Chen, Y., Hou, Y., Bhawamai, S., and Fang, Y. (2020). Suppression of Inflammatory Mediators by Ethanol Extracts of Pennisetum purpureum S. (Napiergrass Taishigrass no. 2) in Activated RAW 264.7 Macrophages. Journal of Food and Nutrition Research, 8(8): 392-398.

5. Chinedu, O., and Buhari, A. (2015). Evaluation of the Anti-Gastric Ulcer Effect of Methanolic Extract of *Pennisetum purpureum* (Schumach) in Male Wistar Rats. International Journal of Current Microbiology and Applied Sciences, 4(10): 466-474.

6. Evinemi, P.A., Enemo, K., Onah, C. M., Uzor, P. F., Omeje, E. O. (2022) In vivo Antimalarial and GC-MS Studies of *Pennisetum purpureum* Leaf Extract and Fractions. Tropical Journal of Natural Product Research. 6(8):1274-1280.

7. Ojo, O. A., Ojo, A. B., Barnabas, M., Iyobhebhe, M., Elebiyo, T. C., Evbuomwan, I. O., Michael, T., Ajiboye, B. O., Oyinloye, B. E., Ede, O. I. O. (2022) Phytochemical properties and pharmacological activities of the genus *Pennisetum*: A review. Scientific African. 16, e01132.

8. Harborne, J.B. (1998) Method of extraction and isolation In. Phytochemical Methods (3rd edition), Chapman & Hall, London. Pp. 60-66

9. OECD (2000) Guideline Number 423 for the Testing of Chemicals: Revised Draft Guideline 423 (Acute Oral Toxicity). Paris, France.

10. Mishra, S. B., Verma, A., Mukerjee, A., Vijayakumar, M. (2012) *Amaranthus spinosus* L. (Amaranthaceae) leaf extract attenuates Streptozotocin-nicotinamide induced diabetes and oxidative stress in albino rats: A histopathological analysis. Asian Pacific Journal of Tropical Biomedicine 2(3): 1647-1652

11. Mishra, S. B., Verma, A., Vijayakumar, M. (2013). Preclinical evaluation of antihyperglycemic and antioxidant action of Nirmali (Strychnos potatorum) seeds in streptozotocin nicotinamide induced diabetic Wistar rats: a histopathological investigation. Biomarker and Genomic Medicine 5, 157–163.

12. Lommel, A.T. L.V. (2002) From Cells to Organs: A Histology Textbook and Atlas. Springer-verlag Germany.

13. D'Souza, J. J., D'Souza, P. P., Fazal, F., Kumar, A., Bhat, H. P., Baliga, M.S. (2014) Anti-diabetic effects of the Indian indigenous fruit Emblica officinalis Gaertn: Active constituents and modes of action. Food and Functions. 5, 635–644.

14. Bak, E. J., Kim, J., Jang, S., Woo, G. H., Yoon, H. G., Yoo, Y. J., Cha, J. H. (2013). Gallic acid improves glucose tolerance and triglyceride concentration in diet-induced obesity mice. Scandinavian Journal of Clinical and Laboratory Investigation, *73*(8): 607–614..

15. Owumi, S., Najophe, E. S., Farombi, E. O., Oyelere, A. K. (2020). Gallic acid protects against Aflatoxin $B_1$ -induced oxidative and inflammatory stress damage in rats kidneys and liver. Journal of Food Biochemistry, 44(8): e13316.

16. Yusuf, B. O., Yakubu, M. T., Akanji, M. A. (2021). Chromatographic fractions from *Chrysophyllum albidum* stem bark boost antioxidant enzyme activity and ameliorate some markers of diabetes complications. Journal of Traditional and Complementary Medicine, 11(4): 336–342.

Current Trends in Biotechnology and Pharmacy
Vol. 18(2) 1705-1712, April 2024, ISSN 0973-8916 (Print), 2230-7303 (Online)
DOI: 10.5530/ctbp.2024.2.19



# Formulation and Evaluation of Piroxicam Liquid Fill Formulations

**Sudhir Maddela[1*], R. R Manjula, B. Pamula Reddy, Sahithi Kodali[1], Bindu Patibandla[1], Suchitra Singavarapu[1], Raasi Maathangi[1].**

[1]Department of Pharmaceutics, Nirmala College of Pharmacy, Atmakur, Mangalagiri.*Corresponding Author: sudhir.spark@gmail.com

## Abstract

The present investigation includes the preparation and evaluation of liquid filling formulations of Piroxicam (PXM), a non-steroidal anti-inflammatory drug, to improve its dissolution properties. Liquid fills were prepared using various excipients like polyethylene glycol 400 (PEG 400), propylene glycol (PG), and methanol as co-solvents, poly vinyl pyrrolidone (PVP K-30) as solubilizing agent, and hydroxyl propyl methyl cellulose as gelling agent. The prepared PXM liquid fills were evaluated for appearance, recrystallization, viscosity, clarity, assay and *in vitro* drug release studies. The compatibility of PXM and excipients in liquid fills was confirmed by FTIR. DSC studies together with XRD confirmed the absence of PXM recrystallization within the liquid fills. The viscosity of the prepared liquid fills was found to be in the range of 60.9–591.7 cps. Liquid fills containing PVP K 30 gave better dissolution properties when compared to formulations without PVP K 30, and complete PXM release was observed within 60 min for all PXM liquid fills and the PXM release from liquid fills followed diffusion mechanism. The liquid fills showed 98-102% PXM content even after 6months time period indicating that the PXM was stable in liquid fill formulations.

**Keywords:** Piroxicam, liquid fill formulations, recrystallization, diffusion, and dissolution.

## Introduction

The dissolution and bioavailability of the newly developed entities especially the BCS class II drugs remain challenged because of its poor biopharmaceutical properties. They show poor aqueous solubility at varying pH conditions throughout the gastro intestinal tract. To come across these impediments that are associated with the BCS class II drugs, the formulations scientists developed several alternative dosage forms to improve the biopharmaceutical properties of the drug substances. In this context, the liquid orals, semisolids, liquid fills (soft gels) gained importance to address the issues of bioavailability by administering the drugs through soft gelatin capsules. Initially this technology of delivering the drugs through soft gelatin capsules was widely used for the delivery of oily liquids such as cod liver oil etc (1-3). Therefore, these soft gels contain the active pharmaceutical ingredient(API) either as solution, suspension or emulsion which will enhance the absorption of API. Thus, soft gels can be considered as a best tool for the delivery of compounds with poor biopharmaceutical properties (4).

Piroxicam is a nonselective, non-steroidal anti-inflammatory drug (NSAID) which belongs to “oxicam” class and used for treating rheumatoid arthritis, osteoarthritis and other inflammatory diseases, acts by inhibiting

both COX-1 and COX-2 inhibitors (5). PXM is a drug of poor solubility and included in class II of Biopharmaceutical Drug Classification System, thereby, PXM absorbs slowly and gradually through the GIT leading to slow onset of action (6).

Various formulations have been developed for PXM like fast dissolving tablets (7), transferosme gel (6), microsponge tablet (5), solid self-micro emulsifying dispersible tablets (8), and dispersible tablets (9) to improve its solubility property. No one developed PXM liquid fills for soft gels. So, the present investigation was aimed at developing PXM liquid fills for soft gels and their evaluation to improve the biopharmaceutical properties of PXM. As these liquid fills/soft gels are used for enhanced bioavailability, many drugs are formulated in the form of soft gels. The present study deals with the formulation of piroxicam liquid fill formulations/soft gels to improve its dissolution properties.

## Materials and Methods

PXM was obtained from Darwin laboratories, Vijayawada. PEG 400, PG, were purchased from Thermo Fisher Scientific India Pvt. Ltd. PVP, Sodium metabisulfite, and Methanol was obtained from Qualigens fine chemicals, Mumbai.

## Methodology

### Construction of calibration curve

PXM calibration curve was constructed using a series of standard solutions containing 1, 2, 3, 4, 5 µg PXM per ml. the solutions were scanned in the 200-400nm region using Shimadzu UV-1800 UV-Visible spectrophotometer. The absorbance of the standard solutions was measured at 334nm against blank (pH 1.2 buffer)

### Preparation of PXM liquid fills

Liquid fill formulations were prepared by accurately weighing required quantities of PXM and other excipients as per the formulae given in Table 1. PEG 400 and PG (half of the quantity) were taken in a suitable container and then PXM was added under continuous stirring to completely dissolve the PXM. The stirring was continued till the remaining ingredients added were dissolved and a homogenous solution was obtained. Finally, the volume as adjusted with PEG 400. The prepared formulations were sonicated for 3 minutes to remove any entrapped air. The prepared formulation (equivalent to the dose of PXM) was filled in to “0” sized hard gelatin capsule with help of a syringe, the capsule body and cap were then sealed with a band to prevent the leakage of contents (10).

Table 1: Composition of PXM liquid Fills

| Ingredients (mg/cap) | F1 | F2 | F3 | F4 | F5 | F6 | F7 |
|---|---|---|---|---|---|---|---|
| PXM | 20 | 20 | 20 | 20 | 20 | 20 | 20 |
| PEG-400 | 60 | 60 | 50 | 40 | 40 | 40 | - |
| PG | 10 | 20 | 20 | 20 | 20 | 20 | - |
| PVP K-30 | - | - | - | - | 10 | 20 | 10 |
| HPMC | - | - | - | - | - | - | 60 |
| SBS | 0.1 | 0.1 | 0.1 | 0.1 | 0.1 | 0.1 | 0.1 |
| Methanol | 10 | - | 10 | 20 | 10 | - | 10 |
| Total weight | 100 | 100 | 100 | 100 | 100 | 100 | 100 |

Current Trends in Biotechnology and Pharmacy
Vol. 18(2) 1705-1712, April 2024, ISSN 0973-8916 (Print), 2230-7303 (Online)
DOI: 10.5530/ctbp.2024.2.19


**Evaluation of PXM liquid filling formulations**

The PXM liquid fills were evaluated for the following properties

**Morphological properties**

Properties such as homogeneity, color, transparency, and appearance of PXM liquid fills are tested visually against a black background. All the formulations were stored at room temperature (25 ± 3°C) with relative humidity of approximately 65 ± 5% and were tested periodically every month for a period 6 months (9). The results are given in Tables 2 and shown in Fig: 1

**SEM studies**

The PXM liquid fills were further investigated for recrystallization by scanning electron microscopy (SEM-JOEL, JSM-840A, Japan). The samples to be examined were mounted on the SEM sample slab using a double-sided adhesive tape. The samples mounted were coated with gold ($200A^0$) under reduced pressure (0.001 torr) for 5min to improve the conductivity using an Ion sputtering device (JOEL, JFC-1100E, Japan) (10).

**DSC analysis**

Thermograms of PXM and selected PXM liquid fills were recorded using Differential Scanning Calorimeter (Schimadzu, DSC-60, Japan). Samples weighing 5mg were sealed in aluminum pans and heated to 400ºC at a rate of 10ºC per minute. Samples were heated from 50-400ºC (10).

**X- RD analysis**

XRD studies of PXM and selected PXM liquid fills were performed using X-Ray Diffractometer (Schimadzu, XRD-7000, Japan) with Cu-K$\alpha$ radiation at 40kV and 30mA. X-Ray diffraction patterns were collected over $2\theta$ range of 10-40º at a scan rate of 4º per minute (10).

**FTIR analysis**

Samples were analyzed using ATR-FTIR spectrometer (Bruker, Germany). ATR spectra were measured over the wave number range of 4000-500 $cm^{-1}$ at a resolution of 1.0 $cm^{-1}$. The powder or liquid fill sample is simply placed onto the ATR crystal and the sample spectrum is collected. FTIR spectra of PXM and mixtures (PXM + excipients in 1:1 ratio) were shown in Fig 5.

**Drug content**

Accurate amount of PXM liquid fills equivalent to dose of PXM was taken in a 10mL volumetric flask and dissolved in 5mL of methanol and the volume was made up with distilled water. Samples were suitably diluted with pH 1.2 buffer and the absorbance was measured at 334nm. The estimations were carried out in triplicate (10).

**Variation of mass:**

Mass variation among the different batches of PXM liquid fills was calculated by measuring the mass of each capsule equivalent to PXM dose. The estimations were carried in triplicate.

**Rheological studies**

The viscosity was measured using Brookfield DV-II + PRO viscometer of cup and bob type. The formulation was taken into the cup of viscometer and measured using spindle CP52 at 10 rpm. The viscosity measurements were made in triplicate using fresh samples each time (10).

***In vitro* drug release studies**

*In vitro* drug release studies were conducted using 900 mL of pH 1.2 buffer as a dissolution medium using USP type II (paddle) apparatus (DISSO 8000, LAB INDIA). A temperature of 37°C and a rotation speed of 50 rpm were maintained. PXM Liquid fills were filled into hard gelatin capsule (size 0) and dissolution studies were performed. As the capsule tends to float in the dissolution medium, sinkers were used. A 5 mL sample was withdrawn at predetermined

time intervals over a period of 1 hr and then replaced with the same volume of fresh dissolution medium. The filtered samples were suitably diluted and analyzed at 334 nm using UV-visible Elico SL150 spectrophotometer. Dissolution experiments were conducted in triplicate (10).

## Results and Discussion

### Preparation of Liquid fills

In the present investigation the liquid fills were prepared for easy administration and quick release of medicament which is also a commercially scalable technique. Initially, placebo liquid fills were prepared with different polymers like HPMC E3, Sodium CMC, Sodium Alginate, PG, and PEG-400 and observed for gel forming capacity and appearance. The liquid fills prepared with PG, PEG and HPMC E3 were transparent and showed good flow ability, whereas, the liquid fills prepared with sodium CMC, sodium alginate were turbid and are highly viscous. So, PG, PEG, and HPMC E3 were selected for further development of liquid fills. The liquid fills prepared with PEG and PG were stable, homogenous and clear even after the addition of PXM. Whereas the liquid fills with HPMC E3 were turbid after the addition of PXM. Hence, further the liquid fills were prepared with PEG and PG only. The PXM liquid fills were prepared as per the formulae shown in Table 1.

### Evaluation of PXM liquid fills

### Morphological properties

The prepared PXM liquid fills were visually tested for homogeneity, transparency, color and smoothness. Soft gels with PEG-400 and PG showed no change in properties even at the end of 6-month time and no crystallization of PXM was observed. The results were given in Table 3. Soft gels formulated with HPMC E3 were opaque which may be due to recrystallization of PXM in liquid fills. The results were shown in Fig1.

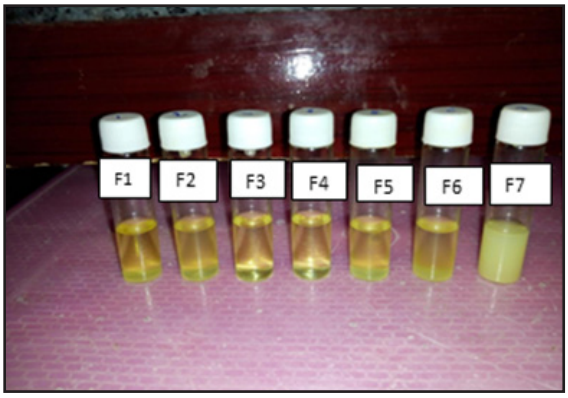


Fig 1: Morphological Properties of PXM liquid Fill Formulations (0-6 months)

### SEM analysis:

The PXM liquid fills were further investigated for PXM recrystallization in liquid fills by SEM analysis. The scanning electron micrographs of PXM and selected PXM liquid fills were shown in Fig 2. The visualized SEM micrographs revealed that the liquid fills were relatively clear and maintained the transparency, this may be due to molecular dispersion of PXM in liquid fills.

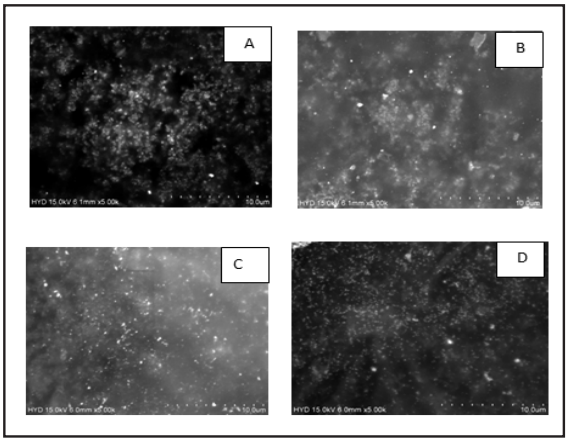


Fig 2: SEM micrographs of PXM Liquid Fills (A) PXM, (B) F4, (C) F6, (D) F7

### DSC analysis:

DSC thermograms obtained for PXM and PXM soft gels were shown in Fig3. PXM showed melting endotherm at 200 ºC. PXM soft

gels showed no, or weak peaks compared to PXM. This may be due to molecular dispersion of PXM within soft gels. Overall DSC curves indicate that there is no interaction observed between PXM and excipients.

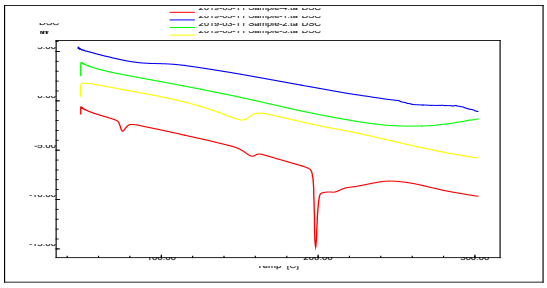

Fig 3: DSC Thermograms of (-----) PXM, (-----) F1, (-----) F4, (-----) F6

**X-RD analysis**

Selected PXM soft gels were subjected to X-RD studies to investigate the crystallographic properties of PXM in soft gels. PXM showed characteristic peaks at 16.54, 19.82, 24.50, 27.32 and 38.07 $2\theta$. The X-ray diffractograms of the PXM liquid fills showed weak or no signals when compared to the characteristic peaks of pure PXM. This may be due to molecular dispersion of PXM within the soft gels. Overall, together with DSC data the X-RD results clearly indicate that the PXM was not in crystalline state in liquid fills. The X-ray diffractograms of PXM and selected PXM liquid fills were shown in are shown in Fig 4.

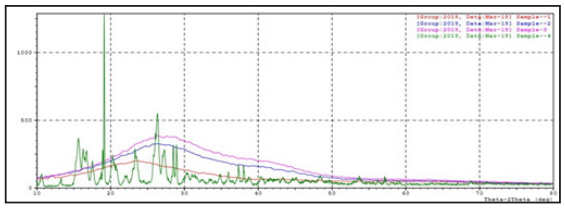

Fig 4: X-RD diffractograms of (----) PXM, (-----) F1, (-----) F4, (----) F6

**FTIR analysis**

The PXM showed characteristic peaks at 1681cm$^{-1}$(ketone C=O stretching), 668cm$^{-1}$ (C=Cl due to Halogen compound), 2311cm$^{-1}$(N-H amino acid stretching). These characteristic peaks of PXM were all retained in the soft gels. These results were given in Table7 and indicate that there is no interaction between PXM & excipients in soft gels. The FTIR spectra of PXM alone and in combination with excipients were shown in Fig 5.

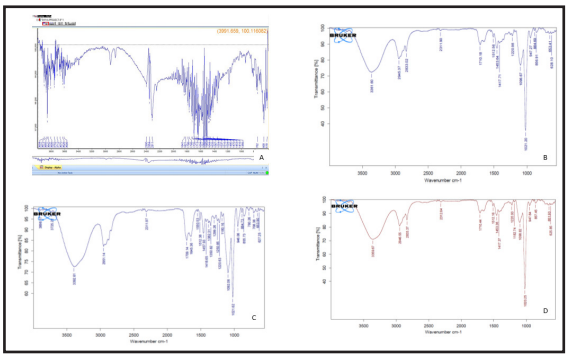

Fig 5: FTIR spectra of (A) PXM, (B) PXM+PEG-400, (C) PXM+PG, (D) PXM+PEG 400+PG+PVP K30

**Drug content**

The PXM content within the liquid fills were found to be in the range of 18.70 to 20.11mg. The results were given in Table 2. The results indicated a good uniformity of PXM within the liquid fill, and overall good solubilization of PXM in liquid fills was observed. The liquid fills formulated with PVP gave superior PXM content compared to liquid fills without PVP.

**Variation of mass**

The mass of PXM liquid fills equivalent to 20mg dose of PXM from three different batches were recorded on electronic balance (shimadzu-ATX224) and the results are shown in Table 2. Same mass of the soft gels was obtained with the three batches of the soft gels indicating the reproducibility of the soft gel preparation method and formulation.

**Rheological studies**

The viscosity of the PXM liquid fills was measured using Brookfield viscometer with spindle 52 was reported in Table 2. From the data obtained it is observed that the consistency of the liquid fills was dependent upon

the concentration of PEG-400. Even though the PEG is selected as co-solvent the high consistency nature of PEG enhanced the viscosity of the prepared liquid fills, hence increased PEG concentration lead to high viscous liquid fills. In fact, the PG has decreased the consistency of the prepared liquid fills, thereby, a 2.05-fold decrease in viscosity was observed F 6 compared to F1. A significant increase in viscosity was observed in liquid fill containing HPMC (F7) compared to other formulations which may be due to the influence of gelling agent (HPMC). However, the addition of PVP to the formulation showed a negligible effect on the viscosity of liquid fill formulations.

Table 2: Evaluation Parameters for PXM Liquid Fill Formulations

| Formulation | Variation of mass± SD | Viscosity± SD | Drug content ± SD |
|---|---|---|---|
| F1 | 100.85 ± 0.204 | 140.8±0.10 | 19.01 ± 0.02 |
| F2 | 100.86 ± 0.287 | 126.9±0.02 | 19.43 ± 0.06 |
| F3 | 100.21 ± 0.085 | 105.8±0.06 | 19.08 ± 0.06 |
| F4 | 100.13 ± 0.170 | 94.5±0.10 | 19.39 ± 0.02 |
| F5 | 100.13 ± 0.047 | 82.6±0.01 | 19.04 ± 0.03 |
| F6 | 100.45 ± 0.108 | 68.5±0.05 | 20.11 ± 0.05 |
| F7 | 100.79 ± 0.152 | 275.5±0.01 | 18.70 ± 0.01 |

### *In vitro* drug release studies

In the present investigation, dissolution of PXM soft gels was carried out using USP Type-II Dissolution Rate Testing Apparatus and 900mL of pH 1.2 buffer was used as dissolution medium. The *in vitro* dissolution profiles of PXM liquid fills were shown in Fig3. The cumulative percent of PXM released at the end of 5 min for F1, F2, is 15.50 ± 2.4, and 35.44 ± 1.9 respectively. A 2.2 folds increase in PXM release was observed in formulation F2 compared to formulation F1 indicating that increased concentration of PG significantly attributed the co-solvency effect and thereby superior dissolution rates were obtained with increased concentration of PG which can be. The comparative dissolution profile of PXM liquid fill F1 and F2 were shown in Fig 6(A). The cumulative percent of PXM release from F2, and F3 is 35.44 ± 1.9, 48.46 ± 3.4 respectively at the end of 5 minutes. A 1.36-fold increase in PXM release was observed in formulation F3 compared to F2, indicating that a decrease in concentration of PEG enhanced the PXM release from liquid fills which might be due to decrease in consistency of the liquid fills due to lesser concentration of PEG compared to F2. The comparative dissolution profile of PXM liquid fill F2 and F3 were shown in Fig 6(B). Further trails were carried out to study the effect of PVP K30 on PXM release rates from the liquid fills. The cumulative percent of PXM released at the end of 5 minutes from F4, F5, and F6 is 53.86 ± 3.7, 77.84 ± 2.4, and 90.15 ± 2.6 respectively. A 1.44-, and 1.67-fold increase in PXM release was observed in F5, and F6 compared to F4 indicating that PVP K30 enhanced the PXM release from liquid fills. The comparative dissolution profile of PXM liquid fills F4, F5, and F6 were shown in Fig 6(C). The cumulative percent of PXM released from F7 is found to be 12.26± 0.5 at the end of 5 minutes, indicating that HPMC significantly lower the PXM release from liquid fills because of its high consistency.

The viscosity of the liquid fills also showed significant effect on PXM release form liquid fills. The liquid fills of high consistency (F1, F2, F3, and F7) showed slow PXM release whereas the liquid fills with low consistency (F4, F5, and F6) showed faster PXM release. Overall, the formulations F5 and F6 containing PVP K30 showed significant superior PXM release compared to F4 without PVP K30.

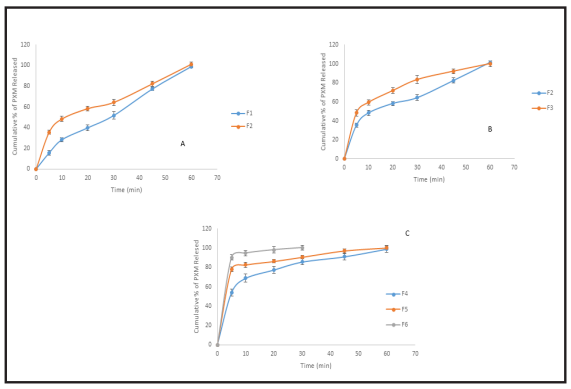


Fig 6: Comparative *in vitro* drug release profile of PXM Liquid Fills

## Drug release kinetics

To better understand the release profiles obtained with PXM liquid fills, the drug release data obtained at different time points was fitted in to different kinetic models such as First order (11), and Higuchi model (12).

The first order release rate constant 'k' ($sec^{-1}$) values and correlation coefficient ($R^2$) values calculated from dissolution data (0-60 min) of PXM liquid fills. The 'k' values for F1to F7 were found to be 0.13, 0.18, 0.27, 0.45, 0.61, 0.7, and 0.12 respectively. A 1.35, and 1.55 fF5, and F6 compared to F4. The liquid fills containing PVP K30 significantly showed higher K values compared to liquid fills without PVP K30.

The Higuchi square root model of all soft gels showed higher correlation coefficient values (0.76-0.98) indicating diffusion as release mechanism.

## Conclusion

The dissolution properties of PXM can be enhanced by using co-solvents (PG and PEG), and solubilizing agent PVP K30 by formulating as liquid fills. The liquid fills with PEG showed more consistency compared to PG. all the liquid fills showed good physico-chemical properties and were stable till the end of 6months. Overall the liquid fills with PVP K30 showed superior dissolution rates compared to liquid fills without PVP K30.

## References

1. Vidyavati, S., Jithan, A. (2010). Development and evaluation of zero order sustained release matrix type transdermal films of ibuprofen. Journal of Global Pharma Technology, 2(2): 51-58.

2. Sarath, S., Menon, B. V., Basavaraj, S., Bharath, R., Deveswaran, V., Madhavan. (2011). Formulation and evaluation of ibuprofen tablets using orange peel pectin as binding agent. Der Pharmacia Letter, 3(4) 241-247.

3. Madhulatha, A., Naga Ravikiran, T. (2013). Formulation and evaluation of ibuporfen transdermal patches. International Journal of Research in Pharmaceutical and Biomedical Sciences, 4(1): 351-362.

4. Nirav, S., Rajan, B. M. (2011). Formulation and evaluation of floating drug delivery system. International Journal of Pharma and Bio Sciences, 2(1): 571-580.

5. Cryer, B., Feldman, M. (1998). Cyclooxygenase-1 and cyclooxygenase-2 selectivity of widely used nonsteroidal anti-inflammatory drugs. Am J Med, 104:413-21.

6. Piao, M. G., Kim, J.H., Kim, J. O., Lyoo, W. S., Lee, M. H., Yong, C. S. and Choi, H.G. (2015). Enhanced oral bioavailability of piroxicam in rats by hyaluronate microspheres. Drug Development and Industrial Pharmacy, 33(4):485-491.

7. Kumar, I., Chaudhary, D., Thakur, B. and Pandit, V.(2020). Formulation and evaluation of fast dissolving tablets using direct compression and sublimation method. Journal of Drug Delivery and Therapeutics, 10(3-s): 17-25.

8. S. H., G., C., S., P., S. B., S., M., Siddaramaiah, K. S., N., & Gowda, D. V. (2021). Formulation and Evaluation of Solid Self

Micro Emulsifying Dispersible Tablet of Piroxicam. International Journal of Applied Pharmaceutics, 13(2): 127–133.

9. Snehalatha, Lakshmi, Radhika., Yogananda, R., Nagaraja, T. S., Vijay, Kumar, M. M. J. and Masareddy, R. S. (2009). Formulation and evaluation of piroxicam dispersible tablets using natural disintegrants. Journal of pharmaceutical Sciences and Research, 1(4): 146-150.

10. Jyothi, S. K. M., Maheswari, Seetha. S., Sravanthi. D., Buchi N. Nalluri.(2013). Preparation and evaluation of valsartan liquid filling formulations for soft gels. Journal of Pharmaceutics, Article ID 418346.

11. Lapidus, H., and Lordi, N. G. (1996). Drug release from compressed hydrophilic matrices. Journal of Pharmaceutical Sciences, 55:840-843.

12. Higuchi, T. (1963), Mechanism of sustained action medication: Theoretical analysis of rate of release solid drugs dispersed in solid matrices, Journal of Pharmaceutical Sciences, 52:.1145-1148.

Current Trends in Biotechnology and Pharmacy
Vol. 18(2) 1713-1724, April 2024, ISSN 0973-8916 (Print), 2230-7303 (Online)
DOI: 10.5530/ctbp.2024.2.20



# A Bibliometric Analysis of Scholarly Publication on Protein Folding From 2018 to 2022

**SK Panda[1], Atul Bhatt[1],Aparna Satapathy[2],SP Chaudhari[1], NK Prasanna[3] & Manohar Pathak[1*]**

[1]Department Library and Information Science, Gujarat University, Gujarat, Ahmedabad 380009, India
[2] Maharshi Dayananda Saraswati University, Ajmer-305009, Rajasthan.
[3]CSIR- National Institute of Information and Policy Research, Pusa Campus, New Delhi-110012, Delhi, India
Email: - prasanna@niscpr.res.in; manoharpathak@gmail.com

**Abstract**

The paper investigates the research output of protein folding published in the last five years, from 2018-2022. The source data are retrieved from the SCOPUS database and analyzed using MS Excel and VOS Viewer software. The VOSViewer software is mainly used for networking and visualization to understand the research pattern. A total of 12515 documents on protein folding are retrieved and considered for the study. The research finds that Uversky, V.N. was the most prolific protein folding author with the highest 42 publications and top 2560 global citations. The most productive countries in this field is the USA (4443 publications), followed by China (1791 publications), and Germany (1197 publications). The four hot keywords in protein folding research are protein binding, protein conformation, and metabolism, but protein folding is a burning author keyword. Most articles have been published by the CNRS (Centre National de la RechercheScientifique). This study will benefit future researchers worldwide in understanding the research pattern of protein folding.

**Keywords**: Protein folding, Bibliometrics, Bibliometrix, Protein conformation,Chaperon

## Introduction

Proteins are large complex biomolecules that play many vital roles in our bodies (1). This complex organic compound makes hormones and enzymes and plays an essential role in building and repairing muscles, bones, cartilage, skin, etc. The basic building blocks of proteins are called amino acids (2) Protein comprises twenty-plus basic chains of amino acids, each called a polypeptide (3). To perform the biological function, these chains adopt the termed structure (native shape) through a physicochemical process known as protein folding (2,4).

The protein folding mechanism goes through 4 steps of a structural process that are primary, secondary, tertiary and quaternary (5). The first structure of the protein is the primary structure, the nascent protein. Then folding occurs in the primary structures, giving the secondary structure like the α-helix and the β-pleated sheet. This is not a well-stabilized protein structure. This secondary structure is three-dimensional in nature but nonfunctional. From the secondary structure, tertiary functional protein structures are formed through a process called hydrophobic effect or hydrophobic collapse (3). Most of the cases, the protein stabilizes at the

tertiary structure, but this is not the final conformation of the protein through protein folding. Sometimes the tertiary structure transforms into the quaternary structure (6). In this process, the nonfunctional nascent protein is transformed into a final stabilized functional form called a native protein (7). To fold the nascent protein to its native state, the favorable interactions are Hydrophobic effect, Electrostatic effects, Enthalpy from Vander walls packing interaction, and gain of protein-protein H bonds, whereas protein conformational entropy and loss of protein-water H-bonding are the unfavorable interactions (6,8).

Protein folding is crucial for normal physiology, including development and healthy ageing, and failure of this process is related to the pathology (9). Sometimes molten globule (compact intermediate tertiary structure of a protein) aggregates and debates from the folding pattern, and the protein remains unfolded (10). Due to the failure of native structures,inactive proteins are formed (11). Inactive protein functions raise various diseases like Huntington's disease (8), Alzheimer's disease (12), Cystic fibrosis (13), Parkinson's disease (14), Gaucher's disease followed by allergies (15). Chaperon helps to keep the protein on

the right path if the protein debate from the holding pattern.Now a days,various experimental techniques are used for protein folding such as Circular dichroism (16), X-ray crystallography, Fluorescence spectroscopy,X-ray crystallography etc. (17); However, Kubelka et al., reported that the time scale of the protein folding depends on its size and topology (18).

Figure 1 shows that Protein folding has been an emerging area of research in the last few decades. To understanddomain-specificresearch trends, hotspots and their interrelationships with other research areas, we analyzed the global literature on 'protein folding' published in the last 5 years, from 2018 to 2022, using bibliometric methods.

Figure 1 shows that Protein folding has been an emerging area of research in the last few decades. To understanddomain-specificresearch trends, hotspots and their interrelationships with other research areas, we analyzed the global literature on ‘protein folding’ published in the last 5 years, from 2018 to 2022, using bibliometric methods.

Bibliometrics methods are quantitative approaches for evaluating and monitoring written and published research (19). It is *a* valuable tool for tracing a specific research field’s intellectual structure. Pritchard first introduced itin 1996, comprising mathematical and statistical approaches.Itencompasses a set of methods thatmeasure the various aspects of literature like subject, author, citations, affiliation, country, sources etc (20). (Zyoud et al., 2022). Bibliometrics has been considered a standard science policy and research management tool (21)technological innovations like artificial intelligence (AI. Ithelps to monitor the literature growth and research pattern. The science indicators such aspublication trend, authorships, citation statistics, keyword analysis etc., are some of the bibliometric techniques useful for tracking the evolution of science and technology and decision-making (22,23,24). Citation analysis is the most conventional method to measure the scientific quality of individual researchers. Author co-citation analysis was developed by White & Griffith, and this method provides the intellectual structure in sciencedisciplines (25,26). It has also been stated (27) state that this quantitative analysis helps to identify the authorship pattern and literature growth followed by institutional collaboration. Several researchers have tested the bibliometric and scientometric approaches in different subject areas to understand the research patterns.

**Research objectives**

The study aims to analyze the protein folding research output between 2018 and 2022by employing the bibliometrics methods based on information retrieved from the Scopes database. Thefollowing are the main objectives:

To study the year-wise distribution and growth of the publications, To analyze the author's productivity and identify the most prolific researcher in the field, To evaluate the country-wise research trends globally and examine the highly productive organizations and most cited documents in protein folding research, To establish a network of Co-citation and Co-authorship and, To plotnetwork visualization of the co-occurrence of keywords in protein folding global research outputs.

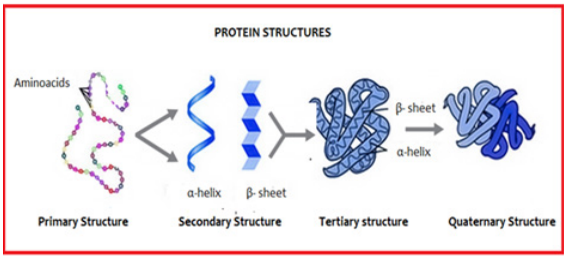


Figure 1:—Protein folding stages (https://www.researchgate.net/publication/298786402_Principles_of_Protein_Folding)

## Materials and Methods

The sample dataset was collected from the Scopus Database,the largest international bibliographic and citation database and is used primarily for bibliometrics research in all parts of the World. The word'proteinfolding'was used as the search string and qualified with the Scopus search criteria 'Article title, Abstract, Keywords'. The instant result is thenlimited to the last 5-year publications data covering 2018 to 2022. The result found 12515 publications during the study period that included all types of documents' erratum' and 'retracted'.We analyzed the collected data using MS Excel andVOSViewer software. This study analyses the number of publications, citations, and productivity of authors, organizations, countries and journals/articles. We also analyzed the quality of the author's and organization's academic production using the H-index. We constructed the co-authorship, co-citation, and keyword occurrence network to study the relationship and visualise the datausing the VOSViewer.

## Results and Discussion

The study discussed the entire results in two parts: (a) performance analysis and (b) science mapping. The performance analysis examines the characteristics of the publications and the perception of quality using different tools and techniques. It accounts for the research's publication patterns, contribution and productivity in the given field. In contrast, science mapping focuses on the relationship between research constituents such as keywords, citations and authorships. It identifies how authors andcountries are related and their evolutionary significance (28,29,30).

### *Performance analysis*

Performance analysis is the simplest methodin the bibliometric study toanalyze the performances of different research constituents, such as articles, authors, institutes, countries, and journals,over a period of time (31,32). We performed all these analyses in this study to present the research trends.

### *Annual publications analysis*

Ofthe total number of 12515 publications on protein folding retrieved from the Scopus database between 2018 and 2022,the highest number of 2674 (21.37%) papers were published in 2018 with most h-index, followed by 2666(21.30%) papers in 2020, 2623 (20.96%) papers in 2019, 2494 (19.93%) papers in 2021 and a comparatively lowest number of 258(16.44%) of papers in 2022 as shown in Table 1.

In contrast,the citation analysis column shows the highest number of citations received in2019, followed by 2018, during the study period. The data show that the annual publication growth slightly decreased from 2018-2022.

Bibliometric analysis of authors,institutions and countries/regions

Table 2 analyses the distribution of the ten mostprolific authors. The author with the most

published papers (42) is Uversky, V.N. from the University of South Florida, Tampa, USA, followed by Gianni, S.(36) and Hassan, M.I.(29). The highest 1125citations isreceived by Vendruscolo, M., from University of Cambridge, UK withmaximum 17 h-index followed by Best, R.B. from NIH, USA having 770 citations with 14 h-index.The author's productivity analysis also shows that the most creativeauthors are from USA and INDIA in protein folding.

Table 1: Distribution of annual growth of scientific publications

| Sr. No | Year | No. of Publications | Citations | h-index |
|---|---|---|---|---|
| 1 | 2018 | 2674 | 65697 | 152 |
| 2 | 2019 | 2623 | 70494 | 133 |
| 3 | 2020 | 2666 | 43109 | 108 |
| 4 | 2021 | 2494 | 31935 | 80 |
| 5 | 2022 | 2058 | 8558 | 42 |

Table 2: Distribution of most prolific authors

| Authors | TP | CT | h-index | Institution | Country |
|---|---|---|---|---|---|
| Uversky, V.N | 42 | 560 | 14 | University of South Florida, Tampa | USA |
| Gianni, S. | 36 | 332 | 10 | Sapienza Università di Roma | Italy |
| Hassan, M.I. | 29 | 313 | 11 | JamiaMilliaIslamia, New Delhi | India |
| Vendruscolo, M. | 28 | 1125 | 17 | University of Cambridge | UK |
| Islam, A. | 27 | 275 | 10 | JamiaMilliaIslamia, New Delhi | India |
| Ahmad, F. | 25 | 270 | 10 | JamiaMilliaIslamia, New Delhi | India |
| Wolynes, P.G. | 24 | 424 | 13 | Rice University | USA |
| Toto, A. | 24 | 172 | 8 | Sapienza Università di Roma | Italy |
| Gruebele, M. | 23 | 310 | 10 | University of Illinois Urbana-Champaign | USA |
| Best, R.B. | 23 | 770 | 14 | National Institutes of Health (NIH) | USA |
| Note: TP-Total no. of publications, CT-Citations | | | | | |

Figure 2 shows the top ten countries in terms of scientific research publications on Protein folding. The data reflects that the USA has published the highest number of 4443 papers, which is 35.5% of total publications, followed by China with 1791(14.32%) papers and Germany with 1197(9.56%) papers.

This studyalso investigated institute-wise scientific researchpublications and their productivity. Table 3 presents the ten most highly productive institutions/organizations in protein folding research. The Institute with the most publications is 'CNRS Centre National de la RechercheScientifique' which is in France and has published the highest 325 publications, followed by the Chinese Academy of Sciences (245) and the National Institutes of Health (231). In contrast, the Howard Hughes Medical Institute, USA has received the highest 8189 number of citations with 42 h-index, followed by the University of Cambridge, UK, with 6643 citations and 36 h-in-

dex. The analysisaslo shows that the USA has participated the most, followed by China in protein folding research globally.

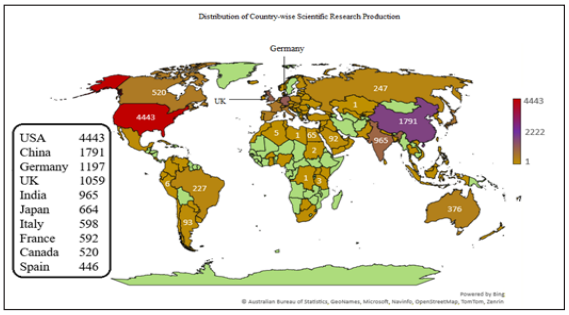


Figure 2 Distribution of County-wise scientific research publications

***Bibliometric analysis of most cited papers***

Table 4 provides the top ten highly cited papers. The paper entitled "Highly accurate protein structure prediction with AlphaFold" published in Nature in 2021 received a maximum of 7366 total citations, followed by "Reactive oxygen species (ROS) as pleiotropic physiological signalling agents" published in Nature Reviews Molecular Cell Biologyin 2020 with 1583 citationsand "Accurate prediction of protein structures and interactions using a three-track neural network"published in science in 2021 with 1384 citations, respectively. Naturejournals were taking leadership in producinghighly citedpapers in protein folding research. Science Mapping

Table 3: Distribution of highly productive organizations

| Affiliations | TP | CT | h-index | Country |
|---|---|---|---|---|
| CNRS Centre National de la RechercheScientifique | 325 | 4911 | 35 | France |
| Chinese Academy of Sciences | 245 | 3596 | 29 | China |
| National Institutes of Health (NIH) | 231 | 5024 | 37 | USA |
| Ministry of Education China | 218 | 3076 | 28 | China |
| University of Cambridge | 175 | 6634 | 36 | UK |
| Inserm | 168 | 3239 | 25 | France |
| Howard Hughes Medical Institute | 155 | 8189 | 42 | USA |
| Harvard Medical School | 142 | 4602 | 35 | USA |
| ConsiglioNazionaledelleRicerche | 137 | 1726 | 22 | Italy |
| University of Chinese Academy of Sciences | 133 | 1850 | 22 | China |
| Note: TP-Total no. of publications, CT-Citations | | | | |

Science mapping is a multifaceted-bibliometric tool to analyze and examine scientific output (28). Thisbibliometrics method uses computational techniquesto analyze the citation data quantitatively, classify them, and visualize the interrelationships between bibliographic objects, and also establish the network links, clusters, overarching structure, evolution of research themes and research fronts, and geographic spread of the body image research (33). In this study, we used VOSviewer software to study the network visualization ofco-author-

ship in relationships with countries, co-occurrence of keywords, and co-citation analysis of documents, authors and organizations.

***Co-authorship network analysis***

The co-authorship method is one of the most verifiable methods to quantify and examine scientific collaboration (34). Figure 3 shows the network visualization of co-authorship analysis with the countries. The circle signifies a country/region, and the size of each circle symbolizes the number of publications of each country, indicating the activity of the country/region. The lines between circles represent the cooperative relationship between two countries/regions. The study considered the criteria of a minimum of 5 papers with 5 citations. As a result, 76 countries met the threshold of 175 countries.These are grouped into 8 clusters,forming8256 total link strength.TheUSAhasthe highest link strength (2713), followed by the UK(1362), Germany (1342), China (884) and France (804).

Table 4: Highly Cited Documents

| Title/Authors | Year | Source Title | Cited by |
|---|---|---|---|
| Highly accurate protein structure prediction with AlphaFold by Jumper J.; Evans R.; Pritzel A.; Green T.; Figurnov M.; Ronneberger O.; Tunyasuvunakool K.; Bates R.; Žídek A.; Potapenko A.; Bridgland A.; Meyer C.; Kohl S.A.A.; Ballard A.J.; Cowie A.; Romera-Paredes B.; Nikolov S.; Jain R.; Adler J.; Back T.; Petersen S.; Reiman D.; Clancy E.; Zielinski M.; Steinegger M.; Pacholska M.; Berghammer T.; Bodenstein S.; Silver D.; Vinyals O.; Senior A.W.; Kavukcuoglu K.; Kohli P.; Hassabis D. | 2021 | Nature | 7366 |
| Reactive oxygen species (ROS) as pleiotropic physiological signalling agents by Sies H.; Jones D.P. | 2020 | Nature Reviews Molecular Cell Biology | 1583 |
| Accurate prediction of protein structures and interactions using a three-track neural network by Baek M.; DiMaio F.; Anishchenko I.; Dauparas J.; Ovchinnikov S.; Lee G.R.; Wang J.; Cong Q.; Kinch L.N.; Dustin Schaeffer R.; Millán C.; Park H.; Adams C.; Glassman C.R.; DeGiovanni A.; Pereira J.H.; Rodrigues A.V.; Van Dijk A.A.; Ebrecht A.C.; Opperman D.J.; Sagmeister T.; Buhlheller C.; Pavkov-Keller T.; Rathinaswamy M.K.; Dalwadi U.; Yip C.K.; Burke J.E.; Christopher Garcia K.; Grishin N.V.; Adams P.D.; Read R.J.; Baker D. | 2021 | Science | 1364 |
| AlphaFold Protein Structure Database: Massively expanding the structural coverage of protein-sequence space with high-accuracy models by Varadi M.; Anyango S.; Deshpande M.; Nair S.; Natassia C.; Yordanova G.; Yuan D.; Stroe O.; Wood G.; Laydon A.; Zídek A.; Green T.; Tunyasuvunakool K.; Petersen S.; Jumper J.; Clancy E.; Green R.; Vora A.; Lutfi M.; Figurnov M.; Cowie A.; Hobbs N.; Kohli P.; Kleywegt G.; Birney E.; Hassabis D.; Velankar S. | 2022 | Nucleic Acids Research | 1278 |

Scholarly publication on protein folding

| | | | |
|---|---|---|---|
| Cellular Senescence: Defining a Path Forward by Gorgoulis V.; Adams P.D.; Alimonti A.; Bennett D.C.; Bischof O.; Bishop C.; Campisi J.; Collado M.; Evangelou K.; Ferbeyre G.; Gil J.; Hara E.; Krizhanovsky V.; Jurk D.; Maier A.B.; Narita M.; Niedernhofer L.; Passos J.F.; Robbins P.D.; Schmitt C.A.; Sedivy J.; Vougas K.; von Zglinicki T.; Zhou D.; Serrano M.; Demaria M. | 2019 | Cell | 995 |
| Deep Mutational Scanning of SARS-CoV-2 Receptor Binding Domain Reveals Constraints on Folding and ACE2 Binding by Starr T.N.; Greaney A.J.; Hilton S.K.; Ellis D.; Crawford K.H.D.; Dingens A.S.; Navarro M.J.; Bowen J.E.; Tortorici M.A.; Walls A.C.; King N.P.; Veesler D.; Bloom J.D. | 2020 | Cell | 978 |
| Highly accurate protein structure prediction for the human proteome by Tunyasuvunakool K.; Adler J.; Wu Z.; Green T.; Zielinski M.; Žídek A.; Bridgland A.; Cowie A.; Meyer C.; Laydon A.; Velankar S.; Kleywegt G.J.; Bateman A.; Evans R.; Pritzel A.; Figurnov M.; Ronneberger O.; Bates R.; Kohl S.A.A.; Potapenko A.; Ballard A.J.; Romera-Paredes B.; Nikolov S.; Jain R.; Clancy E.; Reiman D.; Petersen S.; Senior A.W.; Kavukcuoglu K.; Birney E.; Kohli P.; Jumper J.; Hassabis D. | 2021 | Nature | 914 |
| Site-specific glycan analysis of the SARS-CoV-2 spike by Watanabe Y.; Allen J.D.; Wrapp D.; McLellan J.S.; Crispin M. | 2020 | Science | 866 |
| ColabFold: making protein folding accessible to all by Mirdita M.; Schütze K.; Moriwaki Y.; Heo L.; Ovchinnikov S.; Steinegger M. | 2022 | Nature Methods | 811 |
| The Unfolded Protein Response and Cell Fate Control by Hetz C.; Papa F.R. | 2018 | Molecular Cell | 802 |

***Co-citation network analysis***


Figure 3: Co-authorship network analysis

The co-citation analysis discloses the frequency at which other scholarly articles have cited two publications together, presenting important information regarding the interconnectedness within the literature(Ki, 2023). In this study, the co-citation map includes at least fifty references that appear in the bibliographies of the 12515 publications focused on protein folding. 370cited references met the established co-citation frequency threshold.We found 6 clusters indicated in colours with a total link strength is 22875. Figure 4 shows the network map of the co-citation of references. The circle size represents the number of times the cited

references collaborate,as appears commonlyin the number of citing papers. The larger a circle, the more often vital co-citation seems. The author Walter P. received the highest number of citations (204) with top link strength of 754, followed by Hartl F.U., having 181 citations with 663 link strength. Authors such asAnfisenC.B.andKabsch W. secured 3rdand 4th positions in co-citation network analysis, having 177 and 170 citations with 569 and 488 link strengths, respectively.

### *Co-occurrence of keywords network analysis*

Keywords were grouped into 5clusters with total link strength of 189379. Figure 5depicts a network map of all keywords within the research papersselected for the study. The width of the network lines reflects the intra-relationship among the keywords, i.e., the thicker the network line, the stronger the association. The keywords that appeared most were 'Protein folding'with an occurrence of 10687 and a total link strength of 258779, followed by 'metabolism' (112155;7222), protein expression (72061;2363) and 'protein confirmation'(67249;2642). Other frequently used keywords which are thematically associated are protein structure, protein binding, protein function, protein domain, aminoacid sequence, molecular dynamics, chaperone, gene expression, protein-protein interaction, gene expression, protein aggregation, physiology, protein secondary structure, binding site, protein misfoldinganddrug effect.


Figure 4: Co-citation network analysis


Figure 5: Co-occurrence network of keywords

## Conclusion

Here, we employed both quantitative and qualitative approaches to describe the research trend in protein folding,covering data from 2018 to 2022.The study examined 12515 scientific productions retrieved from the Scopus database. The finding of the study reveals that although a good number of papers published during the study, but the number of publications has been decreasing from 2018 to 2022. The USA has contributed the most papers during the study, and an author named Uversky, V.N from the country has contributed the most. In contrast, the highest number of papers has been published by a France-affiliated organization called CNRS. The co-author network analysis tells that the total strength of the co-authorship links of a given researcher with other researchers was highest in the case of the USA, followed by UK, Germany and China. The most used keyword is 'protein folding',asreporteddur-ing the study period.

### *Strengths and limitations*

Here we have provided an overview of the current literature on 'Protein folding', by analyzingthe information about authors, publishers, publication year, and the number of citations and predicted the current hot topics and the trendsfrom them. In this study, we collected

the data only from Scopus and a specific period. However, there is enough scope for further studies using different metrics on this emerging study area. Even results representation will be different if other databases are also considered.

***Conflicts of Interest***

The author declares no conflict of interest.

**References**

1 Torrisi, M., Pollastri, G., & Le, Q. (2020). Deep learning methods in protein structure prediction. Computational and Structural Biotechnology Journal, 18: 1301–1310. https://doi.org/10.1016/j.csbj.2019.12.011

2 Nunes, E. A., Colenso-Semple, L., McKellar, S. R., Yau, T., Ali, M. U., Fitzpatrick-Lewis, D., Sherifali, D., Gaudichon, C., Tomé, D., Atherton, P. J., Robles, M. C., Naranjo-Modad, S., Braun, M., Landi, F., & Phillips, S. M. (2022). Systematic review and meta-analysis of protein intake to support muscle mass and function in healthy adults. Journal of Cachexia, Sarcopenia and Muscle, 13(2): 795–810. https://doi.org/10.1002/jcsm.12922

3 Agirrezabala, X., Samatova, E., Macher, M., Liutkute, M., Maiti, M., Gil-Carton, D., Novacek, J., Valle, M., & Rodnina, M. V. (2022). A switch from α-helical to β-strand conformation during co-translational protein folding. The EMBO Journal, 41(4): 1–13.https://doi.org/10.15252/embj.2021109175

4 Onuchic, J. N., & Wolynes, P. G. (2004). Theory of protein folding. Current Opinion in Structural Biology, 14(1): 70–75. https://doi.org/10.1016/j.sbi.2004.01.009

5 Hong, H., Choi, H., & Yoon, T. (2022). Untangling the complexity of membrane protein folding. Current Opinion In Structural Biology, 72: 237-247. https://doi.org/10.1016/j.sbi.2021.11.013

6 Minkyung Baek et al(2021).Accurate prediction of protein structures and interactions using a three-track neural network. Science876:373,871-.DOI:10.1126/science.abj8754

7 Laganowsky, A., Clemmer, D. E., & Russell, D. H. (2022). Variable-Temperature Native Mass Spectrometry for Studies of Protein Folding, Stabilities, Assembly, and Molecular Interactions. Annual Review of Biophysics, 51: 63–77. https://doi.org/10.1146/annurev-biophys-102221-101121

8 Windheim, J., Colombo, L., Battajni, N. C., Russo, L., Cagnotto, A., Diomede, L., Bigini, P., Vismara, E., Fiumara, F., Gabbrielli, S., Gautieri, A., Mazzuoli-Weber, G., Salmona, M., & Colnaghi, L. (2022). Micro- and Nanoplastics' Effects on Protein Folding and Amyloidosis. International Journal of Molecular Sciences, 23(18): 1–13. https://doi.org/10.3390/ijms231810329

9 Winklhofer, K. F., Tatzelt, J., & Haass, C. (2008). The two faces of protein misfolding: Gain- and loss-of-function in neurodegenerative diseases. EMBO Journal, 27(2): 336–349. https://doi.org/10.1038/sj.emboj.7601930

10 Housmans, J. A. J., Wu, G., Schymkowitz, J., & Rousseau, F. (2023). A guide to studying protein aggregation. FEBS Journal, 290(3): 554–583. https://doi.org/10.1111/febs.16312

11 Schlebach, J. P., Narayan, M., Alford, C., Mittendorf, K. F., Carter, B. D., Li, J., & Sanders, C. R. (2015). Conformational Stability and Pathogenic Misfolding of the Integral Membrane Protein PMP22.

Journal of the American Chemical Society, 137(27): 8758–8768. https://doi.org/10.1021/jacs.5b03743

12 Veeman, D., Dhamodharan, D., Surendhar, G. J., Natrayan, L., Stalin, B., Ramaswamy, S., Jule, L. T., & Krishnaraj, R. (2022). Systematic review on nine hallmarks of neurodegenerative disease. Indian Journal of Biochemistry and Biophysics, 59(3): 249–257.

13 Santos, L., Nascimento, R., Duarte, A., Railean, V., Amaral, M. D., Harrison, P. T., Gama-Carvalho, M., & Farinha, C. M. (2023). Mutation-class dependent signatures outweigh disease-associated processes in cystic fibrosis cells. Cell and Bioscience, 13(1): 1–22. https://doi.org/10.1186/s13578-023-00975-y

14 Varadharajan, V., Ganapathi, S. T., & Mandal, S. K. (2022). Prediction of protein-protein interaction networks and druggable genes associated with parkinson's disease. Indian Journal of Biochemistry and Biophysics, 59(1): 39–49. https://doi.org/10.56042/ijbb.v59i1.31808

15 Choudhury, M., Sharma, D., Das, M., & Dutta, K. (2022). Molecular docking studies of natural and synthetic compounds against human secretory PLA2 in therapeutic intervention of inflammatory diseases and analysis of their pharmacokinetic properties. Indian Journal of Biochemistry and Biophysics, 59(1): 33–38. https://doi.org/10.56042/ijbb.v59i1.27977

16 Jiang, F., Bian, J., Liu, H., Li, S., Bai, X., Zheng, L., Jin, S., Liu, Z., Yang, G.-Y., & Hong, L. (2023). Creatinase: Using Increased Entropy to Improve the Activity and Thermostability. The Journal of Physical Chemistry B, 127(12): 2671-2682. https://doi.org/10.1021/acs.jpcb.2c08062

17 Dill, K. A., & MacCallum, J. L. (2012). The protein-folding problem, 50 years on. Science, 338(6110): 1042–1046. https://doi.org/10.1126/science.1219021

18 Kubelka, J., Hofrichter, J., & Eaton, W. A. (2004). The protein folding "speed limit." Current Opinion in Structural Biology, 14(1): 76–88. https://doi.org/10.1016/j.sbi.2004.01.013

19 Ellegaard, O., & Wallin, J. A. (2015). The bibliometric analysis of scholarly production: How great is the impact? Scientometrics, 105(3): 1809–1831. https://doi.org/10.1007/s11192-015-1645-z

20 Zyoud, S. H., Koni, A., Al-Jabi, S. W., Amer, R., Shakhshir, M., Al Subu, R., Salameh, H., Odeh, R., Musleh, S., Abushamma, F., & Abu Taha, A. (2022). Current global research landscape on COVID-19 and cancer: Bibliometric and visualization analysis. World Journal of Clinical Oncology, 13(10): 835–847. https://doi.org/10.5306/wjco.v13.i10.835

21 Hossain, M., Sarwar, S. A., Lisako, E., Mckyer, J., & Ma, P. (2020). Applications of artificial intelligence technologies in COVID-19 research: A bibliometric study. Preprints 2020. https://doi.org/10.20944/preprints202006.0161.v1

22 Abumalloh, R. A., Nilashi, M., Yousoof Ismail, M., Alhargan, A., Alghamdi, A., Alzahrani, A. O., Saraireh, L., Osman, R., & Asadi, S. (2022). Medical image processing and COVID-19: A literature review and bibliometric analysis. In Journal of Infection and Public Health,15(1): 75–93. Elsevier Ltd. https://doi.org/10.1016/j.jiph.2021.11.013

23 Mejia, C., Wu, M., Zhang, Y., & Kajikawa, Y. (2021). Exploring Topics in Bibliometric

Research Through Citation Networks and Semantic Analysis. Frontiers in Research Metrics and Analytics, 6(September): 1–16. https://doi.org/10.3389/frma.2021.742311

24 Majumder, N., Chaudhari, S. P., Pandya, M., Bhatt, A., & Trivedi, D. (2021). Measuring the Global Research Output and Visualization on Gender Equality: A Bibliometric Analysis. Library Philosophy and Practice,pp1–21. https://doi.org/10.2139/ssrn.3915981

25 Osareh, F. (1996). Bibliometrics, citation analysis and co-citation analysis: A review of literature II. Libri, 46(4): 217–225. https://doi.org/10.1515/libr.1996.46.4.217

26 Willett, P. (2007). A bibliometric analysis of the Journal of Molecular Graphics and Modelling. Journal of Molecular Graphics and Modelling, 26(3): 602–606. https://doi.org/10.1016/j.jmgm.2007.03.008

27 Baskaran, C., & Sivakami, N. (2014). Swine Influenza Research Output: a Bibliometric Analysis. Journal of Information and Knowledge, 51(1): 13–20.

28 Cobo, M. J., López-Herrera, A. G., Herrera-Viedma, E., & Herrera, F. (2011). Science mapping software tools: Review, analysis, and cooperative study among tools. Journal of the American Society for Information Science and Technology, 62(7): 1382–1402. https://doi.org/10.1002asi.21525

29 Moral-muñoz, J. A., Herrera-viedma, E., Santisteban-espejo, A., Cobo, M. J., Herrera-viedma, E., Santisteban-espejo, A., & Cobo, M. J. (2020). 77520-Texto del artículo-249046-3-10-20200304.pdf. El Profesional de La Informa- Ción, 29: 1–20.

30 Rojas-Sánchez, M. A., Palos-Sánchez, P. R., & Folgado-Fernández, J. A. (2022). Systematic literature review and bibliometric analysis on virtual reality and education. In Education and Information Technologies. Springer US. https://doi.org/10.1007/s10639-022-11167-5

31 Cucari, N., Montera, R., & Profita, S. (2023). A bibliometric performance analysis of publication productivity in the corporate social responsibility field : Outcomes of SciVal analytics. Corporate Social Responsibility and Environmental Management, 30(1): 1–16. https://doi.org/10.1002/csr.2346

32 Donthu, N., Kumar, S., Mukherjee, D., Pandey, N., & Lim, W. M. (2021). How to conduct a bibliometric analysis: An overview and guidelines. Journal of Business Research, 133(March): 285–296. https://doi.org/10.1016/j.jbusres.2021.04.070

33 Andersen, N., & Swami, V. (2021). Science mapping research on body image : A bibliometric review of publications, 2004–2020. Body Image,. 38: 106–119. https://doi.org/10.1016/j.bodyim.2021.03.015

34 Ullah, M., Shahid, A., ud Din, I., Roman, M., Assam, M., Fayaz, M., Ghadi, Y., & Aljuaid, H. (2022). Analyzing Interdisciplinary Research Using Co-Authorship Networks. Complexity, 2022. https://doi.org/10.1155/2022/2524491

Current Trends in Biotechnology and Pharmacy
Vol. 18(2) 1725-1735, April 2024, ISSN 0973-8916 (Print), 2230-7303 (Online)
DOI: 10.5530/ctbp.2024.2.21



# Mapping of Global Research Performance on Molecular Docking: A Bibliometric Study

**Atul Bhatt[1], SK Panda[1], SP Chaudhari[1], Manohar Pathak[1]*, Aparna Satapathy[2] & NK Prasanna[3]***

[1]Department Library and Information Science, Gujarat University, Gujarat, Ahmedabad 380009, India
Maharshi Dayananda Saraswati University, Ajmer-305009, Rajasthan.
[3]CSIR- National Institute of Information and Policy Research, Pusa Campus, New Delhi-110012, Delhi, India
Email: -manoharpathak@gmail.com; prasanna@niscpr.res.in

**Abstract**

The paper examines the global scientific literature on Molecular Docking (MD). MDis a keyapproachusedinbioinformatics to identify and developnovel compounds towards drug discovery.This study uses the bibliometric method to analyze scientific data covered in the Scopus database from 2013 to 2022 using MS Excel,R Studio, andVOS Viewer software.A total of 12173 documents on Molecular Docking were retrieved and considered for the study. The paper provides an in-depth evaluation of the research output of MD. The research found that MuthuS.was a most prolific author in MD scientific research, with 98 publications that received 1481 global citations. The most productivecountries in this field areIndia (4020 publications), followedbyChina (2675 publications), Saudi Arabia (1362 publications) and Egypt (1071 publications). The hot keywords in MD research are molecular modelling, molecular docking simulation, unclassified drug and controlled study, but Molecular Docking is the burning author keyword. The finding also shows that the publications are increasing consistently from 2013onwards.Most articles have been published in the 'Journal of Molecular Structure'. As it is an emerging and a trending topic, it has scope for further studies. This studywillbenefit future researchers and practitioners worldwide in understanding the research pattern on MD and identifying the other key areas related to the topic.

**Keywords:**Molecular Docking, Bibliometrics, Bibliometrix,Protein-Ligand Interaction, Drug design.

## Introduction

Molecular Docking is a computer-assisted drug design model and a vital tool for drug discovery towards predicting the binding affinity between receptors and ligands1,2. During docking"lock and key model" (Figure 1A), which refers to the internal geometry of the receptor and the ligand to find the correct orientation for the "key" to open up the "lock" kept fixed3. The real flexible docking process (Figure 1B) in which the receptor and ligands change their conformation to fit each other is called an"induced fit model"(1,4).

Molecular docking simulations are generally used for reproducing the experimental data through docking validations algorithms, where protein-protein or protein-ligand conformations are obtained by using in silico method (5). Docking is one of the main toolsfor virtual screening procedures. By using this method a library of several compounds is "docked" alongside one drug target and proceeds to the best hit (6).

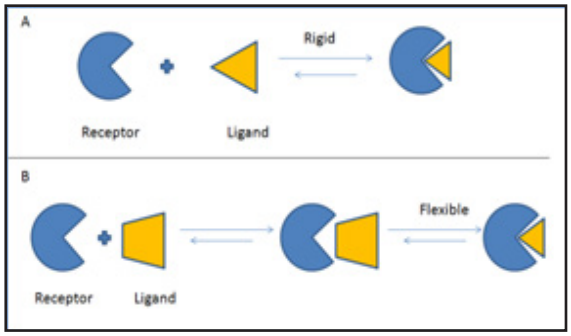


Figure 1:MolecularDockingModels: (A) A lock-and-key model (B) Induced fit model

It is a structure-based drug-designing method that generally stimulates molecular interaction for predicting the binding modeusingshape and electrostatic interactions like van der Waals &Coulombic interactions (1, 7, 8). The sum of all these interactions is calculated by a docking score (9). Various MD software is available to find the best orientation and optimal conformation according to pre-organization and specific complementarity with a definite algorithm, followed by a scoring function to calculate the binding affinity (10,11). The most widely used MD software is Flex X: fragmentation algorithm, Gold: genetic algorithm, Glide: Exhaustive Systematic search, AutoDock: genetic algorithm & Lamarckian genetic algorithm, ZDOCK: Geometric complementarity & molecular dynamics, RDOCK: genetic algorithm, MC (monte carlo) & MIN (Simplex minimization, LeDOCK: Simulated annealing (SA) & Genetic algorithm (GA) followed by AutodockVina: GA genetic algorithm (9). The three main distinct forms of MD are Rigid Docking, Flexible-rigid Docking, and Flexible (soft) Docking. The most widely used software is Flexible-rigid Docking because of its accuracy1. We can analyze the interactive mode of protein-DNA docking with the help of AutodockVina, which is displayed in PyMOL (1, 12, 13) Figure 2 shows the flow chart of the Process of Molecular Docking (14).

Since the 1980s, the molecular docking approach has been widely used to predict the interaction between two proteins, identify the

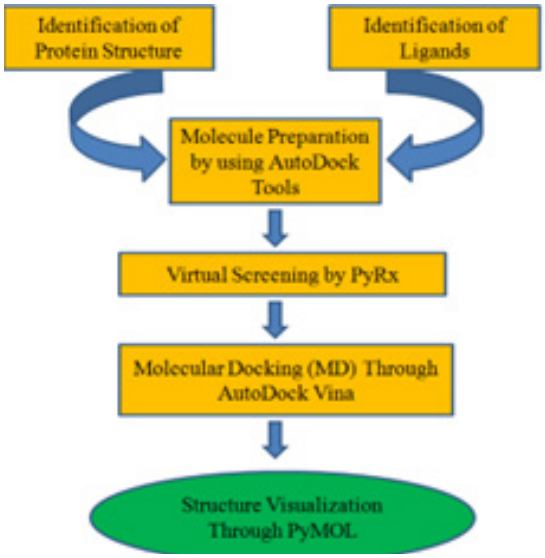


Figure 2: Process of Molecular Docking

ligand binding pocket, and predict the interaction(s) between a protein and a small molecule (15). Now a day's, the development of drug discovery computational docking simulation is the need of today's research (16,17). The impact of molecular Docking is well recognized and established in pharmaceutical industries. Day by day, molecular docking-based virtual screening is growing and significantly enhanced towards the recognition of new lead candidates (18). This paper analyzed the global literature on Molecular Docking (MD) conducted in the last ten years, from 2013 to 2022, using bibliometric methods. Review of Literature

MD research started in the early 1980's, with the establishment of the Molecular Graphics Society in 1982. The major role of Society is to support anddevelop research towards designing bioactive molecules (Willett, 2007). In 2016, Agarwal and Mehrotra reported thatMD helps to form a stable complex by predicting the preferred binding orientation of the ligand to the receptor using novel computational tools and techniques.It aims to attain an optimized docked conformer for ligand and receptor molecules (15,19) in their study discussedthecommonly applied methods in computational biolo-

gy, drug design, computational chemistry, and material science. Computer-aided drug design and discovery (CADDD) plays a major role towards drug discovery and development (19). The use and application of computational methods have facilitated the proliferation of biological databases and become an early driving force for developing MD techniques towards drug designing (20). Molecular Docking is the future of medicinal research as reported recently (21).

This study tries to assess global works of literature on MD using bibliometrics methods based on data retrieved from the Scopes. In 1963, Pritchard stated that bibliometrics is the application of mathematical and statistical methods for quantitative data analysis that extracts patterns from publications such as the growth of publication, journal impact, citations patterns, authorship in the literature, and so on (22,23,24). Bibliometrics comprises a set of methods to examine or measure books, articles and other publications. In recent decades, Bibliometrics has been considered a standard science policy and research management tool (25) It is generally applied to scientific fields to quantitatively measure the various aspects of literature like subject, author, citations, affiliation, country, etc. (26). The study identifies the prominent and impactful(a)authors, (b)geographic regions, (c)research institutions, (d) scholarly documents, (e)significant keywords and research topics, (f) highly cited countries, (g)most publishing sources that have been highly influential in the field over the last ten years. Bibliometric indicators like authorship patterns, citation statistics, and bibliometric techniques are useful for decision-making and tracking the evolution of science and technology (27,28). For specific scientific research, bibliometric studies comprehensively assess and help to identify the number and distribution of publications related to authorship, co-authorship, most cited articles etc.Overthe past few decades, several bibliometric and scientometric approaches have been adopted by researchers to study computational researchin different areas (29). But there isno bibliometric studies have been conducted on Molecular Docking yet. This paper is entirely new and innovative.The main objectives of this study are to provide a systematic overview of MD by employing the bibliometrics methods based on information retrieved from the Scopes database.

***Objective of the study***

The study aims to analyze the global research output on MDbetween 2013 and 2022. Several parameters, such as year-wise growth of publications, authorship patterns, author's keywords and citations, are assessed (30). Th following are the main objectives:

To study the type of research publications and their year-wise growth, To analyze the research trends of MD geographically, To identify the most prolific authors,productivesourcesandtitlesin MD research, To state the mostwidely used keywords in MD research, To assess the worldwide collaborations and institutions in MD research output, and, To visualize the co-authorship, co-citation and co-occurrence networks and map the relationships among the bibliographic entities.

**Methodology**

The sample dataset for the study was collected from the Scopus database in the third week of February 2023. The database Scopus was chosen because it is the oldest and most comprehensive database of records of citation indexes that itself uses an inbuilt analysis tool. The keyword "Molecular Docking"was used as the search string and qualified with the 'title' tag. The instant result was then restricted and downloaded from 2013 to 2022, as the authors felt that the ten years of data were sufficient for viewing the results appropriately and justice to the present study. Subsequently, the data are analyzed using MS Excel and Bibliometrix (R package) to understand the research performance. For science mapping or network visualization, we usedVOSViewer (31, 32).The stage-wise methodologies are shown in figure 3

## Result and Discussions

The result discussed in part: (a) performance analysis and (b) science mapping. The performance analysis examines the characteristics of the publications and the perception of quality using different tools and techniques. The performance analysis accounts for the publication patterns, contribution and productivity of the research in the given field of study. In contrast, science mapping focuses on the relationship between research constituents(Chen et al., 2022; Cobo et al., 2015). It identifies how authors, disciplines, and studies are related to one another and their evolutionary significance. The mapping analysis illustrates the thematic links by examining the co-occurrences of keywords, co-authorship, co-citation etc.(Cobo et al., 2015; Moral-muñoz et al., 2020; Rojas-Sánchez et al., 2022)

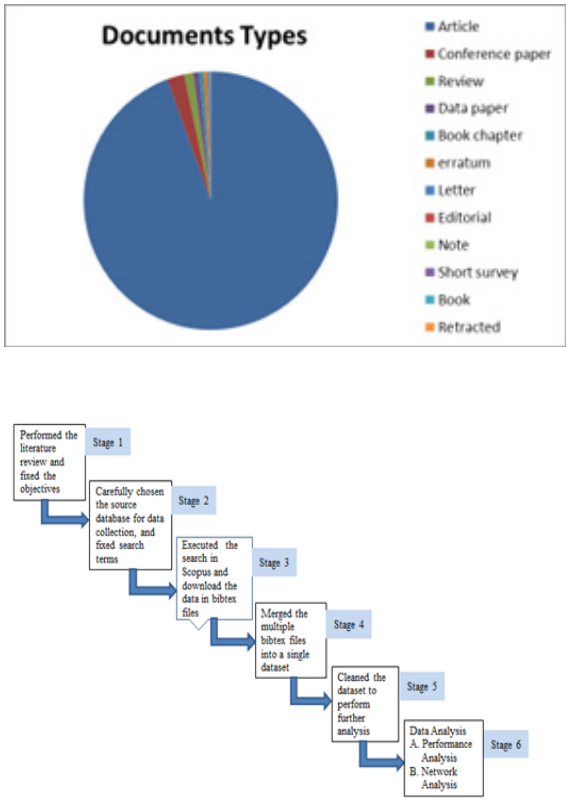


Figure 3: Flowchart of Methods applied to conduct the bibliometric study

### *Performance analysis*

Performance analysis is the easiest way to conduct a bibliometric study. It presents the performance of different research constituents, such as authors, institutes, countries, journals and citations (33). In Performance analysis, we aim to evaluate the different parameters' productivity and popularity based on bibliographic data considered for this study using the metrics such as publication count, citation rates and their impacts as the key performance indicators (34).

### *Distribution of document type, annual scientific production and country-wise scientific production*

A total of 12172 publications on Molecular Docking were identified from the Scopus database between 2013 and 2022. The summary of the findings shows that these articles were published in 1501 journals and had a total of 20629 keywords, followed by 33466 authors who authored these documents. The type of documents included 11493 (94.41%) research articles, 269 (2.21 %) conference papers, 140 (1.15 %) review articles, 114 (0.94%) other forms of publications, including the book, book chapter, data papers, editorial papers, erratum, letter and short review as shown in Figure 3.

Table 1 provides year-wise scientific production and citation impact from 2013 to 2022. There was a consistent rise in publications from 2013 to 2022. The highest 3315 (27.23%) number of papers were published in 2022, followed by 2219 (18.22%) papers in 2021, 1669 (13.71%) papers in 2020 and 1186 (9.74%) papers in 2019. The data indicates that most of the articles were published in the last four years, from 2019 to 2022. The average annual growth rate is 29.70%. The citations increased significantly over the study period, and the highest number of citations was received in 2022. In contrast, an average citation per year (ACPP) was the maximum in 2015 (22.79), followed by 2022 (20.41), 2013 (19.51) and lowest in 2021 (6.85). However, the citation rate (CR)

was highest reported in 2015 (95.59) and the lowest in 2022 (51.89).

Figure 4 shows the top ten countries in terms of scientific research publications on MD. The data reflects that India has published the highest number of 4029 papers, which is 33% of total publications in the MD domain under the study, followed by China with 2675 papers, Saudi Arabia with 1368 papers and Egypt with 1075 papers. At the same time, developing countries like the USA have ranked eighth position in the row.

### *Distribution of most prolific authors and author's productive life*

Table 1: Year-wise Publications and citation impact

| Year | TP | TC | h-Index | CR |
|---|---|---|---|---|
| 2013 | 328 | 6399 | 41 | 93.9 |
| 2014 | 401 | 7792 | 44 | 94.51 |
| 2015 | 544 | 12400 | 52 | 95.59 |
| 2016 | 695 | 12245 | 46 | 94.24 |
| 2017 | 840 | 15059 | 47 | 94.64 |
| 2018 | 975 | 15345 | 45 | 95.28 |
| 2019 | 1186 | 15989 | 46 | 91.99 |
| 2020 | 1669 | 19564 | 49 | 91.31 |
| 2021 | 2219 | 15195 | 63 | 83.42 |
| 2022 | 3315 | 67663 | 38 | 51.89 |

Table 2 indicates the top ten most productive authors on MD Research. It is observed that the highest number of papers are published by 'Muthu, S.' from India and are associated with Arignar Anna Government Arts College. He authored 98 articles with an h-index of 22, 15.11 g-index and received 1481 citations. The second prominent author, ' Taha, M', from Imam Abdulrahman Bin Faisal University, Saudi Arabia, published 83 articles with 28 h-index, 27.33 ACPP and has received the highest 2269 citations. 'Wadood, A.' and 'Rahim, F.' both from Pakistan, secured third and fourth positions with 76 and 75 papers. The table aslo shows that four authors from Pakistan secured positions in the top 10 most prolific authors table in the field of MD.

Table 3 discusses the highly productive institutions in terms of publications, total citations, h-Index, average citation per publication, and their geographic locations. The data shows that the King Saud University of South Arabia was leading in the domain, followed by the Ministry of Education China and the National Research Centre from Egypt in 2nd and 3rd positions, respectively. Regarding citations, King Saud University also received the highest 6437 citations, with an average citation per paper of 15.47, followed by Cairo University (4203 TC, 17.23 ACPP) and Chinese Al-Azhar University (4135 TC, 17.23 ACPP) in the top three positions. It has also been observed that the most productive institutions in molecular docking research belong to Egypt and Saudi Arabia.

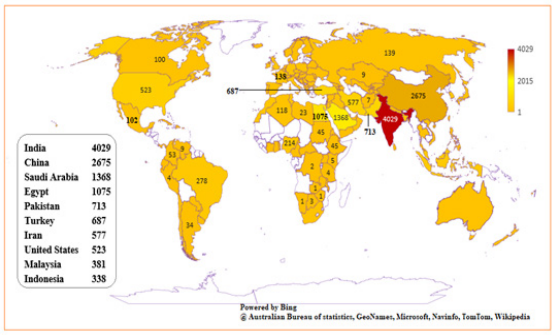


Figure 4: Most productive countries

Table 4 provides the highly productive sources in the MD research with theirPublisher and Scimago ranking. Data exposed that the journal entitled 'Journal of Molecular Structure' (855 total publications, 10111 total citations) was the most productive journal in Molecular Docking research, followed by the 'Journal of Biomolecular Structure and Dynamics' (496 total publications, 4998 total citations), and 'Bioorganic Chemistry' (335 total pub., 7688 total citations). The analysis also discovered that the journal "Molecules" ranked fourth in terms of total publications and total citations (4409 total citations, 7.5 average citations) with an SJR rank

Table 2. Top ten authors the relationship between author, country and institution

| Author Name | TP | TC | h-index | ACPP | Institution | Country |
|---|---|---|---|---|---|---|
| Muthu, S. | 98 | 1481 | 22 | 15.11 | Arignar Anna Government Arts College | India |
| Taha, M. | 83 | 2269 | 28 | 27.34 | Imam Abdulrahman Bin Faisal university, | Saudi Arabia |
| Wadood, A. | 76 | 1828 | 25 | 24.05 | Abdul Wali Khan University Mardan, | Pakistan |
| Rahim, F. | 75 | 1833 | 26 | 24.44 | Hazara University Pakistan | Pakistan |
| Bouachrine, M. | 54 | 306 | 10 | 5.67 | UniversitéMoulay Ismail | Morocco |
| Khan, K.M. | 52 | 1754 | 24 | 33.73 | University of Karachi | Pakistan |
| Saeed, A. | 52 | 826 | 18 | 15.88 | Quaid-i-Azam University, Department of Chemistry | Pakistan |
| Iqbal, J. | 47 | 701 | 17 | 14.91 | COMSATS University Islamabad | Pakistan |
| Hassan, M. | 44 | 693 | 17 | 15.75 | Research Institute at Nationwide Childrens Hospital | USA |
| Khedkar, V.M. | 43 | 662 | 15 | 15.40 | Vishwakarma University | India |

Table 3: Top ten productive institutions

| Affiliation | Country | TP | TC | h-Index | CR | ACPP |
|---|---|---|---|---|---|---|
| King Saud University | Saudi Arabia | 416 | 6437 | 41 | 88.70 | 15.47 |
| Ministry of Education China | China | 279 | 2539 | 25 | 81.72 | 9.10 |
| National Research Centre | Egypt | 279 | 3589 | 32 | 83.15 | 12.86 |
| Cairo University | Egypt | 244 | 4203 | 31 | 90.16 | 17.23 |
| Al-Azhar University | Egypt | 240 | 4135 | 33 | 91.25 | 17.23 |
| College of Pharmacy | Saudi Arabia | 228 | 3995 | 36 | 89.91 | 17.52 |
| College of Sciences | Saudi Arabia | 206 | 2773 | 30 | 86.89 | 13.46 |
| Faculty of Pharmacy | Egypt | 161 | 2801 | 31 | 91.30 | 17.40 |
| University of Karachi | Pakistan | 157 | 2933 | 29 | 89.81 | 18.68 |
| King Abdulaziz University | Saudi Arabia | 151 | 1546 | 21 | 82.78 | 10.24 |

Table 4: Distribution of highly cited sources, their Scimago rank, and Country

| Name of Source Title | Publisher | TP | TC | SJR_2021 | h_index | ACPP |
|---|---|---|---|---|---|---|
| Journal of Molecular Structure | Elsevier | 855 | 10111 | 0.48 | 39 | 15.47 |
| Journal of Biomolecular Structure and Dynamics | Taylor & Francis | 496 | 4998 | 0.561 | 32 | 9.10 |
| Bioorganic Chemistry | Elsevier | 335 | 7688 | 0.728 | 42 | 12.86 |
| Molecules | MDPI | 334 | 4409 | 0.705 | 29 | 17.23 |
| Medicinal Chemistry Research | Springer Nature | 212 | 2146 | 0.357 | 22 | 17.23 |
| Chemistryselect | Wiley-Blackwell | 158 | 838 | 0.407 | 15 | 17.52 |
| SpectrochimicaActa Part a Molecular and Biomolecular Spectroscopy | Elsevier | 154 | 3405 | 0.59 | 32 | 13.46 |
| RSC Advances | Royal Society of Chemistry | 154 | 2681 | 0.667 | 31 | 17.40 |
| Polycyclic Aromatic Compounds | Taylor & Francis | 145 | 227 | 0.228 | 7 | 18.68 |
| Evidence Based Complementary and Alternative Medicine | Hindawi | 141 | 383 | 0.461 | 10 | 10.24 |

of0.705, following the journal 'Bioorganic Chemistry with the highest SJR of 0.728.Elsevier and Taylor &Francisare leading publishers of MD research. Table 5 describes the ten most highly cited papers. The paper, 'Molecular docking and structure-based drug design strategies' by 'Ferreira et al., published in the journal 'Molecules', in 2015, has received the highest number of 864 citations. The second most cited paper 'Software for molecular docking: a review' by 'Pagadala et al., published in 'Biophysical Review', in 2017, has 624 citations,followed by 'Ribavirin, Remdesivir, Sofosbuvir, Galidesivir, and Tenofovir against SARS-CoV-2 RNA dependent RNA polymerase (RdRp): A molecular docking study 'by 'Elfiky A. A., published in 'Life Sciences' has a total of 577 citations and ranked the third position.

Table 5. Highly Cited Documents

| Name of Source Title | TP | TC | SJR_2021 | h_index |
|---|---|---|---|---|
| Journal of Molecular Structure | 855 | 10111 | 0.48 | 39 |
| Journal of Biomolecular Structure and Dynamics | 496 | 4998 | 0.561 | 32 |
| Bioorganic Chemistry | 335 | 7688 | 0.728 | 42 |
| Molecules | 334 | 4409 | 0.705 | 29 |
| Medicinal Chemistry Research | 212 | 2146 | 0.357 | 22 |
| Chemistryselect | 158 | 838 | 0.407 | 15 |
| SpectrochimicaActa Part a Molecular and Biomolecular Spectroscopy | 154 | 3405 | 0.59 | 32 |
| RSC Advances | 154 | 2681 | 0.667 | 31 |
| Polycyclic Aromatic Compounds | 145 | 227 | 0.228 | 7 |
| Evidence Based Complementary and Alternative Medicine | 141 | 383 | 0.461 | 10 |

### *Science mapping*

It is a highly critical method used in bibliometrics analysis to map the scientific output (35). This methodology uses computational techniquestoanalyze the bibliographic objects quantitatively& qualitatively and then visualize their interrelationships. To perform this analysis, we choseVOSviewer software, a highly used-science mapping tool, in order todraw the overarching structure, evolution of research themes and research fronts, and geographic spread of the MD research (36). The VOS Viewer software is mainly used for networking and visualization to understand the research pattern. Further, it exploresthe relationshipofthe authors with countries, the keywords frequently appearing in the papers, and the documents and their citations in terms of total network links, clusters and network strength.

### *Co-authorship network*

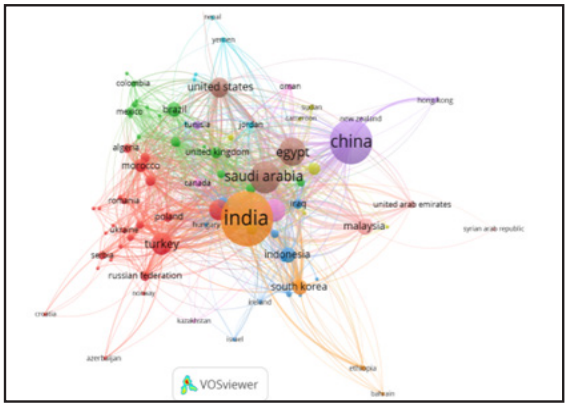


Figure 5: Visualization of co-authorship analysis versus countries

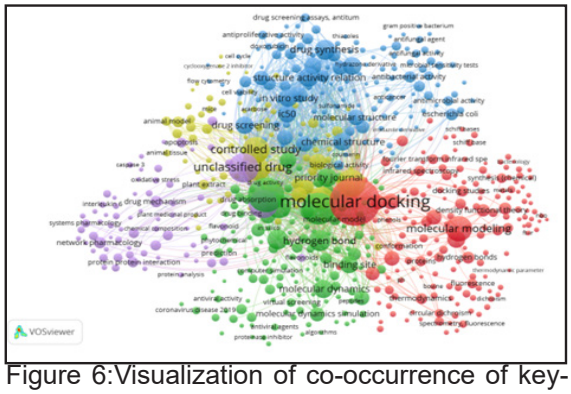

Figure 6:Visualization of co-occurrence of keywords

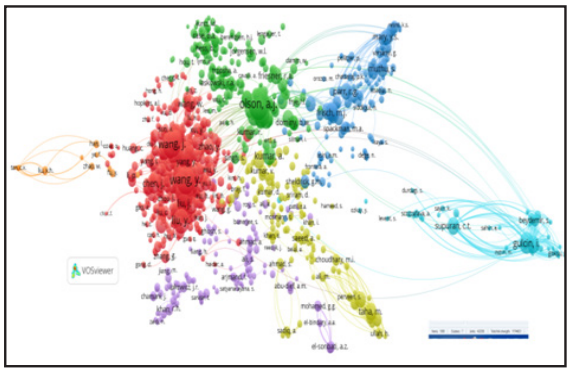

Figure 7: Visualization of co-citation network

Figure 5 plots the co-authorship network versus countries. The circles signify the countries or regions, and the size of the circle symbolizes the number of publications. The links between circles represent the cooperative relationship between two countries/regions. The study considered the criteria of a minimum of 5 papers from the country with 10 citations.Saudi Arabia hasthe highest link strength(2260), followed by India(1665) and Egypt (1098).India secured the firstposition for publishing the most documents, followed by Saudi Arabia and Egypt. Egypt placed in third position receiving 14732 citations after India and Saudi Arabia.

### *Network visualization of co-occurrence of keywords*

Figure6 depicts a network map of all keywords within the research papersselected for the study. The minimum number of occurrences of a keyword is considered to be75. The results show out of a total of 20629 keywords,only 587 keywords met the threshold.The width of the network lines reflects the intra-relationship among the keywords, i.e., the thicker the network line, the stronger the association.The keywords that appeared most were 'Molecular Dockingwith total link strength of 170879,followed by 'unclassified drug' (112155),MD simulation (95466) and 'controlled study'(80694). There are 187 number of clusters of keywords, out of which the most frequently used keywords are Metabolism, Human, Structure activity relation, Molecular dynamics, in vitrostudy, ic50, Neutralizing, binding site, drug screening, structure activity relationship, enzyme inhibition, Drug effects, ligands, Computer model, Molecular dynamic simulation and Drug protein binding.  2.3 Co-citation Network Visualization

Figure 7 shows the network map of co-citation among cited authors. The circle size represents the number of citations in which each author collaborates with another based on the number of co-authors. In general, the larger size of a circle, the more often vital co-citation seems. The author' Olson, A.J.' received the highest number of citations (4464) with top link strength 205881, followed by Wang Y., having 3697  citations with 218016 link strength. Author Wang J and Zhangh Y secured 3rdand 4th positions in co-citation network analysis, having 355 and 3332 citations with 208445 and 190655 link strength, respectively.

## Conclusion

This study performedaquantitative and qualitative analysis of Molecular Dockingresearchovera period of ten years, from 2013 to 2022,to understand the research trends and the contributionsanddistributionsof authors, organizations, countries and journals in the domain. For this study theexperimental data was collected from the Scopus database.Atotalof12172 scientific productions were retrievedduring the study period. The study reveals that most of the MD researchwaspublished in English.Devel-

oped and developing countries like India, China, Saudi Arabia, and Egypt contributed significant researchinMD.Accordingto the study,an author Muthu, S. fromIndia,affiliated with Arignar Anna Government Arts College, dominated the list of publications by publishing 98 documents. The study also finds that most prolific authors belong to India and Saudi Arabia. The article by Ferreira et al., 2015 from the journal MOLECULES has received the highest 864 citations. The authored keyword' Molecular Docking' appeared most, followed by 'Molecular modelling simulation', 'Unclassified Drug' 'Controlled Study', and 'Drug synthesis. The study also discovers that research on MD is increasingexponentially worldwide and collaboratively.The bibliometric study is the most preferred way to measure the productivity of a subject, organization, authors, and source.Still, there is enough scope for further studies on MD because it is an emerging areathat will significantly affect today's Society regarding drug discovery. This study will aid future researchers who wish to undertake bibliometric studies on related domains.

**Conflict of Interest:** There is no conflict of interestrelated to the works in the manuscript.

**References**

1 Fan, J., Fu, A., & Zhang, L. (2019). Progress in molecular Docking. Quantitative Biology, 7(2): 83–89. https://doi.org/10.1007/s40484-019-0172y

2 Ganeshpurkar, A., Chaturvedi, A., Shrivastava, A., Dubey, N., Jain, S., Saxena, N., Gupta, P., & Mujariya, R. (2022). In silico interaction of Berberine with some immunomodulatory targets: A docking analysis. Indian Journal of Biochemistry and Biophysics, 59(8):848–853.https://doi.org/10.56042/ijbb.v59i8.62908

3 Morrison, J. L., Breitling, R., Higham, D. J., & Gilbert, D. R. (2006). A lock-and-key model for protein-protein interactions. Bioinformatics, 22(16): 2012–2019. https://doi.org/10.1093/bioinformatics/btl338

4 Koshland, D. E. (1995). The Key–Lock Theory and the Induced Fit Theory. Angewandte Chemie International Edition in English, 33(23–24): 2375–2378. https://doi.org/10.1002/anie.199423751

5 Sanchez, G. (2006). Protein–Ligand Docking: Current Status and Future Challenges. Proteins: Structure, Function, and Bioinformatics,65(1): 15–26. https://doi.org/10.1002/prot

6 Raquel Dias1 and Walter Filgueira de Azevedo Jr.1, 2. (2008). Molecular Docking Algorithms. Current Drug Targets, 9(12): 1040–1047.

7 Liu, N., Chee, M. L., Niu, C., Pek, P. P., Siddiqui, F. J., Ansah, J. P., Matchar, D. B., Lam, S. S. W., Abdullah, H. R., Chan, A., Malhotra, R., Graves, N., Koh, M. S., Yoon, S., Ho, A. F. W., Ting, D. S. W., Low, J. G. H., & Ong, M. E. H. (2020). Coronavirus disease 2019 (COVID-19): An evidence map of medical literature. BMC Medical Research Methodology, 20(1). https://doi.org/10.1186/s12874-020-01059-y

8 Morris, G. M. (2008). Molecular Docking. Molecular Modelling of Protiens, pp365-382. https://doi.org/10.1007/978-1-59745-177-2

9 Pagadala, N. S., Syed, K., & Tuszynski, J. (2017). Software for molecular Docking: a review. Biophysical Reviews, 9(2):91–102. https://doi.org/10.1007/s12551-016-0247-1

10 Erdogan, T. (2022). Computational evaluation of 2-arylbenzofurans for their potential use against SARS-CoV-2: A DFT, molecular Docking, molecular dynamics simulation study. Indian Journal of Biochemistry and Biophysics, 59(1): 59–72. https://doi.org/10.56042/

ijbb.v59i1.47454

11 Kaur, T., Madgulkar, A., Bhalekar, M., &

Asgaonkar, K. (2018). Molecular Docking in Formulation and Development. Current Drug Discovery Technologies, 16(1):30.39. https://doi.org/10.2174/1570163815666180219112421

12 Briggs, P., Winn, M. D., Bailey, S., & Ashton, A. (2002). Ccp4 Newsletter on Protein Crystallography. Ccp4.Ac.Uk, 4. http://www.ccp4.ac.uk/newsletters/newsletter36.pdf

13 Trott, O., & Olson, A. J. (2009). Software News and Update AutoDock Vina : Improving the Speed and Accuracy of Docking with a New Scoring Function , Efficient Optimization , and Multithreading. https://doi.org/10.1002/jcc

14 Kumar, T. (2021). Molecular Docking Studies of Possible Treatment of Diabetes using Vasicine against Islet Amyloid Polypeptide. International Journal for Research in Applied Science and Engineering Technology, 9(VI): 4202.4209.https://doi.org/10.22214/ijraset.2021.35984

15 Agarwal, S., & Mehrotra, R. (2016). An Overview of Molecular Simulation. JSM Chemistry, 4(2):1024–1028.

16 Rahman, M. M., Karim, M. R., Ahsan, M. Q., Khalipha, A. B. R., Chowdhury, M. R., & Saifuzzaman, M. (2012). Use of computer in drug design and drug discovery: A review. International Journal of Pharmaceutical and Life Sciences, 1(2): 1–21

17 Naresh, P., Shyam Sundar, P., Girija, K., Pradheesh, S. J., Shanthoshivan, A. G., Akashwaran, S., Swaroop, A. K., & Jubie, S. (2021). Drug repurposing of Daclatasvir and Famciclovir as antivirals against dengue virus infection by in silico and in vitro techniques. Indian Journal of Biochemistry and Biophysics, 58(6): 557–564.

18 Bartuzi, D., Kaczor, A. A., Targowska-Duda, K. M., & Matosiuk, D. (2017). Recent advances and applications of molecular Docking to g protein-coupled receptors. Molecules, 22(2): 1–23. https://doi.org/10.3390/molecules22020340

19 Eweas, A. F., Maghrabi, I. A., & Namarneh, A. I. (2014). Advances in molecular modeling and Docking as a tool for modern drug discovery. Der Pharma Chemica, 6(6): 211–228.

20 Song, M., Kim, S., Zhang, G., Ding, Y., & Chambers, T. (2014). Productivity and influence in bioinformatics: A bibliometric analysis using PubMed Central. Journal of the American Society for Information Science and Technology, 65(2): 352–371. https://doi.org/10.1002/asi.22970

21 Ahuja, S., Deep, P., . S., Nair, S., Sambhyal, S., Mishra, D., Pandey, C., Manchanda, P., . K., Dee, A., Kumar, L., Gwalia, P., Arora, R., Singh, B., Attri, S., Singh, D. K., . A., Gupta, M., & Chopra, V. (2022). Molecular Docking; future of Medicinal Research. Ecology, Environment and Conservation, 28(01s):18–18https://doi.org/10.53550/eec.2022.v28i01s.018

22 Barker, K. (2013). Tracing thought through time and space: A selective review of bibliometrics in social work. Bibliometrics in Social Work, 1–34. https://doi.org/10.4324/9780203051467

23 Hicks, D., Wouters, P., Waltman, L., Rijcke, S., & Rafols, I. (2015). Bibliometrics: The Leiden Manifesto for research metrics.Nature, 520: 429-431.https://doi.org/10.1038/520429a

24 Patra, S. K., & Mishra, S. (2006). Bibliometric study of bioinformatics literature. Scientometrics, 67(3):477–489. https://doi.org/10.1556/Scient.67.2006.3.9https://doi.org/10.3329/ijpls.v1i2.12955

25 Hossain, M., Sarwar, S. A., Lisako, E., Mckyer, J., & Ma, P. (2020). Applications of artificial intelligence technologies in COVID-19 research: A bibliometric study.

Preprints. https://doi.org/10.20944/preprints202006.0161.v1

26 Zyoud, S. H., Koni, A., Al-Jabi, S. W., Amer, R., Shakhshir, M., Al Subu, R., Salameh, H., Odeh, R., Musleh, S., Abushamma, F., & Abu Taha, A. (2022). Current global research landscape on COVID-19 and cancer: Bibliometric and visualization analysis. World Journal of Clinical Oncology, 13(10): 835–847. https://doi.org/10.5306/wjco.v13.i10.835

27 Abumalloh, R. A., Nilashi, M., Yousoof Ismail, M., Alhargan, A., Alghamdi, A., Alzahrani, A. O., Saraireh, L., Osman, R., & Asadi, S. (2022). Medical image processing and COVID-19: A literature review and bibliometric analysis. Journal of Infection and Public Health 15: 75–93 https://doi.org/10.1016/j.jiph.2021.11.013

28 Mejia, C., Wu, M., Zhang, Y., & Kajikawa, Y. (2021). Exploring Topics in Bibliometric Research Through Citation Networks and Semantic Analysis. Frontiers in Research Metrics and Analytics, 6(September): 1–16. https://doi.org/10.3389/frma.2021.742311

29 Murillo, J., Villegas, L. M., Ulloa-Murillo, L. M., & Rodríguez, A. R. (2021). Recent trends on omics and bioinformatics approaches to study SARS-CoV-2: A bibliometric analysis and mini-review. Computers in Biology and Medicine, 128(December 2020): 104162. https://doi.org/10.1016/j.compbiomed.2020.104162. https://doi.org/10.56042/ijbb.v58i6.57794

30 Majumder, N., Chaudhari, S. P., Pandya, M., Bhatt, A., & Trivedi, D. (2021). Measuring the Global Research Output and Visualization on Gender Equality: A Bibliometric Analysis. Library Philosophy and Practice, pp1–21. https://doi.org/10.2139/ssrn.3915981

31 Dervis, H. (2019). Bibliometric analysis using bibliometrix an R package. Journal of Scientometric Research, 8(3): 155–160. https://doi.org/10.5530/JSCIRES.8.3.32

32 García-Pascual, V., García-Beltrán, E., & Domenech-Amigot, B. (2022). Eye-Related COVID-19: A Bibliometric Analysis of the Scientific Production Indexed in Scopus. International Journal of Environmental Research and Public Health, 19(16). https://doi.org/10.3390/ijerph19169927

33 Donthu, N., Kumar, S., Mukherjee, D., Pandey, N., & Lim, W. M. (2021). How to conduct a bibliometric analysis: An overview and guidelines. Journal of Business Research, 133:pp285–296. https://doi.org/10.1016/j.jbusres.2021.04.070

34 Cucari, N., Montera, R., & Profita, S. (2023). A bibliometric performance analysis of publication productivity in the corporate social responsibility field : Outcomes of SciVal analytics. 1–16. https://doi.org/10.1002/csr.2346

35 Cobo, M. J., López-Herrera, A. G., Herrera-Viedma, E., & Herrera, F. (2011). Science mapping software tools: Review, analysis, and cooperative study among tools. Journal of the American Society for Information Science and Technology, 62(7):1382–1402. https://doi.org/10.1002/asi.21525

36 Andersen, N., & Swami, V. (2021). Science mapping research on body image : A bibliometric review of publications in Body Image , 2004 – 2020. 38:106–119. https://doi.org/10.1016/j.bodyim.2021.03.015

37 Chen, S., Xu, Z., & Skare, M. (2022). The impact of COVID-19 on the service business industry: insights from a bibliometric review. Total Quality Management and Business Excellence. https://doi.org/10.1080/14783363.2022.2078188

Current Trends in Biotechnology and Pharmacy
Vol. 18(2) 1736-1744, April 2024, ISSN 0973-8916 (Print), 2230-7303 (Online)
DOI: 10.5530/ctbp.2024.2.22



# Molecular Docking Analysis of Christanoate and Christene from *Christia vespertilionis* Plants as Potential Inhibitors of Covid-19

**Suganya Murugesu[1], Tavamani Balan[1], Nurliyana Ismahani Mohd Tamri[1], Lukhman Nul Hakim Zamree[1], Nurul Fathiah Zulkifli Samba[1], Siti Nur Hajar Mohamed Anuar[1], Sharon Fatinathan[1], Vikneswari Perumal[1]**

[1]Faculty of Pharmacy and Health Sciences, Royal College of Medicine Perak, Universiti Kuala Lumpur,30450 Ipoh, Perak,Malaysia.
Corresponding author: vikneswari@unikl.edu.my

**Abstract**

Covid-19 is a global pandemic caused by SARS-CoV-2 virus that caused mortality and world economic collapse. It is almost impossible to break the chain of infection with no intervention except vaccines to prevent worsening symptoms and to build herd immunity in people. Efforts to discover a therapeutic drug to combat the virus are still ongoing. Various medicinal phytoconstituents are also researched for their pharmacological action as antiviral agents against Covid-19. This study explored the antiviral potential of *Christia vespertilionis* bioactive compounds (christene and christanoate) for treating Covid-19 using molecular docking analysis. The Covid-19 protein crystal structures (PDB ID: 6LU7, PDB ID: 6CS2, PDB ID: M1D, PDB ID: 2GHV and PDB ID: 6M71) obtained from the protein data bank were docked to christene and christanoate. The analyses were carried out using the Autodock tool 1.5.6. The control docking was done using favipiravir as the reference drug. The binding interaction of the protein and ligand was observed using the Biovia Discovery visualizer. The binding affinity and interactions indicate that the observed compounds have antiviral action suggesting their potential as Covid-19 inhibitors and can be further considered for therapeutic applications.

**Keywords**: SARS-CoV-2, *Christia vespertilionis*, molecular docking, Covid-19

## Introduction

The outbreak of coronavirus disease (COVID-19) caused a global health emergency at the end of 2019 (1). The RNA virus has caused significant economic and social repercussions providing a significant threat globally (2). According to Chen et al., (3), the virus was most likely transmitted to humans through infected droplets from bats. The majority of those infected with COVID-19 will experience mild to moderate respiratory symptoms and will recover without the need for additional treatment. However, COVID-19 can develop serious illnesses in older people, those suffering from medical conditions such as heart disease, diabetes, chronic pulmonary illness, and cancer. Currently, vaccination has been approved for mass immunization. However, there is decreasing vaccine coverage and an increasing risk of vaccine-preventable disease outbreaks and epidemics due to vaccine hesitancy. Vaccination is perceived as unnecessary by many individuals due to their belief, lack of confidence, and presumed unsafe (4). The key goals to fight against the rapidly evolving virus are developing new therapies or repurposing drugs (5,6).

The SARS-CoV-2 virus belongs to the Coronaviridae family, subfamily coronavirinae and Nidovirales order. It is a protein-sense RNA virus with a single linear RNA segment on a sin-

Current Trends in Biotechnology and Pharmacy
Vol. 18(2) 1736-1744, April 2024, ISSN 0973-8916 (Print), 2230-7303 (Online)
DOI: 10.5530/ctbp.2024.2.22


gle strand. SARS-CoV-2 is a member of Sarbecovirus, which undergo frequent recombination. If there are enough sequenced genomes, building a phylogenetic tree of a virus family's mutation history is possible. The China Centre for Disease Control and Prevention reported five SARS-CoV-2 genomes isolated from Wuhan in early 2020 (7). At the epicentre of the pandemic in Wuhan, SARS-CoV-2 was treated with favipiravir, a therapeutic drug approved for emergency use in Italy as the pandemic expanded through Europe, and it is currently being used in Japan, Russia, Ukraine, Uzbekistan, and Kazakhstan. Favipiravir is a synthetic prodrug found while evaluating the antiviral effectiveness of chemical compounds used to treat influenza strain (A/PR/8/34-H1N1), later identified as T1105. Favipiravir has high bioavailability, protein binding affinity and small distribution volume. It reaches maximum concentration within 2 hours after a single dose. It has a short half-life of 2.5 to 5 hours, leading to rapid renal elimination in the hydroxylated form. Elimination is mediated by aldehyde oxidase and marginally by xanthine oxidase. The pharmacokinetics of favipiravir is dose-dependent as well as time-dependent. The cytochrome P450 system does not metabolize it but blocks one of its components (CYP2C8). As a result, it should be used with caution when coupled with drugs metabolized by the CYP2C8 system (8).

In recent decades, research on the use of medicinal plants for various pharmacological actions has been carried out vastly. Secondary metabolites from plants, such as flavonoids, have been shown to have tremendous bioactivities, including antiviral effects. *Christia vespertilionis* (L.f.) Bakh. F. is an ornamental plant in the Fabaceae family. It is also known as mariposa or butterfly wing for its distinctive trifoliate leaf shape. *C. vespertilionis* is a species native to Southeast Asia and Brazil. This plant has traditionally been used to treat snake bites and facilitate healing in respiratory and tuberculosis cases (9). Furthermore, *C. vespertilionis* is used to treat muscle fatigue, colds, inflamed tonsils, impaired blood circulation, and inflamed bronchitis and to increase blood circulation. According to Bunawan et al., (10), *C. vespertilionis* can treat many diseases and is a viable alternative to modern synthetic medicines. The plant was previously reported to possess antidiabetic activity (11), anti-tumour and antiproliferative activities(12), followed by antimalarial activity (13). Upadhyay et al., (13) reported on the antiplasmodial and antimalarial activities of *C. vespertilionis* roots, leaves, and stems methanolic extracts using *in vitro* and animal model assays. Their study revealed two potential compounds, namely christene and christanoate, with more pharmacological activity to be explored (13,14).

Therefore, this study uses molecular docking analysis to investigate the Covid-19 protein-inhibiting activity of christene and christanoate from *C. vespertilionis*. About five protein structures (PDB ID: 6LU7, PDB ID: 6CS2, PDB ID: 6M1D, PDB ID: 2GHV and PDB ID: 6M71) related to the Covid-19 protein sequence were selected for the analysis.

## Materials & methods

### *Preparation of ligands*

A 3D model of the identified compound was constructed using Chem3D software. The structures and formal charges of the targeted compound were checked through 2D drawing (**Fig. 1**) and subjected to conformational research. Energy minimization was set on all conformers, and the partial charges were automatically calculated. The data obtained was saved in the MDB file for further docking studies.

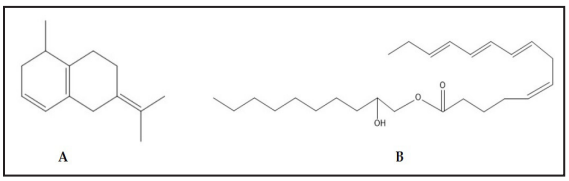


**Fig 1.** A: Christene (7-isopropylidene-1-methyl-1, 2, 6, 7, 8, 9-hexahydronaphthalene) and B: Christanoate (2'- hydroxydecanylpentadec-5, 8, 10, 12-tetraenoate) from *Christia vespertilionis* leaf

### *Optimization of the enzyme active site*

The X-ray crystallographic structure of the proteins displayed in **Fig. 2** (PDB ID: 6LU7, PDB ID: 6CS2, PDB ID: 6M1D, PDB ID: 2GHV and PDB ID: 6M71) was obtained from the Protein Data Bank at https://www.rcsb.org. Hydrogen atoms were added to stabilize the charges of the proteins in their respective standard geometry form. To check errors in atom's type and connection, automatic correction was applied to ease the process. The receptor was selected, and its atom's potential was fixed. All default items were used to search the active site in each enzyme structure with the site finder. The site finder of the pocket was used to create dummy atoms on the enzymes.

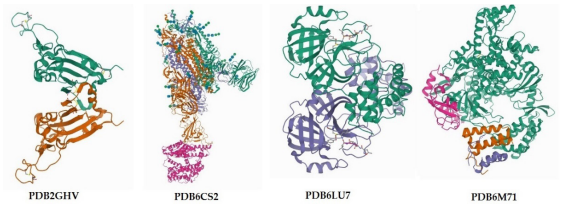


**Fig 2.** The protein structure of SARS-CoV-2; PDB ID: 2GHV, PDB ID: 6LU7, PDB ID: 6CS2, PDB ID: 6M1D, and PDB ID: 6M71

### *Docking analysis*

The docking process between christene and christanoate with the proteins was conducted using AutoDock Tools by uploading the enzyme's active site in PDB file format. Dummy atoms were added and adjusted on the docking site with the program specifications. The active binding site between the ligand and receptor was placed in the centre of the grid box. The grid box size was adjusted up to 126x126x126 to cover all binding sites involved. It was used to calculate the interaction energies between the ligand-receptor interactions. The AutoDock was used to calculate the docking automatically, and each compound's lowest binding energy was selected. The process preceded the study of the illustration of the ligand-receptor interaction in both 2D and 3D structures on the Discovery Studio Visualizer.

The rotatable bonds were set with AutoDockTools, and all torsions can be rotated. Ligand protein tethering was accomplished by adjusting the genetic algorithm (GA) parameters throughout ten runs of the GA criteria. Gasteiger charges were added by default. The maximum grid box size was used with the default spacing. The grid box parameters for X, Y, and Z centres were 142.5142, 131.9530 and 177.2277, respectively. Molecular dynamics (MD) simulations were then applied to multiple conformations of the 6M1D-christanoate complexes. For each compound, the highest-scoring docking poses were selected. Autodock 4.2 and BIOVIA Discovery Studio Visualizer 2021 analyzed the protein-ligand complexes with the lowest binding energy.

## Results and Discussion

All the results are tabulated below with the details on the residues and binding energy that represents the interaction between protein and compounds (christanoate and christene) observed. Based on the results obtained, the binding energy score of the compounds docked indicates the affinity of the compounds towards the protein and its binding site residues. The positive control used in this study is favipiravir prescribed to the Covid 19 patients. Table 1 displayed the interaction of christanoate and christene with the COVID-19 proteins.

PDB ID: 2GHV is the spike protein (S protein) of SARS-CoV targeting the angiotensin-converting enzyme 2 (ACE2) receptors. The positive control, favipiravir, was docked to the residues in Chain E of the receptor where Phe329, Asn330 and Ala331 interacted via hydrogen bonding and other conventional bonding with Thr332, Phe334, Tyr356, Asn357, Thr359, Trp423 and Arg495. The binding energy score of favipiravir was -5.4 kcal/mol, slightly lower than christine (-6.1 kcal/mol) and christanoate (-5.6 kcal/mol). Christene has made only hydrophobic interaction with the chain E residues, namely Arg441, Leu443, Arg444, His445, Asp454, Ser456, Val458, Pro459, Phe460, Ser461,

Table 1. The interaction of christanoate and christene with the COVID-19 proteins

| Proteins (PDB) | Ligands | Hydrogen bond residues | Other residues | Binding affinity (Kcal/mol) |
|---|---|---|---|---|
| 2GHV | favipiravir | Chain E: Phe329, Asn330, Ala331 | Chain E: Thr332, Phe334, Tyr356, Asn357, Thr359, Trp423, Arg495 | -5.4 |
| | Christene | - | Chain E: Arg441, Leu443, Arg444, His445, Asp454, Ser456, Val458, Pro459, Phe460, Ser461, Lys465, Pro466, Cys467, Pro477 | -6.1 |
| | Christanoate | Chain E: Phe329, Arg495 | Chain E: Asn330, Ala331, Thr332, Phe334, Tyr356, Asn357, Ser358, Thr359, Phe360, Phe361, Ser362, Trp423, Asn424, Thr425, Asn427, Ile428 | -5.6 |
| 6LU7 | favipiravir | Chain A: Phe8, Ile106, Phe112, Gln127, Asp153, Thr292 | Chain A: Gln110, Thr111, Asn151, Phe294, Asp295 | -5.4 |
| | Christene | - | Chain A: Phe8, Val104, Ile106, Gln107, Gln110, Asn151, Asp153, Ser158, Phe294 | -6.3 |
| | Christanoate | Chain A: Leu141, Asn142, Gly143, Ser144, Cys145, His163 | Chain A: Thr24, Thr25, Thr26, Leu27, His41, Met49, Tyr54, Phe140, His164, Met165, Glu166, His172, Asp187, Arg188, Gln189 | -5.6 |
| 6CS2 | favipiravir | Chain A: Lys1020<br>Chain B: Glu1013, Lys1020, Arg1021 | Chain A: Glu1013, Ser1019, Arg1021, Val1022<br>Chain B: Ser1019<br>Chain C: Glu1013, Arg1021 | -6.0 |
| | Christene | - | Chain B: Trp101, Ile116, Asn118, Val123, Arg183, Phe185, Phe187, Val196, Lys198, Ile219, Phe220 | -7.5 |
| | Christanoate | Chain A: Lys1020 | Chain A: Trp868, Tyr886, Gly1017, Gln1018, Ser1019, Lys1020, Arg1021<br>Chain B: Glu1013, Lys1020, Arg1021<br>Chain C: Gln1018, Ser1019, Lys1020, Val1022, Tyr1029, Arg1089 | -6.5 |
| 6M71 | favipiravir | Chain A: Ser343, Asp358, Asn360, Tyr374, Tyr530 | Chain A: Ile333, Val342, Thr344, Asn356, Val359, Glu370 | -5.5 |
| | Christene | - | Chain A: Arg33, Ala34, Phe35, Val71, Arg116, Lys121, Thr123, Asp126, Asp208, Tyr217, Asp218 | -6.1 |
| | Christanoate | Chain A: Asn138 | Chain A: Tyr32, Lys47, Asp135, His133, Asp135, Cys139, Ala706, Ser709, Thr710, Gly774, Lys780, Asn781, Ser784 | -4.7 |

Lys465, Pro466, Cys467 and Pro477. Meanwhile, christanoate formed hydrogen bonding with Phe329 and Arg495 and hydrophobic bond with Asn330, Ala331, Thr332, Phe334, Tyr356, Asn357, Ser358, Thr359, Phe360, Phe361, Ser362, Trp423, Asn424, Thr425, Asn427 and Ile428.

The second protein used in this *in silico* study was PDB ID: 6LU7, the main protease of SARS-CoV with chain A and B. All three ligands interacted with the residues from chain A, indicating the potential inhibiting site. The control drug displayed hydrogen bonding with Phe8, Ile106, Phe112, Gln127, Asp153 and Thr292. Meanwhile, the residues bind through other hydrophobic bonding, including Gln110, Thr111, Asn151, Phe294 and Asp295. Christene displayed bonding with Phe8, Val104, Ile106, Gln107, Gln110, Asn151, Asp153, Ser158 and Phe294 in chain A via hydrophobic bond-

ing. Meanwhile, residues from chain A namely Leu141, Asn142, Gly143, Ser144, Cys145 and His163 bind through hydrogen bonding and Thr24, Thr25, Thr26, Leu27, His41, Met49, Tyr54, Phe140, His164, Met165, Glu166, His172, Asp187, Arg188 and Gln189 bind via hydrophobic bonding with christanoate. These two ligands displayed better binding scores than the control (-5.4 kcal/mol) ligand, with binding energy levels of -6.3 and -5.6 kcal/mol.

The SARS-CoV spike glycoprotein with human ACE2 bound particles (PDB ID: 6CS2) was used to dock the two compounds of C. *vespertilionis* leaf. favipiravir, christene and christanoate displayed the lowest binding energy level among all the other receptors docked with the binding score value of -6.0, -7.5 and -6.5 kcal/mol, respectively. The control drug interacted with residues in chain A (Lys1020) and B (Glu1013, Lys1020, and Arg1021) and bound through hydrogen bonding. Meanwhile, Glu1013, Ser1019, Arg1021, and Val1022 from chain A, Ser1019 in chain B, followed by Glu1013 and Arg1021 in chain C, made hydrophobic bonding with favipiravir. Christene showed more affinity towards the residues in chain B involving Trp101, Ile116, Asn118, Val123, Arg183, Phe185, Phe187, Val196, Lys198, Ile219 and Phe220. However, Christanoate has shown binding with residues in all three chains, similar to the control drug. The compound made a hydrogen bond with Lys1020 in chain A. Other than that, it made hydrophobic bond with Trp868, Tyr886, Gly1017, Gln1018, Ser1019, Lys1020 and Arg1021 in chain A, followed by interaction with Glu1013, Lys1020 and Arg1021 in chain B and with Gln1018, Ser1019, Lys1020, Val1022, Tyr1029 and Arg1089 in chain C.

Lastly, the RNA-dependant RNA polymerase PDB ID: 6M71 was used in this study to determine the molecular affinity of the compounds observed against SARS-CoV. Christene (-6.1 kcal/mol) exhibited the highest binding energy score compared to christanoate (-4.7 kcal/mol) and favipiravir (-6.1 kcal/mol). favipiravir interacted with the residues in chain A, including Ser343, Asp358, Asn360, Tyr374 and Tyr530 via hydrogen bond and with Ile333, Val342, Thr344, Asn356, Val359 and Glu370 via the hydrophobic bond. Christene binds to Arg33, Ala34, Phe35, Val71, Arg116, Lys121, Thr123, Asp126, Asp208, Tyr217 and Asp218 in chain A via hydrophobic bonding. Meanwhile, christanoate interacted with Asn138 via hydrogen bonding followed Tyr32, Lys47, His133, Asp135, Cys139, Ala706, Ser709, Thr710, Gly774, Lys780, Asn781 and Ser784 via hydrophobic contact. Both the compounds were found to be interacting with residues in chain A, however, of different potential sites, unlike the control ligand.

The search for novel antiviral drugs targeting various parts of its structure to combat viral infection is ongoing. The current docking analysis using christene and christanoate from the *C.vespertilionis* leaf indicates that the compounds have a high affinity towards the proteins used in the docking analysis. Apart from the active site residues that alter the protein function, other residues that interacted with the compounds were also observed.

The structural details of the Coronaviruses (SARS-CoV) genome were described by Wang et al., (15) as a single-stranded positive-sense RNA (+ssRNA) that is typically larger than other RNA viruses. It is packed with four structural proteins, namely spike protein (S1 and S2), membrane protein (M), envelope protein (E) and nucleoprotein (N). It contains non-structural proteins (NSP1-16), each with distinct functions in the evolution of the viral material. Some of the SARS-CoV proteins that can potentially serve as the therapeutic drugs target include the spike glycoprotein and its binding domain, the RNA-dependent RNA polymerase (RdRp) complex and the main protease (Mpro) (15).

The most vulnerable receptor during SARS-CoV infection is the ACE2 receptor of the host cell. PDB ID: 2GHV is the sequenced spike protein (S protein) of SARS-CoV that tar-

gets the ACE2 receptors in the host, making it a possible therapeutic target for the treatment. Typically, the virus is named coronavirus based on its crown-like shape resembling the trimeric form that the virion takes upon S protein interaction (16). Christene has shown significant binding score towards the spike protein. However, christanoate showed interaction with the residues (Phe329 and Arg495) similar to that of the control drug, favipiravir, thus indicating its target site is similar to the drug and may potentially forbid the interaction of the spike protein with the host cell. Changes in the structural conformation of the protein observed may have contributed to the inhibition of the protein activity (17).

The main protease-Mpro structure plays a crucial role in the viral's proteolytic maturation; thus, its inhibition may interrupt the life cycle (18). Based on the conformational complex of the main protease-Mpro (PDB ID: 6LU7) with the potential inhibitors showed that christanoate has a high affinity towards residues intact in the active site and the catalytic dyad of the protein reported by Khaerunnisa et al., (19). The active site residues of the protein include Thr24, Thr26, Phe140, Asn142, Gly143, Cys145, His163, His164, Glu166 and His172. Paasche et al., (20) in their investigation to find potential inhibitors of 3CLpro, have demonstrated the residues (His41 and Cys145) that define the catalytic dyad of the protein interacted with the inhibitors used. Catalytic dyads indicate sites with residues vital for the catalytic activity of the protein. The docking of favipiravir, christene and christanoate to this protein showed christanoate as the significant inhibitor as it interacted with the amino acids in the active site, and the catalytic dyad of the protein that included Cys145 And His163 interacted through hydrogen bonding; meanwhile, Thr24, Thr26, His41, Phe140, His164, Glu166, and His172 interacted via hydrophobic bonding. Christene displayed interaction similar to favipiravir, indicating its capacity to prevent protein activity. This inhibition pattern serves as evidence that an allosteric binding site may be present in the protein structure with the ability to alter the activity of the protein (21). Favipiravir and christene were observed to bind with the amino acids near the active site pocket, blocking the entrance that may have altered the protein conformation, thus halting the viral activity.

These results are similar to that reported by Sisakht et al., (22), who used phytochemicals from various plant sources against 3CLpro. Ginkgolide M (Asn142, Cys145, Glu166, Gly143, His163, and Phe140), Glycobismine A (Ser144A, Cys145A, Gly143A, Leu141A, His163A, and Asn142A) and mezerein (His163A, Ser144A, Cys145A, Leu141a, Asn142, and Met49A) are the three compounds that displayed high affinity towards the residues in the catalytic site of the protease. Meanwhile, another study reported on luteolin interaction with the allosteric site, potentially inhibiting protein activity. The interaction involved Arg105, Gln110, Thr111 and Ile152 via hydrogen bonding and hydrophobic contact with Phe8, Arg105, Ile106, Gln107, Val104, Gln110, Thr111, Asn151, Ile152, Asp153, Thr292 and Phe294.

Another SARS-CoV spike glycoprotein with human ACE2-bound particles is deposited as PDB ID: 6CS2. Christanoate was observed to bind with the residues similar to the control drug with interaction in all three chains (A, B and C). Compared to christene, christanoate has more affinity towards the residues similar to favipiravir, with more hydrophobic contact rather than hydrogen bonding. The results are contrary to Sharbidre et al., (23) who displayed the interaction of an anti-inflammatory compound, bergenin, with the S-protein Lys715, Asp757, Leu843, Pro845, Asp849, Pro1039 and His1040. Pal and Talukdar (24) reported that the crucial residues of the S-protein active site include Lys26, Asn90 and Phe32. Another study reported potential catalytic sites of the protein involving Thr51, Leu52, Lys291, Ser292 and Phe293 (25). However, the results obtained were contrary to a previous study, thus indicating that the S-protein is likely to have a potential allosteric site that could prevent the interaction of the spike protein

with the host cell receptor.

PDB ID: 6M71 is the RNA-dependent RNA polymerase (RdRp) with a cofactor nsp12. The primary protein catalyzes the viral RNA replication and transcription process. Therefore, inhibiting this enzyme will suppress viral replication and further infection (26). The protein is comprised of several domains, including the N-terminal domain (1-397), finger domain (397-581 and 629-687), the palm region (582-628 and 688-815) and the thumb region (816-596) (27). The docking analysis revealed that christanoate has a higher affinity towards the active residues, which is similar to Remdesivir reported by Alizadehmohajer et al., (26) involving Lys47, His133, Asp135, Ala706, Ser709, Thr710, Gly774, Lys780 and Ser784 via hydrophobic contact in christanoate. Their study mentioned that the residues interacted with would establish an environment cohesive and stable upon forming the complex.

The study revealed that christanoate displayed higher affinity towards the proteins' docked with it of the two compounds analyzed. The long chain structure with one hydroxyl group and ester group played a crucial role in forming a stable complex, thus enhancing the inhibition activity. Comparably, favipiravir contains one hydroxyl group contributing to the hydrogen bond formed with the catalytic residues. Besides that, the amide and amino group in its structure was also observed to make much more stable hydrogen bonding with the proteins observed. Potential inhibitors of SARS-CoV viral proteins may disrupt the activity not just by responding to the catalytic site or the major active site but also by blocking the entry of the virus into the host cells. Inhibitors may achieve this by binding to the active residues and altering the protein structure, which could block the viral receptors' interaction with the host cells. Apart from that, inhibitors could also halt the viral replication and transcription cycle by altering the protein structure upon binding (27,28). Based on the interaction of christanoate with the proteins used in this, it has potential to inhibit the SARS-CoV.

## Conclusion

The study revealed the antiviral activity of two major compounds identified in *Christia vespertilionis* leaf against SARS-CoV-2 using various protein structures modelled based on the virus structure and genome. Molecular docking is a method that can preliminarily illustrate the conformational structure of the viral protein and the potential inhibitor complex. Based on the investigation, christanoate can be further analyzed for its antiviral activity using pre-clinical techniques to confirm its bioactivity against SARS-CoV-2.

## Acknowledgement

The authors thank Dana Penyelidikan & Inovasi Mara (DPIM) 2021 with reference number MARA/DPIM MARA.600-6/4/3(56) for supporting this study.

## References

1. Prasetyo, W. E., Purnomo, H., Sadrini, M., Wibowo, F. R., Firdaus, M., and Kusumaningsih, T. Identification of potential bioactive natural compounds from Indonesian medicinal plants against 3-chymotrypsin-like protease (3CLpro) of SARS-CoV-2: Molecular docking, ADME/T, molecular dynamic simulations, and DFT analysis. Journal of Biomolecular Structure and Dynamics, 41(10), (2023), 4467-4484.
2. Ghufran, Mehreen, Mehran, U., Haider, A. K., Sabreen, G., Muhammad, A., Muhammad, S., Syed, Q. A., Syed, S. U. H., and Simona, B. In-silico lead druggable compounds identification against SARS COVID-19 main protease target from in-house, chembridge and zinc databases by structure-based virtual screening, molecular docking and molecular dynamics simulations. Bioengineering, 10(1), (2023), 100.
3. Chen, Y., Guo, Y., Pan, Y., and Zhao, Z. J. Structure analysis of the receptor binding of 2019-nCoV. Biochemical and Biophysical Research Communications, 525(1), (2020), 135-140.

4. Tzenios, N., Chahine, M., and Tazanios, M. Better strategies for Coronavirus (COVID-19) vaccination. Special Journal of the Medical Academy and Other Life Sciences, 1(2), (2023).

5. Sofi, F., Dinu, M., Reboldi, G., Stracci, F., Pedretti, R.F., Valente, S., Gensini, G., Gibson, C.M. and Ambrosio, G. Worldwide differences of hospitalization for ST-segment elevation myocardial infarction during COVID-19: A systematic review and meta-analysis. International Journal of Cardiology, 3472022, (2022), 89-96.

6. Xue, Y., Husheng, M., Yisa, C., James, D. G., Qingsong, L., Ellen, W., and Jing, Y. Repurposing clinically available drugs and therapies for pathogenic targets to combat SARS-CoV-2. MedComm, 4(3), (2023), e2

7. Zheng, S., Fan, J., Yu, F., Feng, B., Lou, B., Zou, Q., Xie, G., Lin, S., Wang, R., Yang, X. and Chen, W. Viral load dynamics and disease severity in patients infected with SARS-CoV-2 in Zhejiang province, China, January-March 2020: Retrospective cohort study. BMJ, (2020), 369.

8. Agarwal, S., and Agarwal, S. K. Endocrine changes in SARS-CoV-2 patients and lessons from SARS-CoV. Postgraduate Medical Journal, 96(1137), (2020), 412-416.

9. Lee, J. J., Saiful, Y. L., Kassim, N. K., Che, A. C. A., Esa, N., Lim, P.C., and Tan, D.C. Cytotoxic activity of *Christia vespertilionis* root and leaf extracts and fractions against breast cancer cell lines. Molecules, 25(11), (2020), 2610.

10. Bunawan, H., Bunawan, S. N., and Baharum, S. N. The red butterfly wing *(Christia vespertilionis*): A promising cancer cure in Malaysia. International Journal of Pharmacy and Pharmaceutical Sciences, 7(8), (2015), 5.

11. Murugesu, S., Perumal, V., Balan, T., Fatinanthan, S., Khatib, A., Arifin, N. J., Shukri, N. S. S. M., Saleh, M. S. and Hin, L. W. The investigation of antioxidant and antidiabetic activities of *Christia vespertilionis* leaves extracts. South African Journal of Botany, 133, (2020), 227-235.

12. Wu, X. Y., Tang, A. C. and Lu, Q. Y. Study on antitumor effect of the extract from *Christia vespertilionis* in vivo. Chinese Journal of Experimental Traditional Medical Formulae, 8, (2012),202-204.

13. Upadhyay, H. C., Sisodia, B. S., Cheema, H. S., Agrawal, J., Pal, A., Darokar, M. P. and Srivastava, S. K. Novel antiplasmodial agents from *Christia vespertilionis*. Natural Product Communications, 8(11), (2013), 1934578X1300801123.

14. Dash, G. K. An appraisal of *Christia vespertilionis* (LF) bakh. F.: A promising medicinal plant. International Journal of Pharmacognosy and Phytochemical Research, 8(6), (2016), 1037-1039.

15. Wang, M. Y., Zhao, R., Gao, L. J., Gao, X. F., Wang, D. P., and Cao, J. M. SARS-CoV-2: structure, biology, and structure-based therapeutics development. Frontiers In Cellular And Infection Microbiology, 10, (2020), 587269.

16. Hwang, W. C., Lin, Y., Santelli, E., Sui, J., Jaroszewski, L., Stec, B., and Liddington, R. C. Structural basis of neutralization by a human anti-severe acute respiratory syndrome spike protein antibody, 80R. Journal of Biological Chemistry, 281(45), (2006), 34610-34616.

17. Mycroft-West, C., Su, D., Elli, S., Li, Y., Guimond, S., Miller, G., and Skidmore, M. The 2019 Coronavirus (SARS-CoV-2) surface protein (spike) s1 receptor binding domain undergoes conformational change upon heparin binding. BioRxiv. (2020), 2020-02.

18. Liang, R., Wang, L., Zhang, N., Deng, X., Su, M., Su, Y., ... and Yu, F. Development of small-molecule MERS-CoV inhibi-

tors. Viruses, 10(12), (2018), 721.

19. Khaerunnisa, S., Kurniawan, H., Awaluddin, R., Suhartati, S., and Soetjipto, S. Potential inhibitor of COVID-19 main protease (Mpro) from several medicinal plant compounds by molecular docking study. Preprints, (2020), 2020030226.

20. Paasche, A., Zipper, A., Schäfer, S., Ziebuhr, J., Schirmeister, T., and Engels, B. Evidence for substrate binding-induced zwitterion formation in the catalytic Cys-His dyad of the SARS-CoV main protease. Biochemistry, 53(37), (2014), 5930-5946.

21. Günther, S., Reinke, P. Y., Fernández-García, Y., Lieske, J., Lane, T. J., Ginn, H. M., ... and Meents, A. X-ray screening identifies active site and allosteric inhibitors of SARS-CoV-2 main protease. Science, 372(6542), (2021), 642-646.

22. Sisakht, M., Mahmoodzadeh, A., and Darabian, M. Plant-derived chemicals as potential inhibitors of SARS-CoV-2 main protease (6LU7), a virtual screening study. Phytotherapy Research, 35(6), (2021), 3262-3274.

23. Sharbidre, A., Dhage, P., Duggal, H., and Meshram, R. In silico investigation of *Tridax procumbens* phyto-constituents against SARS-CoV-2 infection. Biointerface Research in Applied Chemistry, 11, (2021), 12120-12148

24. Pal, S., and Talukdar, A. Compilation of potential protein targets for SARS-CoV-2: Preparation of homology model and active site determination for future rational antiviral design. (2020).

25. Khandelwal, A., and Sharma, T. Computational screening of phytochemicals from medicinal plants as COVID-19 inhibitors. (2020)

26. Alizadehmohajer, N., Behmardi, A., Najafgholian, S., Moradi, S., Mohammadi, F., Nedaeinia, R., ... and Manian, M. Screening of potential inhibitors of COVID-19 with repurposing approach via molecular docking. Network odeling Analysis in Health Informatics and Bioinformatics, 11(1), (2022), 1-11.

27. Gao, Y., Yan, L., Huang, Y., Liu, F., Zhao, Y., Cao, L., Wang, T., Sun, Q., Ming, Z., Zhang, L,, Ge, J., Zheng, L., Zhang, Y., Wang, H., Zhu, Y., Zhu, C., Hu, T., Hua, T., Zhang, B., Yang, X,, Li, J., Yang, H., Liu, Z., Xu, W., Guddat, L. W., Wang, Q., Lou, Z., and Rao, Z. Structure of the RNA-dependent RNA polymerase from COVID-19 virus. Science, (2020), 779-782.

28. Jakovac, H. COVID-19 and vitamin D—Is there a link and an opportunity for intervention? American Journal of Physiology-Endocrinology and Metabolism. (2020).

29. Quartuccio, L., Sonaglia, A., McGonagle, D., Fabris, M., Peghin, M., Pecori, D., ... and Tascini, C. Profiling Covid-19 pneumonia progressing into the cytokine storm syndrome: Results from a single Italian Centre study on tocilizumab versus standard of care. Journal of Clinical Virology, 129, (2020), 104444.

Current Trends in Biotechnology and Pharmacy
Vol. 18(2) 1745-1764, April 2024, ISSN 0973-8916 (Print), 2230-7303 (Online)
DOI: 10.5530/ctbp.2024.2.23



# BZ-97: A Promising Compound Against *Trypanosoma cruzi*

**Milixza M Botacio[1,2,*], Maria F. Alves-Rosa[1,*], Nerea Escala[3], Michele Ng[1], Lorena M. Coronado[1], Jafeth Carrasco[1], Doriana Dorta[1], Laura Pineda[1], Esther del Olmo[3], Ricardo Correa[1,†], Carmenza Spadafora[1,†]**

[1]Center of Cellular and Molecular Biology of Diseases, Instituto de Investigaciones Científicas y Servicios de Alta Tecnología (INDICASAT AIP), City of Knowledge, Clayton, Apartado 0816-02852, Panama City, Panama.
[2]Programa de Maestría en Microbiología Ambiental, Universidad de Panamá, Panama City, Rep. of Panama.
[3]Departamento de Ciencias Farmacéuticas: Química Farmacéutica, Facultad de Farmacia, Universidad de Salamanca, CIETUS, IBSAL, 37007, Salamanca, Spain.
[†]Corresponding authors' email: rcorrea@indicasat.org.pa,

**Abstract**

Chagas Disease has been considered "the most neglected among the neglected diseases." Only two very toxic drugs developed in the 1960s have been approved to control the disease in its acute phase and are infective in the chronic stage of the illness. It is imperative to find new molecules that can act against the causative parasite, *Trypanosoma cruzi.* BZ-97 is a synthetic product derived from the benzimidazole scaffold. It was tested against other human parasites, showing the best activity (IC50 = 0.76 μM) towards *T. cruzi* intracellular stages. The effects of BZ-97 on epimastigotes of the Y strain were analyzed. Signs of changes in the parasite homeostasis were evident by acidocalcisomes alkalinization, calcium mobilization, changes in their morphology and some signs of apoptotic events with a lack of ROS production, which is a crucial advantage over the behavior of the reference drug, benznidazole. Acidocalcisomes alkalinization was evidenced through fluorescence microscopy analysis and the use of 5-[N-ethyl-N-isopropyl] amiloride (EIPA), an inhibitor of the TcNHE pump, confirmed the involvement of this proton pump in the BZ-97-mediated acidocalcisome alkalinization. BZ-97 is presented as a potential lead compound against *T. cruzi that is* worthy of further studies in the future.

**Keywords:** *Trypanosoma cruzi*, anti trypanosomatid, acidocalcisome, benzimidazole scaffold

## Introduction

*Trypanosoma cruz*i is the causative parasite of American Trypanosomiasis, better known as Chagas Disease. This ailment affects approximately 7-8 million people in Latin America (1). An annual incidence of 30,000 new cases and 10,000 deaths has been reported (2). However, as it is a silent disease, the number of infected people and deaths associated with this disease is probably imprecise and underestimated (3, 4). As a consequence of large waves of migration, a large percentage of people carry the infection to non-endemic areas such as North America (5).

CD has two phases: an initial acute phase, which is usually asymptomatic, and a lifelong chronic phase, which in 60 to 70% of patients is clinically silent, but 20 to 30% of them will develop in years or decades heart problems (20 to 30%), digestive problems, or a combination of both (10 to 15%). Neurological symptoms

* Both authors Milixza M Botacio and Maria F. Alves-Rosa contributed equally to the work.

are also seen in a small proportion of patients (5%) (6).

To kill the parasite, CD can be treated with Benznidazole (BNZ) or Nifurtimox (NFX), both developed over 40 years ago. Both compounds are currently the only drugs available for treating CD and remain as therapeutic options showing certain efficacy in the treatment of CD (7). While both, NFX and BNZ, are effective in treating the acute stages of infection, their efficacy is limited in the chronic phase and varies by geographical location (3).

Furthermore, the frequency of drug side effects is higher in older patients, further limiting their benefits. The treatment regimen with both compounds is long, and many adverse effects can occur, compromising the continuity of the treatment. Regarding the common adverse effects of BNZ, they include allergic dermatitis, nausea, vomiting, anorexia, weight loss, insomnia, and dose-dependent peripheral sensitive neuropathy, among others (8-10). Rare but serious events include neuropathy and bone marrow depression.

In the absence of effective and less toxic chemotherapies against Chagas Disease, new, safer, and more efficient drugs are urgently needed against this disease.

Nitroimidazoles are a well-known class of active compounds that have shown high activity against *T. cruzi* (11). The incorporation of a nitro group into the imidazole ring has been widely studied, as in Benznidazole (*N*-benzyl-2-(2-nitroimidazol-1-il)acetamide); on the other hand Benzimidazoles (BZ), that is, organic compounds that have a benzene ring linked to an imidazole ring in positions 4 and 5 have shown very interesting biological activities. BZ rings are considered good scaffolds for the development of new promising candidates against Chagas disease.

The structure of BZ is related to that of imidazole; however, taking into account their physicochemical properties, the former are weaker bases than the latter due to the benzene ring that can help delocalize electrons from the imidazole nitrogen through a variety of resonance conformations. BZ derivatives as the 2-aminoBZ type represent a group of compounds with interesting biological activity (12), and some of them are drugs of clinical uses as antifungal or anthelmintic properties (e.g. albendazole) among others (Figure 1).

Figure 1. Structures of Benzimidazole (left), Albenzadole (center), and Benznidazole (right)

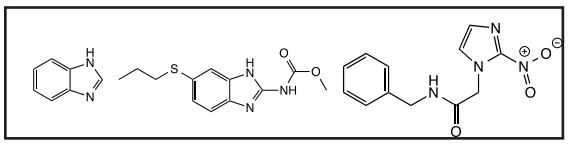

In lieu of the above, a number of new derivatives of BZ were synthesized and screened against tropical human parasites, including *Trypanosoma cruzi*. This report details the screening and characterization of the biological activity of one such derivative, BZ-97, against *T. cruzi*, the causative agent of Chagas Disease.

## Materials and Methods

### *Chemical compounds*

Compound BZ-97 was used in a previous study describing their synthesis (13). The derivative was kept as a lyophilized product that, when ready to be used, was prepared in stock solutions (5 mM) in 100% dimethyl sulfoxide (DMSO; Sigma-Aldrich®). It was stored at 4 ºC until the day of the experiment when it was taken to the corresponding concentration in the plate by diluting it in culture media (13). In the study presented here, compound BZ-1 was tested against Trypanosoma cruzi parasites with the code BZ-97.

### *Parasites and bioactivity assays*

Intracellular antitrypanosomal bioassays were carried out on the recombinant Tulahuen clone C4 lacZ of *T. cruzi* trypomastigotes (American Type Culture Collection (ATCC), Manassas, VA, USA), which expresses the

β-galactosidase enzyme as a reporter of viability (14, 15). Vero cells (ATCC, Manassas, VA) were grown for 24 hours prior to performing the experiment. On the day of the experiment, cells were infected, and BZ-97 was dissolved in DMSO and added to the medium at a single dose of 10 µM for screening purposes (Fig. 2) or at 10, 2, 0.4, and 0.1 µM, for the determination of its IC50. Infected cells were incubated for five days and maintained in RPMI-1640 at 37 °C under a 5% $CO_2$ atmosphere with L-glutamine, 4-(2-Hydroxyethyl)-piperazine-1-ethanesulfonic acid buffer, $NaHCO_3$, 10% FBS and 1% penicillin/streptomycin as supplements. To determine the anti-trypanosomal activity, chlorophenol-red-β-D-galactopyranoside (Roche Applied Science) was used as the substrate of living parasites β-galactosidase, which was allowed to act for 4.5 h. Benznidazole was used as a positive control using 10, 1, and 0.1 µg/ml to determine its IC50. Absorbance was measured at 570 nm using a plate reader (Sinergy HT, BioTek Instruments Inc, Winooski, VT, USA).

For epimastigote assays, the Y strain of *T. cruzi,* grown in LIT medium, was used, as it was chosen as the reference strain for drug discovery programs against Chagas Disease (15,16). Parasites at $5\times10^6$ epimastigotes/mL were incubated at 28 °C in 96-well plates, adding the compound BZ-97 at the concentrations described for the trypomastigote assays. Benznidazole and untreated parasites were used as positive and negative controls, respectively. The antiparasitic activity was evaluated after 72 h of incubation using the MTT method.

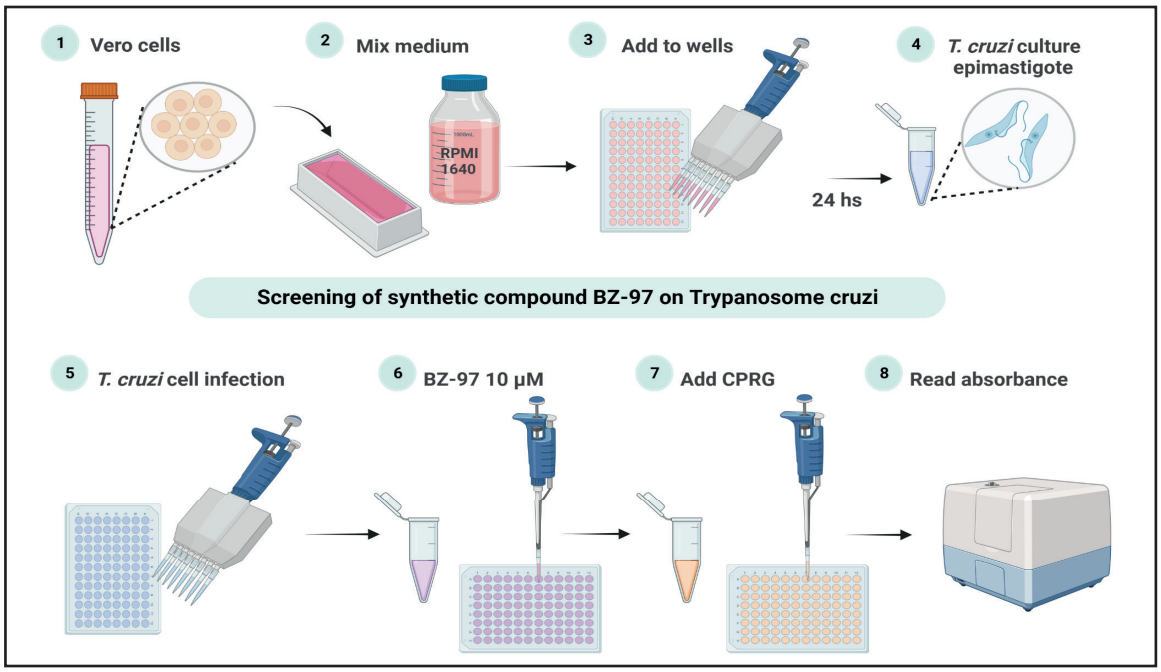


Figure No.2 . Diagram of the screening protocol used for the analysis of active compounds against *T. cruzi* of the Tulahuen strain (clon C4 lacZ) or Y.

**Cytotoxicity determination**

For cytotoxicity assays, Vero cells were cultivated in 96-well plates with RPMI-1640 medium (Sigma- Aldrich, USA) supplemented with 1% penicillin/streptomycin and 10% fetal bovine serum (FBS) (Gibco, Invitrogen, Carlsbad, CA, USA). Cells were allowed to adhere to the bot-

tom of the flask for 24 h before incubating them with the compound for five days. DMSO, the vehicle for BZ-97, was used as a negative control. To obtain the IC50 of the drugs, BZ-97 was assayed at the same concentrations used in the anti-trypanosomal assay, and benznidazole was analyzed with 7 concentrations ranging from 500 to 7.8 µg/ml (1,921 to 30 µM). After incubation, MTT (3-(4, 5-dimethyl-thiazol-2-yl)-2, 5-di-phenyl-tetra-zoliµM bromide) at 2.5 µg/ml was added to each well. Absorbance was determined 4 h later at 570 nm, using a color plate reader, as described earlier by Mosmann et al, 1983 (16) and modified for *T. cruzi* by Muelas-Serrano et al, 2000 (17).

All bioassays were performed in duplicates and some in triplicates. The IC50 of Adriamycin, calculated from using 1, 10, and 100 nM concentrations, was used as a positive control for cytotoxicity assays.

***Detection of reactive oxygen species***

Measurement of intracellular reactive oxygen species (ROS) was evaluated through ROS-dependent 5-(and-6)-chloromethyl-2′,7′-dichlorodihydrofluorescein diacetate (CM-H2DCFDA) (Molecular Probes®, Eugene OR, USA) oxidation. The amount of oxidized DCF indicates the level of intracellular ROS production. Briefly, 10x6 epimastigotes were cultured in a 96-well plate and incubated with LIT medium (control), (20 µM) BZ-97, or (40 µM) BNZ for 3h at 28°C h. After that, parasites were loaded with CM-H2DCFDA (10 µM) and incubated in the dark for 30 min at room temperature. Intracellular ROS production was detected in a fluorometer (Biotek Synergy HT). Excitation was performed at 495 nm, and fluorescence emission was detected at 530 nm. 200 µM Hydrogen peroxide ($H_2O_2$)-treated epimastigotes were used as a positive control. Untreated parasites were used as a negative control. Intracellular ROS production was measured with a fluorometer.

***Mitochondrial membrane potential (ΔΨM) changes***

Mitochondrial membrane potential (ΔΨM) changes were evaluated using 3,3′-dihexyloxacarbocyanine iodide (DiOC6), a lipophilic, permeable dye that emits green fluorescence and demonstrates selectivity towards the mitochondria of living cells when used at low concentrations (18). DiOC6 accumulates in the mitochondria proportionally to the ΔΨm values. The experiments were performed using $5x10^5$ epimastigotes cultured in a 96-well plate and incubated with LIT medium (control), 20 µM BZ-97, or 40 µM BNZ for 3h, 6h and 9 h at 28°C. After that, cells were stained with 10 nM DiOC6 and incubated in the dark for 20 min at 28°C h. After staining, the parasites were washed and suspended in 200 µl of phosphate-buffered saline (PBS) and analyzed immediately by flow cytometry. $5x10^5$ epimastigotes were treated with 50 µM CCCP, a compound known to disrupt mitochondrial membranes, acting as a positive control for depolarization of the mitochondrial membrane.

***Fluorescent microscopy***

All epimastigote images were acquired after a drop of living parasites was placed on a clean glass slide, covered with a coverslip, and sealed. Epimastigotes were visualized with the appropriate lasers with an Olympus FV3000 confocal microscope (Olympus Corporation, Osaka, Japan). A 100 X objective was used to obtain the images.

***Alkalinization of acidocalcisomes detection using acridine orange (AO)***

Changes in the pH of the acidocalcisomes of epimastigotes were monitored by AO staining, a weak base that accumulates in acidic compartments. Its nonionized form dominates in neutral to alkaline environments, emitting green fluorescence and easily diffusing across membranes. In acidic environments, its ionized form prevails, emitting orange fluorescence and being membrane-impermeable (19). Thus, AO accumulation in acidic compartments can be detected as a bright green fluorescence (530 nm) when excited by a 488 nm laser. Thus,

$5x10^5$ epimastigotes cultured in a 96-well plate and incubated with LIT medium (control), 20 µM BZ-97; 40 µM BNZ, 5 µM Mannitol, 20 µM BZ-97 plus 5 µM 5-[N-ethyl-N-isopropyl] amiloride (EIPA); 40 µM BNZ plus 5 µM EIPA, or 1 µM Mannitol plus 5 µM EIPA for 3h at 28°C in 96-well plates. Subsequently, parasites were stained with 5 µM AO, which served as a probe for alkalinization and was then analyzed by fluorometry using a BioTek Sinergy HT fluorometer using the Gen 5 software.

In another set of experiments, $1x10^5$ epimastigotes were cultured in a 96-well plate and incubated with LIT medium (control) or 20 µM BZ-97 for 24 h at 28°C. Parasites were stained with 5 µM OA for 20 minutes in the dark and washed twice with 200 µl of PBS. A 488 nm laser was used to excite the stain.

## Alkalinization of acidocalcisomes detection using LysoSensor™

The LysoSensor™ dye is an acidotropic probe that accumulates in acidic organelles due to protonation. This pH-dependent process also causes the fluorescence quenching of the dye by its weak base side chain to be released, leading to higher fluorescence intensity. LysoSensor staining was performed according to the protocol described by Albrecht et al, 2020 (20), with minor modifications. Briefly, $5x10^5$ epimastigotes were incubated with LIT medium (control), 20 µM BZ-97, 40 µM BNZ, or 20 µM BZ-97 plus 5 µM EIPA for 24 h at 28°C in 96 well plates. After this period of time, the medium containing the stimulus was carefully removed, and 1 µM LysoSensor was added with a freshly tempered LIT medium and incubated for 30 min at 28°C. Subsequently, epimastigotes were washed 3 times with cold PBS (200 µl per wash), mounted on slides, and sealed with a coverslip. The cell-associated green fluorescence (excited with a 488 nm laser) was analyzed in a fluorescent microscope. A comparative analysis of fluorescence intensity was done with the ImageJ software (NIH, USA).

### *Fluorescence microscopy image processing*

Fluorescence microscopy images were processed and analyzed through the Image processing free download software ImageJ 1.x developed by the National Institutes of Health and the Laboratory for Optical and Computational Instrumentation (LOCI, University of Wisconsin) (https://imagej.net/software/imagej).

The data were expressed as the fluorescence intensity value of compound-treated epimastigotes (FI) over baseline (control, LIT medium-treated epimastigotes).

### *Propidium iodide (PI) staining*

Cell membrane damage in epimastigotes can be assayed by quantifying the level of PI incorporated inside treated cells. Briefly, $10x^6$ epimastigotes were cultured in a 96-well plate and incubated with LIT medium (control), 20 µM BZ-97 or 40 µM BNZ for 3 h at 28°C in 96-well plates. Cells were washed once with PBS, and parasites were then resuspended in PBS containing 1 µM PI. Untreated parasites were used as the negative control. As a positive control of cellular damage, epimastigotes were subjected to a high temperature 80 °C in a thermostatic bath for 30 min. Each sample's mean fluorescence intensity (MFI) was determined using the 535 nm laser of a ParteQ CyFlow cytometer (Germany). The experiment was repeated twice in quadruplicates.

### *Changes in cell viability through apoptosis or necrosis*

Apoptosis/ necrosis cellular death was evaluated by flow cytometry using FITC-labeled Annexin V and red-fluorescent propidium iodide (PI) staining (Alexa Fluor™ 488 annexin V/Dead Cell Apoptosis Kit, from Invitrogen™). The assay was performed according to manufacturer instructions with minor modifications. Briefly, 5 x $10^5$ epimastigotes were treated with LIT medium (control), 20 µM BZ-97, 40 µM BNZ, or 1 µM staurosporine for 6 and 24 h at 28°C in 96-well plates. Then, the cells were rinsed once with LIT medium, gently resuspended in 100 µL Annexin V reagent, and incubated in the dark for 15

minutes at 28°C h. The reaction was stopped by adding 200 µL of 1X binding buffer, and cells were analyzed by flow cytometry within one hour for maximum signal. The mean fluorescence intensity (MFI) of FL2 (PI) and FL1 (Annexin V) of each sample was determined using the 535 nm laser of a flow cytometer. All experiments were repeated at least twice in quadruplicates.

### *Statistical analysis*

All experiments were repeated at least twice in quadruplicates. Flow cytometry data are representative of three independent experiments unless otherwise stated. Graphical and One-way ANOVA with Bonferroni's post hoc statistical analysis were performed using GraphPad Prism version 6.04 for Windows, GraphPad Software, (www.graphpad.com)

## Results and Discussion

### *Anti-trypanosomal activity*

During screening of possible antiparasitic compounds, BZ-97 performed well in the low micromolar levels against three parasites: *Leishmania donovani, Trypanosoma cruzi, and Plasmodium falciparum*. The best action was directed against *T. cruzi,* with sub micromolar values (Table I).

Table I. Effect of BZ-97 on intracellular human parasites

| INTRACELLULAR BIOASSAYS | | | | Selectivity Index for *T. cruzi* |
|---|---|---|---|---|
| BZ-97 IC50 (uM) | | | | |
| *L. donovani* | *T. cruzi* | *P. falciparum* | Vero cells | |
| 1.33 | 0.76 | 1.02 | 11.5 | 15.1 |

Given the results obtained in the BZ-97 intracellular IC50 assays, we decided to further study this molecule's effects against *T. cruzi.* A head-to-head anti-*T. cruzi* test was performed to evaluate the effect of this compound on the death of the epimastigotes, comparing it with benznidazole (BNZ), the reference compound. Both BZ-97 and BNZ seem to be less potent against epimastigotes than they were against intracellular forms of the parasite (Table II)

Table II. IC50 of compounds on T. cruzi epimastigotes

| | BZ-97 IC50 (uM) | | Selectivity Index |
|---|---|---|---|
| | *T. cruzi* epimastigotes | Vero cells | |
| BZ-97 | 2.03 ± 1.17 | 11.5 ± 1.8 | 5.1 |
| Benznidazol | 4.59 ± 0.70 | 47.1 ± 7.0 | 10.3 |

### *Effect of BZ-97 on reactive oxygen species production*

It is known that ROS production is a marker of alterations in the parasite's homeostasis caused by various factors, including pH fluctuation, stress, hypoxia, and the presence of heme. The data depicted in Figure 3 show that epimastigotes treated with 20 µM BZ-97 for 3 h do not differ significantly in ROS production from non-treated cells. On the contrary, 40 µM BNZ-treated epimastigotes show an 8-fold increase in ROS synthesis compared with parasites not challenged with any external stimulus. The addition of 200 µM $H_2O_2$ serves the purpose of verifying the integrity of the reagents and analytics used in this experiment.

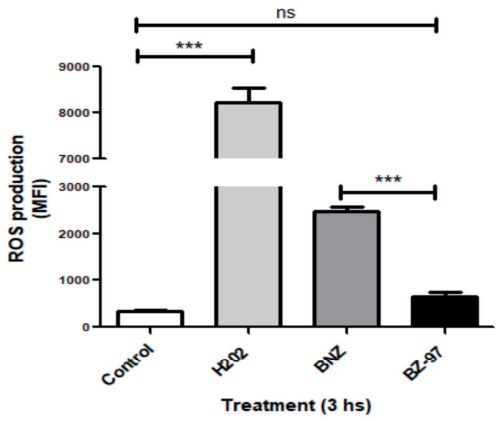


Figure 3. Effect of BZ-97 on epimastigote ROS production.

*T. cruzi* epimastigotes were cultured in

the presence of LIT medium (control), 20 µM BZ-97, 40 µM BNZ, or 200 µM $H_2O_2$ for 3 h prior to detection of ROS production by flow cytometry. Samples were measured with four replicates in each of three independent experiments. MFI: Mean Fluorescence Intensity. One-way ANOVA and Bonferroni's Multiple Comparison Test were used to measure significant variation compared to the untreated control at each time point; *** p <0.001; ns: not significant.

**Effect of BZ-97 on mitochondrial transmembrane potential**

Viable epimastigotes were treated with LIT medium (control), 20 µM BZ-97 or 40 µM BNZ for 3, 6 and 9 h and changes in the transmembrane potential were analyzed by flow cytometry. Results depicted in Figure 4 indicate that while BNZ induces a depolarization of the mitochondrial membrane, at 3 and 6 h, reflected by a decrease in the DiOC6 mean fluorescence intensity (MFI), BZ-97 does not exhibit significant changes at the same time points. The effect of BNZ is reversed at 9 h, showing no significant differences in the DiOC6 MFI compared to either BZ-97 or untreated cells. In these experiments, the low MFI exhibited by CCCP-treated epimastigotes, an inhibitor of mitochondrial oxidative phosphorylation, indicates complete and irreversible depolarization (CCCP-treated vs untreated epimastigotes MFI, *** p< 0.0001).

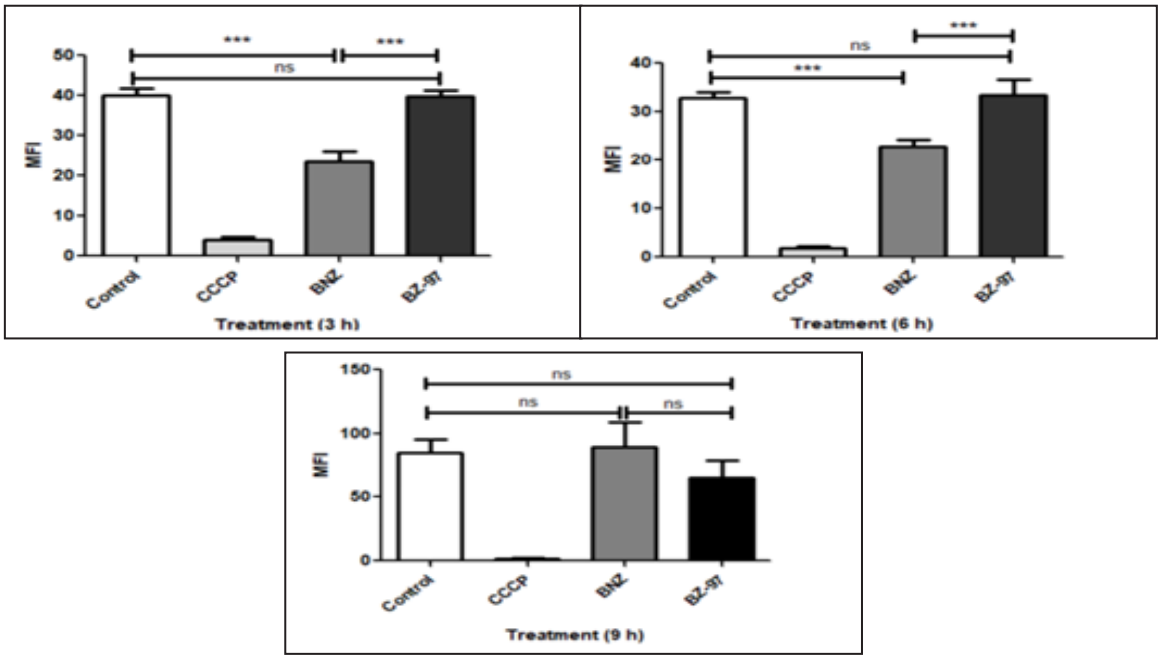


Figure 4. Effects of BZ-97 on the Mitochondrial Membrane Potential in T. cruzi epimastigotes.

Epimastigotes from *T. cruzi* strain Y were incubated with LIT medium (control), 20 µM BZ-97 or 40 µM BNZ for 3, 6 and 9 h before evaluating changes in mitochondrial membrane polarization by flow cytometry. 50 µM CCCP was used as the positive control. MFI: Mean Fluorescence Intensity. One-way ANOVA and Bonferroni's Multiple Comparison Test were used. *** p <0.001; ns: no significant difference.

**Effect of BZ-97 on the acidity of acidocalcisomes**

To evaluate the effect of BZ-97 treatment on epimastigote acidocalcisomes, we further assessed changes in the acidity of this organelle caused by treatments for 3 h using

acridine orange (AO) staining. Fluctuations in the organelle's proton (H+) content are reflected by changes in the AO fluorescence at 530 nm emission.

Figure 5 shows that 20 µM BZ-97-treated epimastigotes exhibit a highly significant increase in AO absorbance, indicative of acidocalcisome alkalinization; similar results were observed in 40 µM BNZ-treated cells. In addition, both compounds show no significant differences in their AO absorbance levels.

EIPA abrogates the effect of BZ-97 and BNZ on acidocalcisomes, resulting in absorbance values similar to those of control cells. Additionally, 5 µM Mannitol strongly induces acidocalcisome alkalinization, and this effect is not prevented by EIPA.

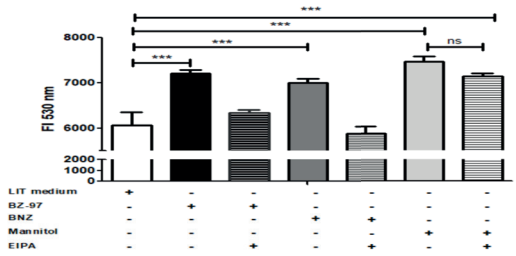


Figure 5. Effect of BZ-97 on acidocalcisomes of epimastigotes.

*T. cruzi* epimastigotes were treated with LIT medium (control), 20 µM BZ-97, 40 µM BNZ or 5 µM Mannitol (positive alkalinization control) with or without 5 µM EIPA for 3 h. 5 µM OA was added to all groups, and their fluorescence was analyzed by fluorometry. FI 530 nm = Fluorescence Intensity at 530 nm One-way ANOVA and Bonferroni's Multiple Comparison Test were used. *** p <0.001; ns: no significant difference.

**Fluorescence microscopy (FM) of acidocalcisomes of BZ-97-treated epimastigotes**

To verify if the observed effect of BZ-97 on the alkalinization of acidocalcisomes persists over time, viable epimastigotes were grown at exponential phase and then treated with LIT medium (control), 20 µM BZ-97, 20 µM BZ-97 + 5 µM EIPA or 40 µM BNZ for 24 h.

Results obtained from FM using LysoSensor™ as an acidic organelle detector probe are depicted in Figure 6. In control epimastigotes, these organelles are visualized as clearly defined green points with high fluorescence intensity (Fig 6A). In contrast, acidocalcisomes from BZ-97- treated epimastigotes show spots with blurry boundaries and lower fluorescence intensity, indicative of acidocalcisome alkalinization (Fig 6B).

BNZ treatment also induces changes in the fluorescence signal similar to BZ-97 (Fig 6C), while incubation of epimastigotes with BZ-97 and EIPA (an inhibitor of primarily Sodium-Hydrogen Exchangers (NHEs) abrogates the effect of BZ-97 (Fig 6D) showing well-defined high fluorescent intracellular spots.

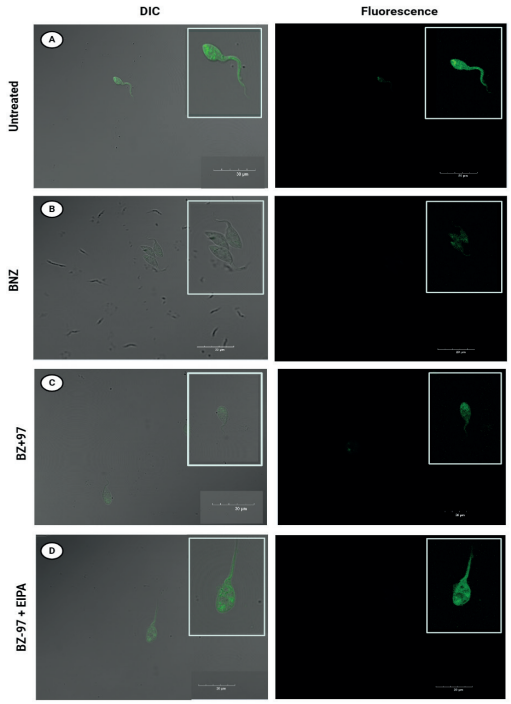


Figure 6. Fluorescence Microscopy of acidocalcisomes of BZ-97-treated epimastigotes using LysoSensor Green probe.

Changes in the pH of acidic organelles of live epimastigotes of *T. cruzi* were assayed using the LysoSensor Green probe. Untreated epimastigotes (A), epimastigotes treated with 20 µM BZ-97 (B), 20 µM BZ-97 + 5 µM EIPA (C), or 40 µM BNZ (D) incubated for 24 h are shown. Inset images have been subjected to digital processing to enhance visualization of parasites. Brightness, exposure, and contrast adjustments were applied solely to improve clarity of these specific regions. All insets received identical image correction parameters to maintain consistency. DIC: differential interference contrast. Pictures are representative of more than 15 fields of one experiment.

These results were also confirmed using acridine orange (AO)-stained epimastigotes. AO is a fluorescent dye that can selectively stain acidic organelles. Untreated epimastigotes exhibited discrete tiny spots throughout the parasite cytoplasm indicative of the presence of acidocalcisomes, and this feature is much less intense after BZ-97 treatment (Figure 7).

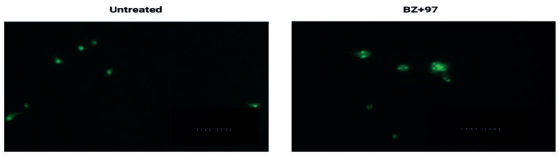


Figure 7. Fluorescence Microscopy (FM) of acidocalcisomes of BZ-97-treated epimastigotes using acridine orange (AO) staining.

Changes in the pH of acidic organelles of live epimastigotes of *T. cruzi* were assayed using acridine orange (AO). Untreated epimastigotes and epimastigotes treated with 20 µM BZ-97 for 24 h were subjected to 5 µM acridine orange (AO) staining. Pictures are representative of more than 15 fields of one experiment. Bar = 30 µm.

FM images were processed and analyzed through the Image processing software ImageJ 1.x Figure 8. Statistical analysis supports the conclusions driven from the FM assay.

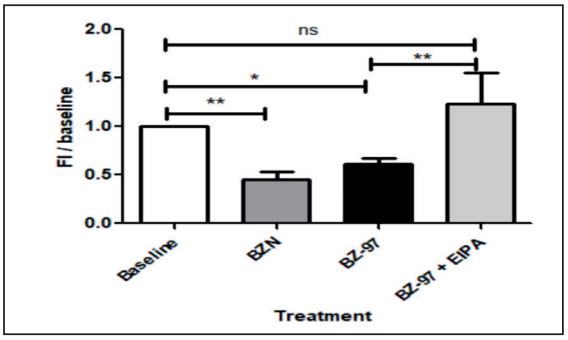


Figure 8. FM image processing analysis.

Epimastigotes of *T. cruzi* strain Y were treated with LIT medium (control), 20 µM BZ-97, 20 µM BZ-97 + 5 µM EIPA or 40 µM BNZ for 24 h and were assayed using the LysoSensor Green probe. FM Image processing and analysis was performed using ImageJ software. Each data is expressed as a FI over baseline (control, LIT medium- treated epimastigote). One-way ANOVA and Bonferroni's Multiple Comparison Test were used. *** p <0.001; ns: no significant difference.

**Intracellular calcium mobilization induced by BZ-97**

This study investigated the initial response (first few minutes) of *T. cruzi* epimastigotes to BZ-97, and compared it to the reference drug BNZ. The release of calcium ions into the cytoplasm, a key signaling event, was monitored using the calcium-binding dye Cal-520 for a period of 2.5 h (Figure 9).

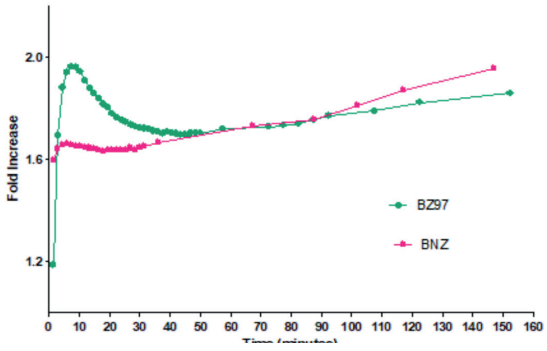


Figure 9. Cytosolic Calcium Changes.

*T. cruzi* epimastigotes were incubated with either 20 µM BZ-97 or 40 µM BNZ. Acridine Orange (5 µM) was subsequently added before fluorescence measurements were taken every 60 seconds for the initial 50 minutes following treatment. Thereafter, readings were collected at less frequent intervals. The data presented represent fold-changes relative to the baseline.

Both BZ-97 and BNZ induce a rapid rise in cytoplasmic calcium levels in *T. cruzi* epimastigotes. While BZ-97 exhibits a faster initial increase compared to BNZ, this effect appears transient. Following the initial peak, the calcium levels induced by BZ-97 progressively decrease, reaching a similar level of that observed with BNZ for over the next 30 minutes. In parasites treated with BNZ, however, the levels of mobilized calcium continue augmenting until it is almost double that of control parasites at the final measured time point.

***Effect of early BZ-97 exposure on epimastigotes apoptosis induction.***

Given that a significant effect on acidocalcisomes acidity is detected as soon as 3 h of BZ-97 treatment, we evaluated the effect of this compound on the induction of apoptosis at this time point. Apoptotic cells can be distinguished from necrotic cells using propidium iodide (PI), as PI can enter necrotic cells with damaged membranes.

Viable epimastigotes were treated with 20 µM BZ-97 or 40 µM BNZ for 3 h prior to PI staining, and changes in their fluorescence were assessed using flow cytometry. Figure 10 shows no significant differences between untreated and treated epimastigotes, indicating no signs of apoptosis as early as 3 hours after exposure to these compounds. Heating the parasites to 80oC, a very aggressive treatment for the membranes, shows a high fluorescence increment (incorporation of PI).

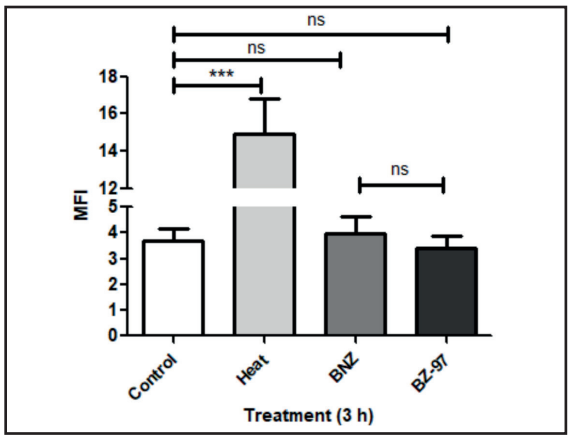


Figure 10. Effect of early BZ-97 exposure on epimastigote apoptosis.

Epimastigotes of the Y strain of *T. cruzi* were treated with 20 µM BZ-97, 40 µM BNZ for 3 h, or submitted to heating at 80 °C for 30 min. PI was added to all groups, and their fluorescence was analyzed using flow cytometry. MFI: Mean Fluorescence Intensity. One-way ANOVA and Bonferroni's Multiple Comparison Test were used. ns: not significant.

***Effect of long-lasting exposure to BZ-97 on the induction of epimastigote apoptosis***

In order to assess whether BZ-97 treatment for 6 and 24 h induces changes in epimastigote viability through apoptosis or necrosis, additional experiments were conducted using the Alexa Fluor® 488 Annexin V/Dead Cell Apoptosis assay. Cells were classified according to these conditions: Annexin V+/PI- (early apoptotic cells), Annexin V+/PI+ (Late apoptotic/ necrotic cells), Annexin V-/PI- (Viable cells) and Annexin V-/PI+ (necrotic cells).

Viable epimastigotes were treated with 20 µM BZ-97, 40 µM BNZ or 1 µM staurosporine for 6 and 24 h and changes in PI uptake and Annexin V cell-associated fluorescence were assessed using flow cytometry.

Data obtained at 6 hours post-incubation indicates that staurosporine induces a mild but significant shift towards Annexin V-/PI+ epi-

mastigotes (necrotic cells) as follows: untreated (0.12% ± 0.02%), staurosporine (4.16% ± 0.08%), BNZ (0.11% ± 0.05%), and BZ-97 (0.17% ± 0.05%). Thus, staurosporine vs BZ-97-treated, BNZ-treated, or untreated parasites show significance ($p < 0.001$). BZ-97-treated, BNZ-treated, and untreated epimastigotes do not differ significantly from each other (ANOVA and Bonferroni's Multiple Comparison Test). Figure 11 shows a representative 2D dot plot of FL1 (Annexin V) vs FL2 (PI) obtained from the flow cytometry analysis of epimastigotes subjected to treatment.

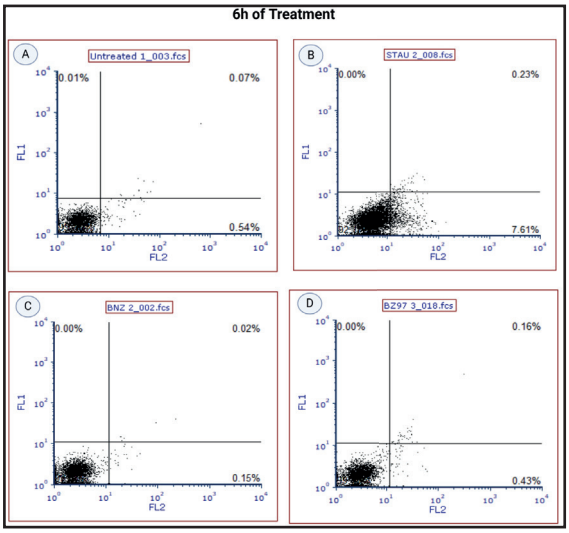


Figure 11. Changes in Fluorescence intensity on epimastigote population following 6 h of staurosporine, BNZ or BZ-97 treatment.

Representative 2D scatter plots (FL1 vs FL2) obtained from flow cytometry analysis of *T. cruzi* epimastigotes strain Y treated for 6 h with culture medium (A), 1 µM staurosporine (B), 40 µM BNZ (C) or 20 µM BZ-97 (D). Values in each quadrant represent the percentage (%) of parasites analyzed which fall on each one of them.

Data obtained at 24 hours post-incubation show significant differences in Annexin V-/PI+ epimastigotes (necrotic cells) as follows: untreated (3.15% ± 1.51 %), staurosporine (50.36 ± 8.8 %), BNZ (2.793 ± 1.03 %), and BZ-97 (11.43 ± 2.18 %). The difference between staurosporine and untreated cells is highly significant ($p < 0.001$), whereas no significant differences were observed between BZ-97-treated, BNZ-treated or untreated cells (ANOVA and Bonferroni's Multiple Comparison Test). See Figure 11 for a representative sample.

Annexin V+/PI+ epimastigotes (late apoptotic/necrotic cells) also show differences as follow: untreated (1.08% ± 0.66 %), staurosporine (11.48 ± 3.9 %), BNZ (4.17 ± 1.59 %), and BZ-97 (8.51 ± 0.8 %). For the comparison between staurosporine vs untreated parasites, the difference between staurosporine and the untreated trypanosomatids is highly significant ($p< 0.001$), whereas no significant differences were observed between BZ-97-treated, BNZ-treated or untreated cells. staurosporine vs BZ-97 or BNZ did not show significant differences suggesting that both imidazoles exert a mild but significant pro-apoptotic effect (ANOVA and Bonferroni's Multiple Comparison Test).

Figure 12 shows a representative 2D dot plot of FL1 (Annexin V) vs FL2 (PI) obtained from the flow cytometry analysis of epimastigotes treated for 24 h.

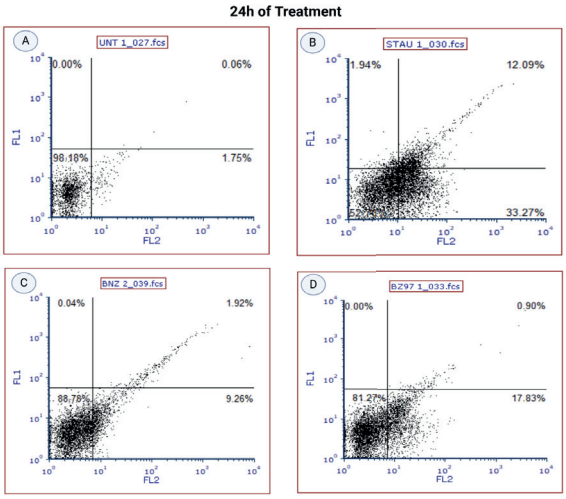


Figure 12. Changes in Fluorescence intensity on epimastigote population following 6h of staurosporine, BNZ or BZ-97 treatment.

Representative 2D scatter plots (FL1 vs. FL2) obtained from flow cytometry analysis of *T. cruzi epimastigotes* treated with culture medium (A), 1 µM staurosporine (B), 40 µM BNZ (C), or 20 µM BZ-97 (D) for 24 h. Values in each quadrant represent the percentage (%) of parasites, from the total acquired, in each one of the quadrants.

### *Effect of treatments on epimastigote structure and morphology*

Figure 13 depicts the results of flow cytometry analysis, where epimastigotes exposed to various treatments are represented as a dot plot based on their fluorescence intensity in two channels (FL1: Annexin V, FL2: PI). Quadrant Q2 encompasses parasites positive for both Annexin V and PI (Annexin V+/PI+). Notably, staurosporine and BZ-97 treatment resulted in the highest proportion of cells in Q2, suggesting a promotion of apoptosis**.**

We also assessed the impact of these compounds on parasite cellular complexity using flow cytometry, with FSC (forward scatter) and SSC (side scatter) serving as measures of cell size and granularity, respectively.

After 6 h of treatment, epimastigotes treated with staurosporine exhibited significant changes in parasite complexity. This was indicated by the appearance of a new cellular sub-population in the lower left quadrant, demonstrating notable differences in both size (FSC, forward scatter) and granularity (SSC, side scattering) compared to the control. Experimental epimastigotes create a new population as follows: untreated (6.37 % ± 0.42 %), staurosporine- (29.87 ± 0.89 %), BNZ- (6.17 ± 0.14 %), and BZ-97- treated (7.65 ± 0.67 %). The difference between staurosporine and BZ-97-treated and BNZ-treated or untreated cells is highly significant ($p<0.001$), whereas no significant differences were observed between BZ-97-treated, BNZ-treated or untreated cells. (ANOVA and Bonferroni's Multiple Comparison Test).

After 24 h of treatment, the percentage of cells in the lower left quadrant increased dramatically in all groups, to finish as follows: untreated (31.7 ± 4.85 %), staurosporine (64.7 ± 0.81%), BNZ (62.17 ± 10.2%), and BZ-97 (64.38 ± 0.63%). The difference between untreated epimastigotes vs those treated with staurosporine, BZ-97 or BNZ is highly significant ($p<0.001$). No significant differences between treated cells were observed (ANOVA and Bonferroni's Multiple Comparison Test).

Figure 12 shows representative 2D scatter dot plots (FSC vs SSC) reflecting epimastigote complexity after being subjected to treatment for 6 h and 24 h.

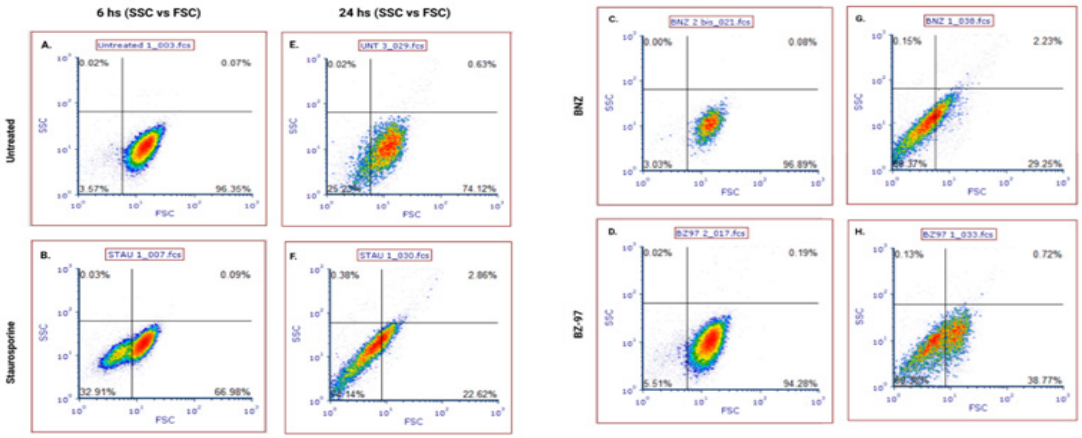


Figure 13. Changes in the complexity of the epimastigote population following BZ-97, BNZ, or staurosporine treatment for 6 and 24 h.

Representative 2D scatter dot plots (FSC vs SSC) reflecting epimastigote complexity were obtained by flow cytometry data analysis. Dot plots from *T. cruzi* epimastigotes treated with culture medium, 1 µM staurosporine, 40 µM BNZ, or 20 µM BZ-97 for 6 h (Figures A, B, C, and D, respectively) and for 24 h (Figures E, F, G, and H, respectively) were divided into four quadrants (Q1-Q4). Q1 and Q2 represent the upper left and right quadrants, respectively, while Q3 and Q4 represent the lower left and right quadrants, respectively. This division was performed to evaluate the percentage of cells in each quadrant (A-F).

Given the observed changes in the morphological complexity of epimastigotes in the SSC vs FSC Lower Left Quadrant after 24 h of treatment, we proceeded to evaluate cell death parameters. After establishing the role of acidocalcisomes in BZ-97 treatment, we study the type of death the parasites were being driven with its treatment, in this specific population.

The results are depicted in Figure 14 and show that the treated epimastigote population predominantly consisted of viable cells (Annexin V-/PI-) except when exposed to staurosporine, which significantly reduced cell viability.

Staurosporine treatment also led to a notable increase in the percentage of necrotic cells (Annexin V-/PI+), whereas BZ-97 or BNZ did not markedly affect this form of cell death. Regarding the late apoptotic/necrotic cell population, approximately 10% of staurosporine-treated epimastigotes underwent this type of cell death. BZ-97 exhibited a mild effect, showing no significant differences from BNZ. Additionally, while the percentage of early apoptotic cells was generally low, it was higher in the group treated with BZ-97 compared to the other treatments.

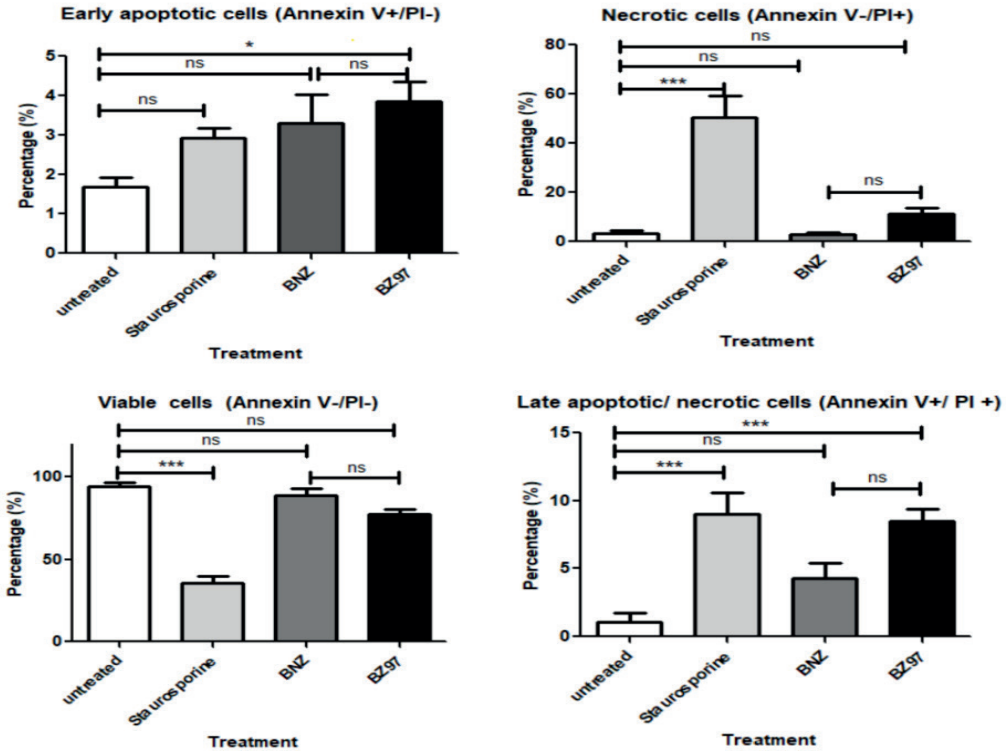


Figure 14. Morphology changes after drug treatment.

Epimastigotes were treated with 1 µM staurosporine, 40 µM BNZ or 20 µM BZ-97. After 24 h of incubation they were stained with Annexin V and Propidium Iodide and analyzed by flow cytometry with the use of quadrants: Annexin V+/PI− (early apoptotic parasites): V+/PI+ (late apoptotic or necrotic parasites);: Annexin V−/PI− (viable parasites); Annexin V-/PI+ (necrotic parasites). * p< 0.05, *** p< 0.001. One-way ANOVA and Bonferroni's Multiple Comparison Test were used. ns: not significant.

## Discussion

Chagas disease (CD), caused by the hemoflagellate *Trypanosoma cruzi* parasite, is a neglected tropical disease endemic to the Americas, affecting over six million individuals (21) (CDC, 2022). While originally confined to this region, migration and environmental changes have propelled CD to a global public health concern (22).

Despite continuous exploration of new treatment possibilities (23), only nitrofurans like nifurtimox (NFX) and the 2-nitroimidazole derivative benznidazole (BNZ), discovered in the early 1960s, remain the mainstay of therapy (22).

Following a 2010 stakeholders' summit in Rio de Janeiro, Brazil, researchers established criteria for further evaluation of Chagas disease drug candidates. These criteria included having an IC50 (concentration inhibiting 50% of parasite growth) equal to or lower than BNZ and a selectivity index (ratio of cytotoxicity to antiparasitic activity) above 10 (16). The benzimidazole derivative BZ-97 fulfilled both criteria in the antiparasitic intracellular assays, warranting further investigations into the compound's mechanism of action against *T. cruzi*.

Given the well-documented association between various drug treatments and the induction of reactive oxygen species (ROS) synthesis as a result of oxidative stress, we first examined the effects of BZ-97 on ROS generation within its target. In fact, ROS production is a marker of alterations in the parasite's homeostasis, i.e., anti- *T. cruzi* treatments (24), hypoxia (25), heme presence as a consequence of heme release during blood digestion (26, 27), starvation and pH stress (28). Elevated ROS production triggers metabolic adaptations in *T. cruzi.* For instance, hypoxia reduces mitochondrial function and energy production, leading to a further increase in ROS (29). Reactive species, thus, can act as a double-edged sword. Studies have demonstrated its diverse effects on the parasite: triggering self-cleaning (autophagy), programmed cell death (apoptosis), or even proliferation (28). Interestingly, when ROS signals proliferation, the parasite's ability to transform into its infective form (metacyclogenesis) is simultaneously suppressed (25).

Our findings indicate that, unlike BNZ, treatment with BZ-97 for 3 hours does not significantly alter the levels of ROS or the mitochondrial membrane potential in *T. cruzi* epimastigotes. This suggests that BZ-97 does not substantially disrupt the mitochondrial electron transport chain, a known source of ROS generation. In contrast, BNZ treatment rapidly induces a significant increase in ROS production and alters the mitochondrial membrane potential within 3 hours. These observations suggest distinct mechanisms of action for these structurally similar imidazole derivatives.

Acidocalcisomes are small, mostly spherical, acidic organelles with an average diameter ranging from 0.2 to 0.6 µm (30). These organelles have several functions including cation and phosphorus storage (31), autophagy, osmoregulation (32), pH homeostasis, and pathogenesis (33). Recent studies have established the role of these organelles not only in phosphate utilization and calcium ion signaling but also on bioenergetics (32) (Docampo et al, 2022). In fact, being the main intracellular reservoir of calcium and phosphate, acidocalcisomes can contribute to signaling in specific processes like pH, homeostasis, and other metabolic processes (32,34,35). It is well known that Ca2+

in the acidocalcisome is bound to a polyanionic matrix of poly P, and can be released after alkalinization of the organelle. This pivotal role underscores their importance in cellular function.

Our data indicate that BZ-97 is able to induce acidocalcisome alkalinization in a similar way as BNZ, which was previously reported as deprotonating the organelle (36). As a control in our experiments, epimastigotes were also subjected to hyperosmotic stress induced by 5 µM Mannitol, leading to alkalinization of acidic vacuoles via a Na+/H+ exchanger (NHE). The BZ-97 and BNZ effects were both blocked by 5-(N-ethyl-N-isopropyl)amiloride (EIPA), an NHE inhibitor, demonstrating the involvement of this pump in the effects caused by the imidazole derivatives.

Differently, the effect of Mannitol was only partially reversed by EIPA. It is important to note that these latter results are not in agreement with those reported by Usorach et al, 2021 (37).

After establishing the role of acidocalcisomes in BZ-97 treatment, we investigated the type of death the parasites were being driven with its treatment. Thus, we used the combination of Annexin V binding and PI uptake, as it is one of the most commonly used assays to measure apoptosis (38). The technique uses double staining with Annexin V, which binds to phosphatidylserine when exposed to the outside of the cytoplasmic membrane as a sign of apoptosis, and PI, since this dye can enter necrotic cells but not early apoptotic cells.

Epimastigotes were analyzed for PI uptake and Annexin V cell-associated fluorescence by flow cytometry at 6 and 24 h. Staurosporine, a protein kinase inhibitor often used to induce apoptosis, was used as a positive control for this process. The use of quadrants helped divide the parasites studied into four possible combinations: Annexin V+/PI- (early apoptotic), Annexin V+/PI+ (late apoptotic), Annexin V-/PI- (viable), Annexin V-/PI+ (necrotic).

Data obtained at 6 hours post-incubation with all drugs indicates that only staurosporine induces a mild but significant shift towards Annexin V-/PI+ epimastigotes indicating that some necrosis is taking place, only with that treatment.

When analyzing the results of the Annexin V+/PI+ epimastigotes (late apoptotic/necrotic cells) at t= 6 h, BNZ-treated parasites show very little apoptosis induction. As for BZ-97, even though the difference is not significant, it already seems to induce more apoptosis than BNZ, once again suggesting a different route of action for both molecules when acting on *T. cruzi* epimastigotes.

Staurosporine, used as a positive control, demonstrated the highest percentage of Annexin V+/PI+ cells, highlighting its significant pro-apoptotic effect. Both BZ-97 and BNZ also increased the proportion of Annexin V+/PI+ but to a lesser extent, compared to the untreated control. Furthermore, no significant differences were observed between BZ-97 and BNZ treatments, indicating that both imidazoles induce a moderate but comparable increase in late-stage apoptosis. It is worth considering several factors that must be taken into account when monitoring the detection of apoptotic markers: (i) Parasite life cycle: *T. cruzi* cell cycle extends beyond 24 hours. The peak apoptotic response induced by BZ-97 and BNZ might occur after this timeframe. (ii) Atypical PS translocation: Imidazoles like BZ-97 and BNZ could potentially trigger alternative apoptotic pathways that do not involve substantial phosphatidylserine (PS) exposure on the cell surface. (iii) Limitations of the assay: As demonstrated by Menna-Barreto et al. (2009), Annexin V/PI staining might not always be sensitive enough to detect apoptosis in T. cruzi epimastigotes, even when other apoptotic markers are present.

The lack of a strong phosphatidylserine (PS) signal in this study does not necessarily exclude apoptosis as a cell death mechanism. In this context, the more detailed information

provided by flow cytometry analysis is worth analyzing, as described below.

Flow cytometry analysis was done to analyze the parasite cellular complexity using epimastigotes exposed to various treatments which were represented as dot plots where FSC (forward scatter) and SSC (side scatter) served as measures of cell size and granularity, respectively. After 6 h of treatment, epimastigotes treated with staurosporine showed significant changes in parasite complexity. This was evidenced by the emergence of a new cellular subpopulation in the lower-left quadrant, characterized by noticeable differences in both size (FSC, forward scatter) and granularity (SSC, side scattering) compared to the control. Experimental epimastigotes fell into a new population where the staurosporine-treated epimastigotes formed the majority of them, with a minor and almost equal representation from the other three groups. The difference between staurosporine and BZ-97-treated, BNZ-treated, and untreated cells is highly significant ($p<0.001$), whereas no significant differences were observed between the latter three groups. By t=24 h, however, the shift to the lower left quadrant is notorious. This suggests that the treatments' effects have impacted the morphology of the parasites, making them smaller and/or less complex.

Further analysis of the cells in this quadrant using FL1 (Annexin V) and FL2 (PI) revealed that approximately 80% of the BZ-97- or BNZ-treated population exhibited morphological changes while remaining viable. This suggests that these drugs primarily induce structural alterations without immediately causing cell death. The precise mechanism underlying these morphological changes in BZ-97-treated cells remains unclear and cannot be definitively determined based solely on the current experiments presented here. While microscopic observations also revealed altered parasite shapes, further investigation is required to elucidate the specific pathways involved.

In addition, the increase of untreated epimastigotes in Q3 indicates that around 30% of the epimastigotes die as a result of an effect not attributable to these compounds.

Our findings suggest that while BZ-97 shares various mechanisms of action with BNZ, it likely targets distinct cellular processes, leading to divergent effects. This is supported by the lack of significant ROS production and the minimal disruption of mitochondrial function observed upon BZ-97 treatment, as discussed below.

Only BNZ appears to alter mitochondrial oxidative phosphorylation, as evidenced by the increased production of reactive oxygen species observed in parasites stimulated by this compound. On the other hand, both BZ-97 and BNZ induce a clear effect on the alkalinization of acidocalcisomes. This is confirmed by studies using acridine orange and LysoSensor, the latter being a probe capable of interacting with the parasite's acidic compartments.

BZ-97 would deliver a pro-apoptotic effect, rather than a necrotic one, on epimastigotes subjected to its treatment. This effect becomes evident after 24 hours of treatment, providing an indication of when the treatment's effect becomes apparent, despite indications that BZ-97, like BNZ, begins to exert effects on the parasite's physiology in the early stages (3 or 6 h) of treatment. This observation is a relevant issue for it would mean that this compound is capable of causing death on the parasite without giving rise to inflammatory processes that result from necrosis.

It is worth noting that in microscopy studies, epimastigotes treated with BZ-97 experienced morphological changes, appearing more "stout" with rounder, less elongated bodies (data not shown). This morphological change is reflected in flow cytometry studies on cellular complexity. There, it is observed that at 24 hours, cellular subpopulations of smaller size and lower granularity appear. These changes are not necessarily accompanied by a decrease

in cell viability, as Annexin V/PI studies on these cells indicate that the majority of cells are viable, with only a small percentage undergoing early apoptosis (around 4%) and even fewer undergoing late apoptosis/necrosis (less than 10%). Similar results are observed with BNZ, with both being significantly different from those obtained from epimastigotes treated with staurosporine.

It is worth noticing that all the effects observed with BZ-97 occur at a dose twice as low as that of BNZ. The fact that this compound can exert a similar effect to one of the treatments considered the gold standard to tackle Chagas Disease deserves further investigation and consideration as a potential therapeutic option for the future.

## DECLARATIONS

### Acknowledgments

CS and LMC are grateful with the Sistema Nacional de Investigación of Panama for partial funding.

### Ethical approval

Not Applicable

### Funding

MB was funded through a Master´s Scholarship from SENACYT. RC was funded through a “Capital Semilla” grant from SENACYT. DD, JC, CS and MN were funded by the BIOBANCO grant from the Ministry of Environment of Panama. CS, LMC and RC were partially funded by the Sistema Nacional de Investigación de Panamá (SNI).

### Availability of data and materials

All data and materials presented here are offered upon request but are subject to availability

### Competing Interests

All authors declare not to have any financial or non-financial interest in this publication.

### Author Contributions

Conceptualization, RC, CS; Methodology, MB, MFER, MN, LMN, JC, RC; Validation, MFER, JC, EdO, CS; Formal analysis, MB, MFER, MN, RC, CS; Investigation, MB, MFER, NE, MN, LMN, JC, DD, LP, RC, CS; Resources, EdO, CS; Data curation, JC, CS; Writing – original draft, MFER; Writing – review & editing, MB, MFER, NE, MN, LMN, JC, DD, LP, EdO, RC, CS; Visualization, MFER; Supervision, MFER, MN, LMN, LP, EdO, CS; Project administration, CS.

All authors read the final manuscript and approved it.

### References

1. CDC website. https://www.cdc.gov/parasites/chagas/epi.html (Accessed on March, 2024)

2. WHO, 2022. World Chagas Disease Day: finding and reporting every case (who.int) (Accessed March 4, 2024)

3. Echeverría L. E., Marcus R., Novick, G., Sosa-Estani S., Ralston K., Zaidel E. J., Forsyth C., Ribeirobn A. L. P., Mendoza I., Falconi M. L., Mitelman J., Morillo C. A., Pereiro A. C., PinazonmM. J., Salvatella R., Martinez F., Perel P., Liprandi Á. S., Piñeiro D. J., & Molina, G. R. *WHF IASC Roadmap on Chagas Disease. Glob Heart.* 2020; 30; 15(1):26. doi: 10.5334/gh.484. PMID: 32489799; PMCID: PMC7218776.

4. Pinheiro E., Brum-Soares L., Reis R., & Cubides J. C. (2017). Chagas disease: review of needs, neglect, and obstacles to treatment access in Latin America. *Revista Da Sociedade Brasileira de Medicina Tropical* 2016; 50: 296–300. https://doi.org/10.1590/0037-8682-0433-2016.

5. Monge-Maillo B., López-Vélez R. Challenges in the management of Chagas disease in Latin-American migrants in Europe. *Clin Microbiol Infect*. 2017; 23 :290-295. doi: 10.1016/j.cmi.2017.04.013.

6. Prata A. Clinical and epidemiological aspects of Chagas disease. *Lancet Infect Dis*. 2001; 1:92-100. doi: 10.1016/S1473-3099(01)00065-2.

7. Meymandi S., Hernandez S., Park S., Sanchez DR., Forsyth C. Treatment of Chagas Disease in the United States. *Curr Treat Options Infect Dis*. 2018; 10:373-388. doi: 10.1007/s40506-018-0170-z. Epub 2018 Jun 26. PMID: 30220883; PMCID: PMC6132494.

8. Castro J.A, de Mecca M.M., Bartel L.C. Toxic side effects of drugs used to treat Chagas' disease (American trypanosomiasis). *H*µM *Exp Toxicol*. 2006 Aµg;25(8):471-9. doi: 10.1191/0960327106het653oa.

9. Rassi A., Rassi A., Marcondes de Rezende J.. American Trypanosomiasis (Chagas Disease). *Infect Dis Clin North Am*. 2012;26 :275–291. doi: 10.1016/j.idc.2012.03.002.

10. Pérez-Molina J.A, Molina I. Chagas disease. The Lancet. 2018;391(10115):82–94. doi: 10.1016/S0140-6736(17)31612-411. Castro J.A., de Mecca M.M., Bartel L.C. Toxic side effects of drugs used to treat Chagas' disease (American trypanosomiasis). *Hum Exp Toxicol*. 2006; 25:471-9. doi: 10.1191/0960327106het653oa.

11. Turrens J.F., Watts B.P. Jr, Zhong L., Docampo R. Inhibition of Trypanosoma cruzi and T. brucei NADH fumarate reductase by benznidazole and anthelmintic imidazole derivatives. *Mol Biochem Parasitol*. 1996; 82: 125-9. doi: 10.1016/0166-6851(96)02722-3. PMID: 8943158.

12. Edwards D.I. Nitroimidazole drugs--action and resistance mechanisms. I. Mechanisms of action. *J Antimicrob Chemother.* 1993; 31:9-20. doi: 10.1093/jac/31.1.9. PMID: 8444678.

13. Escala E., Valderas-García E., Álvarez Bardón M., Castilla Gómez de Agüero V., López-Pérez J.L., Rojo-Vázquez F.A., San Feliciano A., Martínez-Valladares M., Balaña-Fouce R., del Olmo E. Further and new target-based benzimidazole anthelmintics active against *Teladorsagia circumcincta. Journal of Molecular structure* 2022; 1269: 133735 doi.org/10.1016/j.molstruc.2022.133735

14. Buckner F.S., Verlinde C.L., La Flamme A.C., Van Voorhis W.C. Efficient technique for screening drugs for activity against Trypanosoma cruzi using parasites expressing beta-galactosidase. *Antimicrob Agents Chemother*. 1996; 40: 2592-7. doi: 10.1128/AAC.40.11.2592. PMID: 8913471; PMCID: PMC163582.

15. Romanha A.J., Castro S.L., Soeiro M de N., Lannes-Vieira J., Ribeiro I., Talvani A., Bourdin B., Blum B., Olivieri B., Zani C., Spadafora C., Chiari E., Chatelain E., Chaves G., Calzada J.E., Bustamante J.M., Freitas-Junior L.H., Romero L.I., Bahia M.T., Lotrowska M., Soares M., Andrade S.G., Armstrong T., Degrave W., Andrade Z de A. In vitro and in vivo experimental models for drug screening and development for Chagas disease. *Mem Inst Oswaldo Cruz*. 2010; 105:233-8. doi: 10.1590/s0074-02762010000200022.

16. Mosmann T. Rapid colorimetric assay for cellular growth and survival: application to proliferation and cytotoxicity assays. *J Immunol Methods*. 1983; 65: 55-63. doi: 10.1016/0022-1759(83)90303-4.

17. Muelas-Serrano S., Nogal-Ruiz J.J., Gómez-Barrio A. Setting of a colorimetric method to determine the viability of Trypanosoma cruzi epimastigotes. *Parasitol Res*. 2000; 86:999-1002. doi: 10.1007/pl00008532.

18. Sabnis R.W., Deligeorgiev T.G., Jachak M.N., Dalvi T.S. DiOC6(3): a useful dye for staining the endoplasmic reticulum. *Biotech Histochem*. 1997; 72: 253-8. doi: 10.3109/10520299709082249. PMID: 9408585.

19. Palmgren M.G. Acridine orange as a probe for measuring pH gradients across membranes: mechanism and limitations. *Anal Biochem*. 1991; 192: 316-21. doi: 10.1016/0003-2697(91)90542-2.

20. Albrecht L.V., Tejeda-Muñoz N., De Robertis E.M. Protocol for Probing Regulated Lysosomal Activity and Function in Living Cells. *STAR Protoc*. 2020; 1: 100132. doi: 10.1016/j.xpro.2020.100132.

21. CDC. Updated Estimates and Mapping for Prevalence of Chagas Disease among Adults, United States - *Emerging Infectious Diseases journal* 2022; 28: 7.

22. Gómez-Ochoa S.A., Rojas L.Z., Echeverría L.E., Muka T., Franco O.H. Global, Regional, and National Trends of Chagas Disease from 1990 to 2019: Comprehensive Analysis of the Global Burden of Disease Study. *Glob Heart*. 2022; 17: 59. doi: 10.5334/gh.1150

23. Mazzeti A.L., Capelari-Oliveira P., Bahia M.T., Mosqueira V.C.F. Review on Experimental Treatment Strategies Against *Trypanosoma cruzi*. *J Exp Pharmacol*. 2021; 13: 409-432. doi: 10.2147/JEP.S267378.

24. Bombaça A.C.S., Viana P.G., Santos A.C.C., Silva T.L., Rodrigues A.B.M., Guimarães A.C.R., Goulart M.O.F., da Silva Júnior E.N., Menna-Barreto R.F.S. Mitochondrial disfunction and ROS production are essential for anti-*Trypanosoma cruzi* activity of β-lapachone-derived naphthoimidazoles. *Free Radic Biol Med*. 2019; 130: 408-418. doi: 10.1016/j.freeradbiomed.2018.11.012.

25. Saraiva F.M.S., Cosentino-Gomes D., Inacio J.D.F., Almeida-Amaral E.E., Louzada-Neto O., Rossini A., Nogueira N.P., Meyer-Fernandes J.R., Paes M.C. Hypoxia Effects on *Trypanosoma cruzi* Epimastigotes Proliferation, Differentiation, and Energy Metabolism. *Pathogens*. 2022; 11: 897. doi: 10.3390/pathogens11080897.

26. Nogueira N.P., de Souza C.F., Saraiva F.M., Sultano P.E., Dalmau S.R., Bruno R.E., Gonçalves Rde.L., Laranja G.A., Leal L.H., Coelho M.G., Masuda C.A., Oliveira M.F., Paes M.C.. Heme-induced ROS in Trypanosoma cruzi activates CaMKII-like that triggers epimastigote proliferation. One helpful effect of ROS. *PLoS One*. 2011; 6: e25935. doi: 10.1371/journal.pone.0025935.

27. Nogueira N.P., Saraiva F.M.S., Oliveira M.P., Mendonça A.P.M., Inacio J.D.F., Almeida-Amaral E.E., Menna-Barreto R.F., Laranja G.A.T., Torres E.J.L., Oliveira M.F., Paes M.C. Heme modulates *Trypanosoma cruzi* bioenergetics inducing mitochondrial ROS production. *Free Radic Biol Med*. 2017; 108: 183-191. doi: 10.1016/j.freeradbiomed.2017.03.027.

28. Pedra-Rezende Y., Fernandes M.C., Mesquita-Rodrigues C., Stiebler R., Bombaça A.C.S., Pinho N., Cuervo P., De Castro S.L., Menna-Barreto R.F.S. Starvation and pH stress conditions induced mitochondrial dysfunction, ROS production and autophagy in Trypanosoma cruzi epimastigotes. *Biochim Biophys Acta Mol Basis Dis*. 2021; 1867: 166028. doi: 10.1016/j.bbadis.2020.166028.

29. Kung-Chun C.D., Pui-Wah T.A., Law C.T., Ming-Jing X.I., Lee D., Chen M., Kit-Ho L.R, Wai-Hin Yuen V, Wing-Sum Cheu J, Wai-Hung Ho D, Wong CM, Zhang H, Oi-Lin

Ng I, Chak-Lui Wong C. Hypoxia regulates the mitochondrial activity of hepatocellular carcinoma cells through HIF/HEY1/PINK1 pathway. *Cell Death Dis*. 2019; 10: 934. doi: 10.1038/s41419-019-2155-3.

30. Docampo R., de Souza W., Miranda K., Rohloff P., Moreno S.N.J. Acidocalcisomes? conserved from bacteria to man. *Nat Rev Microbiol* 2005; 3; 251. https://doi.org/10.1038/nrmicro1097

31. Docampo R., Moreno S.N. Acidocalcisomes. *Cell Calcium*. 2011; 50: 113. doi: 10.1016/j.ceca.2011.05.012.

32. Docampo R., Huang G. New insights into the role of acidocalcisomes in trypanosomatids. *J Eukaryot Microbiol.* 2022; 69:e12899. doi: 10.1111/jeu.12899.

33. Li F.J., He C.Y. Acidocalcisome is required for autophagy in Trypanosoma brucei. *Autophagy.* 2014;10(11):1978-88. doi: 10.4161/auto.36183.

34. Benaim G., Paniz-Mondolfi A.E., Sordillo E.M., Martinez-Sotillo N. Disruption of Intracellular Calcium Homeostasis as a Therapeutic Target Against *Trypanosoma cruzi*. Front *Cell Infect Microbiol*. 2020;10: 46. doi: 10.3389/fcimb.2020.00046

35. Serrano-Martín X., García-Marchan Y., Fernandez A., Rodriguez N., Rojas H., Visbal G., Benaim G. Amiodarone destabilizes intracellular Ca2+ homeostasis and biosynthesis of sterols in Leishmania mexicana. *Antimicrob Agents Chemother*. 2009 Apr;53(4):1403-10. doi: 10.1128/AAC.01215-08. Epub 2009 Jan 21. PMID: 19164149; PMCID: PMC2663059.

36. Mantilla B.S., Azevedo C., Denny P.W., Saiardi A., Docampo R. The Histidine Ammonia Lyase of *Trypanosoma cruzi* Is Involved in Acidocalcisome Alkalinization and Is Essential for Survival under Starvation Conditions. *mBio.* 2021; 12: e0198121. doi:10.1128/mBio.01981-21.

37. Usorach M., Gimenez A.M., Peppino Margutti M., Racagni GE., Machado E.E. Calcium Signaling Involves $Na^+/H^+$ Exchanger and $IP_3$ Receptor Activation in *T. cruzi* Epimastigotes. *Biologics*. 2021 :384-395. https://doi.org/10.3390/biologics1030022.

38. Reutelingsperger C.P., van Heerde W.L. Annexin V, the regulator of phosphatidylserine-catalyzed inflammation and coagulation during apoptosis. *Cell Mol Life Sci.* 1997; 53:527-32. doi: 10.1007/s000180050067.

39. Menna-Barreto RF., Corrêa J.R., Cascabulho C.M., Fernandes M.C. Pinto A.V. Soares M.J., De Castro S.L. Naphthoimidazoles promote different death phenotypes in Trypanosoma cruzi. *Parasitology.* 2009 ;136 :499-510. doi: 10.1017/S0031182009005745.

Current Trends in Biotechnology and Pharmacy
Vol. 18(2) 1765-1772, April 2024, ISSN 0973-8916 (Print), 2230-7303 (Online)
DOI: 10.5530/ctbp.2024.2.24



# *Dunaliella salina* as a Protein Expression System for the Expression of the Endolysin Lysqdvp001 Against *Vibrio parahaemolyticus*

**Bharath Gunasekaran[1] and Gothandam Kodiveri Muthukaliannan[1*]**

[1]School of Biosciences and Technology, Vellore Institute of Technology, Vellore, Tamil Nadu, India.
*Corresponding Author email: gothandam@gmail.com

**Abstract:**

*Vibrio parahaemolyticus* is a gram-negative, halophilic marine pathogen that is the major cause of infections and death in aquaculture. Consumption of undercooked or raw infected seafood causes gastroenteritis in humans. Because of this rapid rise in the number of cases of vibriosis in fish and Acute hepatopancreatic necrosis disease (AHPND) in crustaceans, the dependence on antibiotics has been on the rise, leading to the occurrence of more antibiotic-resistant bacterial strains. Endolysin, a lysin derived from bacteriophage is a great alternative to antibiotics. The fact that both endolysins and the bacteriophage are both species-specific, makes them even better replacement to antibiotics. In this study, the endolysin Lysqdvp001 which has been shown to be effective against *Vibrio parahaemolyticus*, is expressed and purified from *E. coli.* Further, endolysin Lysqdvp001 is also expressed in *Dunaliella salina,* a microalgae that is a cheap, easy to culture protein expression system. *Dunaliella salina* has many nutritional benefits because of the high concentration of β-carotene. Both the purified Lysqdvp001 and the *Dunaliella salina* expressed Lysqdvp001 are shown to have good antimicrobial properties against *Vibrio parahaemolyticus*.

**Keywords:** Endolysin, *Vibrio parahaemolyticus, Dunaliella salina*, Lysqdvp001, Vibriosis.

## Introduction

Aquaculture is one of the most rapidly growing industries which is a major source of aquatic- based food. However, due to the increase in aquaculture worldwide, diseases affecting aquatic species have also been increasing. The most prevalent and notorious one being the bacterial diseases caused mainly by bacteria belonging to the *Vibrio* species (1,2).

*Vibrio parahaemolyticus* is a halophilic, gram-negative bacteria that is mainly found in warm marine conditions. It is one of the leading causes of all aquatic-related infections and also infects human beings when raw or uncooked seafood is consumed. *Vibrio parahaemolyticus* is known to infect both fishes (causing vibriosis) and crustaceans (causing acute hepatopancreatic necrosis disease) (3). Like most bacterial infections, vibriosis too was traditionally combatted using antibiotics. But the over use of antibiotics has led to the development of antibiotic resistant bacteria that poses a danger to both aquatic and human health (4). This increase in antibiotic resistant bacteria has led to an urgent need for alternative ways to fight off such bacterial infections such as using plant extracts (5) and various other methods (6). One such strategy is using either bacteriophages or its derivative lysins such as endolysins, which are known to be effective against specific bacteria.

Bacteriophages and endolysins are already being used as effective control agents against many bacterial diseases (7,8). One such bacteriophage is qdvp001, which is specific against the bacteria *Vibrio parahaemolyticus.* The main endolysin derived from this phage is called Lysqdvp001 which has been characterized and is known to have strong lytic activity against *Vibrio parahaemolyticus* (9). *Vibrio parahaemolyticus* has a thick peptidoglycan outer membrane that make it difficult for endolysins to act effectively from outside, to counteract this (10) suggested adding cationic amino acids to the endolysins. In order to increase the sustainability and for easier administration of endolysin a proper expression system is required. One such system is the microalgae *Dunaliella salina.* It is a green unicellular, halophilic microalgae that thrives in salty waters like salt water lakes and many marine habitats. While many micro and macroalgae are already used for the control of various pathogens, the concept of expressing a protein in algae itself is a fairly new idea (11). *Dunaliella* is widely studied for its potential use in food and cosmetic industry because of its ability to produce high levels of beta carotene and antioxidant properties (12). *Dunaliella* is also known to be easy to cultivate and combining with its nutritional benefits, makes it a novel and effective platform for recombinant protein expression (13,14).

The current study compares the difference in efficiency between pure Lysqdvp001 and the Lysqdvp001 expressed in Dunaliella salina against Vibrio parahaemolyticus. For this purpose, Lysqdvp001 was first expressed in *Escherichia coli* BL21 DE3 and purified. It was then expressed in *Dunaliella salina* by using the vector pMDC45. Our biochemical results showed that *Dunaliella salina* expressed endolysin, Lysqdvp001 exhibit antimicrobial properties which is comparable to the *E. coli* purified endolysin.

## Materials and Methods

### Strains, gene and vectors

*Vibrio parahaemolyticus* ATCC 17802 was purchased from American type culture collection. The lyophilized culture was stored in -80℃ deep freezer until further use. The culture was revived in a Mueller Hinton broth containing 3% NaCl and was allowed to grow overnight at 37℃. *E. coli* BL21 DE3 competent cells were purchased from TAKARA which were used for expression of the endolysin Lysqdvp001 and stored in -80℃ deep freezer. The gene sequence for the endolysin gene (ORF 60) was retrieved from Genbank-NCBI and the synthesized gene was obtained from Macrogen, Korea.

*Dunaliella salina* was obtained from ICAR-CIBA. Filtered seawater supplemented with Walnes/Conway medium, thiamin HCl (0.1µg/100ml) and cyanocobalamin (0.1µg/100ml) was used as a growth medium. The cells were grown at 25℃ with 12 hour lights on/off cycle in a static condition.pET-28a was used for expression in *E.coli* BL21. pENTR/D-TOPO vector (Thermofisher scientific, USA) was used as an entry vector for Gateway cloning. pMDC45 which has a CaMV35s promoter was used as a destination vector.

### Cloning, expression and purification of lysqdvp001

The ORF60 gene was amplified using gene- specific primers that were obtained Xetra biosolutions, Coimbatore, India:

The underlined portions denote the *BamH1* and *Xho1* restriction sites. A 7 cationic amino acid sequence was added to the reverse primer (highlighted region in Table1). The amplified gene was cloned between the *BamH1* and *Xho1* sites of the plasmid pET -28a+. The gene containing plasmid was then transformed into *E.coli* BL21 DE3 competent cells using heat shock method and was grown in Luria Bertani broth containing 100µg/ml kanamycin. Once

Table 1: Gene-specific primers for the ORF60 gene. The underlined portions are restrictions corresponding to *BamH*1 and *Xho*1 in forward and reverse primers respectively. The highlighted region is a 7 cationic amino acid

| | |
|---|---|
| Forward primer | 5'- CGGGATCCAATGACTTTAATTCGTAAGGGTAGTCG -3' |
| Reverse primer | 5'-CCGCTCGAGGCGCATGCGCAGGGGCGAAGATGAAGACGAATTAAGCTTCG TTATTACTAGTTACATCTGA -3' |

the broth reaches 0.4-0.6 OD (log phase) at 600nm, isopropyl-β-D-1-thiogalactopyranoside (IPTG) was added to make a final concentration of 500µM to induce the expression of the endolysin Lysqdvp001. After addition of IPTG, the cells were incubated at 16℃ overnight at 150rpm. The overnight culture was centrifuged and the pellet was resuspended in phosphate buffered saline (PBS). The cells were then disrupted by ultrasonication and the endolysin was purified by using the His60 Ni gravity columns (TAKARA, China) according to manufacturer's instructions. The purified protein was then stored in -80℃ deep freezer. The concentration of the purified endolysin was determined by using Bradford's assay (15). SDS-PAGE was run to verify the presence and size of the endolysin Lysqdvp001.

**Cloning and expression of protein in *Dunaliella salina***

The endolysin gene ORF60 was amplified using gene-specific primer, but the forward primer has the sequence CACC at the 5' end to ensure that the PCR product is inserted into the topo vector in the right orientation. The pENTR-D-TOPO cloning kit (Thermofischer scientific) helps in inserting the PCR amplified ORF60 gene into the TOPO vector that acts as an entry vector for the gateway cloning process(16). To confirm that the ORF60 gene has been cloned into the TOPO vector in the correct orientation, M13 forward and reverse primers are used along with the gene specific primers.

Table 2: Primers used for orientation confirmation of ORF60 gene in TOPO vector.

| | |
|---|---|
| M13 forward:<br>Gene specific reverse: | 5´-GTAAAACGACGGCCAG-3´<br>5'CCGCTCGAGGCGCATGCGCAGGGGCGAAGATGAAGACGAATTAAGCTTCGT TATTACTAGTTACATCTGA -3' |
| Gene specific forward:<br>M13 reverse: | 5'- CGGGATCCAATGACTTTAATTCGTAAGGGTAGTCG -3'<br>5´-CAGGAAACAGCTATGAC-3´ |

The plant vector pMDC45 is used as the destination vector and by using the LR clonase enzyme (INVITROGEN, USA), the endolysin gene ORF60 is transferred from the entry TOPO vector to the destination pMDC45 vector by incubating the said mixture at 25℃ for 1 hour. The pMDC45 plasmid with the ORF60 gene is then transformed into pre-prepared electrocompetent *Dunaliella salina* cells which were prepared according to the published protocol and grown in the medium containing hygromycin (50µg/ml) at 25℃ for 15 days. To confirm the presence of the ORF60 gene, the genomic DNA was isolated by using the CTAB method (17). PCR using gene-specific primers were done to confirm the presence of ORF60 gene in the transformed *D.*

*salina* cells. The *Dunaliella salina* cells are then centrifuged and the pellet is resuspended in PBS for ultra sonification and extraction of protein. SDS-PAGE was run to determine the presence of the expressed Lysqdvp001 endolysin.

**Turbidity reduction assay**

Turbidity reduction assay was carried out for both purified Lysqdvp001 and *Dunaliella salina* expressed Lysqdvp00. An overnight culture of *Vibrio parahaemolyticus* was grown at 37℃ at 150rpm. The overnight culture was centrifuged and the pellet was treated with EDTA for 5 minutes, then washed with water and stored in a freezer. This treated pellet was suspended in a tris-HCl, pH 8.2 buffer. To 100µl of cell suspension, equal volumes of samples were added. Tris buffer was used as a negative control, lysosyme was used as a positive control, 1mg/ml of purified Lysqdvp001 and 100µl of algal expressed protein extract were used. The OD was measured at 450nm (18) for every 5 minutes for a total of 30 minutes.

**Zone of inhibition**

The inhibition zones of both the purified Lysqdvp001 and the algal expressed Lysqdvp001 were carried out according to (10) Lysqdvp001-5aa, Lysqdvp001-10aa and Lysqdvp001-15aa, were designed based on lysin Lysqdvp001 from Vibrio parahaemolyticus (V. parahaemolyticus. *Vibrio parahaemolyticus* was cultivated at 37℃ overnight at 150 rpm. Sterile oxford cups were used to punch even holes on MH agar. Buffer was used as negative control, gentamicin (50µg/ml) was used as positive control (19) 1 mg/ml of purified Lysqdvp001, algal expressed lysqdvp001 and protein extract of wild type *Dunaliella salina* with no recombinant protein was added as control. The plates were then incubated at 37℃ for 24hours.

**Antibacterial activity against *Vibrio parahaemolyticus***

The efficiency of both the purified protein and the algal-expressed protein was analysed by measuring the minimum inhibitory concentration (MIC) and minimum bactericidal concentration (MBC), both of which were done by broth microdilution. *Vibrio parahaemolyticus* was inoculated in its growth medium and incubated at 37℃ overnight at 150rpm. In a ratio of 1:200, the overnight culture was mixed with the growth medium containing negative control (buffer), positive control (gentamicin) (19)which is an important pathogen in aquatic animals worldwide, the antimicrobial activity of CS-GT and the effects of a CS-GT dose on the intestine histopathology and intestinal flora of V. parahaemolyticus-infected shrimps were explored. The results showed that CS-GT possessed broad-spectrum antibacterial activity, with minimum inhibitory concentration (MIC, algae expressed Lysqdvp001 and purified Lysqdvp001 in a 96 well microassay plate. Gentamicin was used from a concentration of 200-0.40µg/ml. Lysqdvp001 was used from a concentration of 2000-2µg/ml, the extracted algal protein was added serially. Since the *Dunaliella salina* expressed Lysqdvp001was a crude extract, the crude extract with the Lysqdvp001 was used to see MIC and MBC. *Dunaliella salina* expressed Lysqdvp001 was used in concentrations of 5 %( v/v) - 0.15 %( v/v). It was incubated at 37℃ for 24 hours and then the plates were read using a microtiter plate reader at 660nm. 100µl of these were then inoculated onto MH agar plates and incubated at 37℃ for 24 hours.

**Results and Discussion**

**Synthesis, expression and purification of lysqdvp001**

The 0.7 kb ORF60 gene which encodes the endolysin Lysqdvp001 was synthesised and was inserted into the vector pET 28a and transformed into *E.coli* DH5α. The presence of the ORF60 gene in *E.coli* was confirmed by PCR using the gene-specific primers. Fig 1A shows the presence of the desired gene fragment in pET-28a vector. This pET-28a vector containing the ORF60 gene was then transformed into *E.coli* BL21 DE3 cells for protein expression.

IPTG was used for protein induction. The expressed protein was purified using a His60 Ni gravity columns. SDS-PAGE shows the presence of Lysqdvp001 in both crude as well as purified sample as shown in Fig 1B. Upon doing Bradford's assay, the concentration of the purified endolysin Lysqdvp001 was calculated to be 27.3mg/ml.

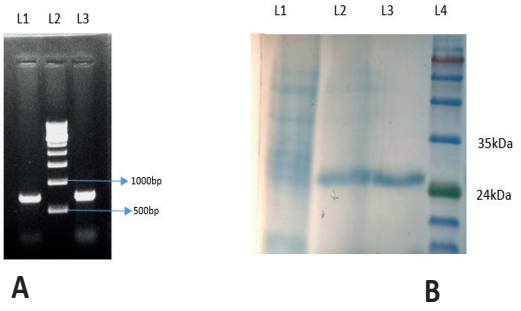


Fig 1: A- PCR confirmation for the presence of the ORF60 gene after inserting in pET-28a plasmid. L1 and L3 shows bands at ~700bp (The size of the ORF60 gene is 711bp). L2 is a 500bp ladder. B- is the SDS-PAGE where L1 is the crude protein from a non transformed *E.coli* BL21, L2 is the crude protein with Lysqdvp001 which shows the expected prtein size of 26kDa, L3 is the purified protein and L4 is the medium ranged protein ladder.

**Cloning and expression of lysqdvp001 in *Dunaliella salina*:**

In order to express the ORF60 gene in *Dunaliella salina,* the gene fragment was cloned into TOPO vector which acts as the entry vector for Gateway cloning. The orientation of the gene in TOPO vector is confirmed by using the M13 primers as shown in Fig 2A. With the help of LR clonase, the ORF60 gene was then transferred into the destination vector pMDC45 through homologues recombination. This was confirmed by PCR as shown in Fig 2B. The pMDC45 with ORF60 was introduced into *Dunaliella salina* through electroporation. The genomic DNA was isolated and PCR was carried out to identify the presence of transgene (ORF60 gene) in the *Dunaliella* genome (Fig 2C).

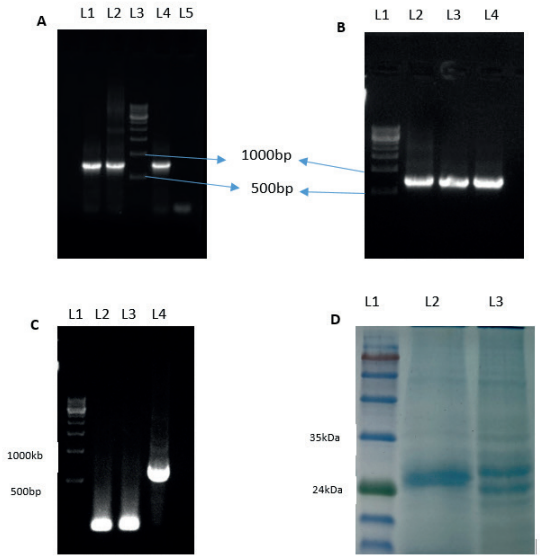


Fig 2: A- Orientation confirmation of ORF60 in TOPO using M13 primers using PCR. L1 is PCR product of M13 forward with gene specific reverse primer, L2 is gene specific forward and M13 reverse primer, L3 is a 500bp ladder, L4 is the positive control where the synthesised gene was used as template. B- PCR confirmation after ORF60 gene was was inserted into pMDC45 plasmid, L1 is 500bp ladder, L2 L3 L4 show positive bands. C- PCR confirmation of presence of ORF60 gene in genomic DNA of transformed *Dunaliella salina*. L1 is 500bp ladder, L2 and L3 show no bands, L4 shows presence of ORF60 gene in the genomic DNA of transformed *Dunaliella salina*. D- SDS-PAGE of extracted protein from *Dunaliella salina*, L1 is a medium ranged protein ladder, L2 is the crude protein extract from transformed *Dunaliella salina* which shows the expected band at ~26kDa, L3 is the crude protein extract from wild type *Dunaliella salina*

**Turbidity reduction assay**

The OD of the EDTA treated *Vibrio parahaemolyticus* cells with added controls, purified Lysqdvp001 and algal expressed Lysqdvp001 were measured at 450nm. Fig 3 shows the lytic activity of both the purified Lysqdvp001 and the

algal expressed Lysqdvp001were significant. This was similar to the results of the positive control, Lysosyme.

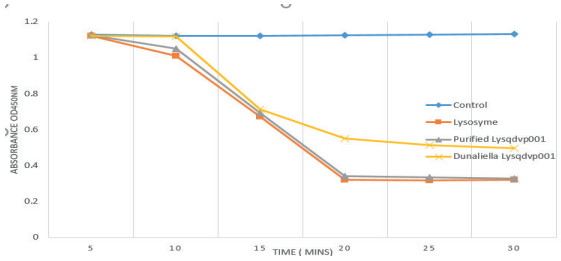


Fig 3: The graph shows the lytic activity of both Lysqdvp001 and *Dunaliella salina* expressed Lysqdvp001 against EDTA treated *Vibrio parahaemolyticus*. The lytic activity was measured for 30 minutes at 25℃.

## Zone of inhibition

The antimicrobial activities of both purified Lysqdvp001 and *Dunaliella salina* expressed Lysqdvp001 were evaluated by measuring the zone of inhibition. As shown in Fig 4 both purified endolysin and algal expressed endolysin, both showed significant lytic activity. Their zones of inhibition were similar to the zone of inhibition of the positive control gentamicin.

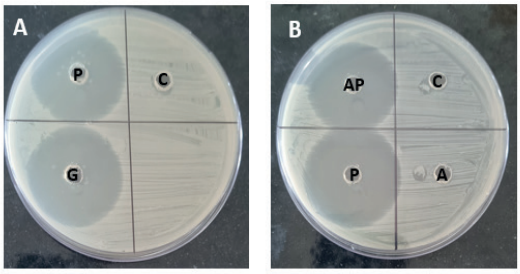


Fig 4: A- shows the zone of inhibition of G-gentamicin, P-purified protein and C- control(water). B- Zone of inhibition of AP- *Dunaliella* expressed Lysqdvp001, P- purified Lysqdvp001, A- wild type *Dunaliella salina* extract , C- control

## Anti-microbial activity against *Vibrio parahaemolyticus* (MIC and MBC)

MIC and MBC were measure to calculate the antibacterial activity of both purified Lysqdvp001 and algal expressed Lysqdvp001. The minimum concentration at which no growth of new cells were found is known as the minimum inhibitory concentration. The MIC for purified Lysqdvp001 was 0.25mg/ml and when these were plated, the minimum concentration at which no colonies are formed is called the minimum bactericidal concentration. The MBC for the purified Lysqdvp001 was found to be to 1mg/ml. The MIC of *Dunaliella salina* expressed Lysqdvp001 was 1.25 % (v/v) and MBC was found to be 2.5 % (v/v) as shown in Table 3.

Table 3: Shows the MIC and MBC values of the positive control gentamicin, Purified Lysqdvp001 and *Dunaliella salina* expressed Lysqdvp001.

| Sample | MIC | MBC |
|---|---|---|
| Gentamicin (control) | 12.5µg/ml | 25µg/ml |
| Purified Lysqdvp001 | 250µg/ml | 1mg/ml |
| *Dunaliella salina*- Lysqdvp001 | 1.25%(v/v) | 2.5%(v/v) |

## Discussion

Endolysins, for quite some time have been considered an alternative to antibiotics, as over exposure to antibiotics can lead to the emergence of multi-drug resistant bacteria (20). One such pathogen is *Vibrio parahaemolyticus*, which is the cause of majority of the bacterial infections in aquaculture and also a major cause of food borne illnesses. The specificity of bacteriophages against specific bacteria make its endolysins all the more important and effective as an alternative to antimicrobials (21). One such endolysin is Lysqdvp001 which is known to be very effective against *Vibrio parahaemolyticus* as shown by (9,10,22)However, unlike gram-positive bacteria, gram-negative bacte-

ria tend to have a thicker peptidoglycan outer membrane. In this study, a 7 cationic amino acid was added to the Lysqdvp001 to increase the hydrolytic activity. The cells were also treated with EDTA to increase the cell permeability and increase the effectiveness of Lysqdvp001. Apart from using EDTA there are also other methods such as adding hydrophobic peptides or by using organic acids (23,24)Using microalgae such as *Dunaliella salina* as an expression system has its advantages like low cost, ease of culturing and easy to manipulate transgenically (25). In this study, the gene ORF60 was transformed into electrocompetent *Dunaliella salina* cells (17) and then grown in a hygromycin supplemented media. The protein extracted from this *Dunaliella salina* containing Lysqdvp001 showed similar antimicrobial activity as the purified Lysqdvp001 as shown by the Fig 4B.

Collectively, this study shows that *Dunaliella salina* can be used as a very good eukaryotic system to express recombinant protein and the Lysqdvp001 endolysin expressed in *Dunaliella salina* has shown to have similar activity to the purified Lysqdvp001.

**References**

1. Austin B, Zhang XH. Vibrio harveyi: A significant pathogen of marine vertebrates and invertebrates. Letters in Applied Microbiology. 2006; 43(2):119-124
2. Toranzo AE, Magariños B, Romalde JL. A review of the main bacterial fish diseases in mariculture systems. Aquaculture. 2005;246(1–4).
3. Nelapati S, Nelapati K, Chinnam BK. Vibrio parahaemolyticus- An emerging foodborne pathogen-A Review. Veterinary World. 2012; 5(1):48-62.
4. Defoirdt T, Sorgeloos P, Bossier P. Alternatives to antibiotics for the control of bacterial disease in aquaculture. Current Opinion in Microbiology. 2011; 14(3):251-258.
5. Vijaya Bharathi S, Rajesh P. Efficacy Of Ficus benghalensis Aerial root Against Seafood Pathogens As A Biopreservative. Current Trends in Biotechnology and Pharmacy. 2023;17(4):1383–9.
6. Terry T, Raj S. The Antibacterial and Antibiotic Potentiating Activity of Marine Sponge Ircinia fusca Against Fish Pathogens. Current Trends in Biotechnology Pharmacy. 2022;16(1):133–40.
7. Borysowski J, Weber-Dąbrowska B, Górski A. Bacteriophage endolysins as a novel class of antibacterial agents. Experimental Biology and Medicine. 2006; 231(4):366-377.
8. Schmelcher M, Tchang VS, Loessner MJ. Domain shuffling and module engineering of Listeria phage endolysins for enhanced lytic activity and binding affinity. Microb Biotechnol. 2011;4(5).
9. Wang W, Li M, Lin H, Wang J, Mao X. The Vibrio parahaemolyticus-infecting bacteriophage qdvp001: genome sequence and endolysin with a modular structure. Arch Virol. 2016;161(10).
10. Ning H, Cong Y, Lin H, Wang J. Development of cationic peptide chimeric lysins based on phage lysin Lysqdvp001 and their antibacterial effects against Vibrio parahaemolyticus: A preliminary study. Int J Food Microbiol. 2021;358.
11. Praveen AS, Vinitha S, Vinayalekshmi VS, Ramya P, Vanavil B. Seaweed Metabolites for Targeting Pel Polysaccharide Biosynthesis in Pseudomonas aeruginosa– A Novel Strategy for Biofilm Control. Current Trends in Biotechnology and Pharmacy. 2023;17(3):1316–26.
12. Masojídek J, Torzillo G. Mass Cultivation of Freshwater Microalgae. In: Reference Module in Earth Systems and Environmental Sciences. 2014.
13. Drepper T, Krauss U, Meyer Zu Bersten-

horst S, Pietruszka J, Jaeger KE. Lights on and action! Controlling microbial gene expression by light. Applied Microbiology and Biotechnology. 2011; 90:23-40.

14. Potvin G, Zhang Z. Strategies for high-level recombinant protein expression in transgenic microalgae: A review. Biotechnology Advances. 2010; 28(6):910-918.

15. Bradford MM. A rapid and sensitive method for the quantitation of microgram quantities of protein utilizing the principle of protein-dye binding. Anal Biochem. 1976;72(1–2).

16. Reece-Hoyes JS, Walhout AJM. Gateway recombinational cloning. Cold Spring Harbor Protocols. 2018.

17. Velmurugan A, Kodiveri Muthukaliannan G. Homologous and heterologous expression of phytoene synthase gene in marine microalgae Dunaliella salina and its potential as aquaculture feed. Aquac Int. 2023;31(6).

18. Nelson D, Loomis L, Fischetti VA. Prevention and elimination of upper respiratory colonization of mice by group A streptococci by using a bacteriophage lytic enzyme. Proc Natl Acad Sci U S A. 2001;98(7).

19. Li L, Liang F, Li C, Hou T, Xu DA. Antibacterial Mechanism of Chitosan-Gentamicin and Its Effect on the Intestinal Flora of Litopenaeus vannamei Infected with Vibrio parahaemolyticus. Mar Drugs. 2022;20(11).

20. Gondil VS, Harjai K, Chhibber S. Endolysins as emerging alternative therapeutic agents to counter drug-resistant infections. International Journal of Antimicrobial Agents. 2020; 55(2):105844.

21. Sillankorva S, Oliveira D, Moura A, Henriques M, Faustino A, Nicolau A, et al. Efficacy of a broad host range lytic bacteriophage against E. coli adhered to urothelium. Curr Microbiol. 2011;62(4).

22. Ning HQ, Lin H, Wang JX. Synergistic effects of endolysin Lysqdvp001 and ε-poly-lysine in controlling Vibrio parahaemolyticus and its biofilms. Int J Food Microbiol. 2021;343.

23. Vaara M. Agents that increase the permeability of the outer membrane. Microbiol Rev. 1992;56(3).

24. Lim JA, Shin H, Kang DH, Ryu S. Characterization of endolysin from a Salmonella Typhimurium-infecting bacteriophage SPN1S. Res Microbiol. 2012;163(3).

25. Feng S, Li X, Xu Z, Qi J. Dunaliella salina as a novel host for the production of recombinant proteins. Applied Microbiology and Biotechnology. 2014; 98:4293-4300.

Current Trends in Biotechnology and Pharmacy
Vol. 18(2) 1773-1778, April 2024, ISSN 0973-8916 (Print), 2230-7303 (Online)
DOI: 10.5530/ctbp.2024.2.25


# Biosorption of Zn (II) ion from Aqueous Solutions Using Nut Grass

**P. Bangaraiah**

Department of Chemical Engineering, VFSTR University, Vadlamudi,Guntur-AP.
Corresponding author:pbangaraiah79@gmail.com

**Abstract**

The present investigation, removal of Zn (II) ion from industry effluent was examined by using Nut grass as a biomass. The process conditions of agitation time and dosage were estimated using batch biosorption. The equilibrium data analyzed with Freundlich and Langmuir isotherms. The results revealed that removal of Zn (II) using Nut grass well followed to the Freundlich model than Langmuir model. The first order and pseudo- second order kinetic expressions were tested to find the best fit for the given kinetic data. It was observed that second order kinetics was the best fit for biosorption of Zn (II) ion. The maximum biosorption capacity of the nut grass for biosorption of Zn (II) ion was occurred at 40 mg/g.

**Keywords:** Biosorption; Nut grass; isotherms; kinetics; Zinc.

## Introduction

The contamination of water by toxic heavy metals is a worldwide environmental problem. Metals are known to be essential to plants, humans and animals, but they can also have adverse effects if their availability in water exceeds the permissible limits. Many industries, especially electroplating, battery and plastic manufacturing release heavy metals such as cadmium and zinc in wastewater (1,2) Zinc, which is generally considered nontoxic, the recommended upper limit for discharge is about 5 mg/L (3). Recovery of Zinc from wastewater will become increasingly important when conservation of essential metals becomes more essential (4). Conventional techniques have limitations (5) and often are neither effective nor economical especially for the removal of heavy metals at low concentrations. New separation methods are effective and environmentally acceptable at affordable cost (6,7). Several methods are utilized to remove Zinc from industrial wastewater. It includes Chemical Precipitation, Lime Coagulation, Reduction, Activated carbon Adsorption, Electrolytic removal, Ion- exchange, Reverse Osmosis, Membrane Filtration and Solvent Extraction (8). Among the various wastewater treatment techniques described, adsorption is generally preferred for the removal of heavy metal ions due to its high efficiency, easy handling, availability of different adsorbents and cost effectiveness (9). Biosorption is a passive immobilization of metals by biomass which is capable of removing traces of heavy metals and other elements from dilute aqueous solutions (10). Many biomaterials such as Peels, husks, plant wastes, bacteria fungi and many more are available for sorption of zinc from waste water (11). The agricultural waste products are also used for the sorption of heavy metal and many researchers are worked on these biomaterials and found suitable for removal of heavy metals (12).

The objective of this study was to evaluate the potential of Nut Grass for the removal of Zinc ion from aqueous solution.

Batch tests were conducted for evaluation of Zn in aqueous solutions under various conditions (contact time and adsorbent dose).

## Materials and Methods

### *Chemicals*

All chemicals and reagents used were of analytical purity. The stock solution of Zn (II) was prepared in 1.2 g/L concentration using $ZnCl_2$ and then diluted to appropriate concentrations for each test (13).

### *Preparation of bio-sorbent*

Nut Grass (NG) an agricultural waste used in this study was obtained from local area. The wet NG was washed several times with tap water and de-ionized water to remove particulate material and dried under sun for 6 days, ground and sieved in to different fractions (200-130 µm) (14).

### Batch adsorption experiments

Batch adsorption experiments were carried out at room temperature by agitating 0.2 -3.0 g/L of adsorbent at a stirring speed of 160 rpm for a contact time of 300 min. For each batch experiment, zinc solution of 10 mg/L concentration was used. Isotherms were obtained by adsorbing different concentrations of metal ions. After prescribed contact times the solutions were centrifuged and the concentrations of metal ions were determined by atomic spectrometry (15).

## Results and Discussion

### *Characterization of bio-sorbent before adsorption*

The characteristics of the bio-sorbents like specific gravity, density, Iodine number and Loss on Ignition were found and listed in Table 1.

### *Effect of contact time*

The adsorption of Zn (II) ion onto NG was studied as a function of contact time in order to determine the necessary equilibrium time. Fig. 1 illustrates the adsorption profile of Zn (II) onto NG. The curve exhibits characteristics of a single, smooth and continuous leading to saturation. Initially a large number of vacant sites are available for adsorption. The adsorption rate is very fast thus rapidly increasing the amount of adsorbate accumulated on the NG surface mainly within 160 min of adsorption. As a result, the remaining vacant surface sites are difficult to be occupied due to the formation of repulsive force between the Zn (II) ion on the solid surface and in the bulk phase (16)

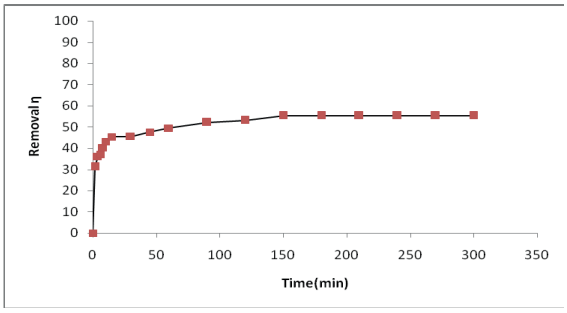


Fig. 1 Effect of Contact Time on Zn (II) uptake by Nut Grass

### *Adsorption kinetics*

Kinetic modeling provides thorough details on the sorption mechanism of solute onto an adsorbent. In this study, kinetic models of Lagergren pseudo- first and second order models were used to examine chemical reaction as rate-controlling parameter for Zn (II) ion adsorption mechanism (17). Linear forms of pseudo-first-and pseudo-second order kinetic equations are given in Eqs. (1) and (2), respectively.

Table 1 Characteristics of the Bio-sorbents

| Bio-sorbent | Specific Gravity | Density (Kg/m$^3$) | Iodine number | Loss on Ignition (%) |
|---|---|---|---|---|
| Nut Grass | 0.915 | 914 | 411 | 70 |

$$\log(q_e - q_t) = \log(q_e) - \frac{k_1}{2.303} t \quad (1)$$

$$\left(\frac{t}{q_t}\right) = \frac{1}{k_2 q_e^2} + \frac{1}{q_e}(t) \quad (2)$$

solute adsorb per unit weight of adsorbent at time ($mgg^{-1}$), $k_1$ is rate constant of pseudo-first-order sorption and $k_2$ is rate constant of pseudo-second-order sorption. Linear plots of pseudo-first- and second-order kinetic model for Zn (II) adsorption onto NG are given in Figs. 2 and 3 respectively. The correlation coefficient obtained from the first order kinetic is 0.974. Whereas the correlation coefficient obtained from the second order kinetic is 0.998 which is still better than the correlation coefficient of first order kinetics. Hence the Zn (II) ion adsorption on to the NG was found to be in conformation to pseudo-second-order kinetic model, suggesting that chemical reaction is a rate-controlling parameter (18). Table 2 shows the pseudo first and second- order kinetic model constants for Zn (II) ion batch adsorption system.

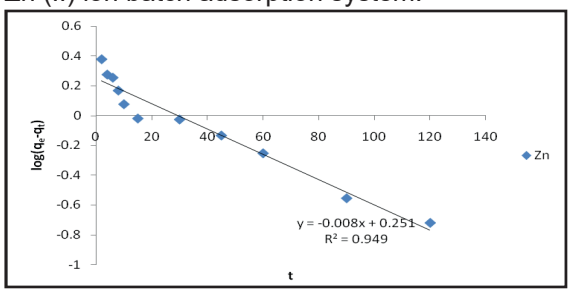


Fig. 2. Pseudo First Order Kinetics for uptake of Zn (II) by Nut Grass

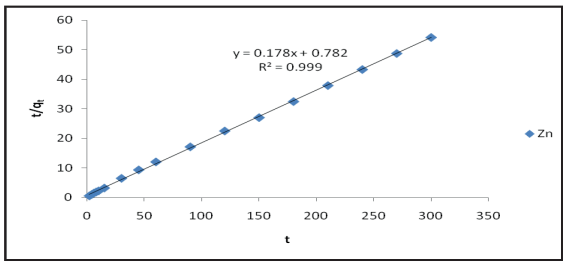


Fig. 3 Pseudo Second Order Kinetics for uptake of Zn (II) by Nut Grass

### *Effect of adsorbent dosage*

The study on biosorbent dosage of Nut Grass for the removal of Zn (II) ion from aqueous solution was carried out at different doses (0.2-3.0 g/L) using 10.0 mg/L of Zn (II) solution. The effect of adsorbent dosage on the Zn (II) removal efficiency is shown in Fig. 4. It was observed that the amount of Zn adsorbed increases with an increase in adsorbent dosage from 0.2 to 2.0 g/L. For biosorbent dosage higher than this value, the Zn (II) removal remained almost constant. Increase in percentage of Zn (II) removal with adsorbent dosage could be attributed to increase in the adsorbent surface areas, augmenting the number of biosorption sites available for biosorption (19).

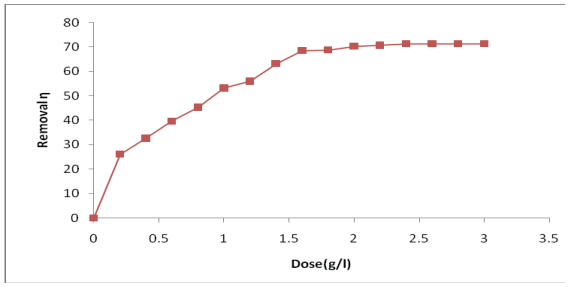


Fig.4 Effect of adsorbent dose for the adsorption of Zn (II) onto the Nut Grass

### *Adsorption isotherms*

Adsorption isotherm is basically an important criterion in optimizing the use of adsorbents as they describe the nature of interaction between adsorbate and adsorbent. Langmuir and Freundlich isotherm models are widely used to investigate the adsorption process. The Langmuir isotherm was developed on the assumption that the adsorption process will only take place at specific homogeneous sites within the adsorbent surface with uniform distribution of energy level. Once the adsorbate is attached on the site, no further adsorption

Table.2 Kinetic parameters of the Pseudo-first and second order model for Zn (II) adsorption

| Metal | Pseudo 1st Order Kinetics Coefficients | | | Pseudo 2nd Order Kinetics Coefficients | | | $q_e$exp (mg/g) |
|---|---|---|---|---|---|---|---|
| | $q_e$cal(mg/g) | $K_1$ | $R^2$ | $q_e$(mg/g) | $K_2$ | $R^2$ | |
| Zn | 1.791 | 0.016 | 0.974 | 4.615 | 0.042 | 0.998 | 5.528 |

Table 3 Langmuir and Freundlich Constants for the removal of Zn (II) ion

| Metal | Langmuir Isotherm constants | | | Freundlich Isotherm constants | | |
|---|---|---|---|---|---|---|
| | $q_{max}$ (mg/g) | b | $R^2$ | n | $K_f$ (mg/g) | $R^2$ |
| Zn | 40.000 | 0.034 | 0.907 | 1.062 | 1.236 | 0.926 |

can take place at that site; which concluded that the adsorption process is monolayer in nature. Contrarily to Langmuir, Freundlich isotherm was based on the assumption that the adsorption occurs on the heterogeneous sites with non-uniform distribution of energy level (20). The linear form of Langmuir and Freundlich equations are represented by Eqs.(3) and (4), respectively.

$$\frac{1}{X/M} = \frac{1}{q_{max}} + \frac{1}{q_{max} b} \frac{1}{C_e} \quad (3)$$

$$\log q_e = \log K + \frac{1}{n} * \log C \quad (4)$$

Where $q_e$ is amount of adsorbate adsorbed at equilibrium (mgg-1), $C_e$ (mmol$^{-1}$) is the equilibrium concentrations of metal ions in the liquid and the solid phases, respectively. $Q_m$, b, K and n are the Langmuir and Freundlich constants respectively. Fig. 5 and 6 exhibit the linear plots of Langmuir and Freundlich for Zn (II) adsorption onto Nut Grass.

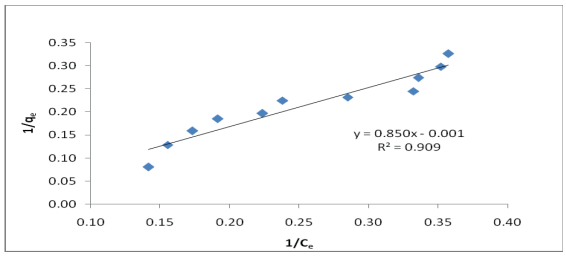


Fig.5 Langmuir adsorption isotherm plot for Zn (II) ion uptake by Nut Grass

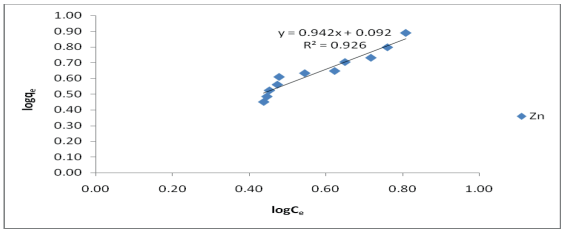


Fig. 6. Freundlich adsorption isotherm plot for Zn (II) ion uptake by Nut Grass

The Langmuir and Freundlich Constants for the removal of Zn (II) ion are shown in Table 3. The $R^2$ value shown in Table 3 is evident that the Zn (II) adsorption in this study is well fitted to Freundlich model.

## Conclusions

The biosorption of Zn (II) ion on Nut grass was investigated. Nut Grass is a suitable sorbent for the removal of Zn (II) ion from aqueous solution. The Zinc removal was a function of contact time and adsorbent dose. The Freundlich isotherm has higher correlation coefficient than those of Langmuir isotherm. The adsorption of Zn (II) from aqueous solution by Nut Grass obeys the pseudo-second-order kinetics. Low cost and availability of Nut Grass, and significant high adsorption capability make it a promising and potentially attractive adsorbent for treating wastewater contaminated with heavy metal like Zinc and consequently provides a step towards a sustainable society.

## References

1. Ajitha R. Meena, Devi V. N. and Murugan, M. (2015). Biosorption of Zn (II) from aqueous solution onto the Alexandrian laurel oil cake. Journal of Chemical and Pharmaceutical Research, 7:643-648.

2. Abdus-Salam, N. and Adekola, S.K. (2018). Adsorption studies of zinc(II) on magnetite, baobab (Adansonia digitata) and magnetite–baobab composite. Applied water science, 8: 222-231.

3. Karima, R. Hana, F. Amel, D. Touhida, H. et.al. (2023). Biosorption of zinc (II) from synthetic wastewater by using Inula Viscosa leaves as a low-cost biosorbent: Experimental and molecular modeling

studies. Journal of Environmental Management. 326: 116742-116752.

4. Dias, M. Pinto, J. Henriques, B. Figueira, P. et al. (2021). Nutshells as Efficient Biosorbents to Remove Cadmium, Lead, and Mercury from Contaminated Solutions. International Journal of Environmental Research and Public Health, 18:1580-1587.

5. Xu, L. Xing, X. and Peng, J. (2022). Removal of Zn2+ from Aqueous Solution Using Biomass Ash and Its Modified Product as Biosorbent. International Journal of Environmental Research and Public Health, 19: 9006-9012.

6. Ighalo, J.O.and Eletta, O.A.A. (2020). Response surface modelling of the biosorption of Zn(II) and Pb(II) onto Micropogonias undulatus scales: Box–Behnken experimental approach. Applied Water Science, 10:197-218.

7. Kour, R. Jain, D. Bhojiya, A.A. Sukhwal, A. et al. (2019). Zinc biosorption, biochemical and molecular characterization of plant growth-promoting zinc-tolerant bacteria. 3 Biotech, 9:421-432.

8. Moein, S. and Salman, A.A. (2018). Biosorption of zinc from aqueous solution by cyanobacterium Fischerella ambigua ISC67: optimization, kinetic, isotherm and thermodynamic studies. Water Science Technology,78: 1525–1534.

9. Kanchana,S. and Sivaprakash, P. (2021).Biosorption of zinc from industrial wastewater using three different Algal species. Indian Journal of Environmental Protection, 4: 924-930.

10. Kalyania, G. Gokulanb, R. and Sujathac,S. (2021). Biosorption of zinc metal ion in aqueous solution using biowaste of Pithophora cleveana Wittrock and Mimusops elengi. Desalination and Water Treatment, 218: 363–371.

11. Mwandira, W. Nakashima, K. Kawasaki, S. et al. (2020). Biosorption of Pb (II) and Zn (II) from aqueous solution by Oceanobacillus profundus isolated from an abandoned mine, Scientific Reports. 10: 21189-21198.

12. Rezgui, A. Hannachi, Y. Guibal, E. and Boubaker, T. (2015). Biosorption of zinc from aqueous solution by dried activated sludge biomass. Desalination and Water Treatment, 56: 2699-2705.

13. Duraisamy, R. and Antony, J.T. (2019). Biosorption of Zinc from aqueous solution by the bacterial strain, Morganella morganii ACZ05. Asian Journal of Biological Sciences,12: 869-876.

14. Bangaraiah,P. and Sarath Babu.B.(2017). Kinetic and equilibrium studies on biosorption of zinc using tamarindus indica L. Research Journal of Pharmacy and Technology,10: 2641-2644.

15. Feng, C. Li, J. Li, X. Li, K. et al. (2018). Characterization and mechanism of lead and zinc biosorption by growing Verticillium insectorum J3. PLOS ONE, 13(12):1-16.

16. Denisova, V. Tihomirova, K. and Mezule, L. (2017). Biosorption of zn(ii) by sphagnum peat. Chemical Engineering Transactions, 57: 385-390.

17. Preetha, B. and Viruthagiri, T. (2020). Biosorption of zinc (II) by Rhizopus arrhizus: equilibrium and kinetic modelling. International Journal of Biochemistry and Biotechnology. 9: 001-003.

18. Zeynep, K. Orhan, A. Sümer, A. Demet, C.D. et al. (2014). Biosorption properties

of zinc(II) from aqueous solutions by Pseudevernia furfuracea (L.) Zopf, Journal of the Air & Waste Management Association, 64:1112-1121.

19. King, P. Anuradha, K. Lahari, S.B. et al. (2008). Biosorption of zinc from aqueous solution using Azadirachta indica bark: equilibrium and kinetic studies. Journal of Hazardous Materials, 152:324-329.

20. Zhang, Y. Zheng, R. Zhang, Y. Ma, F. (2012). Biosorption Mechanisms of Zinc from Aqueous Solution by Using H3PO4-Modified Rice Husk. Journal of Biobased Materials and Bioenergy, 6: 669-672.

Current Trends in Biotechnology and Pharmacy
Vol. 18(2) 1779-1787, April 2024, ISSN 0973-8916 (Print), 2230-7303 (Online)
DOI: 10.5530/ctbp.2024.2.26



# Relative Performance of Bedside Mobility Assessment Tool 2.0 (BMAT) Over Others for Acute Care Patient Recovery

**Charumathi Polavarapu[1], Bhavana Raja[2]**

[1]St. Luke's Health Memorial Hospital, 1717 US-59 Loop North, Livingston, Texas 77351, USA
[2]Department of Physical Therapy, School of health sciences, University of the Pacific, Stockton, CA 95211, USA
Corresponding author: charu.physio@gmail.com

**Abstract**

Immobility compromises almost all of the body's systems. Research indicates that individuals who were mobile before being admitted to the hospital may spend approximately 83% of their hospital stay in bed, and over one-third of hospitalized patients over the age of 70 are released from the hospital with a significantly higher physical limitations than prior to hospital admission. Healthcare professionals should be able to accurately assess patient's mobility status in order to implement interventions to mobilize patients even in the presence of deficiencies. The purpose of this review is to assess the Bedside Mobility Assessment Tool 2.0 (BMAT 2.0), to objectively identify patient mobility function deficiencies and assist the healthcare team in choosing the right equipment for patients to be handled and moved safely. BMAT 2.0 is best used by the interdisciplinary team, involved in patient care, and can be recorded in the electronic health record (EHR). Further, a comparative account of other methods being practiced vis-à-vis the BMAT is given in this article.

**Keywords**: BMAT 2.0, Acute care, Bedside Mobility assessment tool (BMAT), Banner Bedside mobility assessment tool, Length of stay, Safe patient handling and Mobility (SPHM)

## Introduction

Extended bed rest for those who are hospitalized may result in loss of muscle strength, soft tissue changes, psychological issues, long term pressure-ulcers, skin deterioration, and nosocomial pneumonia, among other unexpected consequences (5). During immobilization, muscle strength decreases at a rate of 20% per week (1). Furthermore, pressure ulcers, falls, and functional decline are among the additional hospital hazards that are predicted by low mobility (1). Nurses play a vital role in patient care at hospitals and must have a thorough understanding of the patient's health. Although it is widely known that assessing a patient's mobility early on is crucial for preventing falls, nurses often struggle to do so at the patient's bedside (1). The amount of effort, patience, and expertise the physician needs to complete the current tools for assessing patients' mobility status limits the evaluation. Additionally, there are a limited reliable and valid tool to assess the mobility of hospitalized patients. To effectively monitor a patient's progress and deliver appropriate care, acute care nurses require a reliable instrument

for bedside mobility assessments that is simple to use. BMAT could also be a part of physiotherapists assessments, since they are an important member of the early mobility team (11). The purpose of this review is to investigate the application of BMAT 2.0 as a mobility assessment tool for hospital staff and compare it to the other more commonly used assessment tools.

***Banner mobility assessment tool (BMAT)***

According to nurses, Banner Mobility Assessment Tool (BMAT) is an efficient resource (2) to assess early mobility in patients in the hospital. It is usually stored in hospital's electronic medical record (EMR) (2) for ease of access.

***Performing assessment***

Patients are categorized as having a mobility level of 1, 2, 3, or 4 based on how effectively or poorly they perform at each evaluation level of the BMAT tool (2). Nurses and support personnel are trained on the appropriate technology for patients at each station using educational resources and how-to apply the tool to the patients depending on their needs. The tool explicitly specifies the following criteria: (i) the use of walkers, crutches, canes, and prosthetic legs by progressing patients. (ii) the assessment process and determination of pass or fail. (iii) the role of the nurse in assessing, strengthening, and advancing patients. (iv) the growth from level 3 to level 4.

BMAT 2.0 primarily focuses on the previous level of function (PLOF), discharge planning, and goals for mobilizing patients who meet all four assessments. Additionally, it addresses the management of bilateral non-weight-bearing patients and patients under bed rest orders. Nurses typically perform BMAT 2.0 upon patient admission, during each shift, and whenever there is a significant change in the patient's condition. This assessment generally takes about two minutes to complete. In "safe mode," it enables the care team to evaluate the patient's degree of mobility, plan and organize ways to reinforce and to improve mobility, aim for the appropriate piece of equipment.

The BMAT is a valuable tool for care teams to evaluate mobility. It can be utilized by nurses to assess patients' mobility, integrated into early assessments by physiotherapists, and serve as a means for the interdisciplinary team to discuss mobility status.

***Bedside mobility assessment tool (BMAT)***

The BMAT was created to evaluate a patient's functional state securely rather than relying solely on gait analysis (14). Historically, mobility evaluation was carried out without a procedure. A mobility evaluation should be chosen with the needs of the population it is intended for in mind (16). Clinicians can access a baseline of patient mobility capability with the BMAT (14). The score gives the healthcare provider a person-specific intervention that involves the patient and helps lower falls when a patient's functional ability fails to advance through the phases. Using EMR tools that connect assessment results with safe patient handling and mobility (SPHM) technology, mobility assessment documentation has been utilized to enhance communication within the care team.

As discussed above, BMAT is a mobility assessment tool used primarily by the nurses. The tool classifies a patient in four levels depending on completion of a task, equipment used, and caregiver assistance. The detailed description of the tool is provided in table 1.

Table 1: Describes the BMAT assessment tool in details. Each cell also clearly describes the steps to complete the assessment and grading.

| Response | Task | Response & No. of Caregivers | Fail =choose most appropriate equipment/ device(s) | Pass |
|---|---|---|---|---|
| Assessment level 1 assessment of:<br><br>-trunk strength<br><br>-seated balance | Sit and shake: Ask the patient to sit up straight and rotate* to a sitting position at the side of the bed from a semi-reclined position; they can use the bedrail to do so.<br><br>Observe how well the patient can stay in the bedside posture.<br><br>Make sure the patient crosses his or her midline when you ask them to reach out and grasp your hand for a shake. | Sit: The patient can follow orders and has some trunk strength; if a patient can maintain a sitting balance for more than two minutes (without caregiver assistance).<br><br>Caregivers may try weight-bearing.<br><br>Shake: the patient has significant upper body strength, awareness of the body in space, and grasp strength.<br><br>Caregivers: Minimum 2 or more | mobility level 1<br><br>Use total lift with sling and/or repositioning sheet and/or straps.<br><br>Use lateral transfer devices such as roll board, friction reducing (slide sheets/tube), or air assisted device.<br><br>Note: if patient has 'strict bed rest' or bilateral 'non-weight bearing' restrictions, do not proceed with the assessment; patient is mobility level 1. | Passed assessment level 1 = proceed with assessment level 2. |
| Assessment level 2 assessment of:<br><br>-lower extremity strength<br><br>-stability | Stretch and point: Place the patient's both feet on the floor (or a stool) with their knees no higher than their hips while they are seated at the side of the bed.<br><br>Request that the patient extend one leg, straighten the knee, and flex the ankle pointing the toes. Repeat with the opposite leg if necessary. | Patient exhibits lower extremity stability, strength, and control.<br><br>May test only one leg and proceed accordingly (e.g., stroke patient, patient with ankle in cast).<br><br>Caregivers: Minimum 2 or more | mobility level 2<br><br>Use total lift for patient unable to weight- bear on at least one leg.<br><br>Use sit-to-stand lift for patients who can weight-bear on at least one leg. | Passed assessment level 2 = proceed with assessment level 3. |

| | | | | |
|---|---|---|---|---|
| Assessment level 3 assessment of:<br><br>-lower extremity strength for standing | Stand: Have the patient use an assistive equipment (cane, bedrail) to raise themselves from the bed or chair (sitting to standing).<br><br>The patient must be able to lift their buttocks off the bed and hold them there for five counts and may come back<br><br>Note: consider your patient's cognitive ability, including orientation and Confusion Assessment Method (CAM) assessment if applicable. | Patient exhibits upper and lower extremity stability and strength.<br><br>May test with weight-bearing on only one leg and proceed accordingly (e.g., stroke patient, patient with ankle in cast).<br><br>If any assistive device (cane, walker, crutches) is needed, patient is mobility level 3.<br><br>Caregivers: 1 to 2 | mobility level<br><br>Use non-powered raising/stand aid; default to powered sit-to-stand lift if no stand aid available.<br><br>Use total lift with ambulation accessories.<br><br>Use assistive device (cane, walker, crutches).<br><br>Note: patient passes assessment level 3 but requires assistive device to ambulate or cognitive assessment indicates poor<br><br>safety awareness; patient is mobility level 3. | Passed assessment level 3 and no assistive device needed = proceed with assessment level 4. Consult with Physical therapist when needed and appropriate. |
| Assessment level 4 assessment of:<br><br>-standing balance<br><br>-gait | Step: At the bedside, ask the patient to march in place.<br><br>Ask the patient to take a step forward and then to put each foot back.<br><br>The patient should be stable when carrying out tasks. Check for stability and an awareness of safety. | Patient exhibits steady gait and good balance while marching, and when stepping forwards and backwards.<br><br>Patient can maneuver necessary turns for in-room mobility.<br><br>Patient exhibits safety awareness.<br><br>Caregivers: 0 to 1 | mobility level 4<br>If patient shows signs of unsteady gait or fails assessment level 4, refer back to mobility level 3; patient is mobility level 3. | mobility level 4 modified independence<br><br>Passed = no assistance needed to ambulate; use your best clinical judgment to determine need for supervision during ambulation. |

***Other current patient mobility assessment options and their limitations***

Various types of mobility assessment tools are used in healthcare settings to evaluate an individual's ability to move and perform daily activities. Each tool has its unique characteristics, strengths, and limitations (4). Table 2 provides an overview of the description, benefits, and drawbacks of each tool used to evaluate patient mobility (4).

| Patient mobility assessment tools | Description | Advantages | Limitations |
|---|---|---|---|
| **Timed Up and Go (TUG) Test** | This test measures the time it takes for an individual to stand up, walk a short distance, turn, walk back, and sit down | The advantage of this tool is quick to administer, and minimal equipment requirement | Primarily it assesses the basic mobility, but may not capture the complex movements |
| **Berg Balance Scale (BBS)** | BBS assesses the balance through tasks like standing on one foot, turning, and reaching | Its advantages include providing a detailed assessment of balance | Time-consuming, and may have a ceiling effect for mild impairments |
| **Functional Independence Measure (FIM)** | FIM evaluates an individual's ability to perform activities of daily living, including mobility tasks | It comprehensively assesses the functional independence | Time-consuming, and relies on observer ratings |
| **Dynamic Gait Index (DGI)** | DGI assesses an individual's ability to modify gait in response to various tasks | It focuses on dynamic aspects of gait and balance | It may not be suitable for severe gait impairments |
| **Six-Minute Walk Test (6-MWT)** | 6-MWT measures the distance an individual can walk in six minutes | It assesses the endurance and cardiovascular fitness | It gives limited information on specific components of mobility |
| **Instrumented Gait Analysis (IGA)** | IGA uses technology such as motion capture systems to analyze various aspects of gait | It provides objective data on gait parameters | The main disadvantage of this test is it requires specialized equipment and expertise |
| **Self-Reported Scales (Activities-Specific Balance Confidence Scale)** | In this test, individuals rate their confidence in performing specific activities without falling | It incorporates the patient's perspective | It is subject to bias, and may not align with objective measures, which is the major disadvantage |
| **Gait Speed Assessment (GSA)** | GSA measures the time it takes for an individual to walk a specific distance | The method is quick and easy to measure | limited in assessing dynamic movements |
| **Quick Five and Quick Three** | The Quick 5, developed by a registered nurse and a PT, formed the foundation for a research project that evolved into the Quick 3. | It is more accessible and easier to administer | This tool guides patients through three functional tasks but falls short in fully accommodating patient limitations or addressing the abilities of ambulatory patients. |

Relative performance of bedside mobility assessment tool 2.0 (BMAT) over others for acute care patient recovery

| | | | |
|---|---|---|---|
| **Egress test** | Created by a physical therapist. The patient begins by doing three repetitions of the sit-to-stand exercise, marching in place, and advancing one foot forward and back with each step at the bedside. | The advantage of this test is quick to administer, and minimal equipment requirement | This test ignores the patient's bed mobility, also it is inappropriate for some patients such as those unable to bear weight on one or both legs and only provides minimal guidelines for nurses regarding the use of SPHM<br><br>technology. |
| **Bedside Mobility Assessment Tool** | Focuses on assessing a patient's mobility, transfers, and functional movements at the bedside | Accessibility: Can be conducted at the patient's bedside, minimizing disruptions and discomfort.<br>Real-world simulation: Provides insights into practical challenges faced by patients in the hospital environment.<br>Timeliness: Offers a quick assessment of mobility, suitable for dynamic acute care settings. | |

**Limitations of current mobility assessment tools**

While numerous mobility assessment instruments are available, they all have distinct shortcomings. The patient is first asked to get out of an armchair, walk three meters, turn, and then return to the chair before taking a seat in the Timed Get Up and Test. However, it offers no advice on what to do if the patient cannot support their weight, walk, or maintain a seated balance (3). On the other hand, a tool like Quick 5 offers very few suggestions on safe patient handling and the use of mobility technology. Next, the egress test, ignores the patient's bed mobility or standing technique, or it may be inappropriate for some patients (such as those unable to bear weight on one or both legs) and only provides minimal guidelines for nurses regarding the use of safe patient handling and the use of mobility technology (3).

***Applications of BMAT***

***Utilizing the bedside mobility assessment tool to reduce the length of stay***

The length of stay (LOS) in acute care hospitals is a critical metric influencing patient outcomes and healthcare costs. Prolonged hospital stays are associated with increased risks of complications, functional decline, and healthcare expenses. But the effective use of bedside mobility assessment tools presents an opportunity to identify early mobility issues, implement targeted interventions, and potentially reduce the length of hospital stays (5).

**Rationale for bedside mobility assessment**

Bedside mobility assessments offer a practical and timely means of evaluating a patient's functional status directly in their hospital environment. By focusing on mobility, transfers,

A streamlined and targeted approach to patient care, guided by bedside mobility assessments, has the potential to reduce healthcare costs associated with prolonged hospital stays, unnecessary tests, and increased resource utilization (6).

BMAT can be adequately applied in different departments of a hospital, from Emergency department to the ICU.

**Use of the bedside mobility assessment tool to improve emergency department (ed) safety**

The most frequent adverse event in acute care settings documented in the healthcare industry is avoidable patient falls (12). Nearly seven hundred thousand to one million Americans fall in hospitals each year (Agency for Healthcare Research and Quality (AHRQ), 2021). ED is usually the first hospital location most patient's encounter. A detailed analysis of the patient demographics and the features of the patients who fall in the ED are necessary to determine the best approach for preventing the falls. Most individuals who fall in the ED are younger than the 65-year-old, and usually fell between 15.00 and 18:00 hours (13). Hospital staff can more effectively assess the risk of patients' fall using standardized fall risk instruments and strategies. Following which, safe patient handling and mobility technology can prevent as many as 13% of falls (16, 19, 20). Along with improving worker safety, this approach also complies with the American Nurses Association's (2015) recommendations to reduce manual lifts, a standard procedure for patient transfers and moves at the project site. By determining a patient's degree of mobility, the BMAT assessment equips patient caregivers with valuable information and helps them quickly identify the appropriate equipment for better healing and recovery (Boynton et al. 2020) (14).

**Implementation of the bedside mobility assessment tool in the ambulatory care setting**

Safe patient care depends on the effectiveness of nursing assessments. The nursing process is a systematic, patient-centered manual. The five crucial steps associated with this are evaluation, diagnosis, preparation, execution, and assessment. In order to keep patients safe, nurses must take all necessary precautions (7). Almost 30% of patient injuries happened during post-procedural sedation treatment, particularly during lateral transfers and repositioning. Falls among the elderly are common and can cause serious injuries as well as occasionally result in death (8). A systematic analysis of literature focusing on fall risk assessment revealed that the mobility assessment category was the most trustworthy area to evaluate in order to determine fall risk (9). Mobility strategies have been shown in an increasing amount of research to protect patients and nursing personnel while handling patients (10). Appropriate operation and training of each unique body system is facilitated by mobility, to ensure the safety and proper assessment of patients prior to their discharge which is imperative.

**Early mobility in the intensive care unit**

An intensive care unit (ICU) patient's immobility may have a detrimental effect on their condition and extend their LOS. An evidence-based strategy for early mobility was found to be lacking at the site where treatment is being given. The impact of this protocol on ICU LOS has been ascertained. For four weeks, the research was carried out in a southern California urban community hospital (17). Patients in the neighborhood hospital ICU where these experiments were conducted stayed mostly immobile despite research suggesting that mobility is advantageous. Therefore, it is suggested that the hospital needs a protocol in place for mobilizing patients. While creating mobility programs, organizational culture has a significant influence to play (17). The lack of programs in the project context indicated an inferior level of care at a potentially higher cost, given the magnitude of the benefits associated with mobility. In the community hospital ICU context, Jones et al. (15) noted the significance of applying evi-

dence-based treatments to support early mobility programs using the BMAT. Early mobility programs in the ICU have reduced the pressure, generation of ulcers and ICU length of stay, if patient care is improved (18;19). A few of these programs have used the BMAT, but research has yet to reveal how well the BMAT works in a community hospital context compared to the other tools. Mobility treatment is used in the BMAT program as an evaluation and treatment tool to standardize and enhance the movement patterns of ICU patients.

In an investigation, two groups of ICU patients have been compared using a quasi-experimental design (17). A quantitative methodology centered on the gathering of discrete data was employed for this research. The patients in the medical-surgical ICU made up the population. The project's participants were given mobility therapies based on the BMAT or current practice interventions before the BMAT-based program. In Los Angeles, California, a 101-bed community hospital housed a 12-bed medical-surgical intensive care unit (17). In this study the BMAT intervention served as the independent variable, while the ICU LOS served as the dependent variable. By utilizing the BMAT items for mobility, the study further supports early mobility programs in the ICU. Further, the project can serve as a model for other establishments attempting to introduce mobility initiatives.

## Conclusions

In summary, BMAT holds a significant position among various tools for assessing mobility, each offering unique contributions to patient care across diverse healthcare environments. The comprehensive scope of BMAT, which includes assessments of transfers, sitting balance, and functional movements at the bedside, aligns effectively with the requirements of acute care facilities. However, its value is further amplified when used alongside other mobility assessment tools. The integration of BMAT within acute care settings presents a practical approach to identifying, addressing, and preventing mobility-related issues, leading to reduced hospital stays. By incorporating these assessments into a holistic and interdisciplinary framework, healthcare professionals can optimize patient outcomes, streamline care delivery, and facilitate a smooth transition from hospitalization to home or other care settings. Introducing e-learning initiatives to educate nurses about BMAT usage in acute care settings represents a strategic and innovative method to enhance clinical practice standards. Leveraging technology to provide targeted and accessible training equips nursing staff with the necessary knowledge and skills for conducting effective bedside mobility assessments, thereby enhancing patient care quality and outcomes.

## Acknowledgements

CP would like to thank the management of the Hospital for helping in many ways and permitting to carry out the research.

## Conflict of interests

There are no known conflicts of interests.

## Ethical committee approvals

Not applicable.

## Data availability

Not applicable.

## References

1. Brown, C.J., Friedkin, RJ., and Inouye, SK. (2004). Prevalence and outcomes of low mobility in hospitalized older patients. Journal of American Geriatric Society, 52: 1263-1270.

2. The Bedside Mobility Assessment Tool 2.0 - American Nurse Journal, www.myamericannurse.com/the-bedside-mobility-assessment-tool-2-0/. Accessed 9 Dec. 2023.

3. Hignett, S., and Emma, C. (2005). Development of a patient handling assessment tool. International Journal of Therapy and

Rehabilitation, 12: 178-181.

4. Soubra, R. et al. (2019). A Systematic review of thirty-one assessment tests to evaluate mobility in older adults. BioMed Research International, Hindawi, Article ID 1354362.

5. Werdati, S. et al. (2023). Physical mobility and immobility nursing care plan and management. Nurseslabs, 12 Oct. 2023, nurseslabs.com/impaired-physical-mobility/.

6. Walters, DM. (2022). Grand Canyon University ProQuest Dissertations Publishing, 28649874.

7. Ambulatory Health Care: 2021 National Patient Safety Goals. (2021). The Joint Commission. https://www.jointcommission.org/standards/national-patient-safety-goals/ambulatory-health-care-national-patient-safety-goals/

8. Palumbo, P., Palmerini, L., Bandinelli, S., and Chiari, L. (2015). Fall risk assessment tools for elderly living in the community: Can we do better? PLOS ONE, 12: e0146247.

9. Nunan, S., Wilson, C. B., Henwood, T., and Parker, D. (2018). Fall risk assessment tools for use among older adults in long-term care settings: A systematic review of the literature. Australasian Journal on Ageing, 37: 23-33.

10. Dickinson, S., Taylor, S., and Anton, P. (2018). Integrating a standardized mobility program and safe patient handling. Critical Care Nursing Quarterly, 41: 240-252.

11. Boynton, T., Kelly, L., and Perez, A. (2014). Implementing a mobility assessment tool for nurses: A nurse-driven assessment tool reveals the patient's mobility level and guides SPHM technology choices. American Nurse Today, September 2014, 13-16.

12. LeLaurin, J.H., and Shorr, R.I. (2019). Preventing falls in hospitalized patients: State of the science. Clinics in Geriatric Medicine, 35: 273-284.

13. McErlean, D.R., and Hughes, J.A. (2017). Who falls in an adult emergency department and why-A retrospective review. Australasian Emergency Nursing Journal, 20: 12-16.

14. Boynton, T., Kumpar, D., and VanGilder, C. (2020). The bedside mobility assessment tool 2.0: Advancing patient mobility. American Nurse Journal, 15: 18-22.

15. Jones, D. M., and Eagerton, G. (2020). Reducing preventable injuries through the safe patient handling and mobility program bundle. International Journal of Safe Patien Handling & Mobility (SPHM), 10: 134-139.

16. Soubra, R., Chkeir, A., and Novella, J. L. (2019). A systematic review of thirty-on assessment tests to evaluate mobility in older adults. BioMed Research International, 20: 1354362.

17. Dirkes, S. M., and Kozlowski, C. (2019). Early mobility in the intensive care unit Evidence, barriers, and future directions. Critical Care Nurse, 39: 33-42.

18. Azuh, O., Gammon, H., Burmeister, C., Frega, D. N.D., DiGiovine, B., and Siddiqui, A. (2016). Benefits of early active mobility in the medical intensive care unit: A pilot study. The American Journal of Medicine, 129: 866-871.

Current Trends in Biotechnology and Pharmacy
Vol. 18(2) 1788-1797, April 2024, ISSN 0973-8916 (Print), 2230-7303 (Online)
DOI: 10.5530/ctbp.2024.2.27



# Synthesis, Charectertisation and Antitubercular Evaluation of Pyarzoline Clubbed Thiazole Hybrids

**Pasumarthy N V Gopal[1], S.Poda[1*], Boggula Sourya Swetha[2], Samatha Gadde[1]**

[1]Department of Biotechnology, Acharya Nagarjuna University,
Guntur, Andhra Pradesh, India.
[2]Department of Biotechnology, Yogi Vemana University, Kadapa, Andhra Pradesh, India
Pin Code: 516005
Corresponding Author: sudhakarpodha@gmail.com

**Abstract:**

In our previous work, we have synthesised novel isoxazole conjugated pyrazoline derivatives by reacting isoxazolyl chalcones (1-15) with thiosemicarbazide in glacial acetic acid. From these compounds, 15 isoxazole conjugated pyrazoline carbothioamides were synthesised, compounds 24 and 25 are selected for further optimisation. In continuation to this work, pyrazoline-clubbed thiazole hybrids were synthesied by using potential antimycobacterial isoxazole conjugated pyrazoline carbothioamides – 24 and 25. The pyrazoline-1-carbothioamides- 24 (3-(isoxazol-5-yl)-5-(3,5-dimethoxyphenyl)-4,5-dihydro-1H-pyrazole-1-carbothioamide) and 25 (3-(isoxazol-5-yl)-5-(2,3,4-trimethoxyphenyl)-4,5-dihydro-1H-pyrazole-1-carbothioamide) were further optimized and synthesized eight more compounds (24a-24d, 25a-25d) which have a substituted thiazole ring. These compounds are purified by recrystallisation and charecterised by FT IR, $^1$H NMR and Mass spectra. Compound 24a have shown potent antimycobacterial activity.

**Keywords:** Thiazole;FTIR; NMR; Mass; antitubercular activity; *Mycobacterium tuberculosis* H37Rv; MABA assay.

## Introduction

*Tuberculosis (TB)* caused by the bacteria Mycobacterium tuberculosis (Mtb), is one of the world's most serious problems today. According to WHO forecasts, TB killed 1.4 million people in 2019, including 208,000 HIV-infected patients. The main factor guiding Mtb's supremacy over humans is its ability to dwell inside its host. It is highly skilled at eluding the host's developed immune defences against it and can exhibit transitions between the active and latent stages of the sickness. Rifampicin-resistant (RR-TB) and multidrug-resistant (MDR-TB) tuberculosis were detected in 206,030 cases globally in 2019. The number of cases reported in 2018 was 186,883, which is a 10% increase (1).

The field of medicinal chemistry has recently seen the emergence of a potential method known as molecular hybridization. This technique enables the synthesis of molecules by combining two or more heterocyclic scaffolds. The topic of drug resistance has been addressed by the use of this technique, which has been essential in the generation of potent molecules against a variety of infectious illnesses and malignancies. It is important to note that the conjugation of numerous heterocycles has been shown to have a synergistic impact on the biological activity of drugs that have recently been synthesized.

A great amount of research in the field of medicinal chemistry has been directed toward pyrazoline and thiazole derivatives because of the strong biological activity that they possess.

Current Trends in Biotechnology and Pharmacy
Vol. 18(2) 1788-1797, April 2024, ISSN 0973-8916 (Print), 2230-7303 (Online)
DOI: 10.5530/ctbp.2024.2.27


Only few of the research that have shed light on the amazing antibacterial potential of these compounds (2-5). In addition, the effectiveness of these substances as antifungal agents has been shown in a number of studies (6-8). Moreover, the cytotoxic (10-13) , anticancer (14-16) and antitubercular activities (17-21) of these compounds have been demonstrated.

Our research efforts in medicinal chemistry have been oriented towards a pioneering synthesis and evaluation of pyrazoline clubbed thiazole hybrids. The purpose of this strategic endeavor was to encourage the development of powerful lead compounds that selectively target tuberculosis. We used a strategy that was founded on the utilization of molecular hybridization principles, with the objective of developing novel molecules that exhibited increased bioactivity against these essential therapeutic targets.

## Materials and methods

### General

Isoxazole-3-carbaldehyde, 4-Trifluoromethoxy acetophenone, thiosemicarbazide and substituted phenacyl bromides were purchased from Aldrich, Mumbai and remaining chemicals were obtained from local supplier-National Scientific, India. Pre-coated silica gel 60 F254 (Merck, Mumbai) and iodine crystals were purchased by silica gel-G for TLC. On a melting point device, melting points were determined in open tube capillaries and stated in °C without being adjusted. The (Shimadzu) KBr pellet technique was used to record infrared spectra. Inter standard (TMS) was used to record NMR ($^1H$, $^{13}C$) data in $CDCl_3$ and chemical shifts are provided in units. Mass spectra was recorded on Agilent LC-MS instrument.

### Synthesis of thiazole derivatives (24a - 24d) of 5 - (3, 5 - dimethoxyphenyl) -3-(isoxazol-5-yl)-4,5-dihydro-1H-pyrazole-1-carbothioamide (24):

Compound 24 (1 mmol) was dissolved in 20-30 mL of ethanol and stirred at 30°C. Subsequently, the solution was refluxed (100-130°C) for 45 minutes to 1 hour in the presence of different phenacyl bromides (1 mmol). The progress of the reaction was monitored using TLC. When the reaction was completed, the reaction mixture was cooled to room temperature where we observed the formation of an impure precipitate. Further, the precipitate was filtered using a Buchner funnel and dried in a desiccator. The dried product was purified using recrystallization either by methanol or ethanol as the recrystallizing solvent to get the pure crystals of target compounds (24a-24d) (22). (Scheme 1)

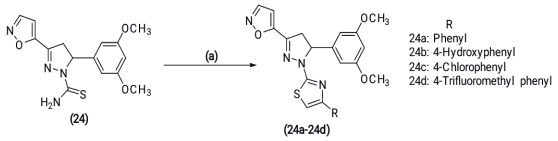


Scheme 1: Synthesis of compounds 24a-24d. (a) Phenacyl bromides, ethanol, refluxed for 45 min to 1 h.

Table 1 outlines the reaction parameters, in-

Table 1. Reaction conditions employed for the synthesis of the compounds (24a-24d)

| S.No | Compound code | Reactants and Solvent | Temperature (°C) | Time (min) | Recrystallizing solvent | Yield (%) |
|---|---|---|---|---|---|---|
| 1 | **24a** | Compound **24** (1 mmol) + Phenacyl bromide; 25 mL ethanol | 100 | 45 | Methanol | 71 |
| 2 | **24b** | Compound **24** (1 mmol) + 4-Hydroxy phenacyl bromide; 20 mL ethanol | 120 | 45 | Methanol | 61 |
| 3 | **24c** | Compound **24** (1 mmol) + 4-Chlorophenacyl bromide; 25 mL ethanol | 115 | 50 | Ethanol | 81 |
| 4 | **24d** | Compound **24** (1 mmol) + 4-Trifluorophenacyl bromide; 30 mL ethanol | 130 | 60 | Ethanol | 79 |

volved reagents, and the choice of recrystallization solvents applied in the production of the specified compounds, namely compounds-24a, 24b, 24c, and 24d.

Synthesis of thiazole derivatives (25a - 25d) of 3 - (isoxazol - 5 - yl) - 5 - (2,3,4 - trimethoxyphenyl)-4,5-dihydro-1H-pyrazole-1-carbothioamide (25):

Compound 25 (1 mmol) was dissolved in ethanol (20-30 mL) and stirred at 30°C. Following this, the solution was refluxed within a temperature range of 100-130°C for a duration of 45 minutes to 1 hour, employing various phenacyl bromides (1 mmol) as reactants. The progression of the reaction was traced by TLC analysis. Upon completion of the reaction, the reaction mixture was cooled to room temperature, resulting in the formation of an impure precipitate. This precipitate was isolated through filtration using a Buchner funnel and subsequently dried within a desiccator. The dried product underwent purification via recrystallization, utilizing either methanol or ethanol as the recrystallizing solvent, yielding pure crystals of the targeted compounds (25a-25d) (22). (Scheme 2)

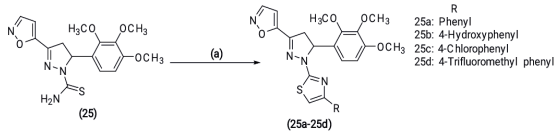


Scheme 2: Synthesis of compounds 25a-25d. (a) Phenacyl bromides, ethanol, Reflux for 45 min to 1 h.

Table 2. Reaction conditions employed for the synthesis of the compounds **(25a-25d)**

| S.No | Compound code | Reactants and Solvent | Temperature (°C) | Time (min) | Recrystallizing solvent | Yield (%) |
|---|---|---|---|---|---|---|
| 1 | **25a** | Compound **25** (1 mmol) + Phenacyl bromide; 20 mL ethanol | 115 | 45 | Ethanol | 64 |
| 2 | **25b** | Compound **25** (1 mmol) + 4-Hydroxy phenacyl bromide; 20 mL ethanol | 110 | 60 | Methanol | 72 |
| 3 | **25c** | Compound **25** (1 mmol) + 4-Chlorophenacyl bromide; 30 mL ethanol | 115 | 45 | Ethanol | 82 |
| 4 | **25d** | Compound **25** (1 mmol) + 4-Trifluorophenacyl bromide; 25 mL ethanol | 130 | 50 | Ethanol | 80 |

Table 2 outlines the reaction conditions, reagents, and recrystallization solvent used for the synthesis of target compounds compounds-25a, 25b, 25c, and 25d.

**5-(5-(3,5-dimethoxyphenyl)-1-(4-phenylthiazol-2-yl)-4,5-dihydro-1H-pyrazol-3-yl) isoxazole (24a):** Yield 71%; m.p. 218-220 °C; FT-IR (KBr, $cm^{-1}$): 1548 (C=C), 1586 (C=N); 1H NMR (400 MHz, DMSO-$d_6$, ppm): $\delta$ 6.22-8.62(10H, Ar-H); 5.27 (1H, Hx, dd, $J_{AX}$ = 3.6Hz, dd, $J_{BX}$=12Hz), 3.81 (1H, $H_B$, dd, $J_{AB}$ = 16Hz, dd, $J_{BX}$= 12Hz), 3.19 (1H, $H_A$, dd, $J_{AX}$ = 3.6Hz, dd, $J_{AB}$=16Hz), 2.48 (6H, 2x-$OCH_3$), 2.12 (3H, -$OCH_3$); Mass Analysis (m/z, %): 463.52 (M+1, 99.66); Anal. Calcd for: $C_{24}H_{22}N_4O_4S$: C, 60.26; H, 4.67; N, 11.71; Found: C, 60.72; H, 4.96; N, 11.91.

**4-(2-(5-(3,5-dimethoxyphenyl)-3-(isoxazol-5-yl)-4,5-dihydro-1H-pyrazol-1-yl)thiazol-4-yl)phenol (24b): Yield** 61%; **m.p**. 256-258°C; FT-IR (KBr, $cm^{-1}$): 1533 (C=C), 1579 (C=N); 1H NMR (400 MHz, DMSO-$d_6$, ppm): $\delta$ 6.12-8.71 (11H, Ar-H); 5.26 (1H, Hx, dd, $J_{AX}$ = 3.6Hz, dd, $J_{BX}$=12Hz), 5.10 (1H, Ar-OH), 3.74 (1H, $H_B$, dd, $J_{AB}$ = 16Hz, dd, $J_{BX}$= 12 Hz), 3.14 (1H, $H_A$, dd, $J_{AX}$ = 3.6 Hz, dd, $J_{AB}$=16Hz), 2.37 (6H, 2x-$OCH_3$); Mass Analysis (m/z, %): 449.50 (M+1, 99.41); Anal. Calcd for: $C_{24}H_{20}N_4O_4S$: C, 61.66; H, 4.52;

N, 12.53; Found: C, 61.84; H, 4.57; N, 12.75.

**5-(1-(4-(4-chlorophenyl) thiazol-2-yl)-5-(3,5-dimethoxyphenyl)-4,5-dihydro-1H-pyrazol-3-yl)isoxazole (24c) :** Yield 81%; m.p. 193-195°C; FT-IR (KBr, $cm^{-1}$): 1546 (C=C), 1589 (C=N) 1H NMR (400 MHz, DMSO-$d_6$, ppm): $\delta$ 6.25-8.69 (11H, Ar-H); 5.29 (1H, Hx, dd, $J_{AX}$ = 3.6Hz, dd, $J_{BX}$=12Hz), 3.84 (1H, $H_B$, dd, $J_{AB}$ = 16Hz, dd, $J_{BX}$= 12Hz), 3.18 (1H, $H_A$, dd, $J_{AX}$= 3.6Hz, dd, $J_{AB}$=16Hz), 2.32 (6H, 2x-$OCH_3$) ; Mass Analysis (m/z, %): 466.94 (M+1, 99.66), 468.94 (M+2, 33.35); Anal. Calcd for: $C_{23}H_{19}ClN_4O_3S$: C, 59.22; H, 4.16; N, 12.12; Found: C, 59.39; H, 4.33; N, 12.20.

**5-(5-(3,5-dimethoxyphenyl)-1-(4-(4-(trifluoromethyl)phenyl)thiazol-2-yl)-4,5-dihydro-1H-pyrazol-3-yl)isoxazole (24d):** Yield 79%; m.p. 176-178°C; FT-IR (KBr, $cm^{-1}$): 1548 (C=C), 1591 (C=N); 1H NMR (400 MHz, DMSO-$d_6$, ppm): $\delta$ 6.28-8.91 (11H, Ar-H), 5.29 (1H, Hx, dd, $J_{AX}$ = 3.6Hz, dd, $J_{BX}$=12 Hz), 3.84 (1H, $H_B$, dd, $J_{AB}$ = 16 Hz, dd, $J_{BX}$= 12 Hz), 3.23 (1H, $H_A$, dd, $J_{AX}$ = 3.6 Hz, dd, $J_{AB}$=16 Hz), 2.35 (6H, 2x-$OCH_3$); Mass Analysis (m/z, %): 501.50 (M+1, 99.35); Anal. Calcd for: $C_{24}H_{19}F_3N_4O_3S$: C, 57.66; H, 3.86; N, 11.28; Found: C, 57.85; H, 3.91; N, 11.33.

**5-(1-(4-phenylthiazol-2-yl)-5-(2,3,4-trimethoxyphenyl)-4,5-dihydro-1H-pyrazol-3-yl) isoxazole (25a):** Yield 64%; m.p. 292-294°C ; FT-IR (KBr, $cm^{-1}$): 1559 (C=C), 1588 (C=N); 1H NMR (400 MHz, DMSO-$d_6$, ppm): $\delta$ 6.20-8.63(10H, Ar-H), 5.27 (1H, Hx, dd, $J_{AX}$ = 3.6Hz, dd, $J_{BX}$=12Hz), 3.84 (1H, $H_B$, dd, $J_{AB}$ = 16Hz, dd, $J_{BX}$= 12Hz), 3.13 (1H, $H_A$, dd, $J_{AX}$ = 3.6Hz, dd, $J_{AB}$=16Hz), 2.42 (3H, -$OCH_3$), 2.34 (6H, 2x-$OCH_3$); Mass Analysis (m/z, %): 463.14 (M+1, 99.32); Anal. Calcd for: $C_{24}H_{22}N_4O_4S$: C, 62.42; H, 4.82; N, 12.18; Found: C, 62.69; H, 4.85; N, 12.25.

**4-(2-(3-(isoxazol-5-yl)-5-(2,3,4-trimethoxyphenyl)-4,5-dihydro-1H-pyrazol-1-yl)thiazol-4-yl)phenol (25b):** Yield 72%; m.p. 266-268°C; FT-IR (KBr, $cm^{-1}$): 1535 (C=C), 1581 (C=N), 1H NMR (400 MHz, DMSO-$d_6$, ppm): $\delta$ 6.22-8.75 (9H, Ar-H); 5.29 (1H, Hx, dd, $J_{AX}$ = 3.6Hz, dd, $J_{BX}$=12Hz), 5.12 (1H, Ar-OH), 3.68 (1H, $H_B$, dd, $J_{AB}$ = 16Hz, dd, $J_{BX}$= 12 Hz), 3.16 (1H, $H_A$, dd, $J_{AX}$ = 3.6 Hz, dd, $J_{AB}$=16Hz), 2.32 (6H, 2x-$OCH_3$), 2.39 (3H, -$OCH_3$); Mass Analysis (m/z, %): 479.13 (M+1, 99.41); Anal. Calcd for: $C_{24}H_{22}N_4O_5S$: C, 60.31; H, 4.68; N, 11.83; Found: C, 60.36; H, 4.73; N, 11.96.

**5-(1-(4-(4-chlorophenyl)thiazol-2-yl)-5-(2,3,4-trimethoxyphenyl)-4,5-dihydro-1H-pyrazol-3-yl)isoxazole (25c) :** Yield 82%; m.p. 178-180°C; FT-IR (KBr, $cm^{-1}$): 1548 (C=C), 1585 (C=N), 1H NMR (400 MHz, DMSO-$d_6$, ppm): $\delta$ 6.28-8.77(9H, Ar-H); 5.27 (1H, Hx, dd, $J_{AX}$ = 3.6Hz, dd, $J_{BX}$=12Hz), 3.86 (1H, $H_B$, dd, $J_{AB}$ = 16Hz, dd, $J_{BX}$= 12Hz), 3.19 (1H, $H_A$, dd, $J_{AX}$ = 3.6Hz, dd, $J_{AB}$=16Hz), 2.41 (3H, -$OCH_3$), 2.35 (6H, 2x-$OCH_3$); Mass Analysis (m/z, %): 497.10 (M+1, 99.71), 499.10 (M+2, 33.27); Anal. Calcd for: $C_{24}H_{21}ClN_4O_4S$: C, 58.10; H, 4.28; N, 11.29; Found: C, 58.22; H, 4.36; N, 11.35.

**5-(1-(4-(4-(trifluoromethyl)phenyl)thiazol-2-yl)-5-(2,3,4-trimethoxyphenyl)-4,5-dihydro-1H-pyrazol-3-yl)isoxazole (25d) :** Yield 80%; m.p. 158-160°C; FT-IR (KBr, $cm^{-1}$): 1550 (C=C), 1583 (C=N); 1H NMR (400 MHz, DMSO-$d_6$, ppm): $\delta$ 6.33-8.85 (9H, Ar-H); 5.31 (1H, Hx, dd, $J_{AX}$ = 3.6Hz, dd, $J_{BX}$=12 Hz), 3.86 (1H, $H_B$, dd, $J_{AB}$ = 16 Hz, dd, $J_{BX}$= 12 Hz), 3.26 (1H, $H_A$, dd, $J_{AX}$ = 3.6 Hz, dd, $J_{AB}$=16 Hz), 2.43 (3H, -$OCH_3$), 2.38 (6H, 2x-$OCH_3$); Mass Analysis (m/z, %): 531.12 (M+1, 99.35); Anal. Calcd for: $C_{25}H_{21}F_3N_4O_4S$: C, 56.63; H, 3.41; N, 10.61; Found: C, 56.71; H, 3.45; N, 10.79.

### In vitro antitubercular activity

The antitubercular activity of the target compounds was performed by the use of Microplate Alamar Blue Assay (MABA).

#### *Principle of MABA assay*

The MABA assay is an essential method used to assess how effective compounds are against *Mycobacterium tuberculosis*, the bacterium responsible for tuberculosis. First introduced by Franzblau *et al*., (1998), this assay

works by evaluating the bacteria's metabolic activity to gauge their viability when exposed to different compounds (23). Essentially, the MABA starts by introducing the test compound to cultures of *Mycobacterium tuberculosis*. Then, a dye called Alamar Blue is added to these cultures. Alamar Blue is a dye that changes color from blue to pink when it encounters bacteria that are actively metabolizing. The effectiveness of the compound in fighting tuberculosis is measured by its ability to hinder the growth and metabolic activity of the bacteria. Consequently, the change in color shown by the Alamar Blue dye acts as a measurable indicator, showing how much the bacterial metabolic activity has reduced and giving us an idea of how well the compound works in inhibiting *Mycobacterium tuberculosis*. (23)

### *Protocol for the MABA assay of the compounds*

Target isoxazole linked 1-carbothioamido-4,5-dihydro-1H-pyrazoles were tested for their antimycobacterial activity against the *M. tuberculosis* H37Rv strain. All medications' minimum inhibitory concentrations (MICs), or the lowest concentration of the medicine that inhibits 99% of the bacteria present at the start of the experiment, were calculated using a broth dilution test. All of the substances under study had their MICs measured and compared to those of Isoniazid. Middlebrook 7H9 broth with 10% albumin-dextrose-catalase and 0.2% glycerol was used to dilute the culture to 105 cfu mL-1 after it had been thawed. All of the working compounds were dissolved in DMSO and then diluted twice in broth to reach the required concentration. After that, 0.05 mL of standardised culture was introduced into each U-tube and the cultures were grown at 37°C for 21 days. U-tubes were used to track development, with isoniazid serving as a "positive control" and untreated inoculum serving as a "negative control" (24-26)

### Results and discussion on the synthesis and characterization of pyrazoline clubbed thiazole hybrids

The synthesis of the target pyrazoline-clubbed thiazole hybrids 24a-24d and 25a-25d are represented in Schemes-1 and 2 respectively. Additionally, the melting point, percentage yield, spectral characterization and elemental analysis data are provided for all the eight compounds. All the eight compounds were synthesized by refluxing pyrazoline-1-carbothioamides (24 and 25) with different kinds of phenacyl bromides in the presence of ethanol as solvent. The yield of the eight compounds was ranging between 61-85%.

In the FT-IR spectrum of target compounds 24a-24d and 25a-25d, the disappearance of absorption band at 3369 $cm^{-1}$ and the appearance of strong absorption bands corresponding to C=N and C=C confirmed the formation of pyrazoline clubbed thiazole hybrids. Further, the 1H NMR spectrum showed signals of pyrazoline scaffold as doublet of doublets at chemical shift values-5.26-5.35 (1H, Hx, dd, $J_{AX}$ = 3.6Hz, dd, $J_{BX}$=12Hz), 3.74-3.88 (1H, $H_B$, dd, $J_{AB}$ = 16Hz, dd, $J_{BX}$= 12Hz) and 3.16-3.29 (1H, $H_A$, dd, $J_{AX}$ = 3.6Hz, dd, $J_{AB}$=16Hz) ppm respectively. Additional peaks pertaining to aromatic protons were seen in between 6-9 ppm. The M+1 peak in their mass spectrum confirmed the molecular weight whereas the elemental analysis data is agreement with the chemical composition of the expected structures.

To contextualize our findings, we compared our results with existing literature. Our synthesis approach aligns with methodologies utilized in prior studies (4,27). However, our spectral characterization, particularly the FT-IR and 1H NMR profiles, exhibit distinctive signals and patterns not reported previously, signifying unique structural attributes (28). Notably, the disappearance of the 3369 $cm^{-1}$ band in our hybrids resonates with observations made by Hawaiz *et al*., (2014) in similar compound formations (29). These deviations warrant further investigation into the potential implications for biological activities and structural modifications.

**Antitubercular activity**

The pyrazole-1-carbothioamides 24 and 25 had shown highest antitubercular activity among the target compounds 16-30. Based on their efficient activity of the two compounds 24

Table 3. Antitubercular activity of pyrazoline clubbed thiazole hybrids (24a-24d and 25a-25d) (expressed as MIC in µg/mL)

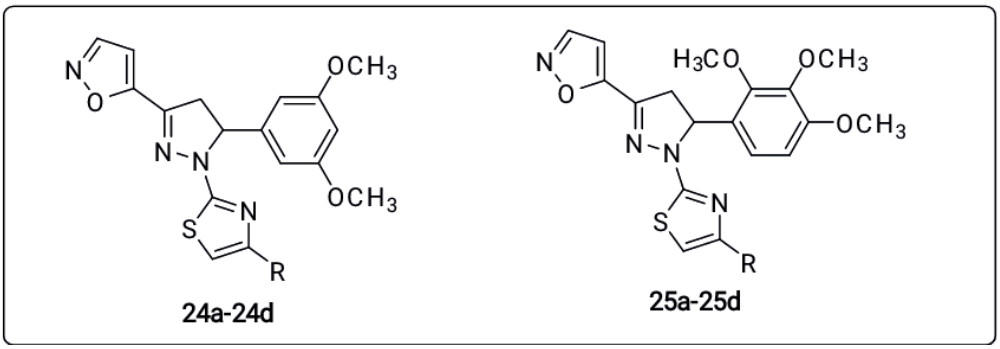


.

| S.No | Compound code | R | *M. tuberculosis* H37Rv |
|---|---|---|---|
| 1 | **24a** | Phenyl | 0.1 |
| 2 | **24b** | 4-Hydroxyphenyl | 1 |
| 3 | **24c** | 4-Chlorophenyl | 0.5 |
| 4 | **24d** | 4-Trifluoromethyl phenyl | 0.5 |
| 5 | **25a** | Phenyl | 0.25 |
| 6 | **25b** | 4-Hydroxyphenyl | 0.25 |
| 7 | **25c** | 4-Chlorophenyl | 0.5 |
| 8 | **25d** | 4-Trifluoromethyl phenyl | 1 |
| 9 | **Isoniazid** | - | 0.25 |

and 25, we further optimized and synthesized eight more compounds (24a-24d, 25a-25d) which have a substituted thiazole ring conjugated with the pyrazoline scaffold in order to improve their antitubercular potency. The activity was performed using the same protocol discussed by other researchers (30-32) i.e MABA assay and the positive control used in the study was isoniazid. The results of antitubercular activity of the pyrazoline conjugated thiazoles (24a-24d, 25a-25d) are summarized in Table 3.

The synthesized eight new compounds (24a-24d, 25a-25d) were evaluated for antitubercular activity using isoniazid as a positive control. Among the four compounds in 24a-24d, the activity of compound 24a is same as compared to 24. The compounds 24b, 24c and 24d had reduced activity than 24 with an MIC value of 0.1 µg/mL, 0.5 µg/mL and 0.5 µg/mL respectively. The above results suggest that the conversion of pyrazoline carbothioamide to pyrazoline conjugated thiazole is not a much useful strategy to enhance the antitubercular potency. However, the retaining of the activity of compound 24a with MIC value 0.1 µg/mL is interesting and this compound may be explored further by substituting the phenyl ring on the ortho, meta and para-positions with groups other than -OH, -Cl and -$CF_3$.

The compounds 25a and 25b had shown same antitubercular potency as that of the compound 25 with an MIC of 0.25 µg/mL whereas the compounds 25c and 25d had an antitubercular potency of 0.5 and 1 µg/mL which

is less than the lead compound 25. This shows that the modification of compound 25 to 25c and 25d is not a much useful strategy for increasing the antitubercular potency of the synthesized pyrazoline conjugated thiazole derivatives. However, the similar potency of the derivatives 25a and 25b indicates that the phenyl ring on the thiazole scaffold can be incorporated with other kinds of small polar substituents that may have marginal effect on improving the activity.

In assessing the antitubercular efficacy of the synthesized pyrazoline-conjugated thiazole derivatives, our study revealed noteworthy comparisons to existing literature. According to Dawood et al., (2023), a similar strategy employing pyrazoline-thiazole derivatives demonstrated varied outcomes in contrast to our findings. Within our synthesized compounds, 24a manifested sustained potency akin to the lead compound 24, suggesting promising potential (Dawood et al., 2023). However, the conversion of pyrazoline carbothioamide to pyrazoline-conjugated thiazole, as explored in compounds 24b, 24c and 24d, resulted in decreased antitubercular activity compared to compound 24, diverging from the expected enhancement strategy (Dawood et al., 2023).

Regarding compounds 25a-25d, comparative findings from Bhandare et al., (2022) align with our observations to a certain extent. Both our study and study of Bhandare et al., (2022) research reported analogous antitubercular potency for compounds 25a and 25b, maintaining equivalence to compound 25. However, the alteration from compounds 25a and 25b to 25c and 25d within our synthesized derivatives led to reduced antitubercular efficacy (33).

Our results suggest potential avenues for further exploration. Specifically, the sustenance of activity in compound 24a proposes an avenue for future investigation by substituting the phenyl ring at various positions with alternate groups, as proposed by Sever et al., (2019). Sever et al.'s work indicated that diversifying substituents on the phenyl ring might yield improvements in the antitubercular properties of pyrazoline-thiazole derivatives (10).

## Conclusion

A novel series of pyrazoline-clubbed thiazole hybrids were synthesied by using potential antimycobacterial isoxazole conjugated pyrazoline carbothioamides – 24 and 25 of our previous work. Among 8 compounds (24a, 24b,24c and 24d) synthesised by thiazole linking, 24a exhibited potent antimycobacterial agent bearing phenyl subtituent at 4$^{th}$ position of thiazole ring with an MIC at 0.1 µg/mL which is better than Isoniazid. Further studies are underway to know about the possible mode of action of the optimised compound.

## References

1. WHO. Global tuberculosis report. 2020. Available online: https://www.who.int/news-room/fact-

2. Ansari MI, Khan SA. Synthesis and antimicrobial activity of some novel quinoline-pyrazoline-based coumarinyl thiazole derivatives. Medicinal Chemistry Research. 2017;26(7):1481-96.

3. Edrees MM, Melha SA, Saad AM, Kheder NA, Gomha SM, Muhammad ZA. Eco-friendly synthesis, characterization and biological evaluation of some novel pyrazolines containing thiazole moiety as potential anticancer and antimicrobial agents. Molecules. 2018;23(11):2970:1-13.

4. Masoud DM, Azzam RA, Hamdy F, Mekawey AA, Abdel-Aziz HA. Synthesis of some novel pyrazoline-thiazole hybrids and their antimicrobial activities. Journal of Heterocyclic Chemistry. 2019;56(11):3030-41.

5. Radini AM, Khidre IE, El-Telbani RM, E. Synthesis and antimicrobial evaluation of new pyrazoline and pyrazolinyl thiazole derivatives bearing tetrazolo [1, 5-a] quin-

oline moiety. Letters in Drug Design & Discovery. 2016;13(9):921-31.

6. Sadashiva R, Naral D, Kudva J, Kumar SM, Byrappa K, Shafeeulla RM, Kumsi M. Synthesis, structure characterization, in vitro and in silico biological evaluation of a new series of thiazole nucleus integrated with pyrazoline scaffolds. Journal of Molecular Structure. 2017;1145:18-31.

7. Altıntop MD, Özdemir A, Turan-Zitouni G, Ilgın S, Atlı Ö, Demirel R, Kaplancıklı ZA. A novel series of thiazolyl–pyrazoline derivatives: Synthesis and evaluation of antifungal activity, cytotoxicity and genotoxicity. European journal of medicinal chemistry. 2015;92:342-52.

8. Elewa SI, Mansour E, Nassar IF, Mekawey AA. Synthesis of Some New Pyrazoline-Based Thiazole Derivatives and Evaluation of Their Antimicrobial, Antifungal, and Anticancer Activities. Russian Journal of Bioorganic Chemistry. 2020;46(3):382-92.

9. Havrylyuk D, Roman O, Lesyk R. Synthetic approaches, structure activity relationship and biological applications for pharmacologically attractive pyrazole/pyrazoline–thiazolidine-based hybrids. European journal of medicinal chemistry. 2016;113:145-66.

10. Sever B, Altıntop MD, Radwan MO, Özdemir A, Otsuka M, Fujita M & Ciftci HI. Design, synthesis and biological evaluation of a new series of thiazolyl-pyrazolines as dual EGFR and HER2 inhibitors. European journal of medicinal chemistry. 2019; 182:111648.

11. Gomha SM, Abdallah MA, Abbas IM, Kazem MS. Synthesis, cytotoxicity evaluation, molecular docking and utility of novel chalcones as precursors for heterocycles incorporating pyrazole moiety. Medicinal Chemistry. 2018;14(4):344-55.

12. George RF, Samir EM, Abdelhamed MN, Abdel-Aziz HA, Abbas SE. Synthesis and anti-proliferative activity of some new quinoline based 4, 5-dihydropyrazoles and their thiazole hybrids as EGFR inhibitors. Bioorganic chemistry. 2019;83:186-97.

13. Mansour E, Aboelnaga A, Nassar EM, Elewa SI. A new series of thiazolyl pyrazoline derivatives linked to benzo [1, 3] dioxole moiety: Synthesis and evaluation of antimicrobial and anti-proliferative activities. Synthetic Communications. 2020;50(3):368-79.

14. Lin Z, Wang Z, Zhou X, Zhang M, Gao D, Zhang L, Wang P, Chen Y, Lin Y, Zhao B, Miao J. Discovery of new fluorescent thiazole–pyrazoline derivatives as autophagy inducers by inhibiting mTOR activity in A549 human lung cancer cells. Cell death & disease. 2020;11(7):1-2.

15. Wang HH, Qiu KM, Cui HE, Yang YS, Xing M, Qiu XY, Bai LF, Zhu HL. Synthesis, molecular docking and evaluation of thiazolyl-pyrazoline derivatives containing benzodioxole as potential anticancer agents. Bioorganic &medicinal chemistry. 2013;21(2):448-55.

16. Lv PC, Li DD, Li QS, Lu X, Xiao ZP, Zhu HL. Synthesis, molecular docking and evaluation of thiazolyl-pyrazoline derivatives as EGFR TK inhibitors and potential anticancer agents. Bioorganic & medicinal chemistry letters. 2011;21(18):5374-5377.

17. Reddy MR, Prasad AR, Spoorthy YN, Ravindranath LR. Synthesis, characterization and antimicrobial activity of certain novel aryl hydrazone pyrazoline-5-ones containing thiazole moiety. Advanced pharmaceutical bulletin. 2013;3(1):153-159.

18. Zaki YH, Al-Gendey MS, Abdelhamid AO. A facile synthesis, and antimicrobial and anticancer activities of some pyridines, thioamides, thiazole, urea, quinazoline, β-naphthyl carbamate, and pyrano [2, 3-d] thiazole derivatives. Chemistry Central Journal. 2018;12(1):1-4.

19. Bondock S, Fouda AM. Synthesis and evaluation of some new 5-(hetaryl) thiazoles as potential antimicrobial agents. Synthetic Communications. 2018;48(5):561-73.

20. Shaik A, Shaik MS, Puttagunta SB. (E)-1-(2′,4′-Dimethyl)-(5-acetylthiazole)-(2,4″-difluorophenyl)-prop-2-en-1-one. Molbank 2018; M1019;1-5.

21. Palleapati K, Kancharlapalli VR, Shaik AB. Synthesis, characterization and antitubercular evaluation of some new isoxazole appended 1-carboxamido-4, 5-dihydro-1H-pyrazoles. Journal of Research in Pharmacy. 2019;23(2):156-63.

22. Munikrishnappa CS, Puranik SB, Kumar GV, Prasad YR. Synthesis, Characterization and Pharmacological Evaluation of Some Novel 4, 5-Dihydro Pyrazole Derivatives Bearing Thiazole and Furan as Potent Antimicrobial and Anticancer Agents. Research journal of pharmaceutical, biological and chemical sciences.2016;7(4):768-83.

23. Franzblau SG, Witzig RS, McLaughlin JC, Torres P, Madico G, Hernandez A, Degnan MT, Cook MB, Quenzer VK, Ferguson RM, Gilman RH. Rapid, Low-Technology MIC Determination with Clinical Mycobacterium tuberculosis Isolates by Using the Microplate Alamar Blue Assay. Journal of Clinical Microbiology. 1998; 36(2): 362–366.

24. Afzal BS, Lohitha SV, Puttagunta SB, Shaik A, Supraja K, Sai HK. Synthesis and screening of novel lipophilic diarylpropeones as prospective antitubercular, antibacterial and antifungal agents. Biointerface Research in Applied Chemistry. 2019; 9: 3912-8.

25. Lokesh BV, Prasad YR, Shaik AB. Synthesis, Biological evaluation and molecular docking studies of new pyrazolines an antitubercular and cytotoxic agents. Infectious Disorders-Drug Targets (Formerly Current Drug Targets-Infectious Disorders). 2019 Sep 1;19(3):310-21.

26. Lagu SB, Afzal BS, Rajendra PY. Synthesis. antibacterial, antifungal antitubercular activities and molecular docking studies of nitrophenyl derivatives. International Journal of Life science and Pharma Research.2019; 9(1): 54-64.

27. Khan Y, Khan S, Hussain R, Maalik A, Rehman W, Attwa MW, Masood R, Darwish HW, Ghabbour HA. The Synthesis, In Vitro Bio-Evaluation, and In Silico Molecular Docking Studies of Pyrazoline–Thiazole Hybrid Analogues as Promising Anti-α-Glucosidase and Anti-Urease Agents. Pharmaceuticals. 2023; 16(12): 1650.

28. Dawood DH, Sayed MM, Tohamy ST, Nossier ES. New Thiophenyl-pyrazolyl-thiazole Hybrids as DHFR Inhibitors: Design, Synthesis, Antimicrobial Evaluation, Molecular Modeling, and Biodistribution Studies. ACS omega.2023; 8(42): 39250-39268.

29. Hawaiz FE. Synthesis and characterization of some new 4, 5-dihydropyrazolyl thiazoles. Chemical Science Transactions. 2014;3(4): 1583-1589.

30. Shaik S, Bhandare RR, Palleapati K, Nissankararao S, Kancharlapalli V, Shaik A. Antimicrobial, antioxidant, and anticancer activities of some novel isoxaz-

ole ring containing chalcone and dihydropyrazole derivatives. Molecules. 2020 Jan;25(5);1047;1-11.

31. Shaikh AB, Lohitha K, Vani S, Basu PS, Shaik A, Supraja K, Harish SH. Synthesis and screening of novel lipophilic diarylpropeones as prospective antitubercular, antibacterial and antifungal agents. Biointerface Research in Applied Chemistry. 2019; 9:3912–3918.

32. Shaik AB, Bhandare RR, Nissankararao S, Lokesh BV, Shahanaaz S, Rahman MM. Synthesis, and biological screening of chloropyrazine conjugated benzothiazepine derivatives as potential antimicrobial, antitubercular and cytotoxic agents. Arabian Journal of Chemistry. 2021;14(2);102915:1-15.

33. Bhandare RR, Munikrishnappa CS, Kumar GS, Konidala SK, Sigalapalli DK, Vaishnav Y, Chinnam S, Yasin H , Al-karmalawy AA and Shaik A B. Multistep synthesis and screening of heterocyclic tetrads containing furan, pyrazoline, thiazole and triazole (or oxadiazole) as antimicrobial and anticancer agents. *Journal of Saudi Chemical Society*. 2022; *26*(3):101447.

Current Trends in Biotechnology and Pharmacy
Vol. 18(2) 1798-1812, April 2024, ISSN 0973-8916 (Print), 2230-7303 (Online)
DOI: 10.5530/ctbp.2024.2.28



# Comparison of Analytical Method validation guidelines used for release, stability in Biosimilar Manufacturing process.

**Narra Naga Pavan Kumar[1], Ajay Pakalapati[1], K. Chandrasekhar[1,*], Chandrasai Potla Durthi[2,#]**

[1] Department of Biotechnology, Vignan's Foundation for Science, Technology and Research, Vadlamudi, 522213, Guntur, Andhra Pradesh, India
[2]Department of Biotechnology, National Institute of Technology Warangal, Warangal, Telangana, India
*Corresponding author:chanduvfstr@gmail.com; #Co-corresponding author: chandrasaip@gmail.com

**Abstract**

Analytical method validation is the process of verifying a method for its purpose of fit, whether it suffices its intended application or not. Analytical method validation is a mandatory requirement to be fulfilled for measuring critical quality attributes (CQA) during the manufacturing process to get a drug approval for human, and veterinary use. As the drug approval process differs from one country to another in a similar way method validation guidelines also differ from one country to another, these requirements will be added as your country of approval differs, In the present review an attempt was made to bring all method validation guidelines in a comparative manner by comparing country-specific requirements these countries/organizations hold the major pharma market and the Stringent regularity countries. The paper majorly focuses on the analytical method used in the Biosimilar manufacturing process and its validation approach by comparing the method validation guidelines from the International Council for Harmonisation of Technical Requirements of Pharmaceuticals for Human Use (ICH), USA, European Medicines Agency (EMA), Japan and India with the CQAs monitored during the biosimilar manufacturing process.

**Key Words:** Food and Drug Administration, European Medicines Agency, ICH, critical quality attribute, Method Validation, QTPP.

**Introduction:**

According to the US Food and Drug Administration (FDA) and European Medicines Agency (EMA), a biosimilar is a biological medicine highly similar to an already approved biological drug (commonly referred to as a Reference product) in that respective region (1,2). Biosimilars and generics show similar effects to the innovator product/Reference product which undergoes an extensive analytical characterization followed by minimal clinical studies in comparison with the innovator product/ Reference product (1). Significant differences exist between the generic drug/biosimilar drug and reference product considering the various stages starting from the Synthesis stage till it encounters the market (3,4). Generic drugs are chemical entities with low molecular weight and are produced majorly through chemical synthesis, where the process and its critical quality attribute (CQA) are more controlled, and the final product will be an exact match with the innovator product/Reference product. whereas in the case of biosimilars,, the molecules are produced

in live cells, due to the complex nature of cells and other factors the control on the process and CQA's are considerably less when compared with generic molecules and by the definition of FDA and EMA, it is clearly understood that the Biosimilars are highly similar molecules but not the exact match to the reference product (1-5). Due to the complex nature of Biosimilars, the Analytical methods used for Quality attribute monitoring should be highly robust and should serve the intended purpose at each stage of the Manufacturing operations, release, stability, and in assessing the Analytical similarity/Biosimilarity.

**Critical quality attribute involved in biosimilars:**

As per the International Council for Harmonisation of Technical Requirements of Pharmaceuticals for Human Use (ICH) Q8 CQA is defined as physical, chemical, biological, or microbiological property or characteristic that should be within an appropriate limit, range, or distribution to ensure the desired product quality. CQAs are generally associated with the drug substance, excipients, intermediates (in-process materials), and drug product (6). As per ICHQ8 the CQA's are defined based on the QTPP data generated from the reference product along with prior product and process development knowledge and excipients (As depicted in the Figure 1). CQA's represents all product characteristics like structure, quality, safety, and efficacy[6].

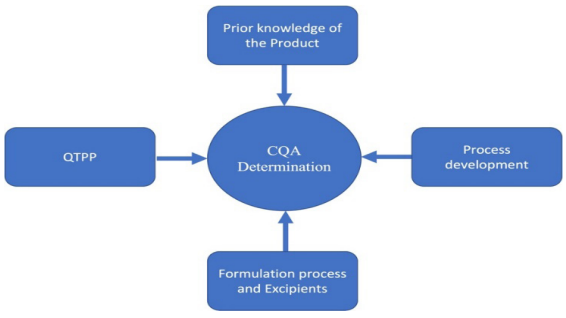


Figure 1:Determination of the CQA as per ICHQ8

CQA's play an important role in determining the Structure, Quality, safety, and Efficacy of the Drug product used for patients. CQA's are measured by various methods at each step of the biosimilar process.

**Typical biosimilar manufacturing and approval process**

Any typical Biosimilar Manufacturing process involves 5 major steps, Amino acid sequencing of Reference product, cloning development and optimization, cell culture process development, Purification process development (Capture step, polishing step, filtration process) and Formulation and fill finish (7,8).

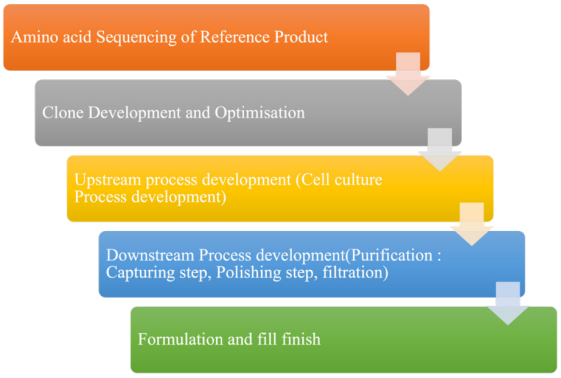


Figure 2: Typical Biosimilar Manufacturing Process.

Amino acid sequencing of Reference product: The Biosimilar program development starts with the sequencing of reference products using various basic analytical techniques.

*Clone Development and Optimization*: Clone development starts with the synthesis of the gene with a similar amino acid sequence obtained from the Reference product, followed by cloning this gene into a microbial or mammalian cell line by using a suitable vector (7). Based on the titer, clonality of the cell line, and minimal quality attributes (charge variants, glycosylation pattern, aggregates), the top clone will be selected followed by the generation of MCB with a set CQA specifications. Upstream process development: MCB generated from the

top clone selected will be used for the generation of WCB followed by process development during which various conditions required for cell growth and production of the desired product are optimized. Optimized process will be scaled up in step-by-step increments up to commercial scale ensuring the quality of the desired product is maintained (8).

Downstream process development: The downstream process majorly concentrates on the isolation and purification of the desired product utilizing various types of chromatography by keeping the CQA within the set specifications range. Various types of filters are also evaluated during downstream process development to ensure the product is free of viral and other contaminants. Optimized process will be scaled up in step-by-step increments up to commercial scale ensuring the quality of the desired product is maintained (8). Formulation and fill finish: The Purified Product is then concentrated/diluted based on the target set concentration/dosage along with the addition of excipients at the set range kept for the formulation process followed by sterile filling. The final drug product will be tested and compared with the reference product (7,8) ensuring similarity between both. During the biosimilar manufacturing process as depicted in Figure 2 various tests are involved at each stage of the process to ensure the final product CQA is comparable with Reference product (7,8). The technique/type of the method used for monitoring the CQA is referenced in Table 1. Methods used in biosimilar manufacturing can be categorized into various types based on its usage and its purpose.

The method outlined in the table above should be robust and their intended purpose should be fulfilled. The major objective of the analytical method validation is to demonstrate that the method is fit for its intended use and to identify the errors that might occur deliberately during the analytical procedure execution. Data generated during the analytical method validation [9,10,11,12] defines the robustness and the variability of the method. As per the ICH, Japa-

Table 1: List of Techniques/Methods used in monitoring the CQA and other Quality attributes (9,10).

| Steps in Biosimilar Manufacturing | Methods/ Technique | Purpose | Classification of the methods based on purpose |
|---|---|---|---|
| Amino Acid sequencing | LC-MS | Amino acid identification | Identity |
| Clone Development / Master Cell bank creation | Protein A/ UV-spectroscopy | Product Titer Quantification | Assay |
| | SDS_PAGE | Product Identification/Size Variants | Identification/Purity |
| | SEC_H(U) PLC/CE-SDS | Size variants Quantification | Purity |
| | IEX_H(U) PLC/ icIEF | Charge variants Quantification | Purity |
| | Glycan | Glycan Content estimation | Purity |
| | Sialic acid | Sialic Acid Estimation | Assay |
| | DNA Barcode assay | Identity test for the cell line | Identity |
| | Sterility test | Microbiological Contaminants | Identification |
| | PCR | Viral contaminants and specific virus tests | Identification |
| Upstream Development | Protein A/ UV-spectroscopy/ Solo-VPE | Product Titter Quantification | Assay |
| | SEC_H(U) PLC/CE-SDS | Size variants Quantification | Purity |

| | | | |
|---|---|---|---|
| | IEX_H(U) PLC /icIEF | Charge variants Quantification | Purity |
| | Glycan | Glycan Content estimation | Purity |
| | Sialic acid | Sialic Acid Estimation | Assay |
| | Process related impurity generated/ added to improve the process efficiency | Estimation and clearance | Assay |
| | Bioburden | Estimation and Identification | Assay and identification |
| | BET | Estimation | Assay |
| Down-stream | Protein A/ UV-spectroscopy/ Solo-VPE | Product Titter Quantification | Assay |
| | SEC_H(U) PLC/CE-SDS | Size variants Quantification/fragments | Purity |
| | IEX_H(U) PLC /icIEF | Charge variants Quantification | Purity |
| | Process related impurity generated during Upstream/ down-stream | Estimation and clearance | Assay |
| Formulation and fill finish | Protein A/ UV-spectroscopy/ Solo-VPE | Product Titer Quantification | Assay |
| | SEC_H(U) PLC/CE-SDS | Size variants Quantification | Purity |
| | IEX_H(U) PLC /icIEF | Charge variants Quantification | Purity |
| | pH | Estimation | Measurement |
| | Osmolality | Estimation | Measurement |
| | Colour/ Clarity/Appearance | Identity | Identity |
| | Potency/ Biopotency | Identity and estimation | Identity and estimation |
| | BET | Estimation | Assay |
| | Bioburden | Estimation/ Identification | Assay and Identification |
| | Sterility | Identification | Identification |
| | Fill volume | Estimation | Assay |
| | Visible/ Sub visible Particles | Estimation | Assay |
| | Excipients | Estimation | Assay |
| | Impurity | Estimation | Clearance |
| | Elemental impurities | Estimation | Clearance |

nese Pharmacopoeia (JP), United States Pharmacopoeia (USP), FDA and other major guidelines, various analytical methods are classified into four major types based on their intended purpose: (i) Identification tests (ii) Quantitative tests for impurities' content (iii) Limit tests for the control of impurities (iv) Quantitative tests of the active moiety in samples of drug substance or drug product or other selected component(s) in the drug product.

Parameters that has to be evaluated are defined based on the classification of the method into types mentioned above. The method validation parameters are depicted in the Figure 3.

Comparison of analytical method validation guidelines used for release, stability in biosimilar manufacturing process

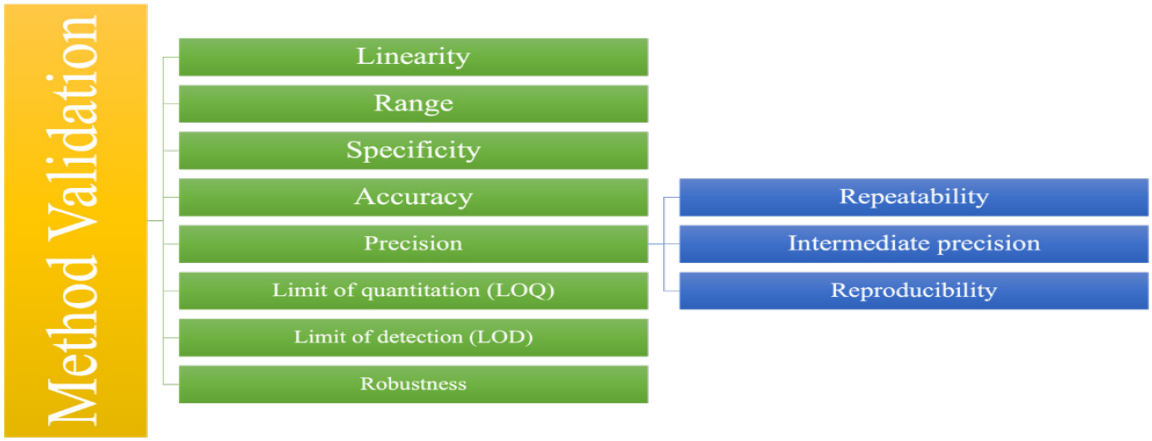


Figure 3:Analytical method validation parameters

As mentioned before, the extent of method validation depend on the purpose of the method and its regulatory requirements. The detailed explanation about each method was extensively mentioned in the further sections. Table 2 depicts the method validation requirements based on the methods categorified as per the Table 1.

Table 2: Method validation parameters based on the method requirement (12,13).

| Parameter | Identity Methods | Assay methods | Purity/Impurity | Clearance |
|---|---|---|---|---|
| Linearity | N | Y | Y | Y |
| Range | N | Y | Y | Y |
| Specificity | Y | Y | Y | Y |
| Accuracy | N | Y | Y | Y |
| Precision | | | | |
| Repeatability | N | Y | Y | Y |
| Intermediate Precision | Y | Y | Y | Y |
| Reproducibility | N | Y | Y | Y |
| LOQ | N | Y | Y | Y |
| LOD | N | May be required | May be required | Y |
| Robustness | Y | Y | Y | Y |

N – Validation of the specific parameter is not required, Y – Validation of the parameter is required.

## Linearity

### *Definition*

The linearity of a method is expressed as the ability of a method to elicit a response in the form of linear or a mathematical expression form proportional to the amount of the analyte present in the sample. The linear or mathematical response majorly depends on the instrument and the detector used. For HPLC, UV, and the majority of the methods the relationship between the amount of analyte present in the sample and the response should be linear. For CAD detectors based on methods, the response can be linear, or quasi-linear [9,10,11,12,13,14].

### *Procedure*

The linearity of the method will be evaluated graphically by plotting the response from the detector connected to the analytical instrument and to the theoretical concentration or the content of the analyte present in the sample being tested. The responses should be directly proportional or proportional by means of the amount of analyte present in the sample. The relation should be explained either by a linear equation or by an appropriate mathematical/statistical equation as applicable. Linearity has to be tested around the range as applicable[12,13,14]. For the majority of the methods the Linearity was expressed in terms of Linear regression as mentioned in the

, $R^2$

Here the Y–axis represents the analyte response generated from the Instrument detector.

X – axis represents the theoretical concentration of the analyte present in the sample (the sample will be diluted into multiple determinations to cover the range of the method with the representative diluent/buffer)

m – slope of the curve

$R^2$ – coefficient of regression

Number of determinants/concentrations used for linearity majorly depends on the range required for the method, a minimum of 5 determinants should be used.

### *Acceptance criteria/test requirements*

The correlation coefficient, Y-intercept, slope of the regression line, and the sum of least squares should be submitted.

Table 3: Linearity Test acceptance criteria (15,16).

| **Parameter** | **ICH**[9] | **USA**[15] | **EU**[16] | **Japan**[10] | **India**[13] |
|---|---|---|---|---|---|
| Minimum number of concentration | 05 | 05 | 05 | 05 | 05 |
| Regression coefficient ($R^2$) | - | - | - | - | 0.999* |
| Graphical plot – Response Versus Concentration | Required | Required | Required | Required | Required |

∗ *For methods with usage of CAD as a detector, criteria can be relaxed with proper justification and supporting data.*

## Range

### *Definition*

The range of a method will be derived from the linearity studies covering the lower and upper limit of analyte concentration to be measured with that analytical method. All the determinants present in the range should have acceptable degree of linearity, accuracy and precision.

***Procedure and acceptance criteria***

The range of a methodwill be derived from the linearity data showing acceptable linearity, accuracy and precision. Table 4 represents the minimum ranges that has to be considered for range based on its application of use:

Table 4:Minimum acceptable ranges based on its intended use (15,16).

| Nature of the analyte | Purpose of the method | Minimum Range to be tested | | | | |
|---|---|---|---|---|---|---|
| | | ICH (9) | USA (15) | EU (16) | Japan (10) | India (13) |
| Drug substance/ Drug product | Assay | 80 – 120 % | 80 – 120 % | 80 – 120 % | 80 – 120 % | 80 – 120 % |
| Impurity | Assay | Reporting level to 120 % of Specification | Reporting level to 120 % of Specification | Reporting level to 120 % of Specification | Upper , lower and middle limit | Reporting level to 120 % of Specification |
| Impurity | Assay/Clearance | LOQ/LOD till upper limit/120 % of specification | LOQ/LOD till upper limit/120 % of specification | LOQ/LOD till upper limit/120 % of specification | Upper , lower and middle limit | Reporting level to 120 % of Specification |

In order to cover the impurity for clearance/assay it is advisable to perform the range test from the LOQ/LOD level till the 150 % of the upper limit of specification (17).

**Specificity**

***Definition***

Specificity is the ability of the analytical method to measure the analyte unequivocally in the presence of other inevitable sample components. For example the sample used for testing should contain impurities, Degradation products, or process raw materials or excipients. Method used should specifically identify the analyte (DS/DP/Impurity/Degradation product) of measurement without the interference of other sample matrix components.

***Procedure***

The specificity of the method can be established in multiple ways depending on the usage of the method. (i) DS/DP, purified Impurity, Degradants of the products, and other analytes were spiked into the matrix /Placebo and their response was evaluated over the amount of materials spiked into the respective matrix (15). (ii) In a Situation where impurities/ degradants products/Standards are not available for spiking , then a well characterised alternative/orthogonal method should be employed. It is preferable to use the method which is compendial or validated to check the specificity (16). (iii) For chromatographic methods respective impurities/ degradants product peaks should be collected and analysed by using Mass spectroscopy technique. (iv) For Assay and impurity tests, the test sample and the respective buffer should be analysed side by side to check the interference of the product. There should not be any interface at/with the peak of analyte (17).

***Acceptance criteria***

No interference should be observed in the measurement of the analyte. The requirements for the specificities across the selected are mentioned in the

Table 5:Country specific requirements for Specificity (15,16).

| **ICH** (9) | **USA** (15) | **EU** (16) | **Japan** (10) | **India** (13) |
|---|---|---|---|---|
| All the components in the sample from the result should be properly labeled with proper resolution | All the components in the sample from the result should be properly labeled with proper resolution | All the components in the sample from the result should be properly labeled with proper resolution | All the components in the sample from the result should be properly labeled with proper resolution | All the components in the sample from the result should be properly labeled with proper resolution |
| Impurities and other samples should be spiked into the placebo/ Sample matrix | Impurities and other samples should be spiked into the placebo/Sample matrix | Impurities and other samples should be spiked into the placebo/ Sample matrix | Impurities and other samples should be spiked into the placebo/Sample matrix | Impurities and other samples should be spiked into the placebo/Sample matrix |
| When Impurities are not available other well characterized method should be used to demonstrate specificity | When Impurities are not available other well characterized method should be used to demonstrate specificity | When Impurities are not available other well characterized method should be used to demonstrate specificity | When Impurities are not available other well characterized method should be used to demonstrate specificity | When Impurities are not available other well characterized method should be used to demonstrate specificity |
| - | For a stability indicating method Accelerated stress samples should be used to show the specificity for degradants | – | In case the reference standard of the impurities/degradants are not available then Accelerated stress samples should be used to show the specificity | - |

## Accuracy

### *Definition*

The accuracy of the analytical method defines how close is the method result value to the actual value (amount of analyte present in the sample) (15). Generally accuracy of the method is expressed in terms of recovery of the analyte present in the solution to the amount of analyte spiked into the solution.

### *Procedure acceptance criteria*

The accuracy of the method was performed by spiking the known amount of analyte into placebo/Background buffer/sample matrix, and the results were expressed in terms of percentage recovery as mentioned in the below equation (16).

$$\% \text{ Recovery} = \frac{(\text{Amount of analyte present in the sample})}{(\text{Amount of analyte spiked or added ino the palcebo})} \times 100$$

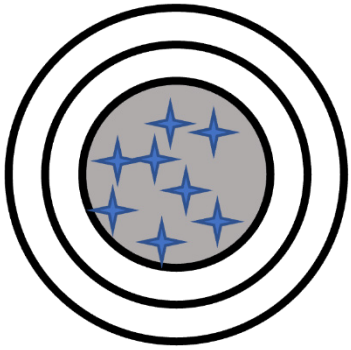

Figure 4: Accuracy of the analytical method

In the Figure 4 stars represent the results obtained from the analytical method whereas the circle with the coloured portion is the true value with accepted method variabili-

ty. The accuracy of a method should cover the linearity and range of the method with at least 9 determinants covering the entire range of a method with at least 3 concentrations (upper limit, middle and lower limit of the range).

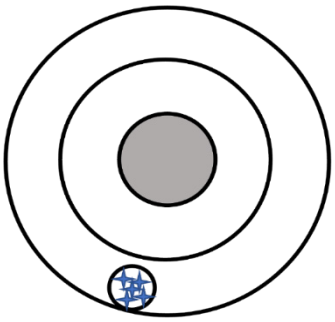

Figure 5: Results are Precise but not accurate

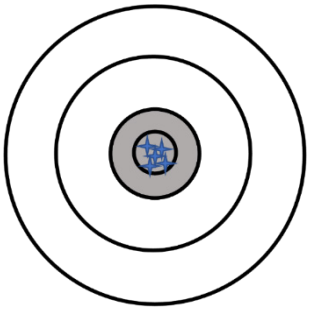

Figure 6: Results are Accurate and Precise

of an analytical method but it can't assure the accuracy of the method. Figure 5 and Figure 6 illustrate the precision and the relationship between accuracy and precision.

It was expressed in three ways as mentioned below: (i) *Repeatability/Intra-assay precision,* (ii) *Intermediate precision,* (iii) *Reproducibility*

***Repeatability/Intra-assay precision***

***Definition***

The repeatability of a method was assessed by defining the variability of the method within a short period of time under the same conditions with the homogenous sample (15,16). The variability of the method was estimated with the same operator, same instrument and sample etc.

**Precision**

Precision is measured as the closeness of the analytical results obtained from a sample with allowed variability. the precision of the method estimates how close the measurement

***Procedure***

The repeatability of a method was estimated by analyzing the sample multiple times with the same analyst, in fact, the repeatability merely depends on the analytical instrument, and the detector responsible for measurement (17). Repeatability depicts the precision of the instrument as well.

| **ICH** (9) | **USA** (15) | **EU** (16) | **Japan** (10) | **India** (13) |
|---|---|---|---|---|
| A minimum of nine determinants covering the entire range of the method with 3 replicates covering 3 Concentrations of the range | A minimum of nine determinants covering the entire range of the method with 3 replicates covering 3 Concentrations of the range | A minimum of nine determinants covering the entire range of the method with 3 replicates covering 3 Concentrations of the range | Variance and standard deviation should be established with 90 % confidence intervals | A minimum of nine determinants covering the entire range of the method with 3 replicates covering 3 Concentrations of the range |
| A minimum of 6 determinants with 100 % test sample concentrations | A minimum of 6 determinants with 100 % test sample concentrations | A minimum of 6 determinants with 100 % test sample concentrations | | A minimum of 6 determinants with 100 % test sample concentrations |

***Acceptance Criteria***

The repeatability of the method will be established by keeping the % RSD criteria for the output value between the determinants analyzed for the study (18). The % RSD criteria depend on the type of method and its requirements for its uses in the process.

***Intermediate precision***

***Definition***

Intermediate precision of the method estimates the variability of the method within laboratories, different days, analysts, equipment, etc.,

***Procedure***

Repeatability sequence can be repeated with different analysts, days, equipment, lots of chemicals, columns, etc., used in the method (19). The variations in the method execution can be done one factor at a time or by using a design of experiments.

***Acceptance criteria***

Intermediate precision of the method was established by keeping the % RSD criteria for the output value between the determinants analyzed for the study (20,21). The % RSD criteria depend on the type of method and its requirements for its uses in the process.

**Reproducibility:**

***Definition***

*Reproducibility is the precision expressed between the two different laboratories.*

***Procedure***

*The reproducibility experiment will be done by executing two sets of experiments as described in repeatability in two different laboratories.*

***Acceptance criteria***

The repeatability of the method was established by keeping the % RSD criteria for the output value between the determinants analyzed for the study (21,22). The % RSD criteria depend on the type of method and its requirements for its uses in the process.

***Limit of quantification(LOQ)***

***Definition***

Estimation of the Lowest concentration or amount of the analyte present in the sample with accuracy and precision, in other words, lowest concentration of an analyte measured by the analytical method (22,23).

***Procedure***

The LOQ of a method is estimated by using the known concentration of the sample at the lowest amount with acceptable accuracy and precision (24,25). For the Chromatographic methods, the LOQ of the method was established by using the signal to Nosie ratio with acceptable accuracy and Precision.

***Acceptance criteria***

For chromatographic methods, the LOQ will be identified at a concentration where the signal-to-noise ratio is equal or more than 10 with acceptable accuracy and precision. The LOQ is estimated by injecting the same sample six times with an acceptable % RSD between the six preparations of the sample.

***Limit of detection (LOD)***

***Definition***

Detection of Lowest concentration or amount of the analyte present in the sample, in other words, the LOD depicts the presence of the analyte in the sample which is not accurate in terms of quantity.

***Procedure***

The LOD method is estimated by evaluating the response which should be higher than the response for the blank sample (25). For the Chromatographic methods, the LOQ of the method was established by using the signal to Noise ratio.

***Acceptance criteria***

For chromatographic methods, the LOD will be determined at a concentration where the signal-to-noise ratio is equal to or more than 3.

***Robustness***

***Definition***

The robustness of a method is the ability of the method to remain unaffected with small deliberate changes with are unavoidable during the method execution (26,27). Expected changes are purposely introduced during the robustness study to understand the effect of these variations on the analytical method outcome.

***Procedure***

Expected changes/variations that might occur in the routine analysis will be introduced during the method validation. For example pH of the buffer and column temperature will be varied and will be studied during the robustness activity. The stability of the prepared sample(diluted/undiluted) solution will also be evaluated.

***Acceptance criteria***

Based on the outcome of the results, the method parameters with a defined range will be finalized for routine analysis. The Method validation parameters vary depending on the above types and based on the application of the method in the Bio-pharmaceutical /pharmaceutical manufacturing (28). In the current review process, the method validation approaches will be majorly categorized based on their application, type of method and manufacturing process requirements. Method validation guidelines from different regulatory bodies resulted in certain method validation characteristics and the same are discussed further.

**For identification methods**

The identification methods are used to confirm the identity of the analyte present in the sample. These tests are performed based on the spectrum of the method or in comparison with the reference standard available (29). Specificity, intermediate precision, and Robustness study are evaluated for the methods used for the identification of analyte such as Amino Acid sequencing by LC-MS, SDS PAGE, PCR, DNA bar code assays method. For Colour/Clarity/Appearance testing methods the whole sample consisting of a drug substance/drug product with its impurities along with its background buffer/matrix will be evaluated as there is no estimation of a specific analyte. The majority of the time this method of analysis is of pharmacopeial methods, and the validation/verification will be done by analyzing the three batch samples or a single batch in triplicates which is intended for commercial process and the similarity of the results will be considered (29). For the microbial methods like Sterility and bioburden matrix/background interference, evaluation estimates the condition buffer for the microbial growth along with positive and negative control.

**For assay methods:**

For better ease of understanding the application of assay methods, the assay methods are divided in to various types as mentioned in Figure 7.


Figure 7: Assay methods and its types

***Assay measurement***

Methods like pH, and osmolality estimation majorly come under assay measurement, where the solution will be analyzed rather than a specific analyte. As pH, and osmolality plays a major role in the stability of the molecule and their interaction within the body when injected, their control is very critical in the process[29]. The method validation will be done by measuring pH and osmolality of three batch samples intended for commercial process or a single batch in triplicates and the similarity of the results will be

considered[30]. These methods has to be applied for release as well as for stability as the sample/ solution should be within the limits till the end of the shelf life of the molecule.

### *Assay concentration estimation*

The method used for estimation of product titer, size variants, charge variants and other quality attributes comes under this category. For the methods used to estimate the active substance in in-process samples, drug substance and drug product, validation will be performed considering the parameters as mentioned in Table 2. However, the method used to estimate active substance in DS and DP method need not be validated for LOQ and LOD limits as the concentration of the analyte in DS and DP samples will be as per the dosing requirement of the concerned medicine (29,30). Also, the range of these methods will be validated as per the process limits with a variation of 10 – 20 % from the lower and upper side of the process limits. These methods should be applied for release as well as for stability as the molecule concertation should be within the limits till the end of the shelf life of the molecule.

### *Identity method and assay*

The Method used to estimate the potency of the molecule can be used as identity and assays. In the Bioassay analysis, the DS/ DP binding with its respective molecular target will be used and the potency will be estimated, as binding is highly specific the method can be used as identity also (30). Potency can be measured, and it is linked to the molecule's efficacy towards the molecule. These methods are majorly done by ELISA or cell-based methods (30). These methods should be applied for release as well as for stability as the molecule concertation should be within the limits till the end of the shelf life of the molecule.

### *Limit tests for impurities*

Limit tests for impurities will be used to estimate the amount the impurities present in the sample, in the biologics manufacturing process there are impurities that majorly come from various stages in the manufacturing process Figure 8 represents the impurities generated in the manufacturing process.

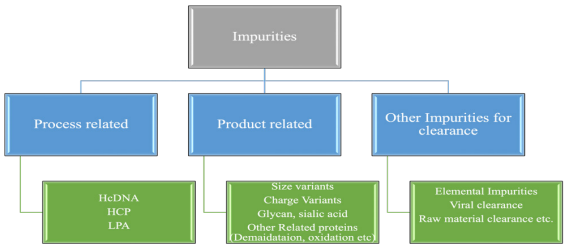


Figure 8: Impurities generated in the Biologics manufacturing process

### *Process-related impurities*

The Process-related impurities like HcDNA , LPA and HCP have a defined calculation for the amount as per agency requirement, the method should be validated to the limits based on daily intake and the process consistency (29,30,31). The method validation must include LOQ and LOD limits. The method validation range should include the process limits as well as the respective health agencies requirement (31). These methods have to be applied for the DS/DP Release and is not required for stability as these impurities will not change based on the time.

### *Product-related impurities*

Product-related impurities like size variants, charge variants, deamidation, oxidation etc, generate over time and increase as the product nears the end of its shelf life. The method validation range for this limit should include the lower limit and the upper limit of the particular impurity, the limit will be decided based on the safety and efficacy data generated from the clinical trial, In the case of biosimilars these limits are set based on the QTPP data generated form the innovator drug procedure from the indented marketing region (30,31). In case where

the impurity limit is very high than the LOQ of the method then the LOD of the method is not required to be generated. These methods have to be applied for the DS/DP Release and is not required for stability as these impurities will not change based on the time (30). The Impurities like Glycan and Sialic acid will not increase over the period of time due to this the method will be used for release and need not be tested on stability.

***Other impurities for clearance***

Impurities like elemental impurities clearance should be performed at the DP stage based on the elemental impurities limits linked to their safety, for method validation of this method the LOQ and LOD have to be established as the limits will be highly minimal except few elemental impurities (31). These will be demonstrated based on the consistency of the process and need not be used for routine release however the measurement of impurities will be evaluated case by case and respective metal ions will be estimated as per the requirement (31). For the method used to test for Viral impurities and other advantageous elements method should be validated with LOD and LOQ, as these impurities absence should be demonstrated in the method, in these cased the amount of some impurities will be spiked as a positive control to show the absence of the impurities, as these will not increase over the period of time due this the method will be used for release and need not to be tested on stability.

*Methods used for the Assay of Excipients:*

The excipients method will be used to check its content in the final DS and DP, as per the label claim or not, for the validation of these methods the range will be established along with the limits as per the label claim, the establishment of LOQ and LOD is not required as per the excipients until there is special consideration of the method (30,31). or if the lower limit of the method coincides/is near the LOQ limit.

**Conclusion:**

The method validation is one of the important requirements for the health agencies to check its performance as the safety, and efficacy of the drug entirely depend on CQA and the stability of the drug which are governed by the analytical method used to estimate the Quality attributes of the method being used. Validation of the method majorly relies on the requirements of the process and the regulators it is always recommended to use the validation parameters to cater to all the agencies' requirements as depicted in the present paper. The Validation should always be planned in such a way as to cover the requirements of all the regulatory agencies, and this requirement should be seen not only to fulfill the requirements of the countries but also in a scientific way these are important for checking the suitability of the method also.

**References:**

1. https://www.fda.gov/files/drugs/published/Biological-Product-Definitions.pdf accessed on 14/03/2022.

2. https://www.ema.europa.eu/en/human-regulatory/overview/biosimilar-medicines-overview#:~:text=A%20biosimilar%20is%20a%20biological,apply%20to%20all%20biological%20medicines. Accessed on 14/03/2022.

3. Sitte, H., Freissmuth, M. (2013). Biosimilars versus generics: scientific basics and clinical implications. memo 6, 202–206

4. Sekhon B,. Saluja V,. (2011). Biosimilars: an overview, Dove Press, Volume 2011:1 Pages 1-11.

5. van de Vooren, K., Curto, A. & Garattini, L. (2015). Biosimilar Versus Generic Drugs: Same But Different?. Appl Health Econ Health Policy 13, 125–127.

6. ICH Q8 (R2) 2009. Pharmaceutical development.

7. Ahmed, I., Kaspar, B,. and Sharma, U,. (2012) 'Biosimilars: impact of biologic product life cycle and European experience on the regulatory trajectory in the United States', Clinical therapeutics, 34(2), pp. 400–419. Available at: https://doi.org/10.1016/J.CLINTHERA.2011.12.005.

8. Amgen explains the steps of manufacturing a biosimilar, Gaba online Journal, BIOSIMILARS/GENERAL posted on 29/05/2020 https://gabionline.net/biosimilars/general/Amgen-explains-the-steps-of-manufacturing-a-biosimilar accessed on 22/03/2023.

9. ICH Q2(R1) Validation of Analytical Procedures: Text and Methodology - ECA Academy (no date). Available at: https://www.gmp-compliance.org/guidelines/gmp-guideline/ich-q2r1-validation-of-analytical-procedures-text-and-methodology (Accessed: 10 April 2024).

10. Validation of Analytical Procedures, <G1-1-130>, Japanese Pharmacopoeia 18th edition

11. Validation of Compendial Procedures, USP <1225>, US Pharmacopoeia 36 edition

12. Federal Register :: Analytical Procedures and Methods Validation for Drugs and Biologics; Guidance for Industry; Availability (no date). Available at: https://www.federalregister.gov/documents/2015/07/27/2015-18270/analytical-procedures-and-methods-validation-for-drugs-and-biologics-guidance-for-industry (Accessed: 10 April 2024).

13. Validation of Analytical Methods, Indian pharmacopeia Commission, IPC/GD/04, version :01

14. Gamache, P., Muellner, T., Eggart, B., Lovejoy, K., & Acworth, I. (2019). Charged aerosol detection – use of the power function and robust calibration practices to achieve the best quantitative results, thermos fisher technical note – 73299.

15. Q2B Validation of Analytical Procedures: Methodology, Guidance for Industry, November 1996.

16. ICH Topic Q 2 (R1) Validation of Analytical Procedures: Text and Methodology, CPMP/ICH/381/95, June 1995.

17. Crowther, J.B. (2001). Validation of pharmaceutical test methods. In: Ahuja, S. and Scypinski, S. (Eds.), Handbook of Modern Pharmaceutical Analysis, Academic Press, New York.

18. Singh, K., & Mehta, S. (2016). The clinical development process for a novel preventive vaccine: An overview. https://doi.org/10.4103/0022-3859.173187

19. Thompson, T. (2022). The staggering death toll of drug-resistant bacteria. https://doi.org/10.1038/d41586-022-00228-x

20. Differences between biosimilars and reference products. (2016). https://www.gabionline.net/biosimilars/research/Differences-between-biosimilars-and-reference-products

21. Yu, L., Shi, X., Han, C., Chun-ming, R., & Wang, J. (2018). A rapid reporter assay for recombinant human brain natriuretic peptide (rhBNP) by GloSensor technology. https://doi.org/10.1016/j.jpha.2018.04.003

22. Camacho, L H., Frost, C P., Abella, E., Morrow, P K., & Whittaker, S. (2014). Biosimilars 101: considerations for U.S. oncologists in clinical practice. https://www.ncbi.nlm.nih.gov/pmc/articles/PMC4303156/

23. Schiestl, M., Zabransky, M., & Sörgel, F.

(2016). Ten years of biosimilars in Europe: development and evolution of the regulatory pathways. https://www.ncbi.nlm.nih.gov/pmc/articles/PMC5440034/

24. Korkmaz, E., & \, M E. (2020). QUALITY EVALUATION OF BIOSIMILAR MEDICINES: AN OVERVIEW. http://www.ujpr.org/index.php/journal/article/download/390/683

25. Kirchhoff, C F., Wang, X M., Conlon, H D., Anderson, S., Ryan, A., & Bose, A. (2017). Biosimilars: Key regulatory considerations and similarity assessment tools. Biotechnology and bioengineering, 114(12), 2696-2705. https://doi.org/10.1002/bit.26438

26. Research, C. (2022). Overview for Health Care Professionals. https://www.fda.gov/drugs/biosimilars/overview-health-care-professionals

27. Research, C. (2020). Quality Considerations in Demonstrating Biosimilarity of a Therapeutic. https://www.fda.gov/regulatory-information/search-fda-guidance-documents/quality-considerations-demonstrating-biosimilarity-therapeutic-protein-product-reference-product

28. Vandekerckhove, K., Seidl, A., Gutka, H., Kumar, M., Gratzl, G., Keire, D A., Coffey, T., & Kuehne, H. (2018). Rational Selection, Criticality Assessment, and Tiering of Quality Attributes and Test Methods for Analytical Similarity Evaluation of Biosimilars. The AAPS journal, 20(4). https://doi.org/10.1208/s12248-018-0230-9

29. F. Wang, D. Richardson, and M. Shameem, (2015).“Host-Cell Protein Measurement and Control” BioPharm International 28 (6).

30. Harry Yang.( 2013). Establishing acceptable limits of residual DNA, PDA J Pharm Sci Technol ,67(2):155-63.

31. ICH guideline Q3D (R1) on elemental impurities.